

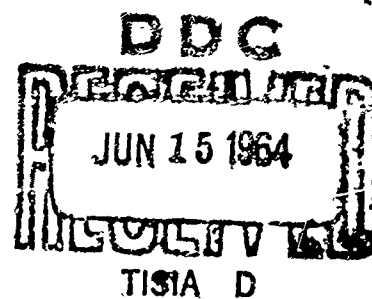
601116

2073

DMIC Report 196  
January 20, 1964

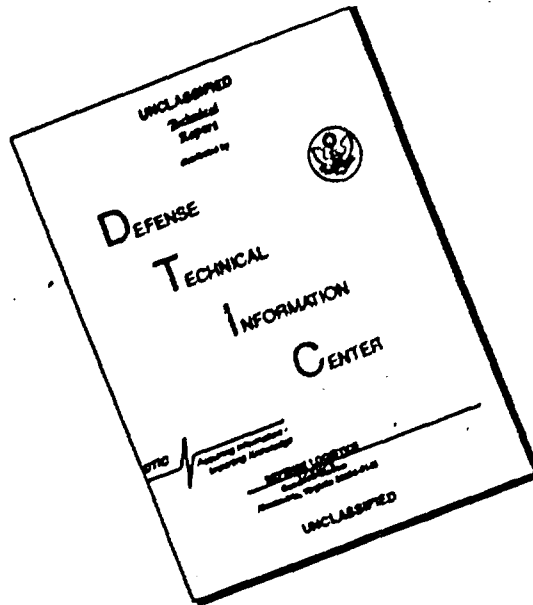
162 P \$3.00

**HYDROGEN-INDUCED, DELAYED, BRITTLE FAILURES  
OF HIGH-STRENGTH STEELS**



**DEFENSE METALS INFORMATION CENTER**  
Battelle Memorial Institute  
Columbus 1, Ohio

# DISCLAIMER NOTICE



THIS DOCUMENT IS BEST QUALITY AVAILABLE. THE COPY FURNISHED TO DTIC CONTAINED A SIGNIFICANT NUMBER OF PAGES WHICH DO NOT REPRODUCE LEGIBLY.

The Defense Metals Information Center was established at Battelle Memorial Institute at the request of the Office of the Director of Defense Research and Engineering to provide Government contractors and their suppliers technical assistance and information on titanium, beryllium, magnesium, aluminum, refractory metals, high-strength alloys for high-temperature service, corrosion- and oxidation-resistant coatings, and thermal-protection systems. Its functions, under the direction of the Office of the Director of Defense, are as follows:

1. To collect, store, and disseminate technical information on the current status of research and development of the above materials.
2. To supplement established Service activities in providing technical advisory services to producers, melters, and fabricators of the above materials, and to designers and fabricators of military equipment containing these materials.
3. To assist the Government agencies and their contractors in developing technical data required for preparation of specifications for the above materials.
4. On assignment, to conduct surveys, or laboratory research investigations, mainly of a short-range nature, as required, to ascertain causes of troubles encountered by fabricators, or to fill minor gaps in established research programs.

Contract No. AF 33(615)-1121  
Project No. 8975

*Roger J. Runck*

Roger J. Runck  
DIRECTOR

"The information in this report came from many sources, and the original language may have been extensively quoted. Quotations should credit the original authors and the originating agency. Where patent questions appear to be involved, the usual preliminary search is advised before making use of the material, and where copyrighted material is used, permission should be obtained for its further publication."

COPIES AVAILABLE FROM OTS \$

DMIC Report 196  
January 20, 1964

HYDROGEN-INDUCED, DELAYED, BRITTLE FAILURES  
OF HIGH-STRENGTH STEELS

by

A. R. Elsea and E. E. Fletcher

to

OFFICE OF THE DIRECTOR OF DEFENSE  
RESEARCH AND ENGINEERING

DEFENSE METALS INFORMATION CENTER  
Battelle Memorial Institute  
Columbus, Ohio 43201



## TABLE OF CONTENTS

	<u>Page</u>
SUMMARY . . . . .	1
INTRODUCTION . . . . .	3
EFFECT OF THE COMPOSITION OF THE MATERIAL . . . . .	3
EFFECT OF STRENGTH LEVEL . . . . .	25
EFFECTS OF APPLIED STRESS AND PLASTIC STRAIN . . . . .	34
THE EFFECT OF HYDROGEN CONTENT . . . . .	56
NEED FOR HYDROGEN MOVEMENT . . . . .	89
Hydrogen Movement Demonstrated . . . . .	89
Temperature Dependence . . . . .	93
Strain-Rate Dependence . . . . .	102
EFFECT OF MICROSTRUCTURE . . . . .	106
EFFECT OF SECTION SIZE . . . . .	114
EFFECT OF NOTCH ACUITY . . . . .	116
EFFECT OF STRESS STATE . . . . .	119
THEORIES OF HYDROGEN EMBRITTLEMENT. . . . .	125
TESTS FOR HYDROGEN EMBRITTLEMENT. . . . .	139
CONCLUSIONS. . . . .	143
REFERENCES. . . . .	146

# HYDROGEN-INDUCED, DELAYED, BRITTLE FAILURES OF HIGH-STRENGTH STEELS

A. R. Elsea and E. E. Fletcher\*

## SUMMARY

Steel which is subjected to a tensile stress exceeding some critical value depending on the strength level of the steel and which contains hydrogen that is free to move is susceptible to failure in a delayed, brittle manner. The problem is especially serious because the minimum stress for failure decreases as the strength of the steel is increased and because failures occur with no appreciable ductility, even though in a tensile test the material may exhibit normal ductility. Under most conditions the strength level of the steel is the most important factor affecting the occurrence of delayed, brittle failure. Both the minimum applied stress that will result in failure and the time required for the failure to occur decrease as the tensile strength of the steel is increased. These failures occur in all types of steel microstructures except austenite. Alloy composition is a relatively unimportant factor in the hydrogen-induced, delayed, brittle failure of body-centered cubic steels.

It has been shown that such failures depend directly on the hydrogen content of the steel, and the way in which the hydrogen gets into the steel is of no importance. Such failures do not occur if hydrogen is kept out of the steel or is removed before the steel is damaged permanently. Normally, the critical amount of hydrogen required to induce failure is not present at the sites where failure initiates, hydrogen must move to these sites, either as the result of a hydrogen-concentration gradient or a stress gradient. The former condition prevails when the steel is exposed to an environment which permits hydrogen to enter its surface. Stress gradients that will cause hydrogen to move to regions of high tensile stress may result from bending or notches.

Since this type of failure involves time for the diffusion of hydrogen, it occurs under low-strain-rate or static-load conditions. Crack propagation is not a continuous process, it has been shown to be a series of individual crack initiations and propagations. Both the incubation period and the propagation of the crack are controlled by the diffusion of hydrogen. However, the mechanism by which hydrogen reduces the ductility of steel and lowers its load-carrying ability still is not known. All of the theories advanced to explain these effects depend on a critical combination of hydrogen and stress.

Whether or not a material under a given set of conditions will fail in a delayed, brittle manner can be determined with certainty only by a sustained-load test. Impact tests are useless, because the time under stress is too short for the failure mechanism to become operative. The results of tensile tests may be misleading, since they may indicate full ductility and yet the material can fail in a brittle manner after a period of time under a sustained stress above the critical level.

---

\*Ferrous and High-Alloy Metallurgy Division, Battelle Memorial Institute.

## INTRODUCTION

DMIC Memorandum No. 180, "The Problem of Hydrogen in Steel", October 1, 1963, was written with the intent of helping the steel user determine if he has a problem of delayed, brittle failure associated with hydrogen in steel, particularly high-strength steel. The effects of hydrogen on the mechanical properties of steel are dealt with, and the general behavior of material susceptible to delayed, brittle failure is described. The most noteworthy characteristic of delayed, brittle failures induced in steel by hydrogen is the loss in ability to support a sustained load. Also, possible sources of hydrogen in steel and the types of tests useful in determining the susceptibility to delayed failure are outlined.

The present report discusses in detail the factors that influence the susceptibility of high-strength steels to this type of failure.

### EFFECT OF THE COMPOSITION OF THE MATERIAL

Many types of steel, including types with a wide variety of alloying additions, comprising both substitutional and interstitial elements, have been examined for resistance to hydrogen embrittlement and hydrogen-induced, delayed, brittle failure. No alloying element has been able to eliminate the propensity toward delayed, brittle failure, and none has been truly effective in retarding failures of this type. All ferritic and martensitic steels investigated under test conditions that promote delayed, brittle failure have been susceptible to this type of failure. However, no instances of hydrogen-induced, delayed, brittle failure of an austenitic steel is known to the authors. Even when severe cathodic charging conditions have been used, no delayed failure and relatively little loss in ductility have been encountered with austenitic steels. However, when austenitic steels are processed so that part of the austenite is transformed to the body-centered cubic form (by cold work or by low-temperature treatment) so that they are no longer fully austenitic, they too become susceptible to such failures. Thus, in the same material, a change in structure can alter what is apparently a completely resistant material into one that is readily susceptible, without change in composition. This has been demonstrated in chromium-nickel, straight-nickel, and manganese austenitic steels. It would seem, then, that the resistance of austenitic materials to this phenomenon is the result of the face-centered cubic structure and not differences in composition.

Because many alloy systems had been investigated and hydrogen embrittlement had been found only in body-centered cubic transition metals, a number of investigators inferred that no face-centered cubic metal can be embrittled by hydrogen: for example, see Reference 1\*. However, Eisenkolb and Ehrlich<sup>(2)</sup> discovered that nickel could become embrittled by hydrogen, so the rule is not universal. Later, Blanchard and Trociano<sup>(3)</sup> verified the embrittlement of nickel and also found that certain nickel-base, nickel-iron alloys were embrittled by hydrogen when charged for several hours at a high current density.

---

\*References appear at the end of the report.

The following paragraphs will describe some of these investigations in greater detail.

Because hydrogen embrittlement limits the use of martensitic steels at high strength levels and no cases of delayed, brittle failure have been found in austenitic steels, most of the studies of delayed, brittle failure have been performed with body-centered cubic steels. For the most part, the early studies were concerned with AISI 4340, a Cr-Ni-Mo steel which is extensively used in the aircraft industry at high strength levels and with which some spectacular delayed, brittle failures have been encountered. The nature of the susceptibility of this steel was well demonstrated by the work of Froiano and co-workers at Case Institute of Technology<sup>(4, 5, 6)</sup>, Elsea and co-workers at Battelle Memorial Institute<sup>(7, 8, 9)</sup>, Sachs and his group at Syracuse University<sup>(10, 11)</sup>, and Rinebolt at the Naval Research Laboratory<sup>(12)</sup>. Examples of the results obtained for this steel heat treated to various strength levels and tested under static loads are shown in Figures 1 and 2. The results shown in Figure 1 were obtained with sharp-notched specimens precharged with hydrogen, while those in Figure 2 were obtained with unnotched specimens cathodically charged continuously while under load.

Elsea's group studied the effects of both interstitial and substitutional alloying elements<sup>(8, 9)</sup>. These investigators used unnotched specimens cathodically charged continuously while under load with standard charging conditions of 4 per cent sulfuric acid electrolyte, phosphorus poison, and a current density of either 8 or 10 ma/in.<sup>2</sup>. Experiments with SAE 4320, SAE 4340, and a high-carbon (about 0.95% C) steel indicated that a considerable change in carbon content had little effect on the delayed, brittle failure (see Figures 3 and 4). The effect of boron, another interstitial alloying element, also was studied. This study was performed with a boron-treated steel, SAE 86B35, heat treated to the 230,000-psi strength level. The results of static loading during continuous cathodic charging with hydrogen at 10 ma/in.<sup>2</sup> are compared with similar data for SAE 4340 in the following tabulation:

<u>Applied Stress, psi</u>	<u>Rupture Time, minutes</u>	
	<u>SAE 86B35</u>	<u>SAE 4340</u>
100,000	15	10
50,000	32	30
40,000	63.5	40
30,000	120	~120(a)

(a) By interpolation.

The addition of boron appeared to have no appreciable effect on the time for failure to occur in this stress range. A brief study of the effect of substitutional alloying elements was made by comparing three steels with the same nominal carbon content and all heat treated to approximately 270,000-psi ultimate tensile strength. The steels were SAE 4340 (Cr-Ni-Mo), SAE 4140 (Cr-Mo), and SAE 1040 (plain carbon). The data from these experiments are shown in Figure 5. The failure times were about the same for the SAE 4140 and 4340 steels. The SAE 1040 steel had shorter delay times than did the other two steels, but it was approximately 2 points Rockwell C higher in hardness, which would tend to give shorter times.

Gasior and Prajsnar<sup>(13)</sup> studied the delayed failure of three plain-carbon steels that differed in carbon content. The steels were studied in the as-quenched condition

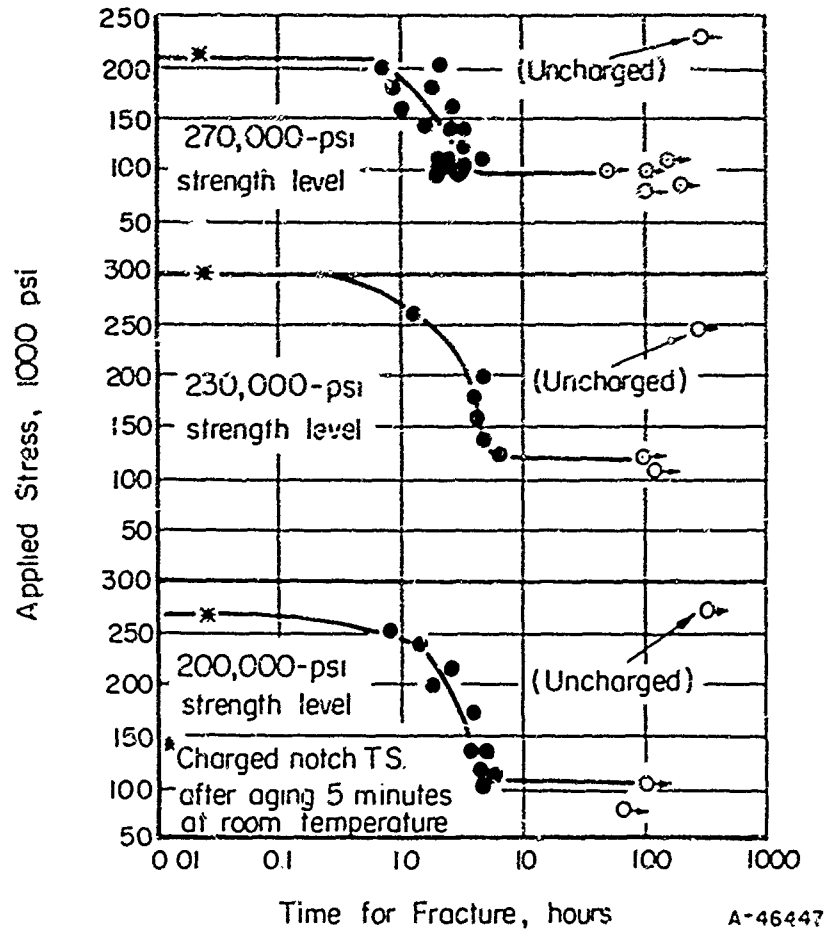


FIGURE 1. DELAYED-FAILURE TESTS ON SAE-AISI 4340 STEEL HEAT TREATED TO SEVERAL STRENGTH LEVELS, SHOWING THE EFFECT OF HYDROGEN<sup>(5)</sup>

Fixed charging conditions, aged 5 minutes, sharp-notch specimens.

Case Institute of Technology Charging Condition A:

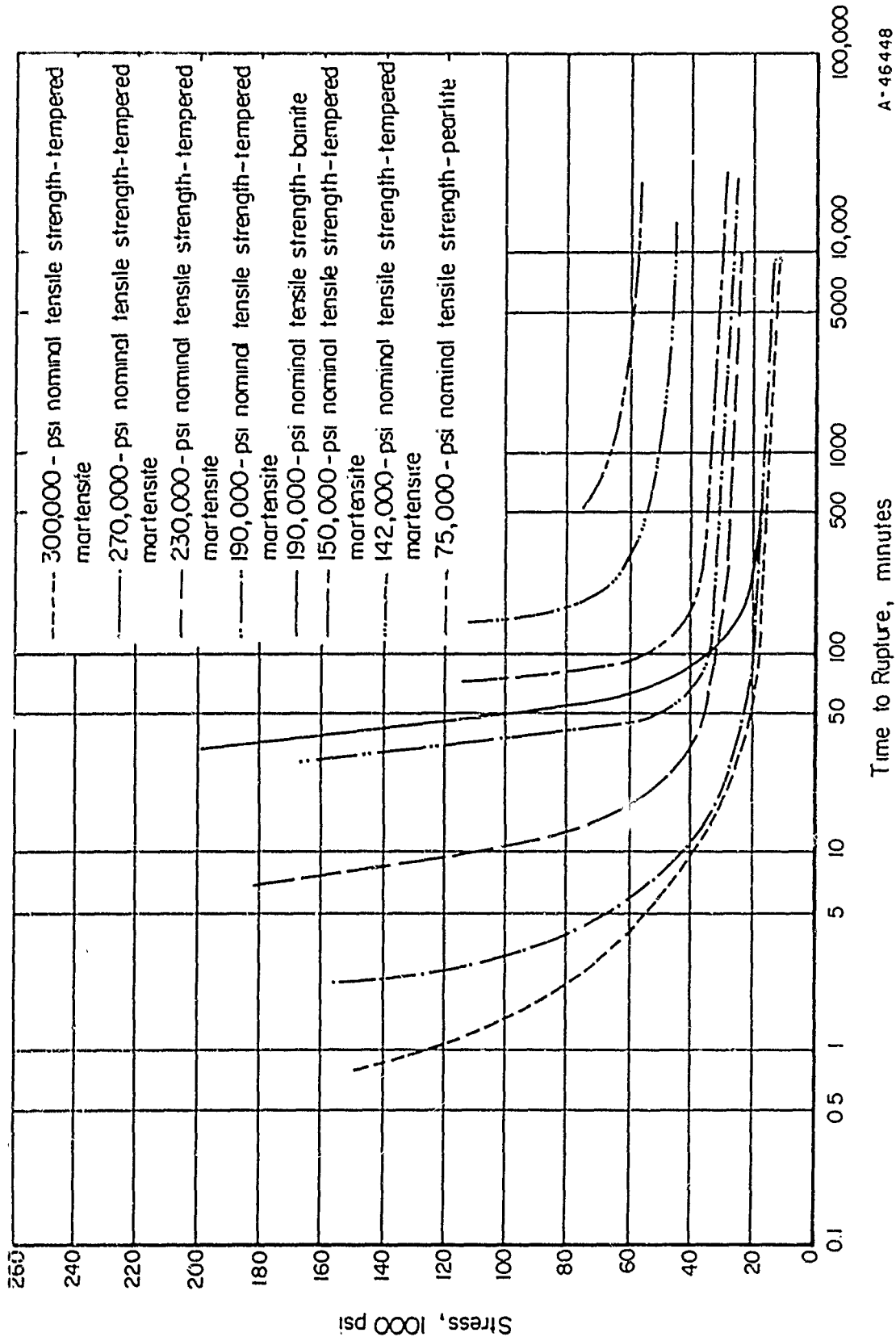
Electrolyte: 4 per cent  $H_2SO_4$  in water

Poison: None

Current density: 20 ma/in.<sup>2</sup>

Charging time: 5 minutes

Aging time: Measured from end of charging to start of test.



A-46448

FIGURE 2. DELAYED-FAILURE CHARACTERISTICS OF UNNOTCHED SPECIMENS OF AN SAE 4340 STEEL DURING CATHODIC CHARGING WITH HYDROGEN UNDER STANDARDIZED CONDITIONS(8)

Battelle Charging Condition A:

Electrolyte: 4 per cent by weight of H<sub>2</sub>SO<sub>4</sub> in water

Poison: 5 drops per liter of cathodic poison composed of  
 2 g phosphorus dissolved in 40 ml CS<sub>2</sub>

Current density: 8 ma/in.<sup>2</sup>

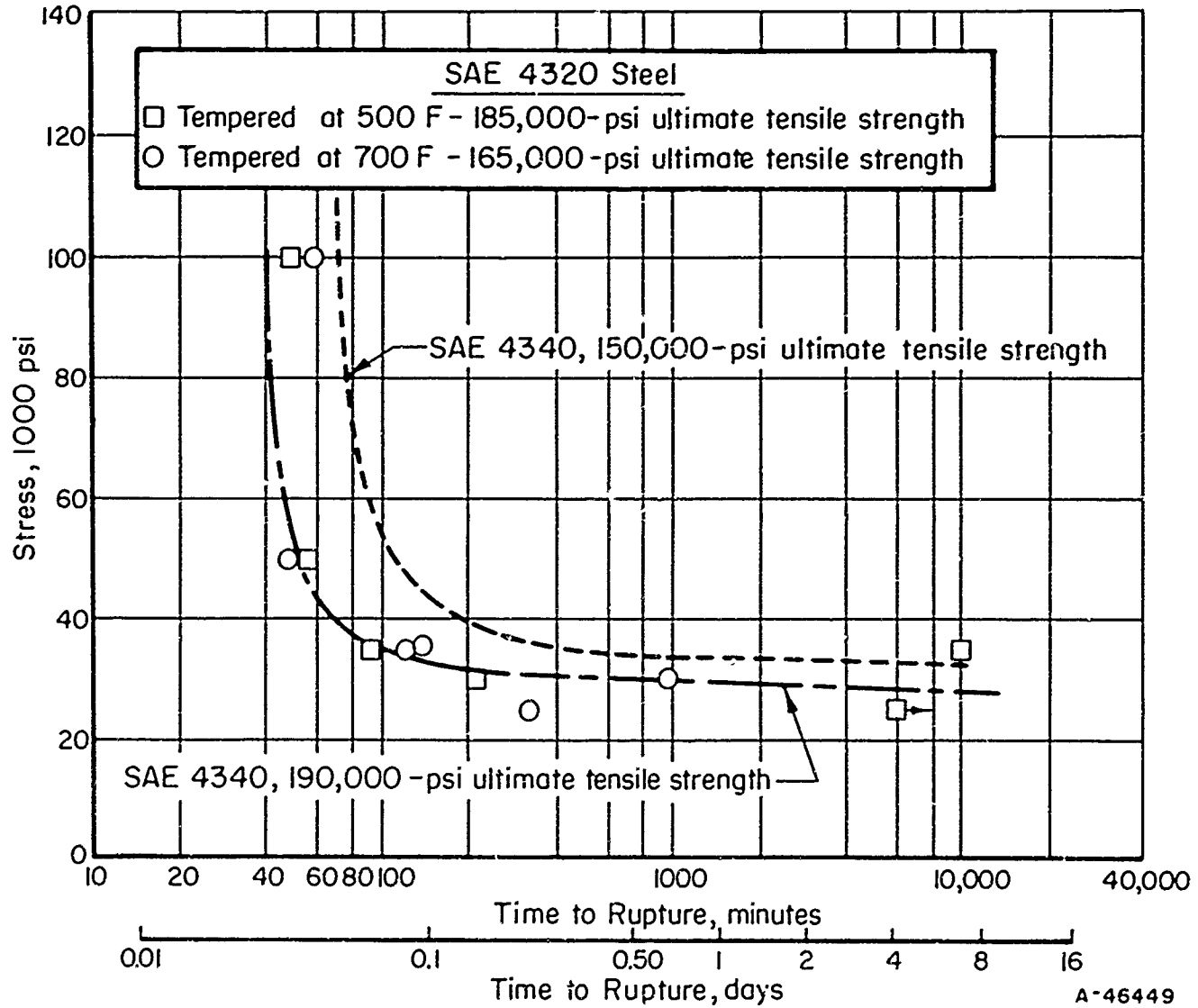


FIGURE 3. DELAYED-FAILURE CHARACTERISTICS OF AN SAE 4320 STEEL DURING CATHODIC CHARGING UNDER STANDARDIZED CONDITIONS<sup>(8)</sup>

Lines representing characteristics of SAE 4340 steel have been added for comparison. Battelle Charging Condition A, as given in Figure 2.

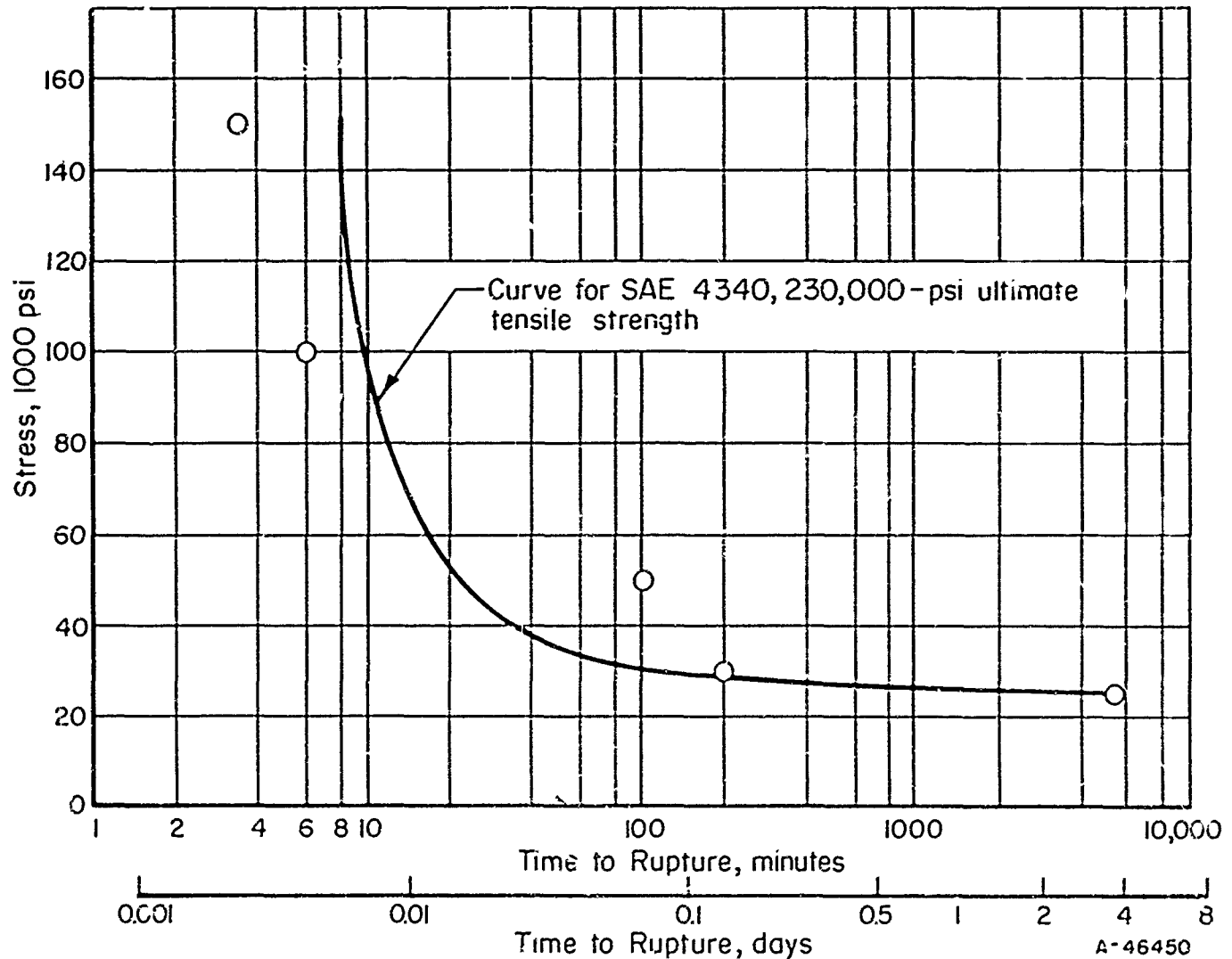


FIGURE 4. DELAYED-FAILURE CHARACTERISTICS, DURING CATHODIC CHARGING UNDER STANDARDIZED CONDITIONS, OF A HIGH-CARBON STEEL (about 0.95% C) HEAT TREATED TO HAVE AN ULTIMAT. TENSILE STRENGTH OF 230,000 PSI<sup>(8)</sup>

The characteristics of SAE 4340 steel at the same tensile strength have been added for comparison.

Battelle Charging Condition A, as given in Figure 2.



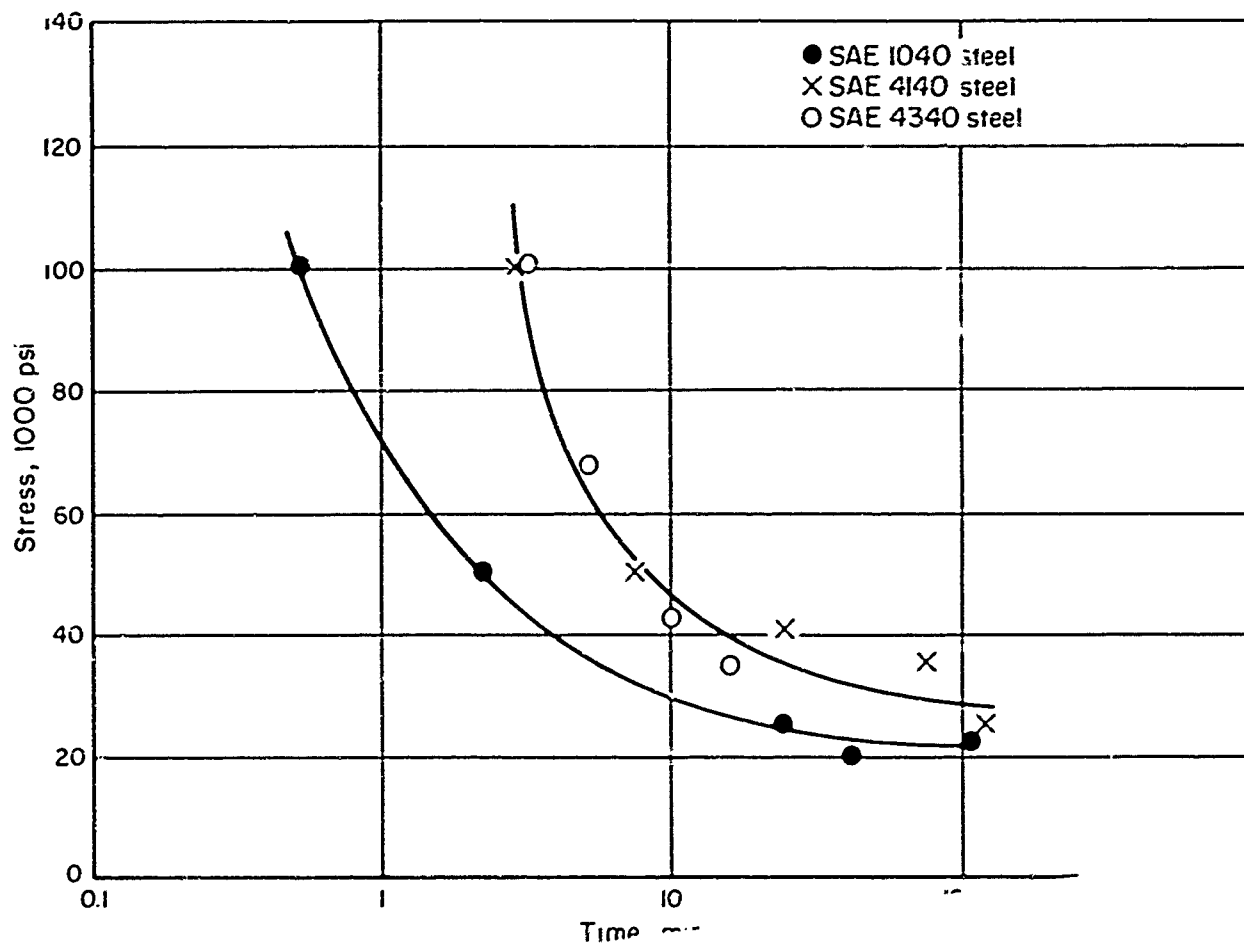


FIGURE 5. FAILURE TIME AS A FUNCTION OF APPLIED STRESS FOR SAE 1040, 4140, AND 4340 STEELS HEAT TREATED TO APPROXIMATELY 270,000-PSI ULTIMATE TENSILE STRENGTH<sup>(9)</sup>

Charging Conditions:

Electrolyte: 4 weight per cent  $H_2SO_4$  in water  
 Poison: 5 drops per liter of cathodic poison  
 composed of 2 g phosphorus  
 dissolved in 40 ml  $CS_2$   
 Current density: 10 ma/in.<sup>2</sup>

and after tempering at various temperatures up to 450 C (840 F). The results, shown in Figure 6, indicate that, the higher the carbon content, the greater is the susceptibility of steel to hydrogen-induced, delayed, brittle failure. However, the comparisons were made on the basis of constant tempering temperature, and constant tempering temperature does not provide constant tensile strength for steels of different carbon content. The steels of higher carbon content would tend to be stronger for a given tempering temperature. The observations of some other workers confirm this finding for plain-carbon steels. However, the work of Elsea's group cited above indicated that a considerable change in carbon content in alloy steels had little effect on delayed, brittle failure, when the steels were compared at about the same tensile strength. In addition to the different bases of comparison, differences in the test methods used may have contributed to the apparent difference in the results of these two investigations.

Troiano and co-workers studied the delayed-failure characteristics of 12 heats of SAE 4340 steel at strength levels of 230,000 and 270,000 psi<sup>(15)</sup>. They used notched specimens precharged with hydrogen. All twelve heats exhibited delayed, brittle failure over a substantial range of applied stress at both strength levels. The lower critical stress for failure was independent of strength level and chemical composition, while the failure time increased linearly with increasing notched tensile strength of charged specimens. The failure time and the notched tensile strength as charged decreased somewhat with increasing amounts of phosphorus plus sulfur. For a given strength level, the ductility of uncharged, smooth specimens decreased with increasing amounts of phosphorus plus sulfur and with increasing carbon content. Traces of the delayed-failure curves obtained are shown in Figure 7.

Blanchard and Troiano<sup>(16)</sup> studied the delayed-failure and notched tensile properties of a vacuum-melted SAE 4340 steel. The notched ductility and notched tensile strength were increased by vacuum melting, and the susceptibility to delayed failure was reduced.

Rinebolt<sup>(12)</sup> and Raring and Rinebolt<sup>(17, 18)</sup> compared the delayed-failure behavior of AISI 4340 steel melted in a vacuum, in argon, and in air. Analyses showed that vacuum and argon melting markedly lowered the oxygen content of this steel compared with that of air-melted steel, but the hydrogen and nitrogen contents were not lowered appreciably. The three materials were heat treated to strengths in the range from 150,000 to 287,000 psi. Delayed fractures did not occur below 97 per cent of the notched tensile strength at the 230,000-psi strength level when the specimens were not charged electrolytically or cadmium plated. Cadmium plating resulted in delayed fractures at stress levels as low as 50 per cent of the notched tensile strength. Cathodic charging with hydrogen resulted in delayed failures at stresses as low as 16 per cent of the notched tensile strength of the uncharged materials. However, melting in a vacuum or in an argon atmosphere had no significant effect on resistance to delayed, brittle fracture as compared with that of air-melted steel. Evidently, the difference in oxygen content among the steels had no substantial influence on the susceptibility to hydrogen-induced, delayed, brittle failure. Values of reduction in area and elongation obtained in short-time tests of unnotched specimens decreased to less than 1 per cent after relatively short charging times.

Because the usual low-temperature baking treatment used to minimize hydrogen embrittlement in high-strength steel generally is not adequate to eliminate harmful hydrogen completely, Klier, Muvdi, and Sachs<sup>(19, 20)</sup> evaluated seven different high-strength steels for susceptibility to delayed failure in the sustained-load test. The

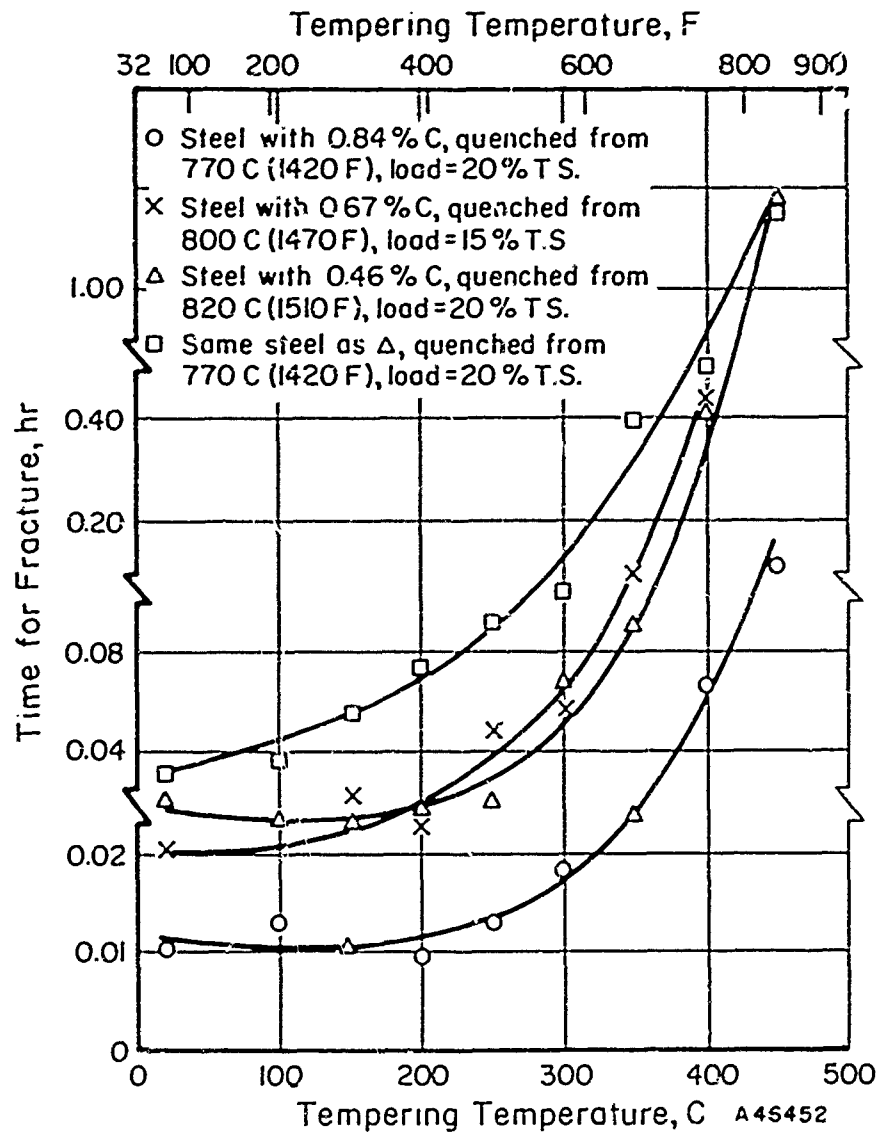


FIGURE 6. TIME FOR FRACTURE VS. TEMPERING TEMPERATURE FOR DIFFERENT CARBON STEELS CHARGED CATHODICALLY WITH HYDROGEN (AFTER GASIOR AND PRAJSNAR)<sup>(14)</sup>

Note the three breaks in the vertical time scale.

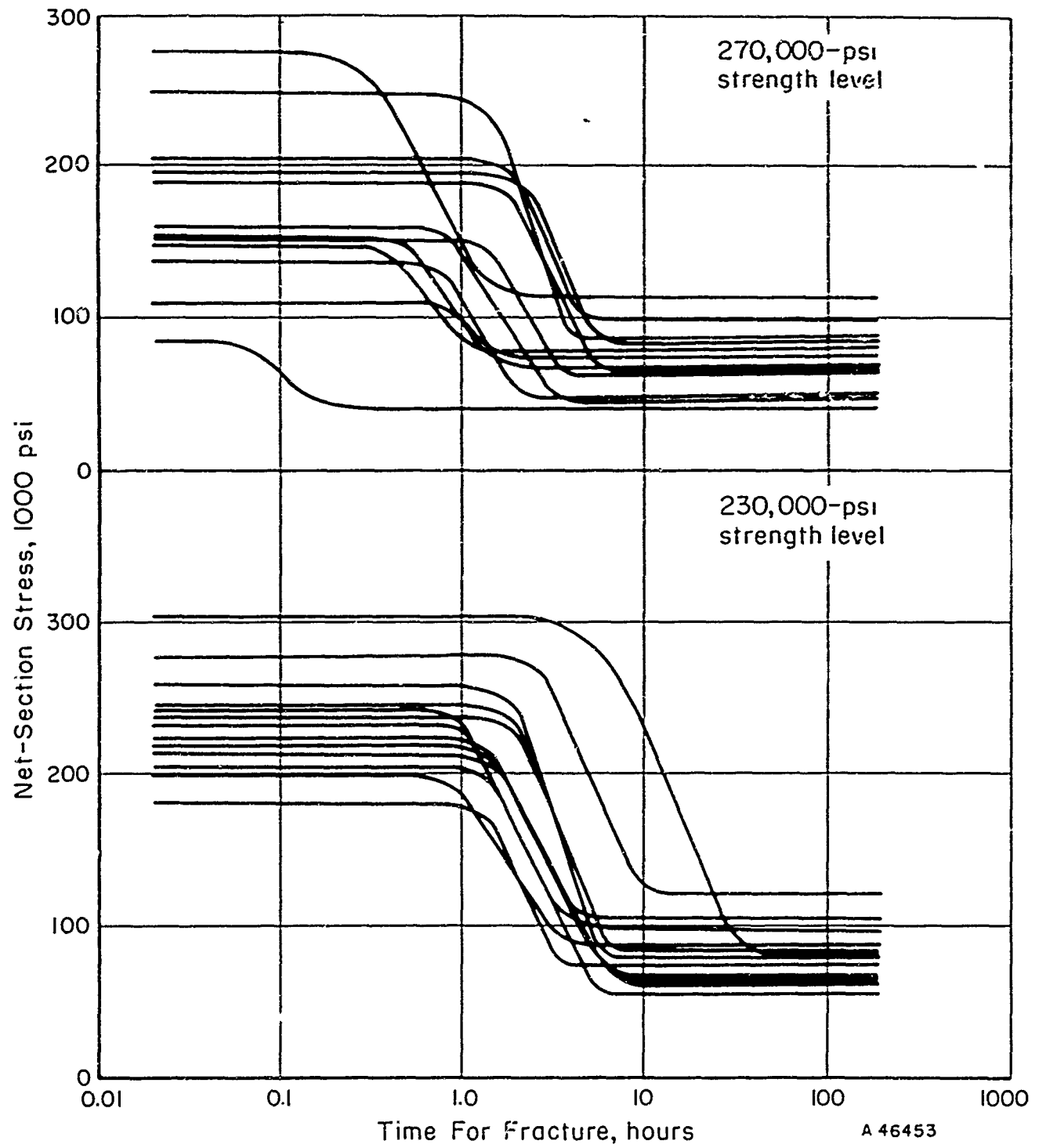


FIGURE 7. DELAYED-FAILURE BEHAVIOR FOR TWELVE HEATS OF SAE 4340 STEEL; NOTCHED SPECIMENS PRECHARGED WITH HYDROGEN(15)

seven materials studied, the heat treatments used, and the resulting strength levels are listed in Tables 1 and 2. Both smooth (unnotched) and notched ( $K_t = 2$  to 10) specimens were used. Hydrogen was introduced into the steel during cadmium electroplating at 200  $\text{mA}/\text{in.}^2$ . By a suitable adjustment of the applied load, specimens of all seven steels including all strength levels examined could be made to fail, with a time delay, under sustained load as the result of hydrogen introduced by cadmium electroplating. Curves of applied stress versus time to failure were presented for each steel and each strength level studied, see Figure 8 for SAE 4340 as an example. From these curves, the rupture strength corresponding to a failure time of 100 hours was determined. This value has been plotted versus tensile strength for four of the steels in Figure 9. From their results, they concluded that the susceptibility of a steel to failure under sustained load after cadmium plating depends on the severity of the notch and on the metallurgical structure of the steel. They found that the silicon-modified steels studied were more resistant to hydrogen embrittlement at intermediate tempering temperatures than were the low-silicon steels. Also, the lower critical stress was higher for the high-silicon steels than for low-silicon steels for the intermediate tempering temperatures. An example of the general behavior of the silicon-rich steels is that exhibited by Hy-Tuf, shown in Figure 10. Although all the steels studied could be made to fail under sustained load after cadmium plating, two steels possessed relatively high resistance to delayed failure at strength levels as high as 270,000 psi when hydrogen was introduced in this manner. Hy-Tuf at a strength level of 230,000 psi showed only slight embrittlement under the cadmium-plating conditions used, as is shown in Figures 10 and 11. UHS-250 also was less sensitive to the embrittling action of electrodeposited hydrogen than were the low-silicon steels. Thus, these results suggest that steels with high silicon contents offer some advantage.

Srawley<sup>(21)</sup> tested a wide variety of steels to obtain more extensive comparative data on the susceptibility to hydrogen embrittlement. He also tested a selection of non-ferrous alloys. The emphasis was on delayed fracture under constant sustained load. The specimens were severely cathodically charged with hydrogen (24 hours at 0.5 amp/ $\text{in.}^2$ ) so that even a slight degree of susceptibility to embrittlement of any of the alloys might be detected. The compositions and conditions of the materials used are given in Tables 3 and 4.

To compare a variety of materials, a convenient index of the susceptibility to hydrogen embrittlement is the ratio of the lower critical stress for failure to the notched tensile strength of the uncharged material. This ratio, which Srawley called the "static-fatigue ratio", will have a low value for materials that are highly susceptible to hydrogen-induced, delayed, brittle failure and will approach a value of 1.00 as the susceptibility becomes negligible. In Srawley's work, the small number of specimens available per material allowed only the determination of the limits between which the static-fatigue ratio should lie. The upper limit, called the failure-stress ratio, was defined as the ratio of the lowest nominal stress at which a specimen failed (within 100 hours) to the notched tensile strength of the uncharged material, the lower limit, called the survival-stress ratio, was defined as the ratio of the highest stress at which a specimen survived (for 100 hours or more) to the notched tensile strength of the uncharged material. These ratios are given in Table 5, along with the properties of the uncharged specimens and the time to failure of the specimen which failed at the lowest nominal stress, i. e., the time corresponding to the failure-stress ratio. In several cases, a specimen fractured while being loaded to the intended stress, so the remark "load increasing" is used in place of the time to failure. In six cases, specimens of relatively soft material which had survived 100 hours or more under load were found to

TABLE 1. CHEMICAL COMPOSITION OF STEELS USED IN A STUDY OF THE EFFECT OF STEEL COMPOSITION ON SUSCEPTIBILITY TO HYDROGEN-INDUCED, DELAYED, BRITTLE FAILURE<sup>(19)</sup>

Steel	Size and Shape	Composition, per cent									
		C	Mn	P	S	Si	Ni	Cr	Mo	V	Cu
4340	4-1/4-in. round	0.41	0.79	0.013	0.016	0.31	1.83	0.77	0.23	--	--
4330 (vanadium modified)	3-1/2-in. round	0.32	0.82	0.010	0.021	0.28	1.82	0.85	0.41	0.07	--
98B40	4-1/2-in. round	0.46	0.80	0.019	0.022	0.41	0.88	0.79	0.20	--	--
Tricent (Inco)	4-1/4-in. square	0.39	0.74	0.014	0.014	1.54	1.83	0.83	0.38	0.07	--
Crucible UHS-260	4-in. square	0.35	1.20	0.023	0.017	1.62	--	1.26	0.32	0.20	--
Hy-Tuf	4-1/2-in. round	0.25	1.30	0.022	0.018	1.47	1.75	0.38	0.37	--	--
Super TM-2	3-in. round	0.41	0.72	0.012	0.014	0.61	2.98	1.15	0.44	--	0.14

TABLE 2. HEAT TREATMENTS AND STRENGTH LEVELS USED FOR THE VARIOUS STEELS LISTED IN TABLE 1<sup>(19)</sup>

Steel	Austenitizing Temperature, F	Tempering Temperature (Strength Level, psi)				
		400 F	500 F	700 F	800 F	1000 F
4340	1525	400 F (275,000)	500 F (270,000)	700 F (235,000)	800 F (215,000)	1000 F (185,000)
4330 (vanadium modified)	1600	250 F (265,000)	500 F (235,000)	750 F (210,000)	1000 F (180,000)	
98B40	1550	400 F (300,000)	575 F (270,000)	700 F (230,000)	800 F (205,000)	900 F (195,000)
Tricent (Inco)	1600	400 F (295,000)	550 F (275,000)	700 F (270,000)		
Crucible UHS-260	1700	500 F (270,000)	800 F			
Hy-Tuf	1575	700 F (230,000)	(250,000)			
Super TM-2	1600	500 F (275,000)				

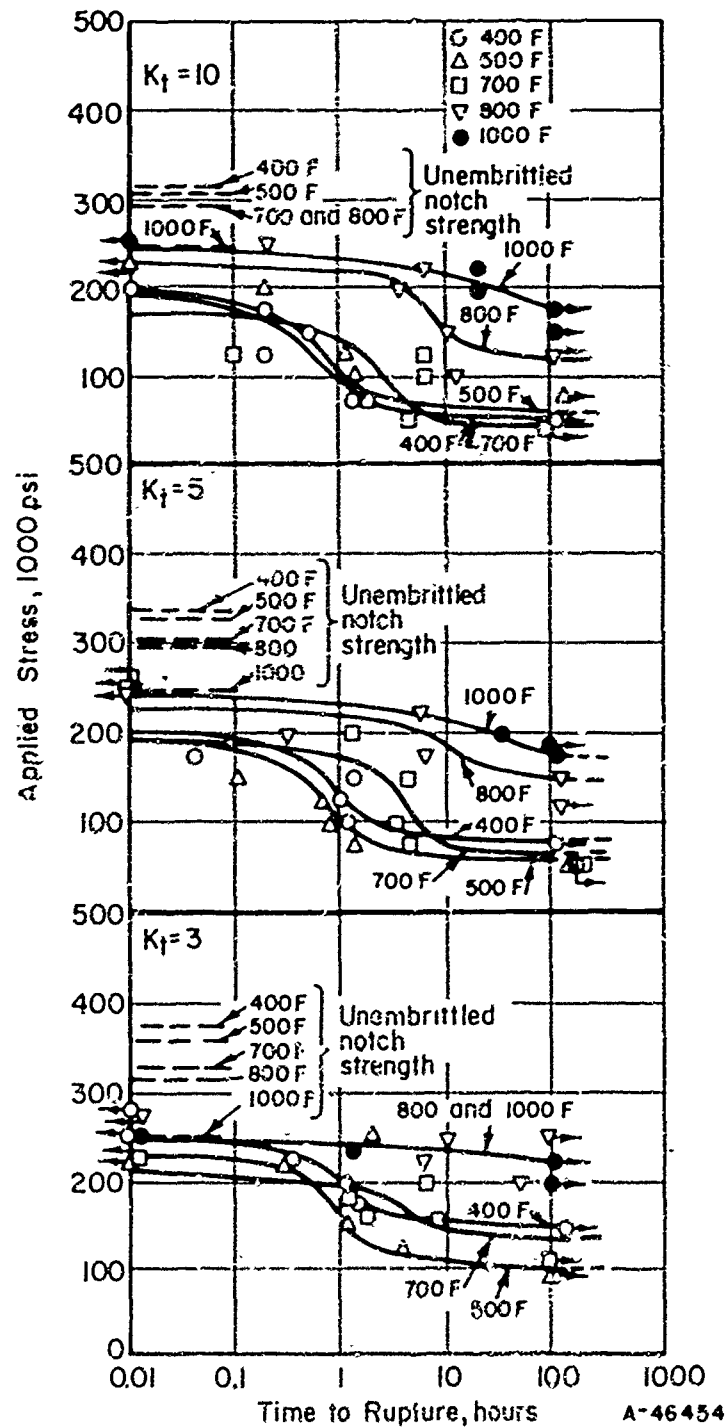


FIGURE 8. PLOTS OF APPLIED STRESS VERSUS TIME TO RUPTURE FOR CADMIUM-PLATED SAE 4340 STEEL TEMPERED AS INDICATED, FOR VARIOUS STRESS CONCENTRATIONS<sup>(19)</sup>

Austenitized at 1525 F, oil quenched.

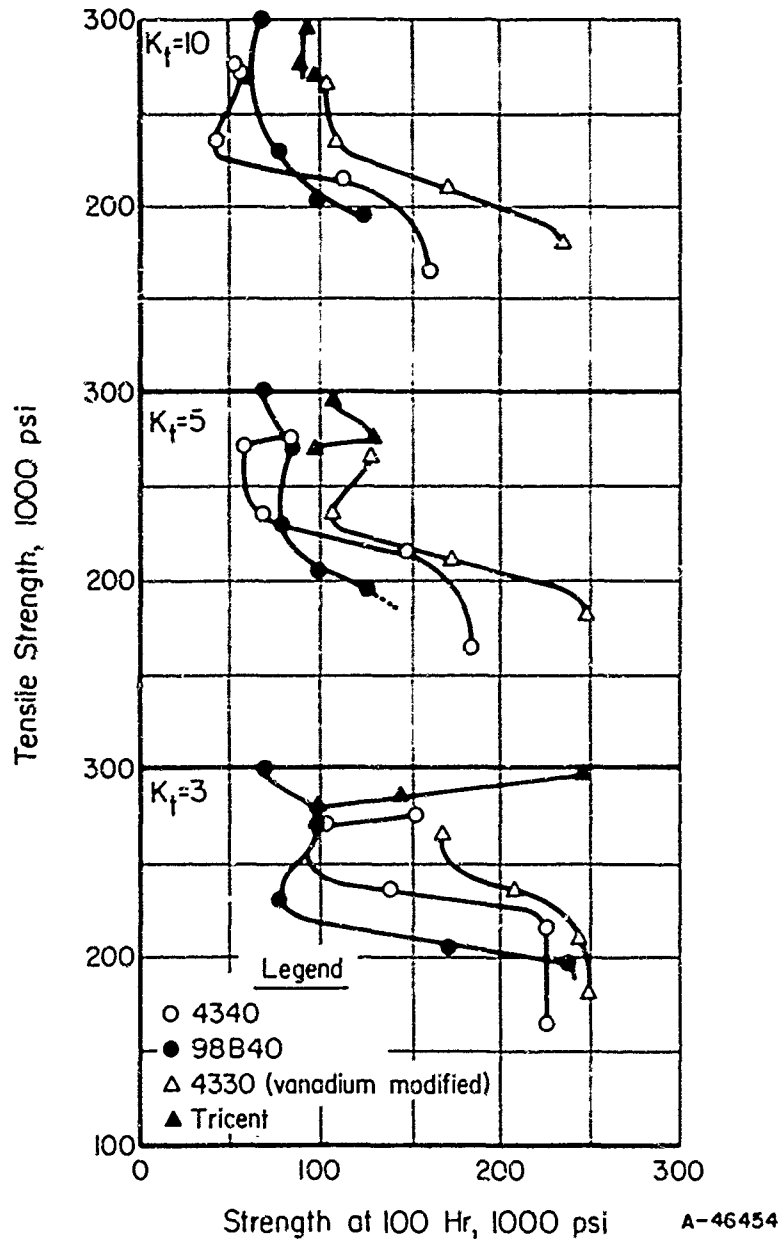


FIGURE 9. PLOT OF THE STRESS WHICH RESULTED IN FAILURE IN EXACTLY 100 HR VERSUS TENSILE STRENGTH FOR THE INDICATED STEELS WITH STRESS CONCENTRATIONS SHOWN(19)



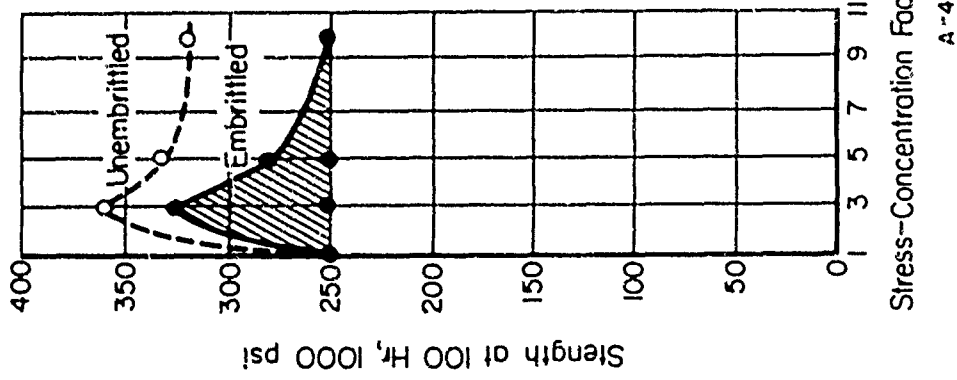


FIGURE 11. THE FRACTURE STRENGTH AT 100 HOURS VERSUS STRESS CONCENTRATION FOR CADMIUM-PLATED HY-TUF STEEL TEMPERED AT 700 F(19)

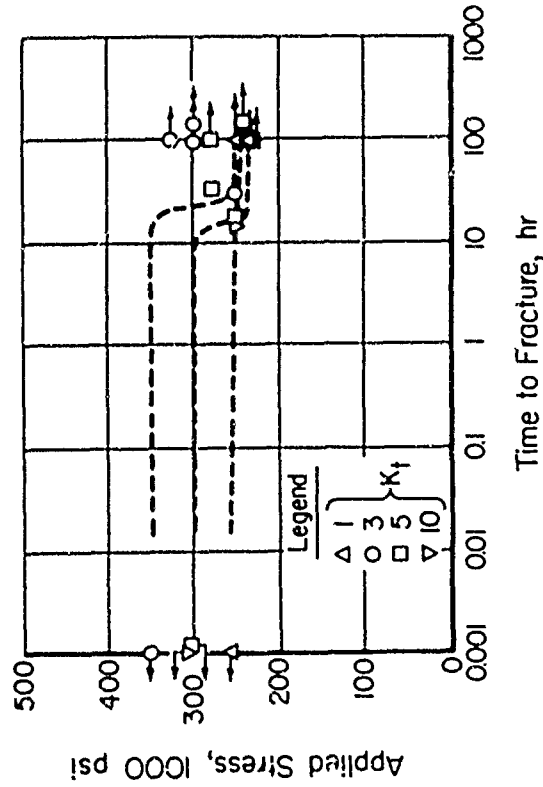


FIGURE 10. PLOT OF STRESS VERSUS TIME TO FRACTURE AT INDICATED STRESS CONCENTRATION FOR CADMIUM-PLATED HY-TUF STEEL TEMPERED AT 700 F(19)

$K_t$  = stress-concentration factor of the notch. Austenitized for 2 hours at 1575 F, oil quenched, and tempered at 700 F.

A-46455

TABLE 3. COMPOSITIONS OF MATERIALS USED IN A COMPARATIVE STUDY OF SUSCEPTIBILITY TO DELAYED, BRITTLE FAILURE<sup>(21)</sup>

Material	Composition, weight per cent
AISI 52100 steel	(Nominal: 1.00 C, 0.35 Mn, 0.3 Si, 1.45 Cr)
AISI 4340 steel	0.41 C, 0.73 Mn, 0.30 Si, 1.82 Ni, 0.76 Cr, 0.28 Mo, 0.009 P, 0.016 S
AISI 4130 steel	0.32 C, 0.45 Mn, 0.26 Si, 0.93 Cr, 0.23 Mo, 0.007 P, 0.020 S
AISI 1020 steel	0.20 C, 0.76 Mn, 0.013 P, 0.027 S
Armco iron	(Nominal: 0.01 C, 0.02 Mn, 0.005 P, 0.025 S)
Malleable cast iron	2.51 C, 0.40 Mn, 1.35 Si, 0.058 P, 0.131 S
AISI 422 steel (modified)	0.23 C, 0.50 Mn, 0.50 Si, 12.40 Cr, 0.50 Mo, 0.31 V, 0.020 P, 0.013 S
PH Steel W	0.07 C, 0.50 Mn, 16.75 Cr, 6.75 Ni, 0.80 Ti, 0.20 Al
PH Steel A	0.07 C, 0.71 Mn, 0.30 Si, 17.07 Cr, 7.24 Ni, 1.18 Al, 0.017 P, 0.006 S
PH Steel B	0.038 C, 0.36 Mn, 0.52 Si, 16.02 Cr, 4.25 Ni, 3.47 Cu, 0.32 Ch, 0.018 P, 0.008 S
Austenitic Steel T	0.09 C, 14.90 Mn, 0.51 Si, 18.12 Cr, 0.022 P, 0.012 S, 0.50 N
AISI 410 steel	0.11 C, 0.55 Mn, 0.32 Si, 11.6 Cr, 0.26 Ni, 0.11 Mo, 0.07 Cu
AISI 304 steel	(Nominal: 0.08 max. C, 2.00 max. Mn, 1.00 max. Si, 18.0-20.0 Cr, 8.0-11.0 Ni)
K Monel	66.4 Ni, 28.9 Cu, 0.9 Fe, 0.55 Mn, 0.19 Si, 0.15 C, 2.90 Al
Monel	66.9 Ni, 30.4 Cu, 1.33 Fe, 0.88 Mn, 0.30 Si, 0.16 C
Inconel	75.6 Ni, 17.4 Cr, 6.5 Fe, 0.04 C, 0.25 Mn, 0.34 Si, 0.02 Cu
Copper Beryllium No. 25	(Nominal: 1.80-2.05 Be, 0.25-0.35 Co)
Bronze	94.9 Cu, 4.8 Sn, 0.04 Zn, 0.15 P, 0.04 Fe, 0.04 Pb
Manganese bronze	(Nominal: 57-60 Cu, 0.8-2.0 Fe, 0.50-1.50 Sn, 0.50 max. Mn)
Aluminum bronze	95.19 Cu, 4.66 Al
Beta brass	52.1 Cu, 47.9 Zn, 0.026 Pb
7075 aluminum alloy	(Nominal: 5.1-6.1 Zn, 2.1-2.9 Mg, 0.18-0.40 Cr)

TABLE 4. CONDITIONS OF MATERIALS TESTED IN A COMPARATIVE STUDY OF SUSCEPTIBILITY TO DELAYED, BRITTLE FAILURE<sup>(21)</sup>

Material	Condition
AISI 52100 steel	Oil quenched from 1550 F (1/2 hr), then tempered as indicated <sup>(a)</sup>
AISI 4340 steel	Oil quenched from 1550 F (1/2 hr), then tempered as indicated <sup>(a)</sup>
AISI 4130 steel	Oil quenched from 1550 F (1/2 hr), then tempered as indicated <sup>(a)</sup>
AISI 1020 steel	Water quenched from 1650 F (1/2 hr), then tempered as indicated <sup>(a)</sup>
Armco iron	Annealed (as received)
Malleable cast iron	Oil quenched from 1500 F (20 min), then tempered at 500 F for 3 hr and water quenched
AISI 422 steel (modified)	Oil quenched from 1850 F (1/2 hr), then tempered as indicated <sup>(a)</sup>
PH Steel W	Received in solution-treated condition, then aged 2 hr at 950 F and air cooled
PH Steel A	Received in solution-annealed condition
RH950	Air cooled from 1750 F (1/2 hr), refrigerated for 16 hr at -100 F, aged at 950 F for 1 hr and air cooled
TH1050	Air cooled from 1450 F (1-1/2 hr), aged 1050 F for 1-1/2 hr and air cooled
PH Steel B	Received in solution-annealed condition
H875	Air cooled from 875 F (1 hr)
Austenitic Steel T	Cold rolled to 30 per cent reduction of area after forging and water quenching from 2000 F (1/2 hr)
AISI 410 Steel	Oil quenched from 1700 F (1 hr), then tempered as indicated <sup>(a)</sup>
AISI 304 Steel	Cold rolled to 46 per cent reduction of area
K Monel	As received (hot rolled)
Monel	As received (hot rolled)
Inconel	As received (hot rolled)
Copper Beryllium No. 25	Received in solution-annealed condition, aged at 600 F for 18 hr and air cooled
Bronze	As received (hot rolled)
Manganese bronze	As received
Aluminum bronze	As received
Beta brass	Air cooled from 1000 F (2 hr) after hot forging to size
7075 aluminum alloy	As received (stress relieved and aged)

(a) See Table 5.

TABLE 5. HARDNESS, ULTIMATE, AND NOTCHED TENSILE STRENGTHS, AND RESULTS OF DELAYED-FAILURE TESTS<sup>(1)</sup>

Material	Condition <sup>(2)</sup>	Uncharged Properties				Hydrogen-Charged Specimens			
		Rockwell Hardness Number	Ultimate	Notched	NTS LTS	Number of Specimens Tested	Survival Stress Ratio, 100 hr	Failure- Stress Ratio, minimum	Time to Failure
			Tensile Strength, 1000 psi	Tensile Strength, 1000 psi					
AISI 52100 steel	T300/1	C-64	--	86.8	--	2	--	0.14	15 sec
	T760/1	C-54	(180)	176.5	(0.63)	3	--	0.15	Load increasing
AISI 4340 steel	T380/1	C-52	298.0	324.0	1.09	5	0.07	0.08	Load increasing
	T600/1	C-46	230.0	288.0	1.25	5	0.10	0.12	Load increasing
	T800/1	C-45	217.5	306.0	1.37	5	0.14	0.16	20 sec
	T1000/1	C-38	178.5	272.0	1.52	4	0.18	0.19	30 sec
	T1100/1	C-35	166.0	252.0	1.51	5	0.25	0.23	5 sec
	T1200/1	C-29	146.0	222.0	1.51	5	0.49	0.54	2 sec
	T1275/1	C-26	132.8	200.0	1.51	5	0.59	0.69	14 min
AISI 4130 steel	T400/1	C-51	(245.0)	273.5	(1.11)	5	0.20	0.23	10 sec
	T600/1	C-48	(225.0)	314.0	(1.39)	2	--	0.22	Load increasing
	T800/1	C-43	(200.0)	276.0	(1.38)	4	0.17	0.18	6 min
	T900/1	C-39	183.5	270.0	1.47	4	0.18	0.19	1 min
	T1000/1	C-35	(160.0)	246.0	(1.53)	4	0.38	0.46	5 sec
	T1100/1	C-30	146.0	227.0	1.55	5	0.35	0.38	30 sec
	T1200/1	C-26	(125.0)	189.0	(1.51)	3	0.80 <sup>(b)</sup>	0.90	7 min
	T1300/1	C-21	118.5	182.0	1.53	5	0.87 <sup>(b)</sup>	0.92	Load increasing <sup>(c)</sup>
AISI 1020 steel	T380/1	C-33	(150.0)	157.0	1.05	4	0.82	0.87	30 sec
Armco iron	Annealed	B-41	44.3	62.2	1.40	2	0.72 <sup>(b)</sup>	0.80	Load increasing <sup>(c)</sup>
Malleable cast iron	T500/3	C-34	129.5	109.0	0.84	6	0.26	0.31	3 min
AISI 422 steel (modified)	T400/4	C-51	262.5	322.0	1.23	5	0.22	0.25	Load increasing
	T900/4	C-51	270.5	185.0	0.68	4	0.33	0.35	Load increasing
	T1050/1	C-45	219.5	322.0	1.46	5	0.18	0.21	108 hr
	T1050/2	C-42	198.8	302.0	1.52	5	0.20	0.25	60 hr
	T1050/4	C-41	157.0	235.0	1.52	4	0.30	0.32	60 hr
	T1100/4	C-42	208.5	307.0	1.47	4	0.22	0.24	27 hr
PH Steel W	T950/2	C-46	209.0	320.0	0.44	4	0.33	0.35	Load increasing
PH Steel A	RH950	C-46	223.0	223.0	1.00	4	0.16	0.27	10 hr
	TH1050	C-40	182.0	256.0	1.40	3	--	0.42	4 hr
PH Steel B	H875	C-42	198.0	320.0	1.62	4	0.18	0.19	1 min
Austenitic Steel T	30% cold rolled	C-42	193.8	313.0	1.61	4	0.89	0.94	6 hr
AISI 410 steel	T400/2	C-41	201.0	310.0	1.54	5	0.22	0.24	4 min
	T500/2	C-40.5	192.5	302.0	1.57	4	0.15	0.16	6 hr
	T600/2	C-40	190.0	300.0	1.58	4	0.29	0.34	10 sec
	T700/2	C-41	197.0	310.0	1.57	4	0.10	0.13	1 min
	T825/2	C-42	193.0	301.5	1.56	5	0.11	0.12	1 min
	T950/2	C-40	196.0	306.0	1.56	5	0.19	0.20	10 sec
	T1000/2	C-35	172.0	274.0	1.59	4	0.18	0.20	4 hr
	T1030/2	C-28	(150.0)	242.0	1.61	2	0.22	0.27	Load increasing
	T1050/2	C-27	139.0	224.0	1.61	5	0.40	0.47	4 min
	T1100/2	C-24	121.0	194.0	1.60	4	0.37	0.44	1 min
	T1200/2	C-21	116.0	187.0	1.61	4	0.38	0.50	39 min

TABLE 5. (Continued)

Material	Condition <sup>(a)</sup>	Uncharged Properties				Hydrogen-Charged Specimens			
		Rockwell Hardness Number	Ultimate Tensile Strength, 1000 psi	Notched Tensile Strength, 1000 psi	NTS UTS	Number of Specimens Tested	Survival- Stress Ratio, 160 hr	Failure- Stress Ratio, minimum	Time to Failure
AISI 304 steel	46% cold rolled	C-28	131.0	203.0	1.55	5	1.00	1.00	Load increasing <sup>(c)</sup>
K Monel	As rec'd.	C-28.5	139.0	220.0	1.58	4	0.93 <sup>(b)</sup>	0.98	Load increasing <sup>(c)</sup>
Monel	As rec'd.	C-24.5	116.0	185.0	1.59	6	0.86 <sup>(b)</sup>	0.95	Load increasing <sup>(c)</sup>
Inconel	As rec'd.	B-72	88.3	115.0	1.31	3	0.79 <sup>(b)</sup>	0.99	Load increasing <sup>(c)</sup>
Copper Beryllium No. 25	600/18	C-41	(185.0)	130.0	(0.70)	4	0.97	1.02	Load increasing <sup>(c)</sup>
Bronze	As rec'd.	B-92	--	135.5	--	4	0.95	1.00	Load increasing <sup>(c)</sup>
Manganese Bronze	As rec'd.	B-96	131.0	156.0	1.19	4	0.90	0.95	49 hr
Aluminum Bronze	As rec'd.	B-81	83.4	106.0	1.27	4	0.95	1.00	Load increasing <sup>(c)</sup>
Beta brass	1000/2	E-84	60.0	75.6	1.26	4	0.61	0.66	20 hr <sup>(d)</sup>
7075 aluminum alloy	As rec'd. (aged)	B-88	80.0	101.5	1.27	4	0.97	1.02	Load increasing <sup>(c)</sup>

(a) The values given are for tempering temperature and time; for instance, T600/1 indicates that a material was tempered for 1 hour at 600 F after the hardening treatment given in Table 4.

(b) Crack detected at notch root after unloading, although load had been sustained for at least 100 hours without fracture.

(c) Lowest stress for fracture was that obtained in the continuous-loading notched tensile test of the charged material.

(d) Delayed fracture of specimens not charged with hydrogen also occurred.

have cracks at the notch roots. These specimens are marked in the table. Apparently, these cracks did not propagate to failure because there was sufficient associated plastic deformation at the notch roots to cause appreciable relaxation of the stress applied by the elastic-ring loading device used.

All the steels harder than Rockwell C 30 were found to be very susceptible to hydrogen-induced, delayed, brittle failure, except AISI 1020 and the cold-rolled austenitic Mn-Cr-N Steel T, which had moderate susceptibility. In the case of the austenitic Steel T, the susceptibility was probably due, at least in part, to the formation of some martensite during cold working. The only steel found to have no susceptibility was the cold-rolled Type 304 austenitic stainless steel. The 12 per cent chromium hardenable stainless steels were particularly susceptible, the Type 410 steel retaining its high susceptibility down to a hardness of Rockwell C 21 (ultimate tensile strength of 116,000 psi). The low-alloy steels were less susceptible in the low-hardness range.

None of the nonferrous alloys (including Monel, Inconel, a number of bronzes, and 7075 aluminum) was found to be appreciably susceptible to hydrogen embrittlement. Beta brass was found to be susceptible to delayed fracture under sustained constant load, whether it was charged with hydrogen or not.

The delay time to failure usually was short compared with other published data. This behavior probably was a result of the severe and prolonged charging with hydrogen that was used. The delay time to failure was believed to depend on the time required for hydrogen to diffuse in sufficient quantity to the region of plastic strain around the notch or crack tip; thus, a high concentration of hydrogen throughout the specimens would tend to reduce the delay time.

Geyer et al. (22) studied the susceptibility to delayed failure in sustained-load tests of SAE 4340 and Thermold J, a hot-work die steel of the SAE H-13 type. The effect of cadmium plating from many different baths was evaluated. The steels were heat treated so that the resulting tensile strength was 290,000 and 283,000 psi, and the notched strength was 435,000 and 425,000 psi for SAE 4340 and Thermold J, respectively. Unplated, notched specimens of both steels were stressed 400 hours at 220,000 psi plus 400 hours at 300,000 psi without failure. After plating from the conventional cadmium cyanide bath and baking 3 hours at 375 F, notched specimens of SAE 4340 generally failed in a few hours at 220,000 psi. After plating from the cadmium fluoborate bath containing peptone, failures were obtained with this steel at the 300,000-psi stress level even though the specimens were baked 23 hours at 375 F prior to loading. When plated from the same baths and baked 23 hours at 375 F, specimens of Thermold J sustained 240 hours at 300,000 psi without failure. The authors concluded that these results indicated a difference in susceptibility to hydrogen embrittlement of the two steels tested. However, the specimens were loaded only to 70 per cent of the notched tensile strength, and they were baked after plating. Thus, from the results of these tests, one cannot conclude that Thermold J was not adversely affected by the various plating procedures.

Probert and Rollinson(23) studied the delayed failure of 11 British steels of widely varying composition when cathodically cleaned in alkaline solution or acid pickled while under a sustained bending stress. All steels with a hardness greater than 302 Brinell were embrittled.

A study of delayed cracking of steel weldments was performed by Beachum, Johnson, and Stout<sup>(24)</sup>. They studied the effects of hydrogen, stress (restraint), and steel composition. Steels studied included AISI 1020 and ASTM A212 plain-carbon steels, and HY-80 and AISI 4140 alloy steels. Delayed cracks were produced in weldments of all four steels.

Schuetz and Robertson<sup>(25)</sup> studied the delayed failure of a series of plain-carbon steels and a series of four nickel steels that contained from 5 to 30 per cent nickel. Hydrogen was introduced into the steels by exposure to H<sub>2</sub>S solution and by cathodic charging. With either method of introducing hydrogen, delayed failures were obtained in the steels in the ferritic or martensitic condition. However, no failure was obtained with the 30 per cent nickel steel when it was treated so as to be fully austenitic at room temperature.

Other investigators have verified that martensitic stainless steels also are subject to hydrogen embrittlement and delayed, brittle failure. Uhlig<sup>(26)</sup> has described the hydrogen embrittlement of a 13 per cent chromium stainless steel, and Lillys and Nehrenberg<sup>(27)</sup> reported on embrittlement of Types 410, 420, and 422 stainless steel.

A few of the other steels reported to be embrittled by hydrogen include SAE 1000<sup>(28)</sup>, SAE 1050 spheroidized-annealed strip<sup>(29)</sup>, SAE 6150<sup>(30)</sup>, clock-spring steel<sup>(31)</sup>, and SAE 4140 cold-drawn wire with a tensile strength of 170,000 psi<sup>(10)</sup>.

Blanchard and Troiano<sup>(3)</sup> performed an investigation to determine whether the hydrogen embrittlement of nickel is of the same nature as that of steel and to determine the effect of alloying on the magnitude of the embrittlement in nickel. The study included 25Cr-20Ni austenitic stainless steel. The materials studied were as follows:

	Composition, per cent		
	Ni	Cr	Fe
"A" Nickel	99.4		0.15
72Ni-28Fe	72.7		27.2
51Ni-49Fe	51		49
Nilvar	36		64
Nichrome I	60	16	24
Nichrome V	80	20	
25-20 stainless steel	19.7	24.9	52.8

Both thermal and cathodic charging were used to introduce hydrogen into the alloys. Thermal charging was used for the 25-20 stainless steel in which the diffusion rate of hydrogen is low at room temperature, the other alloys were charged cathodically. The authors found that the nickel and some of the nickel-base alloys were embrittled by hydrogen when charged for several hours at a high current density. Studies of the strain-rate dependence and the temperature dependence of the embrittlement, and of the recovery of ductility upon aging, showed that this embrittlement was of the same type as that of ferritic and martensitic steels.

The embrittlement was a maximum for pure nickel and nil for the 51Ni-49Fe alloy, Nilvar, and 25-20 stainless steel. The variation in susceptibility toward hydrogen embrittlement of Ni-Cr-Fe alloys is shown in Figure 12. An apparent anomaly is the observation that the hydrogen embrittlement of a nickel-iron alloy decreased with

increasing iron content, even though iron is the easiest metal to embrittle with hydrogen. Because no embrittlement was found in the annealed, austenitic 25-20 stainless steel (83,000-psi tensile strength) and because the susceptibility of metals exhibiting hydrogen embrittlement increases with strength level, a specimen of this steel was cold swaged 67 per cent. This treatment decreased its reduction of area in tension from 76 per cent to 61 per cent and raised its strength level to 146,000 psi for the uncharged condition. By using a complicated procedure designed both to introduce more hydrogen into the steel and to make the superficial skin of hydrogen diffuse into the specimen, a slight embrittlement was produced. The ductility of the cold-worked alloy was reduced from 61 per cent to 53 per cent by introducing hydrogen. These findings indicate that the well-known resistance of austenitic stainless steel to hydrogen embrittlement results from its inherent ductility and from the fact that the hydrogen contents associated with an austenitic structure generally are relatively low.

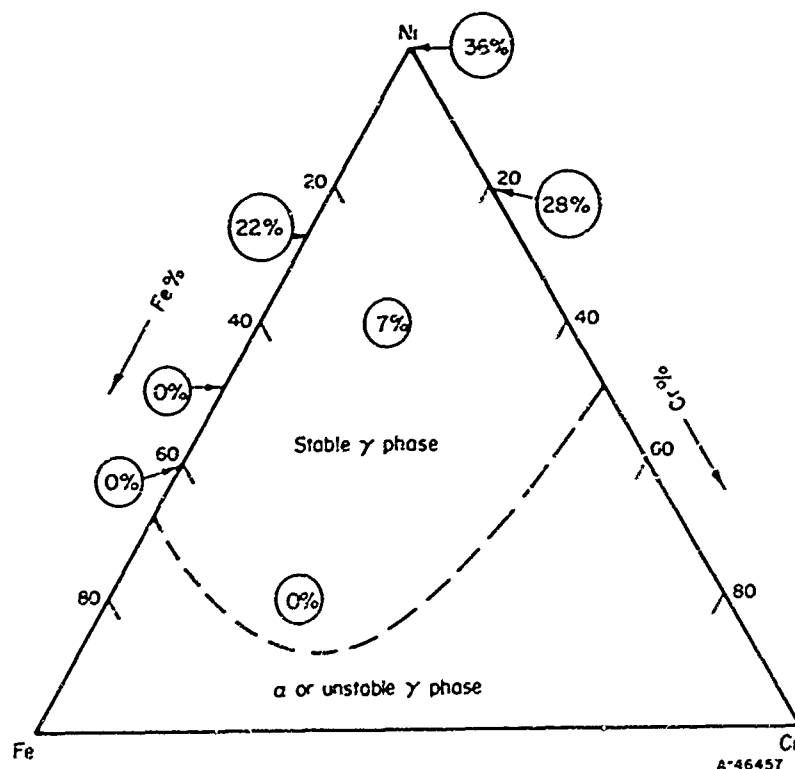


FIGURE 12. INFLUENCE OF THE COMPOSITION OF Ni-Cr-Fe ALLOYS ON THEIR SUSCEPTIBILITY TO HYDROGEN EMBRITTLEMENT<sup>(3)</sup>

All specimens were charged 4 hr at 176 F at a current density of 22 amp/in.<sup>2</sup>. Circled figures represent the reduction of ductility brought on by hydrogen charging.

Only a few studies have dealt with austenitic steels. Virtually no embrittlement has been found in austenitic steels, either of the Cr-Ni stainless type<sup>(1, 32, 3, 33, 34, 35)</sup>, or of the Hadfield austenitic manganese type<sup>(36)</sup>. As reported above, Schuetz and Robertson<sup>(25)</sup> found no embrittlement of an austenitic Fe-30Ni alloy when tested in the



fully austenitic condition, but Blanchard and Troiano<sup>(37, 3)</sup> did find embrittlement of nickel and certain nickel-base austenitic materials under severe charging conditions. Austenitic materials that are resistant to hydrogen embrittlement become susceptible when treated so as to partially transform to body-centered cubic structures, as Jones<sup>(38)</sup> found when chemical milling Type 301 stainless steel that had been cold worked to a high strength level.

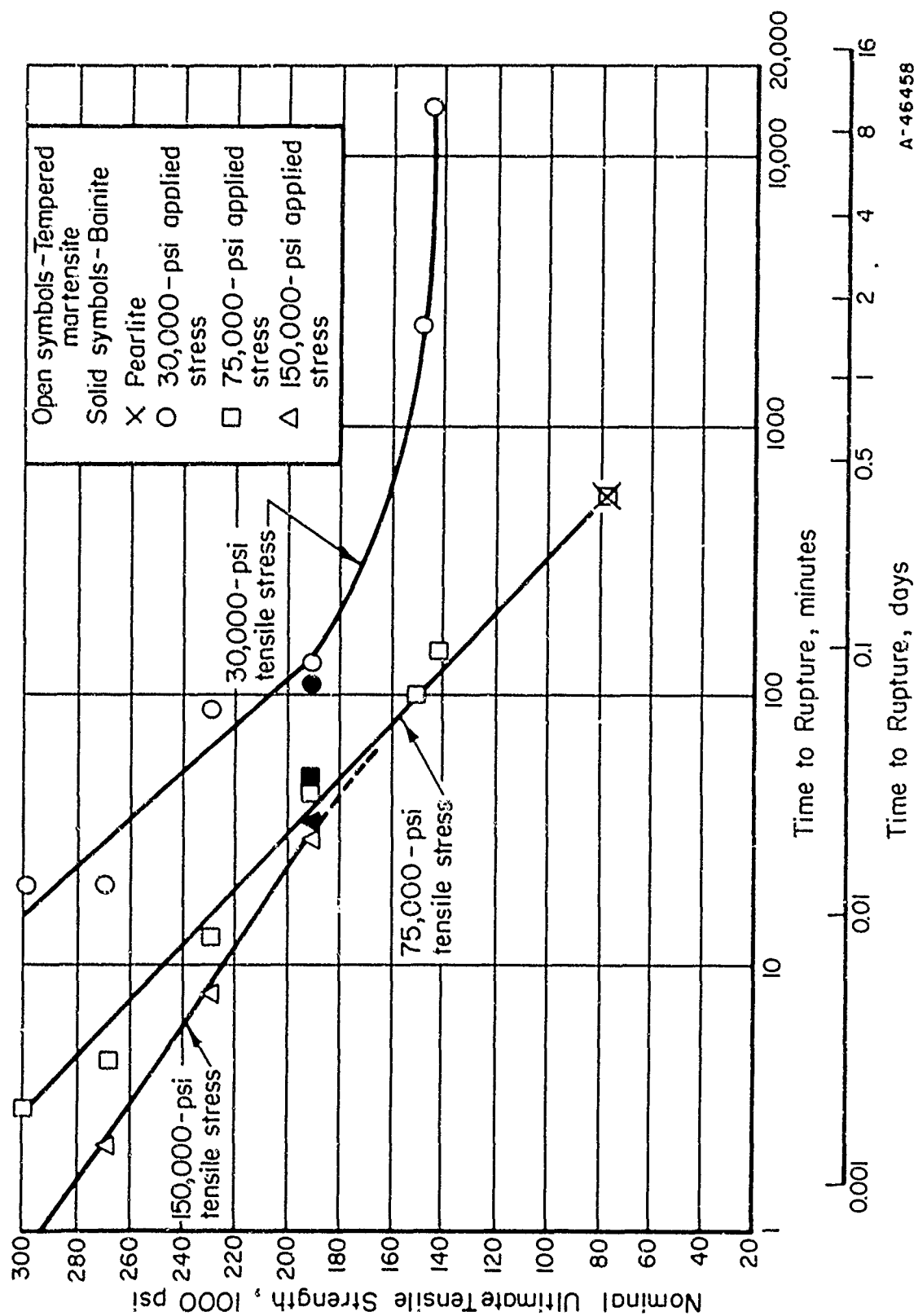
### EFFECT OF STRENGTH LEVEL

Many experiments have shown that both the minimum stress and the time required to produce delayed, brittle failure by hydrogen decrease as the nominal tensile strength of the steel is increased. On the basis of these experiments alone, delayed-type brittle failures would be expected to be an increasingly severe problem as the strength level of steel is increased. Because of the ever-increasing demand for materials of higher and higher strength in the aircraft and missile industries, for weight savings, this general behavior made an understanding of the nature of hydrogen-induced, delayed, brittle failure of steel imperative. The results of some of these experiments that show the effect of strength level on the phenomenon are considered in this section.

Slaughter et al.<sup>(8)</sup> studied the effect of strength level with a group of SAE 4340 steel specimens in which the ultimate tensile strength was varied from approximately 300,000 psi to 142,000 psi. All of these specimens were fully quenched to produce martensitic structures, and then tempered at temperatures in the range from 300 to 1200 F to produce the desired variations in strength. Smooth (unnotched) specimens were continuously charged with hydrogen cathodically while under sustained load. The results are shown in Figures 2 (page 6) and 13. In addition, Figure 13 shows the effect of differences in structure, but this subject will be discussed later. As the strength level was decreased from 300,000 psi to 142,000 psi, the time to rupture in the higher range of stress increased by a factor of approximately 100; the stress required to cause rupture in 10,000 minutes increased from 15,000 to 45,000 psi as the strength level was decreased in that range (see Figure 2).

Although it is unlikely that the conditions of these tests would be encountered in service, the results obtained show that hydrogen entering the steel while it is under stress can cause it to lose more than 90 per cent. of its ability to withstand a sustained load, in the case of steel heat treated to a high strength level. Even at the lowest strength level tested for the tempered martensite (142,000 psi), the steel lost approximately two-thirds of its load-carrying ability. In these experiments, rupture occurred in a tempered-martensite structure having a tensile strength as low as 142,000 psi. However, service failures nearly always have been restricted to steels having a higher strength level. This was attributed to the fact that in these experiments the specimens contained more hydrogen than would be expected in service.

The same steel was isothermally transformed at 1200 F to produce a pearlitic structure which had a tensile strength of 75,000 psi. Under the same charging and test conditions, delayed failures were obtained in unnotched specimens at this strength level, as indicated by the following tabulation and by the appropriate curve in Figure 2 (page 6).



A-46458

FIGURE 13. EFFECT OF NOMINAL STRENGTH OF AN SAE 4340 STEEL ON THE TIME TO RUPTURE DURING CATHODIC CHARGING WITH HYDROGEN UNDER STANDARDIZED CONDITIONS WHILE UNDER STRESS(8)

Battelle Charging Condition A:

Electrolyte: 4 per cent by weight of H<sub>2</sub>SO<sub>4</sub> in water

Poison: 5 drops per liter of cathodic poison composed of 2 g phosphorus in 40 ml of CS<sub>2</sub>

Current density: 8 ma/in. <sup>2</sup>.

<u>Applied Stress, psi</u>	<u>Time to Rupture, minutes</u>
75,000	516
71,000	630
70,000	978
64,000	1872
50,000	Did not fail in 13,242 min (221 hr)
50,000	Did not fail in 14,334 min (239 hr)

Frohberg, Barnett, and Troiano<sup>(5)</sup> at Case Institute of Technology studied the effect of strength level of SAE 4340 steel by using sharp-notched specimens cathodically precharged with hydrogen. Sharp notches were used to localize the region of fracture and to provide a multiaxial stress state. The results obtained are shown in Figure 1 (page 5). With their conditions, applied stresses as low as 40 per cent of the yield strength caused failure in a matter of only a few hours. Identical notched specimens in the uncharged condition were stressed at high loads, as indicated in the figure, and remained unbroken after times of more than 250 hours. Regardless of the strength level, the time to failure was always of the same order of magnitude (approximately 1 to 8 hours).<sup>\*</sup> For a given strength level, there appeared to be only a slight dependence of failure time on the applied stress. Thus, they found that the delay in time for failure was evidently independent of strength level and only slightly dependent upon applied stress for the particular test conditions used. Material at the highest strength level exhibited a lower value of the upper critical stress than did material at the other two strength levels. Barnett and Troiano<sup>(39, 6)</sup> showed the effect of the same cathodic charging conditions on the mechanical properties of both smooth and notched specimens of this steel heat treated to three strength levels. The results are shown in Table 6. For the 240,000-psi strength level, the lower critical stress was 75,000 psi. In studying 12 heats of SAE-AISI 4340 steel, the Case research workers<sup>(15)</sup> found that the lower critical stress was independent of the strength level for their test conditions, but the charged notched tensile strength tended to be inversely related to the strength level, at least at the higher strengths.

Figure 14 shows the results Rinebolt<sup>(12)</sup> obtained for tensile tests of AISI 4340 steel heat treated to three different strength levels and cathodically charged for various times. These comparisons are based on per cent of original tensile strength. The data show that 60 per cent of the tensile strength was lost by a steel of 209,000-psi tensile strength (uncharged specimen) after charging for 4 hours under the conditions used. The same loss in tensile strength was obtained for the steel heat treated to the 287,000-psi strength level after only 1/2 hour of charging. Table 7 presents the actual values obtained. Note that for many charging conditions the material that was the strongest in the uncharged condition became the weakest. Also, note that the reduction in area and elongation decreased to less than 1 per cent after charging for only 5 minutes for all strength levels investigated.

Sachs and co-workers at Syracuse University<sup>(19)</sup> studied the effect of strength level on delayed failures for several materials when the hydrogen was introduced

<sup>\*</sup>These results seem to be somewhat contrary to those obtained by Slaughter et al.<sup>(8)</sup>. Much of the difference is probably the result of differences in test procedure in the two investigations. Slaughter and co-workers used unnotched specimens that were cathodically charged continuously while under sustained stress, while the Case Institute investigators used notched specimens that were precharged with hydrogen and were not charged during the time they were under the sustained stress. It will be shown later that such differences in stress concentration and in the amount and distribution of hydrogen in the test specimen do affect the initiation and propagation of brittle fracture.

TABLE 6. EFFECT OF CATHODIC CHARGING ON MECHANICAL PROPERTIES OF SAE 4340 STEEL HEAT TREATED TO SEVERAL STRENGTH LEVELS(a)(39)

Nominal Strength Level, psi	230,000	240,000	270,000
<u>Uncharged</u>			
Tensile Strength, psi	227,000	236,000	279,000
Yield Strength, psi	--	220,000	235,000
Reduction in Area, per cent	45.5	46	44
Fracture Strength, psi	318,000	345,000	388,000
Notched Tensile Strength, psi	306,000	315,000	330,000
<u>Cathodically Charged(b),</u> <u>5-Minute Age</u>			
Tensile Strength, psi	227,000	236,000	255,000
Reduction in Area, per cent	16	11	3
Fracture Strength, psi	265,000	261,000	265,000
Notched Tensile Strength, psi	251,000	250,000	207,000

(a) All tests run at a crosshead speed of 0.05 inch/min.

(b) Case Institute of Technology Charging Condition A:

Electrolyte: 4 per cent  $H_2SO_4$  in water

Poison: None

Current density: 20 ma/in.<sup>2</sup>

Charging time: 5 minutes.

simply by cadmium electroplating at a fixed current density (200 ma/in.<sup>2</sup>). Their results for SAE 4340 steel will be used to illustrate their findings. Strength levels ranging from 275,000 to 165,000 psi were obtained by tempering at the following temperatures:

<u>Tempering Temperature, F</u>	<u>Ultimate Tensile Strength, psi</u>
400	275,000
500	270,000
700	235,000
800	215,000
1000	165,000

It will be well to refer to these values in studying their results, shown in Figure 8 (page 15) since only tempering temperatures are given on the figure. For notched specimens, delayed failures were encountered for all strength levels studied. For the more severe notching conditions ( $K_t = 10$  and 5), nearly the same curves of load versus time to rupture were obtained for material tempered at 400, 500, or 700 F (strengths between 275,000 and 235,000 psi), and delayed failures occurred at stresses as low as about 50,000 to 75,000 psi. Tempering at 800 and 1000 F to provide lower strength levels led to a displacement of the curves of applied stress versus rupture time to the right and upward. The indicated improvement in properties increased progressively as

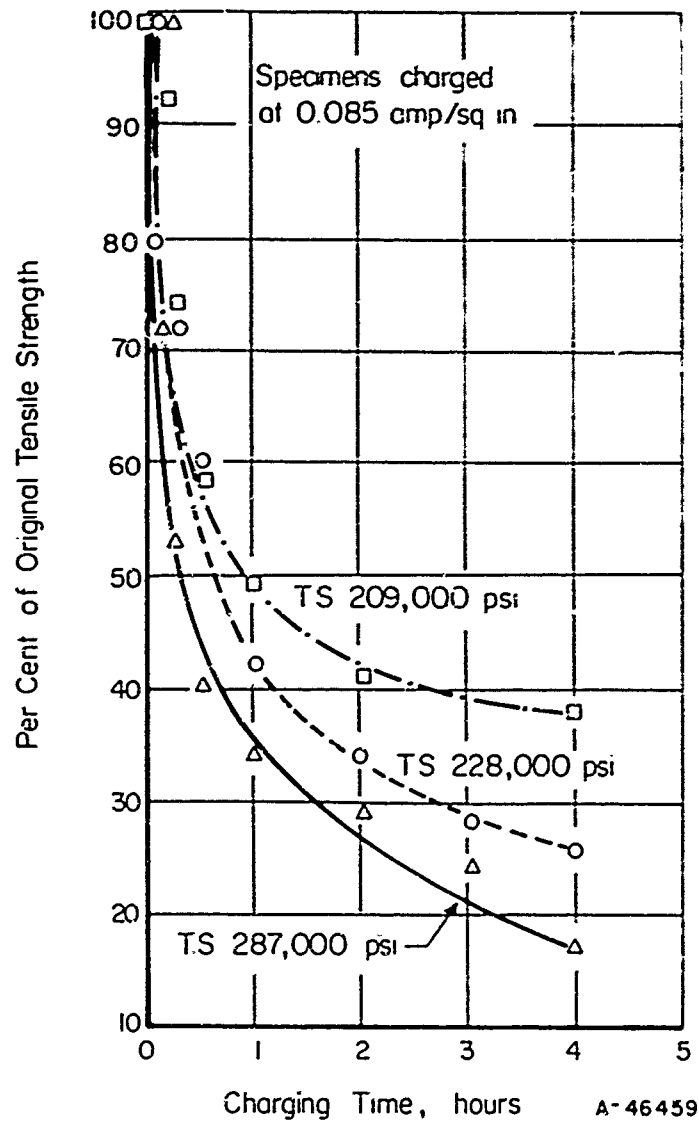


FIGURE 14. EFFECT OF HYDROGEN CHARGING ON TENSILE PROPERTIES FOR AIR-MELTED STEEL AT THREE STRENGTH LEVELS(12)

AISI 4340 steel.

TABLE 7. EFFECT OF CATHODIC CHARGING TIME ON THE TENSILE PROPERTIES OF AISI 4340 STEEL HEAT TREATED TO THREE DIFFERENT STRENGTH LEVELS<sup>(12)</sup>

Original Tensile Strength, psi	Charging Time, minutes	Tensile Strength, psi	Reduction of Area, per cent	Elongation, per cent	Per Cent of Original Tensile Strength
209,250	0	209,250	49	14	100
	7.5	193,500	0.5	0	92
	15	154,000	0	0	74
	30	122,850	0	0	59
	60	103,000	0	0	49
	120	86,000	0	0	41
	240	80,000	0	0	38
228,000	0	228,000	52	14	100
	5	182,000	0	0	80
	15	163,500	0	0	72
	30	130,750	0	0	60
	60	95,350	0	0	42
	120	76,650	0	0	34
	180	64,650	0	0	28
240	59,400	0	0	26	
286,750	0	286,750	41	14	100
	7.5	205,750	0	0	72
	15	153,000	0	0	53
	30	116,100	0	0	40
	60	98,200	0	0	34
	120	82,000	0	0	29
	180	68,500	0	0	24
240	48,400	0	0	17	

the tempering temperature was raised from 700 F. Even after tempering at 1000 F (165,000-psi ultimate tensile strength), delayed failures occurred as the result of hydrogen electrodeposited during cadmium plating. Figure 15 shows the change in "minimum fracture stress", taken as the fracture stress corresponding to a rupture time of 100 hours, with change in tempering temperature (change in strength level). The minimum stress was raised considerably by tempering at the higher temperatures (800 to 1000 F). By comparing these data with the data for smooth specimens ( $K_t = 1$ ) in Figure 16, it is seen that the curve of breaking stress at 100 hours versus tempering temperature for cadmium-plated smooth specimens in Figure 15 differs little from that measured for unembrittled smooth specimens. Although sustained-load failures occurred with a delay for smooth specimens in which the hydrogen was introduced only by commercial cadmium electroplating (Figure 16), such failures took place with little drop in stress.

Data for 98B40 steel tempered at various temperatures are shown in Figures 17 and 18. These data are rather similar to those obtained for SAE 4340 steel. Similar results also were obtained for the vanadium-modified SAE 4330 steel (see Figure 19).

Valentine<sup>(28)</sup> studied the delayed failure of zinc-plated lockwashers made from SAE 1060 wire. Acid pickling was used prior to plating. The lockwashers were tested by placing them between case-hardened flat washers on a bolt and drawing them down flat with a nut, they were examined periodically for failures while clamped on the bolts. This investigator found a strong dependence of the tendency towards delayed failure on strength level, the lower the hardness (strength), the smaller the percentage of failures encountered. Some of his results that show the effect of strength level (in terms of hardness) are given in Table 8. Stefanides<sup>(29)</sup> studied the delayed failure of electroplated dome lockwashers fabricated from SAE 1050 steel strip; these were acid descaled and cadmium plated after hardening. Upon loading to a fixed load for a week, he, too, found that the percentage of failures was directly related to the hardness.

TABLE 8. RESULTS OF TESTS MADE ON HEAVY LOCKWASHERS ELECTROPLATED WITH ZINC<sup>(a)</sup>(28)

Treatment After Plating	Rockwell C Hardness	Number Tested	Number Broken After 1 Week	Per Cent Broken
None	62	200	200	100
None	55	200	184	90
None	50	200	74	37
None	47	200	31	15
None	42	200	0	0
Heated at 400 F for 4 hours	52	200	17	8
Heated at 400 F for 4 hours	50	200	0	0
Heated at 400 F for 4 hours	47	200	0	0
Heated at 400 F for 4 hours	42	200	0	0

(a) 7/16-inch heavy lockwashers plated with 0.0002 inch of zinc plate.

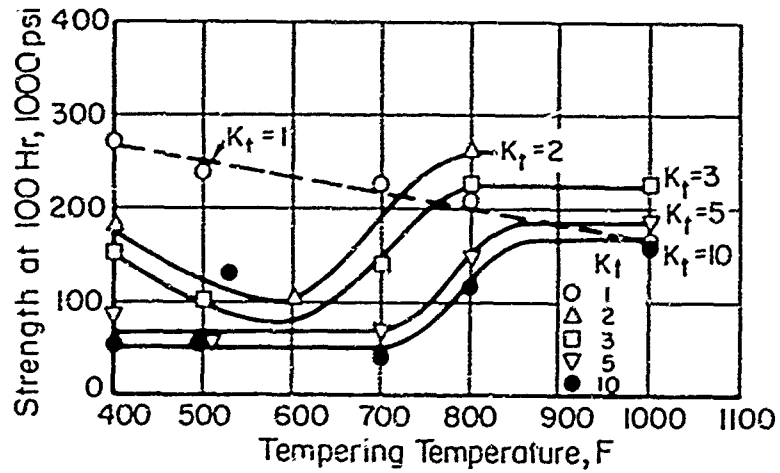


FIGURE 15. PLOT OF THE STRESS CORRESPONDING TO A RUPTURE TIME OF 100 HR VERSUS TEMPERING TEMPERATURE, WITH STRESS CONCENTRATION AS PARAMETER, FOR CADMIUM-PLATED SAE 4340 STEEL.<sup>(19)</sup>

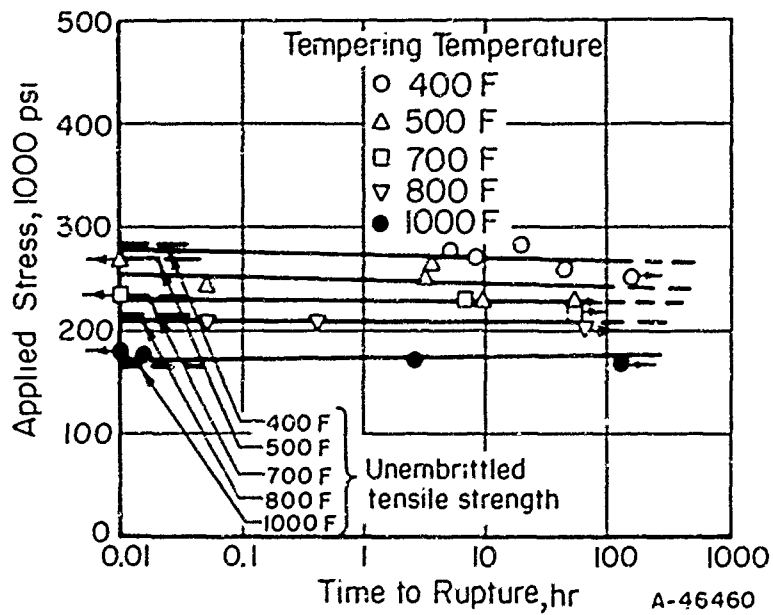


FIGURE 16. THE DELAYED-FAILURE BEHAVIOR OF CADMIUM-PLATED SAE 4340 STEEL TEMPERED AS INDICATED; STRESS CONCENTRATION  $K_t = 1$ <sup>(19)</sup>

Austenitized at 1525 F and oil quenched.



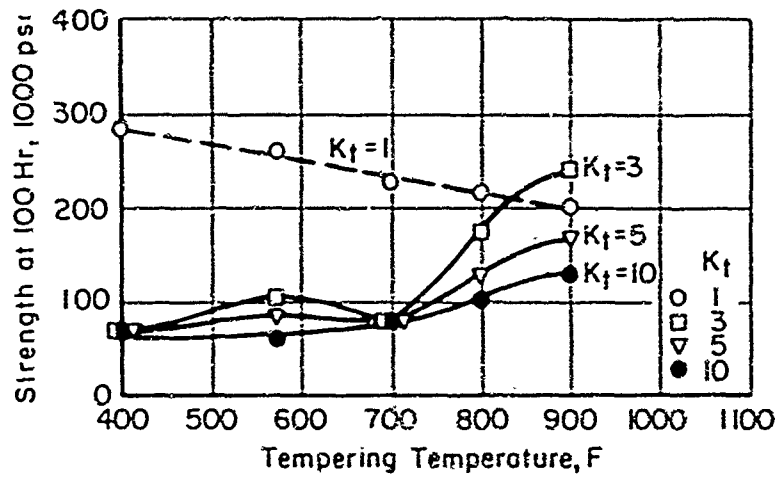


FIGURE 17. THE FRACTURE STRENGTH AT 100 HR VERSUS TEMPERING TEMPERATURE WITH STRESS CONCENTRATION AS PARAMETER FOR CADMIUM-PLATED 98B46 STEEL(17)

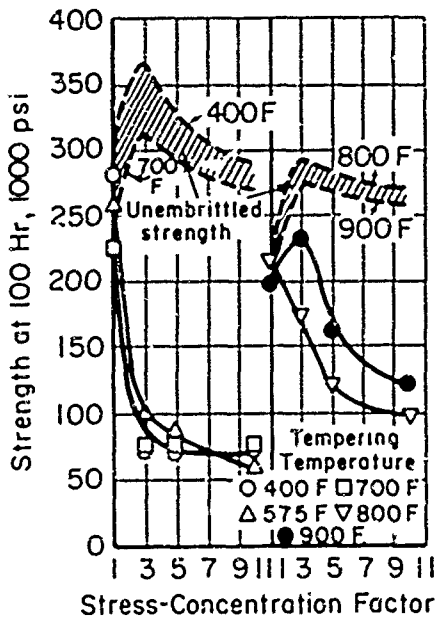


FIGURE 18. THE FRACTURE STRENGTH AT 100 HR VERSUS STRESS CONCENTRATION WITH TEMPERING TEMPERATURE AS PARAMETER FOR CADMIUM-PLATED 98B46 STEEL(19)

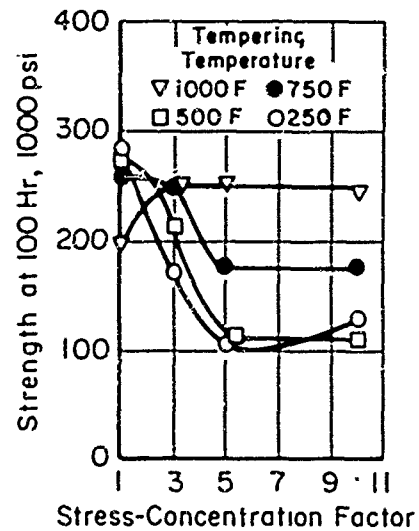


FIGURE 19. THE FRACTURE STRENGTH AT 100 HR VERSUS STRESS CONCENTRATION WITH TEMPERING TEMPERATURE AS PARAMETER FOR CADMIUM-PLATED 4330 VANADIUM-MODIFIED STEEL(19)

A 46461

## EFFECTS OF APPLIED STRESS AND PLASTIC STRAIN

The results of early investigations of hydrogen-induced, delayed, brittle failures performed in various laboratories were in agreement in showing that delayed failure may occur over a wide range of applied tensile stress and that the time for failure is not affected greatly by variations in the applied stress. Also, for given specimens, charging conditions, and test procedures, there is a minimum critical value of applied stress below which failure does not occur in a given material for an indefinite period of time. The results of tests of hydrogenated material under static load usually are plotted as sustained load versus time to failure. Because the resulting curves in some ways resemble fatigue curves, they sometimes are called "static-fatigue curves", in which case the lower critical stress is considered to be a "static endurance limit". However, this terminology may be confusing to some, since fatigue carries the connotation of cyclic loading, while the test used to study hydrogen-induced, delayed, brittle failure employs a static load. Hence, the terms "delayed-failure curves" and "lower critical stress" would appear to be preferable. The lower critical stress is important because, for a given hydrogen concentration and strength level (and a given notch sharpness in the case of notched specimens), it is the lowest applied stress sufficient to initiate a crack. In other words, the lower critical stress is a threshold stress, above which failure is inevitable and below which the steel is undamaged.

Experimental data showing the effect of stress level on the time for delayed failure in the case of notched specimens precharged with hydrogen were shown in Figure 1 (page 5). These data, taken from the work of Frohberg, Barnett, and Troiano<sup>(5)</sup> clearly show the relatively low applied stresses that were sufficient to produce delayed failure. When compared with the yield strengths, it was found that applied stresses of as little as 40 per cent of the yield strength (for a steel of 270,000-psi ultimate tensile strength) caused failure in only a few hours under sustained load. These investigators pointed out that this observed behavior should not be taken to imply that there was no flow, since the unit stress at the root of the notch was considerably greater than the applied stress. Identical notched specimens in the uncharged condition were stressed at high loads, as indicated in Figure 1, and remained unbroken after times of over 250 hours.

For a given strength level, there appeared to be only a slight dependence of failure time on the applied stress. Also, the time to failure was of the same order of magnitude, regardless of strength level. Since the mobility of hydrogen may be expected to remain approximately independent of the strength level and applied stress, even in this early work it appeared that the time to failure may be associated with the diffusion of hydrogen. Furthermore, it was suggested that the time to failure may represent the time to accomplish a critical redistribution of hydrogen.

The plateau of the delayed-failure curves at high applied stress (that is, the upper plateau) coincided with the notched tensile strength for a given strength level. This was determined by applying static loads just above and below the value of the notched tensile strength. The value of the upper critical stress at the 270,000-psi strength level was less than that for the two lower strength levels. This correlated with the marked decrease in notched tensile strength found at the 270,000-psi strength level for hydrogenated specimens.

Probably the most significant relationship these investigators at Case Institute found between applied stress and the time to failure was the occurrence of a minimum

critical value of applied stress below which delayed failure did not occur in material of a given strength level. The test generally was discontinued if a specimen remained unbroken after sustaining the static load for 100 hours, but times as long as 2160 hours without failure were observed. For the specimen geometry, notch acuity, charging conditions, and test conditions used in these experiments, the lower critical stress was nearly the same for the three strength levels (270,000 psi, 230,000 psi, and 200,000 psi). However, this is not always the case for other conditions.

These investigators clearly demonstrated the necessity for exceeding some critical stress value to produce delayed failure, by an experiment in which they varied the notch acuity of the test specimen. The results of this experiment are shown in Figure 20. For the sharp notch (with the highest degree of stress concentration), the smallest load served to produce delayed failure. A greater applied stress was required for failure to occur in the specimens with the milder, 1/32-inch-radius notch. For the specimens with a notch root radius of 2 inches, the stress concentration resulting from the notch was very slight, and the lower critical stress for delayed failure was no more than 5,000 psi below the value of the notched tensile strength of charged specimens. Thus, for these precharged specimens, the lower critical stress was raised markedly as the notch acuity was decreased.

In another experiment, these same workers showed that the lower critical stress is not constant for this type of specimen. Two series of specimens that came from the same bar of steel but which were prepared separately gave the results shown in Figure 21. Despite all the precautions to maintain uniformity between batches, some factor was different. The specimens from which the lower curve was obtained may have had a more severe concentration of residual stress than the specimens from which the upper curve was obtained. In other words, the one set of specimens was, in essence, preloaded and required a smaller applied load to give delayed failure.

In a continuation of this work, Barnett and Troiano<sup>(39)</sup> used the resistance method of crack-propagation measurement to evaluate the effect of applied stress, as well as certain other variables, on delayed, brittle failure. These studies were made with precharged, notched specimens of SAE 4340 steel at the 230,000-psi strength level. Charging conditions were the same as for the work just described. The delayed-failure characteristics for these conditions are illustrated in Figure 22. The increase in electrical resistance was measured as a function of time during static loading at various stresses within the range of 100,000 to 200,000 psi; the results are shown in Figure 23. With the data in Figure 23 and by referring to resistance calibration curves, they obtained crack-area data as a function of time for the indicated applied stresses. Crack area was expressed as a percentage of the area under the notch. These data are shown in Figure 24. In Figure 25, the crack-propagation curves are shown in terms of the alternative parameter, radial crack depth. These figures show that, for the test conditions used, there was little or no incubation time for crack initiation (the minimum time required for a reliable resistance measurement was 30 seconds after application of the load). Immediately upon loading above the lower critical stress, the material was damaged permanently, that is, a crack had been initiated. The extent of damage depended on time and the applied stress. Thus, the magnitude of the applied load influenced the crack-growth behavior. The extent of rapid crack growth incurred in the first stage of the fracture process was, in general, greater the less the magnitude of the applied load. The conditions existing at the end of the third stage, that is at fracture, are summarized in Table 9. The applied stress had no significant effect on the delayed-failure fracture stress, which was slightly higher than the notch-tensile strength of the uncharged base material in every instance.

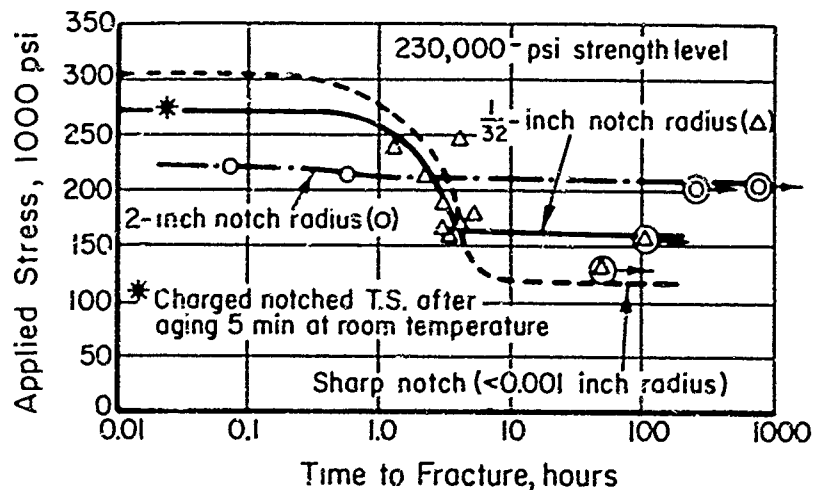


FIGURE 20. COMPARISON OF DELAYED-FAILURE BEHAVIOR OF SAE 4340 STEEL FOR SPECIMENS OF DIFFERENT NOTCH SHARPNESSES<sup>(5)</sup>

Aged 5 minutes

Case Institute of Technology Charging Condition A:

Electrolyte: 4 per cent  $H_2SO_4$  in water

Poison: None

Current density: 20 ma/in.<sup>2</sup>

Charging time: 5 minutes

Aging time: Measured from end of charging to start of test.

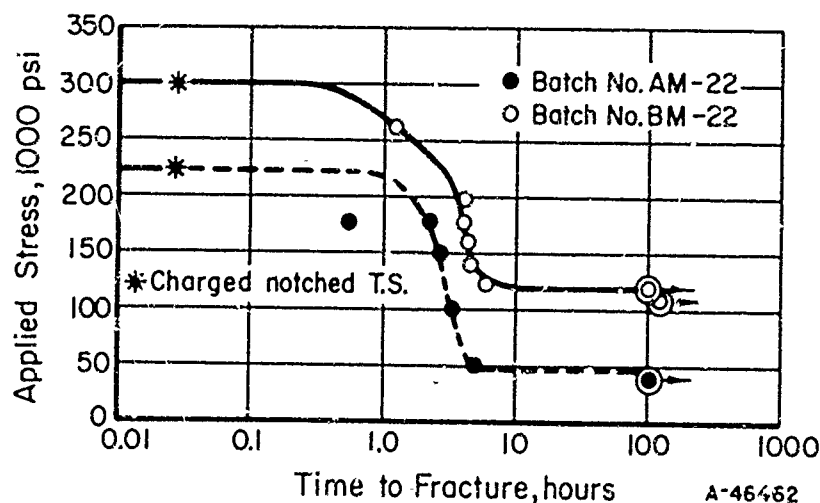


FIGURE 21. STATIC-LOADING TESTS ON SHARP-NOTCH SPECIMENS OF SAE 4340 STEEL HEAT TREATED TO 230,000 PSI<sup>(5)</sup>

Aged 5 minutes.

Case Institute of Technology Charging Condition A, as given in Figure 20.

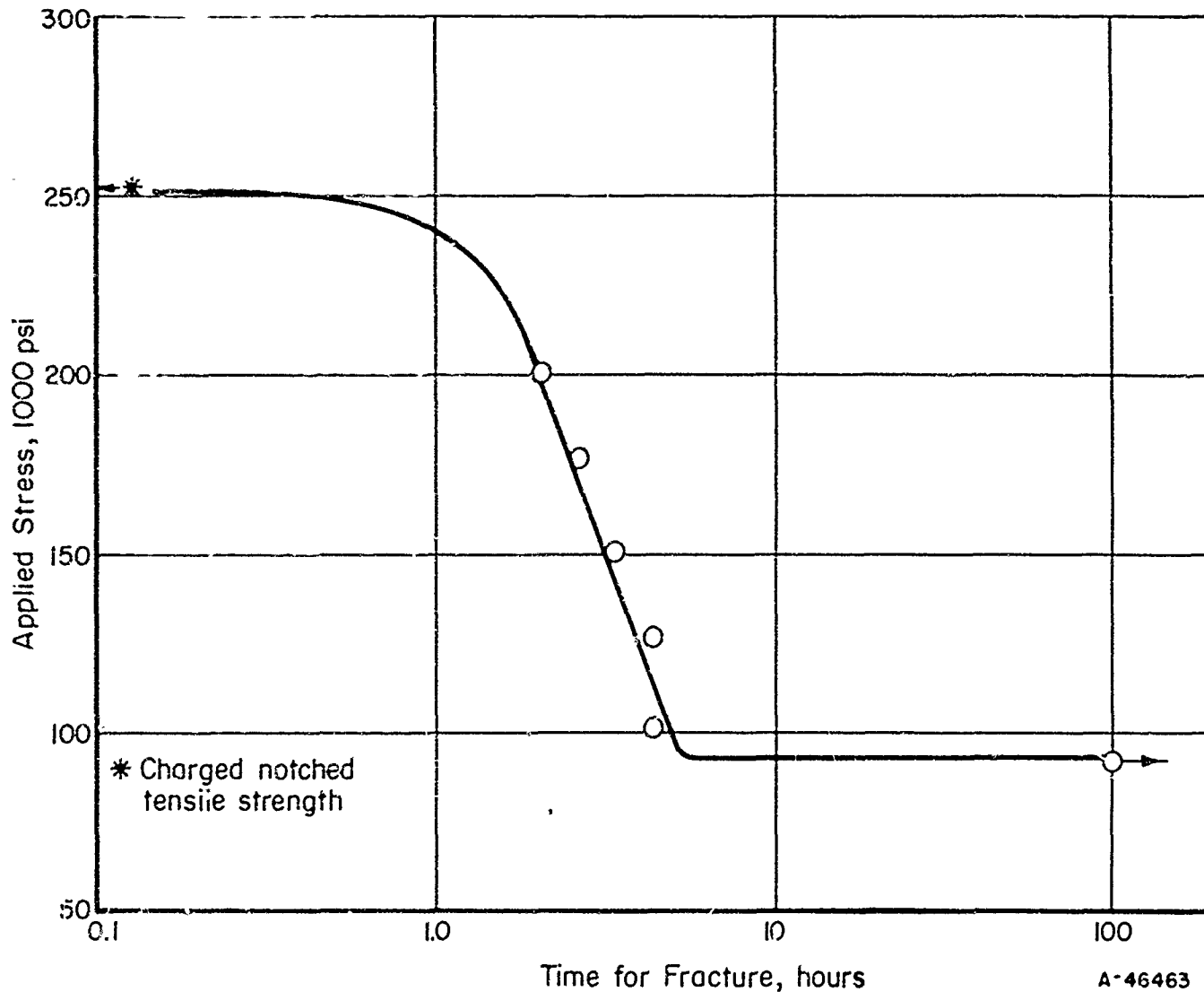


FIGURE 22. DELAYED-FAILURE BEHAVIOR OF SHARP-NOTCH SPECIMENS OF SAE 4340 STEEL AT THE 230,000-PSI STRENGTH LEVEL<sup>(39)</sup>

Aged 5 minutes. Case Institute of Technology Charging Condition A, as given in Figure 20.

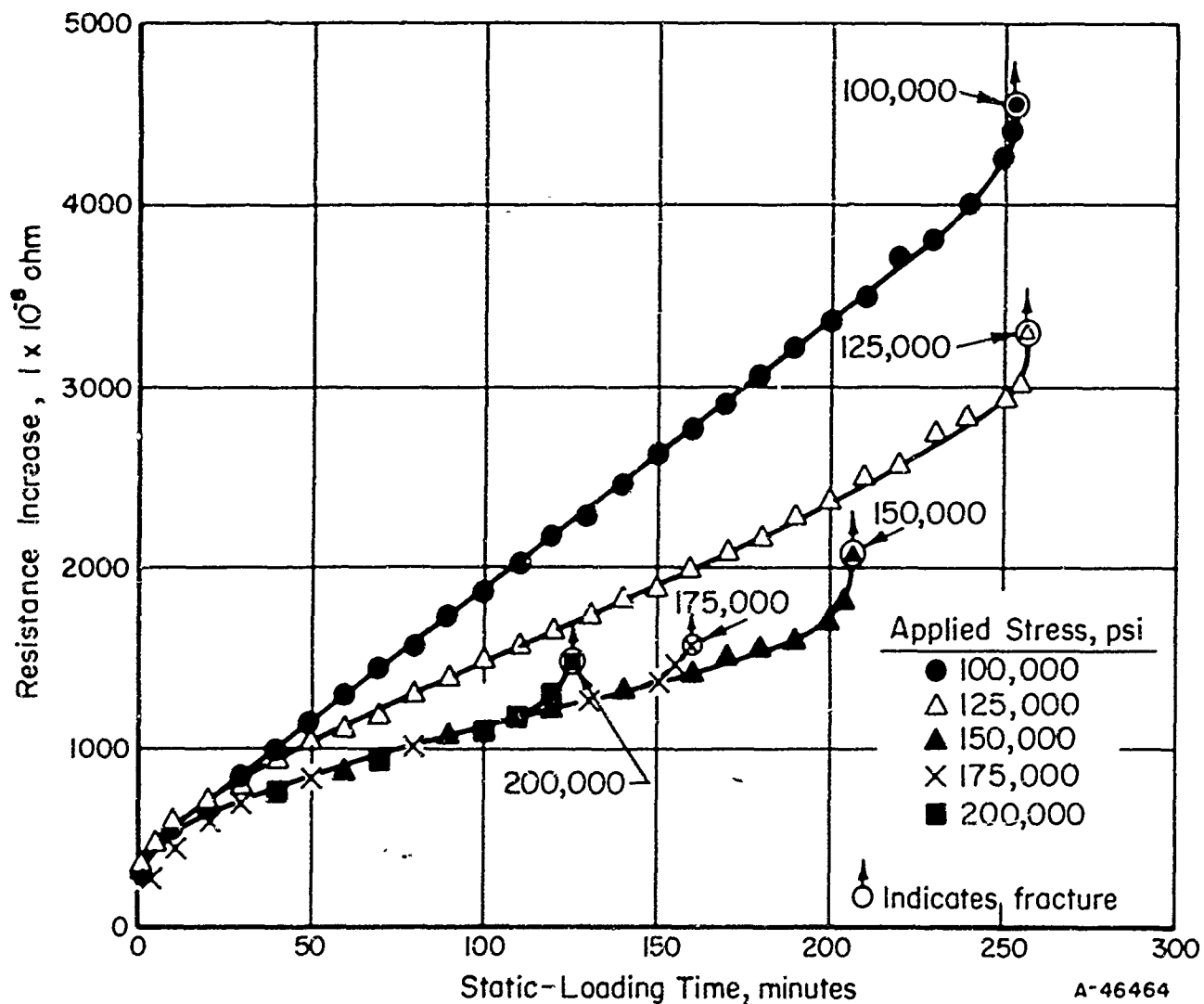
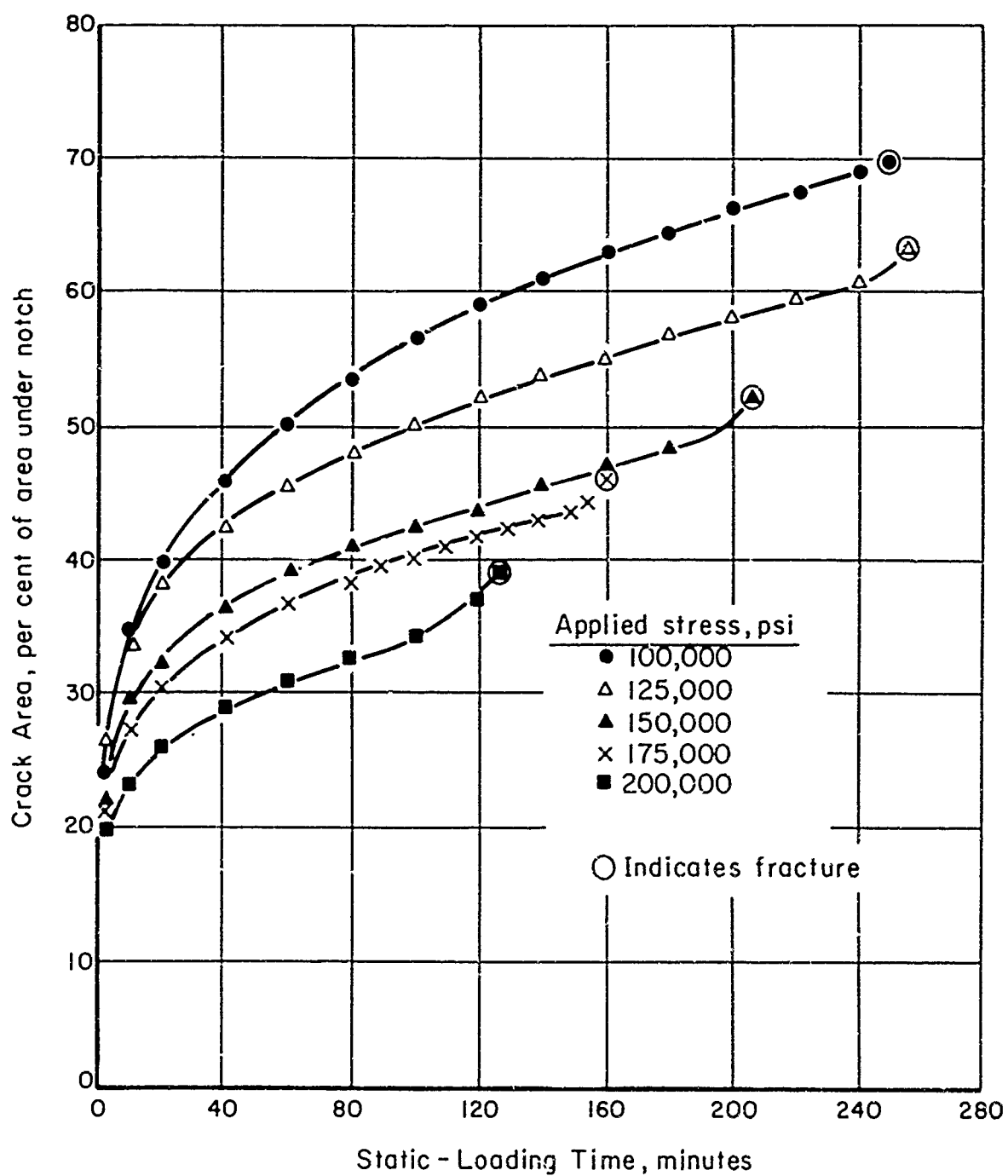


FIGURE 23. EFFECT OF STATIC-LOADING TIME ON THE ELECTRICAL RESISTANCE OF THE SHARPLY NOTCHED SECTION OF SPECIMENS STRESSED WITHIN THE DELAYED-FAILURE RANGE OF SAE 4340 STEEL AT THE 230,000-PSI STRENGTH LEVEL<sup>(39)</sup>

Aged 5 minutes. Case Institute of Technology Charging Condition A, as given in Figure 20.



A-46465

FIGURE 24. EFFECT OF APPLIED STRESS ON CRACK PROPAGATION WITHIN THE DELAYED-FAILURE RANGE OF SHARPLY NOTCHED SPECIMENS OF SAE 4340 STEEL AT THE 230,000-PSI STRENGTH LEVEL(39)

Aged 5 minutes. Case Institute of Technology Charging Condition A, as given in Figure 20.

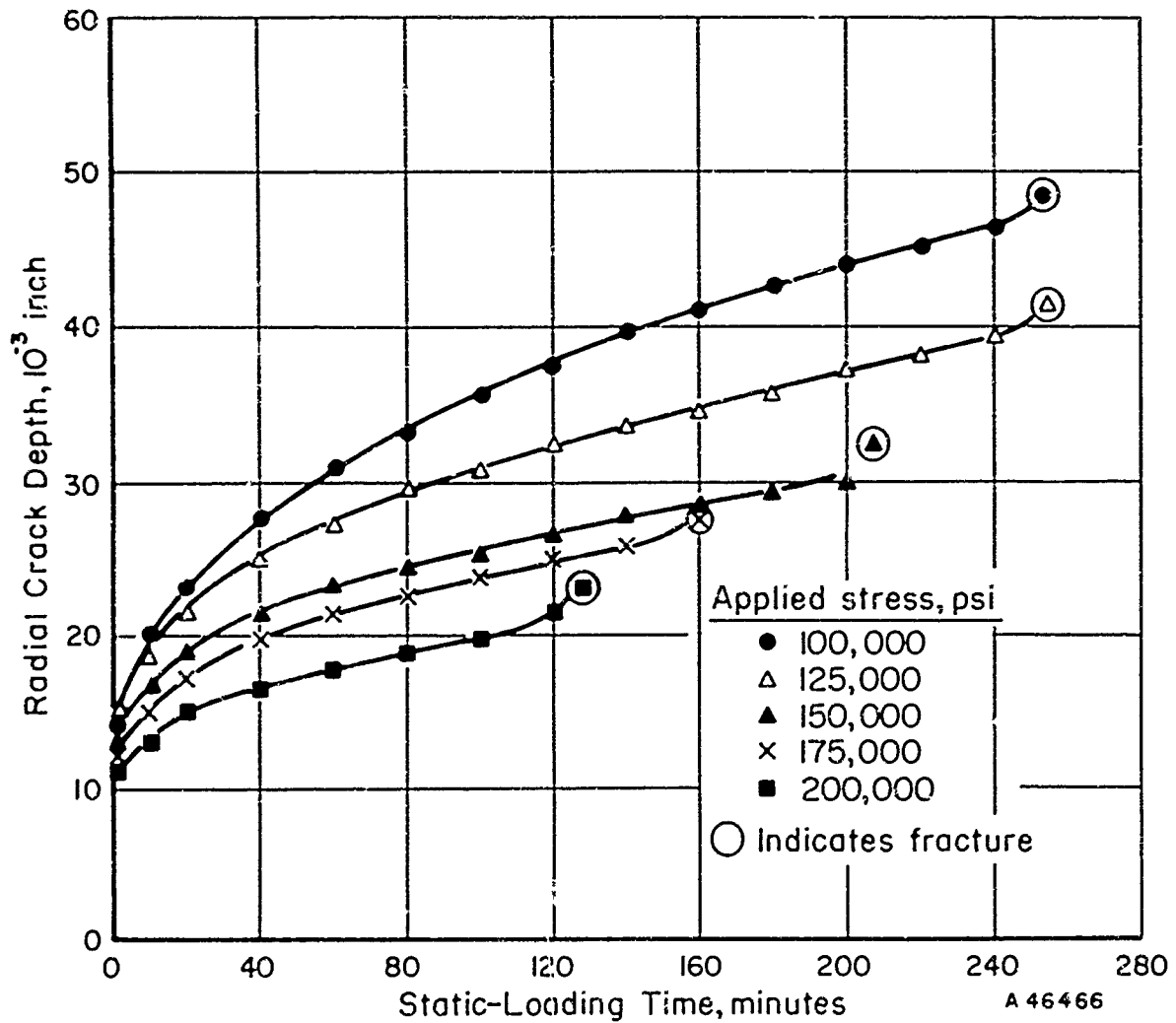


FIGURE 25. EFFECT OF APPLIED STRESS ON THE RADIAL CRACK-PROPAGATION CHARACTERISTICS; DERIVED FROM FIGURE 24(39)



TABLE 9. EFFECT OF APPLIED STRESS ON THE DELAYED-BRITTLE-FAILURE BEHAVIOR OF SAE 4340 STEEL, AT THE 230,000-PSI STRENGTH LEVEL<sup>(39)</sup>

Static Applied Stress, psi	Fracture Time, minutes	Crack Area, per cent of area under notch	Radial Crack Depth, $10^{-3}$ inch	Delayed-Failure Fracture Stress, psi	Surface Energy (S), $10^7$ ergs/cm <sup>2</sup>
100,000	253	70.5	48.0	339,000	4.00
125,000	256	63.5	41.5	343,000	4.60
150,000	207	52.5	32.5	316,000	4.44
175,000	160	45.5	27.5	321,000	4.93
200,000	127	39.0	23.0	328,000	5.40

Note: Case Institute of Technology Charging Condition A, as given in Figure 20.  
Aged 5 minutes at room temperature after charging.

The effect of applied stress when smooth specimens were cathodically charged continuously while under static load was demonstrated by the results of Elsea and co-workers at Battelle Institute<sup>(8)</sup>. Variations in applied stress affected the time to rupture in a similar manner under a wide range of strength levels, compositions, structures, and, to a certain extent, hydrogen contents. When other conditions were held constant, there were two ranges of stress which produced different effects on the time to rupture, as is shown in Figure 2 (page 6). In the higher range of applied stress, the time to rupture was relatively short and was only moderately affected by a change of stress. For example, as the stress was increased from 60,000 psi to 180,000 psi, the time to rupture decreased only from 20 minutes to 6 minutes for a steel heat treated to 230,000-psi ultimate tensile strength and charged under the standardized conditions adopted. These investigators recognized that, in those specimens which failed after a relatively short time, the time to rupture probably was controlled more by the depth of hydrogen penetration than by the failure mechanism. In the lower range of stress, the time to rupture was longer by as much as a factor of 100. Time to rupture was greatly influenced by stress in this range, a slight decrease of stress resulted in a large increase in the time to rupture. For the conditions of the previous example, decreasing the applied stress from 40,000 psi to 25,000 psi increased the rupture time from 40 minutes to approximately 10,000 minutes.

To be certain that the action of the electrolyte at the specimen surface was not influencing the failures in the delayed-failure tests described above, the Battelle investigators performed another series of experiments. In these experiments, specimens were statically loaded in bending and charged cathodically on the compression side, thus eliminating any surface effect of the electrolyte on the side stressed in tension. The specimens used in this series of experiments were bars of SAE 4340 steel 1/2 by 1-1/2 by 8 inches, all heat treated to an ultimate tensile strength of approximately 230,000 psi. An electrolytic cell was cemented to one side of each specimen, with a portion of that side exposed as the cathode. A static bending moment was applied to the specimen so that the side to which the cell was attached was stressed in compression and the side exposed to the atmosphere was stressed in tension. The tension surfaces of the specimens were notched with 0.020-inch-wide transverse slots of varying depth. The stress

on the specimen was computed as the stress at the base of the notch, the effects of stress concentration being neglected. Upon cathodic charging in sulfuric acid electrolyte, a hydrogen gradient was established through the specimen. The hydrogen content was highest at the cathodically charged surface and lowest at the opposite surface, where hydrogen was escaping into the atmosphere. Thus, in the region of highest hydrogen content, compressive stresses existed, while at the surface stressed highly in tension, a low concentration of hydrogen was obtained.

Delayed, brittle fractures were obtained, but none of them originated at the cathodically charged surface. The region near the cathodically charged surface, where the hydrogen content was greatest, behaved in a ductile manner. As in the tensile tests where the static stress was a uniaxial tensile stress, the time to rupture increased as the applied stress was decreased to 80,000 psi. This is shown in Figure 26. One specimen failed after a delay of 15 days. This series of experiments also produced results which supported the conclusion obtained from the static-loading tests that the minimum stress for failure increased with decreasing hydrogen content. This will be discussed more fully in the section dealing with the effect of hydrogen content on delayed failure. The data obtained from both types of test indicated that failure did not occur until a certain combination of hydrogen content and applied stress had been exceeded.

The results of this part of the investigation of Elsea and co-workers may be summarized as follows: Delayed brittle failures were obtained in SAE 4340 steel, heat treated to high strength levels, at stresses even less than 10 per cent of the nominal ultimate tensile strength. These brittle failures occurred in unnotched specimens when a critical combination of stress, hydrogen content, and time were exceeded. Therefore, these investigators concluded that a sustained uniaxial tensile stress is sufficient (biaxial or triaxial stresses are not needed) to cause a delayed, brittle failure in the presence of sufficient hydrogen. The minimum applied stress necessary to cause failure was found to be related to the hydrogen content of the steel; it decreased as the hydrogen content increased. Both the minimum stress for failure and the time required to produce failure were relatively unaffected by differences in the composition or structure of the steel. However, both decreased as the nominal tensile strength of the steel was increased.

The results obtained by Klier, Muvdi, and Sachs<sup>(19)</sup> for the effect of applied stress on notched specimens in which the hydrogen was introduced by electroplating with cadmium were similar to those obtained by Troiano and his co-workers. For example, see Figures 8 and 9 (pages 15 and 16). However, their results for unnotched specimens (shown in Figure 16, page 32) were quite different from those obtained at Battelle Memorial Institute. With smooth specimens in which hydrogen was introduced during cadmium electroplating prior to loading the specimens (Syracuse work), the curve of breaking stress differed little from that obtained for unembrittled smooth specimens, delayed failures were not obtained at stresses appreciably lower than the tensile strength of an unembrittled specimen. However, when the smooth-type specimens were continuously charged with hydrogen while under static load, as was done at Battelle, delayed failures were obtained over a wide range of applied stresses.

Schuetz and Robertson<sup>(25)</sup> studied the delayed fracture of 10 per cent nickel steel wire in both the ferritic and the martensitic states under static stress and precharged with hydrogen for 24 hours at different current densities. They, too, found that fracture was a function of applied stress, time, and hydrogen concentration. Also, they found

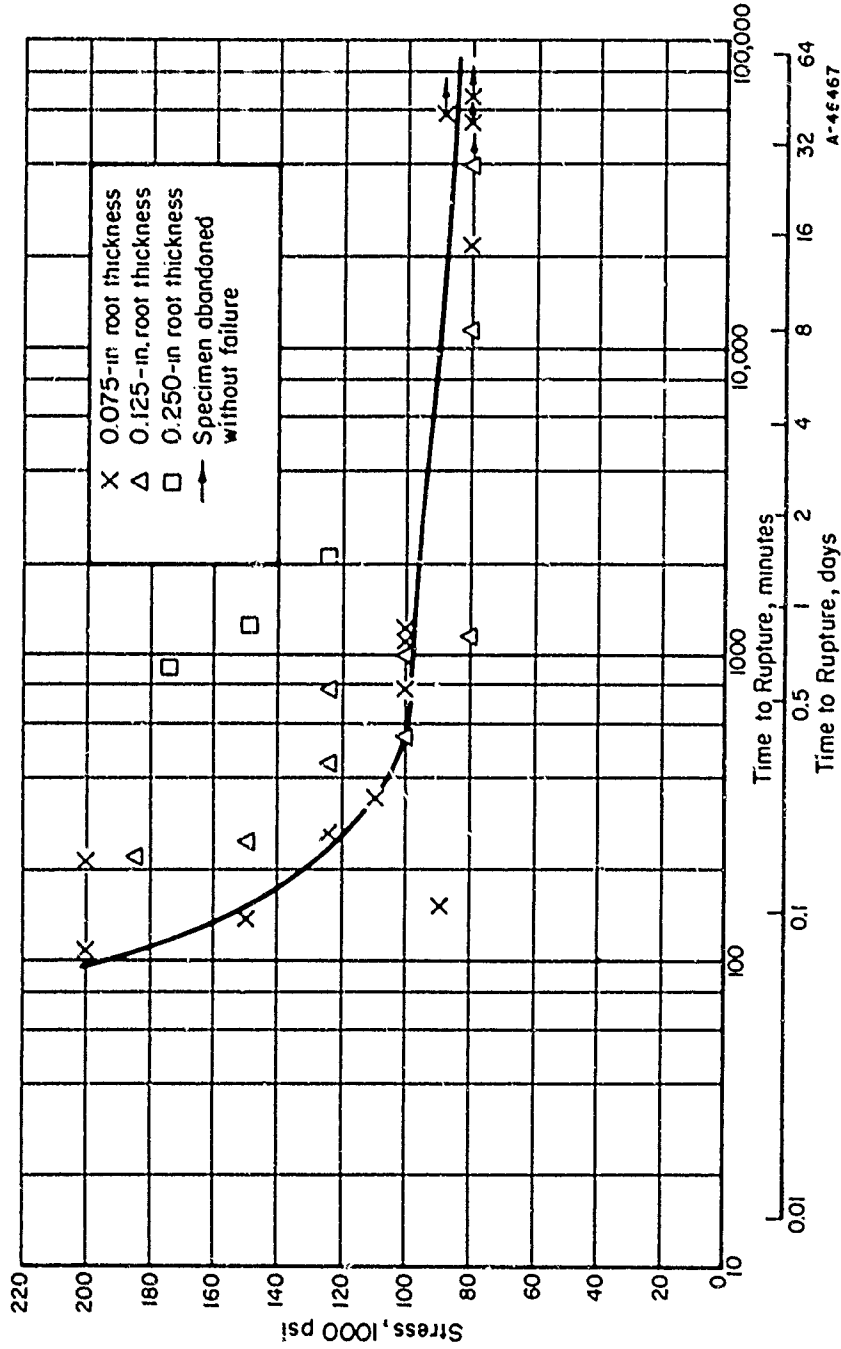


FIGURE 26. DELAYED-BRITTLE-FAILURE CHARACTERISTICS OF NOTCHED SPECIMENS OF AN SAE 4340 STEEL LOADED IN BENDING WHILE BEING CHARGED CATHODICALLY WITH HYDROGEN IN A SULFURIC ACID ELECTROLYTE ON THE COMPRESSION SIDE(8)

The specimens were heat treated to a tensile strength of 230,000 psi.

Charging Conditions:

- Electrolyte: 4 weight per cent H<sub>2</sub>SO<sub>4</sub> in water
- Poison: 5 drops per liter of cathodic poison composed of  
2 g phosphorus dissolved in 40 ml CS<sub>2</sub>
- Current density: 33 ma/in.<sup>2</sup>.

reasonably well-defined "endurance stresses" below which the material appeared to be able to support a stress indefinitely. Some of their results are shown in Figure 27. Fracture in the presaturated wires occurred with no measurable reduction in area, so the observed lower critical stress was compared with the true fracture stress of uncharged material, which was about 275,000 psi for the structure these investigators identified as ferrite. Hydrogen absorption of the magnitude involved in these experiments reduced the load-carrying capacity of the "ferritic" material to 20 to 25 per cent of that of the uncharged material, and the load-carrying capacity of the structure identified as martensite was destroyed almost completely.

Beachum, Johnson, and Stout<sup>(24)</sup> performed a study of the combined effects of hydrogen and stress on the cracking of steel welds in both plain-carbon and alloy steels. The experiments were designed to assess the contribution of hydrogen to delayed cracking of welds by the addition of controlled amounts of hydrogen directly to the welding-arc atmosphere as gaseous hydrogen, water vapor, or propane. Delayed cracks were produced in weldments of all four steels, as was discussed earlier. The results clearly demonstrated that hydrogen and the build-up of stress due to joint restraint caused delayed cracking in these weldments. For a given hydrogen content of the gas, increased restraint lowered the hardness level at which cracking would occur.

The role of stress in hydrogen-induced, delayed, brittle failure of high-strength steel has been considered in greater detail in the work of Steigerwald, Schaller, and Troiano<sup>(40, 41)</sup>.

In the early work at Case Institute of Technology with precharged, notched specimens, it was concluded that plastic flow at the root of the notch was necessary for delayed failure to occur. A specimen with a milder notch which should require a higher applied stress to produce plastic flow at the root of the notch was found to exhibit a higher minimum critical stress to produce delayed failure. However, the workers at Battelle Memorial Institute concluded from their research with continuously charged unnotched specimens, that measurable plastic flow is not a factor in the initial stages of delayed, brittle failure. This conclusion was based on the following reasoning: Within the elastic range, a brittle and a ductile material behave in the same manner. The plastic deformation which distinguishes a ductile material from a brittle material occurs only above the elastic limit. Therefore, ductility would be a factor in the sustained-static-load tests of unnotched specimens only if the stress were increased above the elastic limit or if the elastic limit of the specimens were lowered greatly by the presence of hydrogen. However, several investigators had previously shown that hydrogen does not alter the stress-strain relationship prior to fracture in a conventional tensile test of an unnotched specimen (for example, see Figure 28). Thus, they considered it unlikely that hydrogen has any large effect on the elastic limit. Therefore, the Battelle investigators concluded that, in the initiation of delayed failure, plastic flow was not required but occurred only after a crack had been formed and had grown to an appreciable size. However, the conditions during the initiation of the crack are of most importance to an understanding of the mechanism of hydrogen-induced, delayed, brittle fracture.

One of the early mechanisms<sup>(43)</sup> proposed to explain the delayed, brittle failure of high-strength steels assumed that hydrogen diffuses to defects or dislocation arrays in the lattice. The defects or dislocation arrays could be extended when the hydrogen

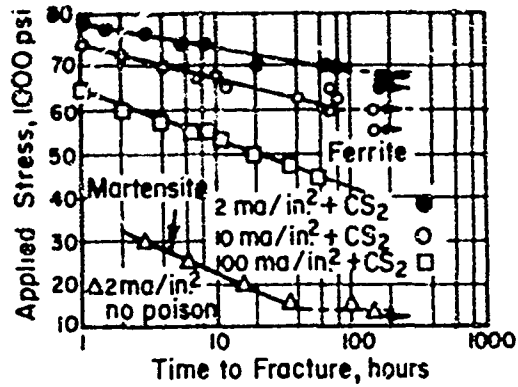


FIGURE 27. DELAYED FRACTURE OF FERRITE AND MARTENSITE IN AN IRON-NICKEL ALLOY (10Ni-90Fe) UNDER CONSTANT APPLIED STRESS AND CONSTANT HYDROGEN (SATURATION) CONCENTRATION<sup>(25)</sup>

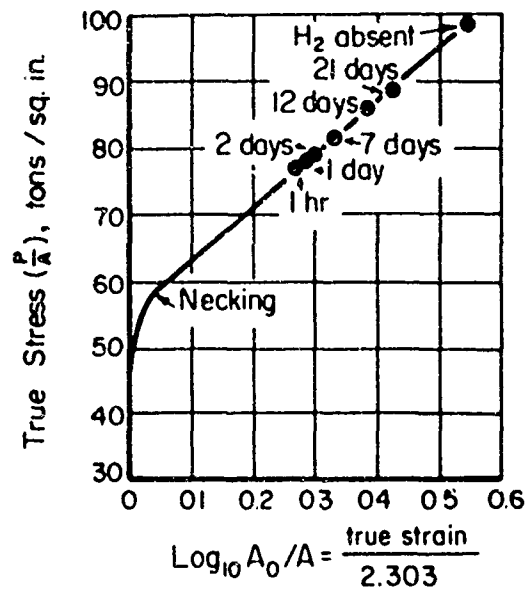


FIGURE 28. TRUE STRESS-TRUE STRAIN CURVES FOR A HYDROGEN-IMPREGNATED 3Cr-Mo STEEL AFTER STANDING IN AIR FOR VARYING PERIODS<sup>(42)</sup>

$P$  = load

$A_0$  = original cross-sectional area

$A$  = instantaneous cross-sectional area at load  $P$ .

precipitates there, either by the internal pressure of molecular hydrogen or by decreased atomic bonding across rows of hydrogen atoms. According to this mechanism, one might expect that plastic strain would have an effect on the time for delayed failures to occur. It could either increase the time by increasing the solubility of the lattice for hydrogen or it could decrease the time by providing more possible nucleation sites for cracks, as Simcoe et al. (9) pointed out. Plastic strain not only would introduce considerably more dislocation arrays but also would tend to alter any pattern of residual microstresses which might be present in the quenched-and-tempered specimens.

Various investigators performed experiments to determine the effect of plastic strain on rupture time. Elsea and co-workers at Battelle<sup>(9)</sup> plastically strained unnotched specimens of SAE 4340 steel (230,000-psi strength level) approximately 2 per cent in uniaxial tension prior to charging with hydrogen. These prestrained specimens were statically loaded and cathodically charged continuously during the test under standard conditions, along with specimens that were not prestrained. The rupture times are shown in Figure 29. For all practical purposes, the 2 per cent prestrain had no effect upon the time for failure to occur. This behavior was considered to indicate that residual stresses may not be responsible for the observed variations in rupture time with ultimate tensile strength. However, the absence of a change in rupture time with an increase in dislocation density brought about by the prestrain was not explained.

Morlet, Johnson, and Troiano at Case Institute<sup>(44)</sup> used a different approach and explored the effect of plastic strain on the subsequent tensile ductility of SAE 4340 steel heat treated to the 230,000-psi strength level and hydrogenated either before or after straining. They, too, used unnotched specimens, the 2-inch radius of the specimen barrel serving merely to insure that the specimens fractured at the midpoint. The specimens were charged with hydrogen electrolytically for 5 minutes under standard conditions and, immediately after charging, were cadmium electroplated under standard conditions. The hydrogen distribution in specimens charged under these conditions was highly nonuniform, the surface layers being high in hydrogen while the core was still hydrogen free. However, previous work had shown that specimens may be homogenized with respect to hydrogen concentration by a baking treatment at 300 F. The baking treatment drives the surface hydrogen into the specimen core, since the cadmium plate acts as a barrier to hydrogen outgassing. Therefore, in their study, a standard baking treatment of 1 hour at 300 F was used.

In one series of experiments, specimens were strained 1.5 per cent at -321 F after hydrogenation. This temperature was used because straining the hydrogenated specimens at room temperature resulted in a multitude of tiny cracks, whereas hydrogen embrittlement disappears at low temperatures, permitting strains much greater than 1.5 per cent without crack formation. The strained specimens were then aged at 150 F in an oil bath. From the results of these experiments, shown in Figure 30, it is apparent that strain caused a remarkable change in the aging characteristics of hydrogenated steel. Three separate stages may be distinguished in the aging curve for the strained specimens. During the first stage, the reduction in area increased from 22 to 37 per cent. The reduction in area decreased from 37 per cent to a minimum value of about 17 per cent in the second stage. In the third stage, the ductility increased and in a manner similar to that of the unstrained specimens. The variation in ductility during the first two stages of aging was particularly striking when compared with the aging curve for the unstrained specimens. In the same time interval, the ductility of the unstrained specimens decreased slightly and then began to increase, presumably due to

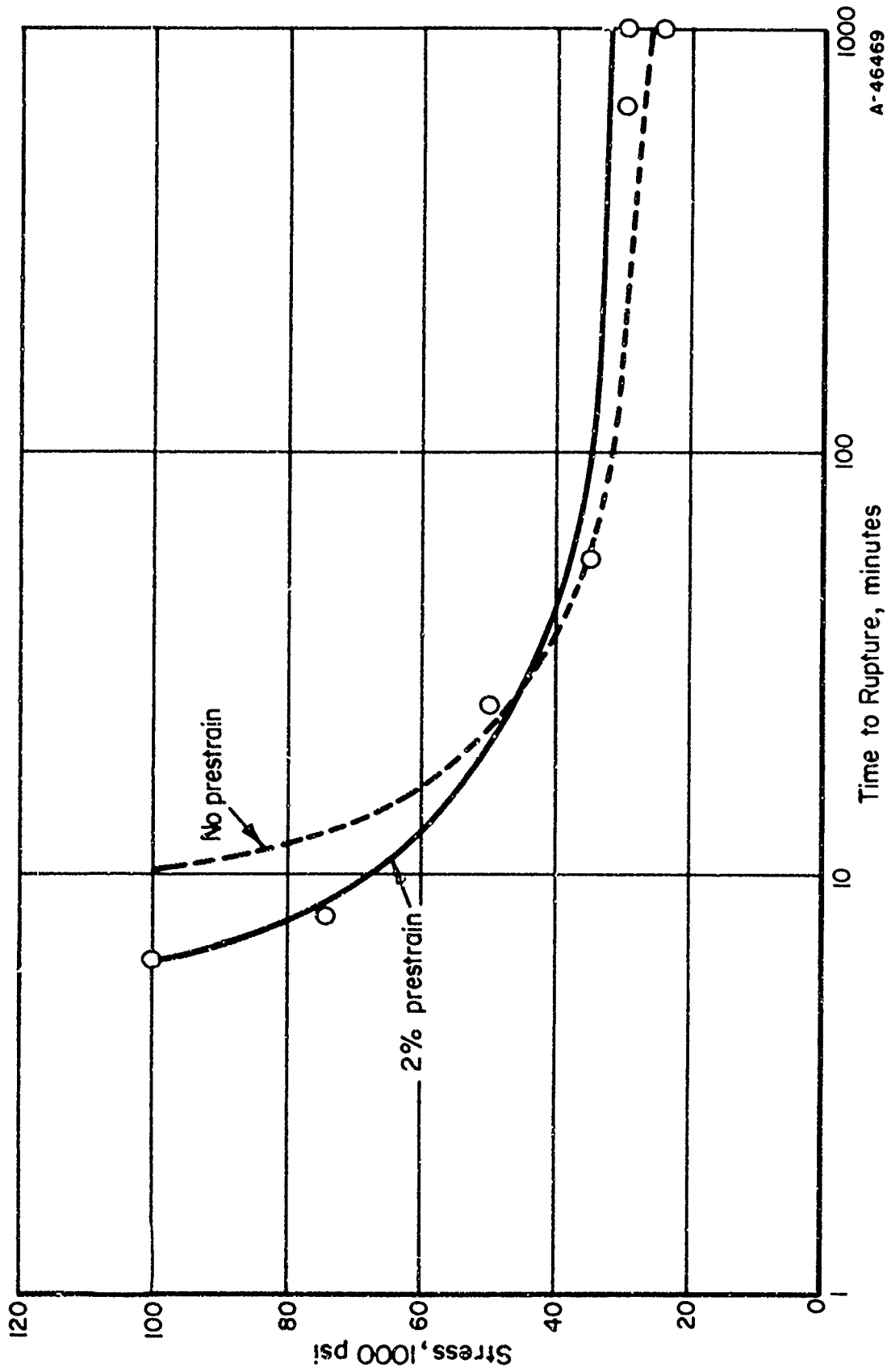


FIGURE 29. TIME FOR FAILURE AS A FUNCTION OF APPLIED STRESS WITH AND WITHOUT 2 PER CENT PLASTIC PRESTRAIN(9)

SAE 4340 steel, ultimate tensile strength 230,000 psi.

Charging Conditions Used:

Electrolyte: 4 per cent by weight of  $H_2SO_4$  in water

Poison: 5 drops per liter of cathodic poison composed of  
2 g phosphorus dissolved in 40 ml  $CS_2$

Current density: 10 ma/in.<sup>2</sup>.

A-46469

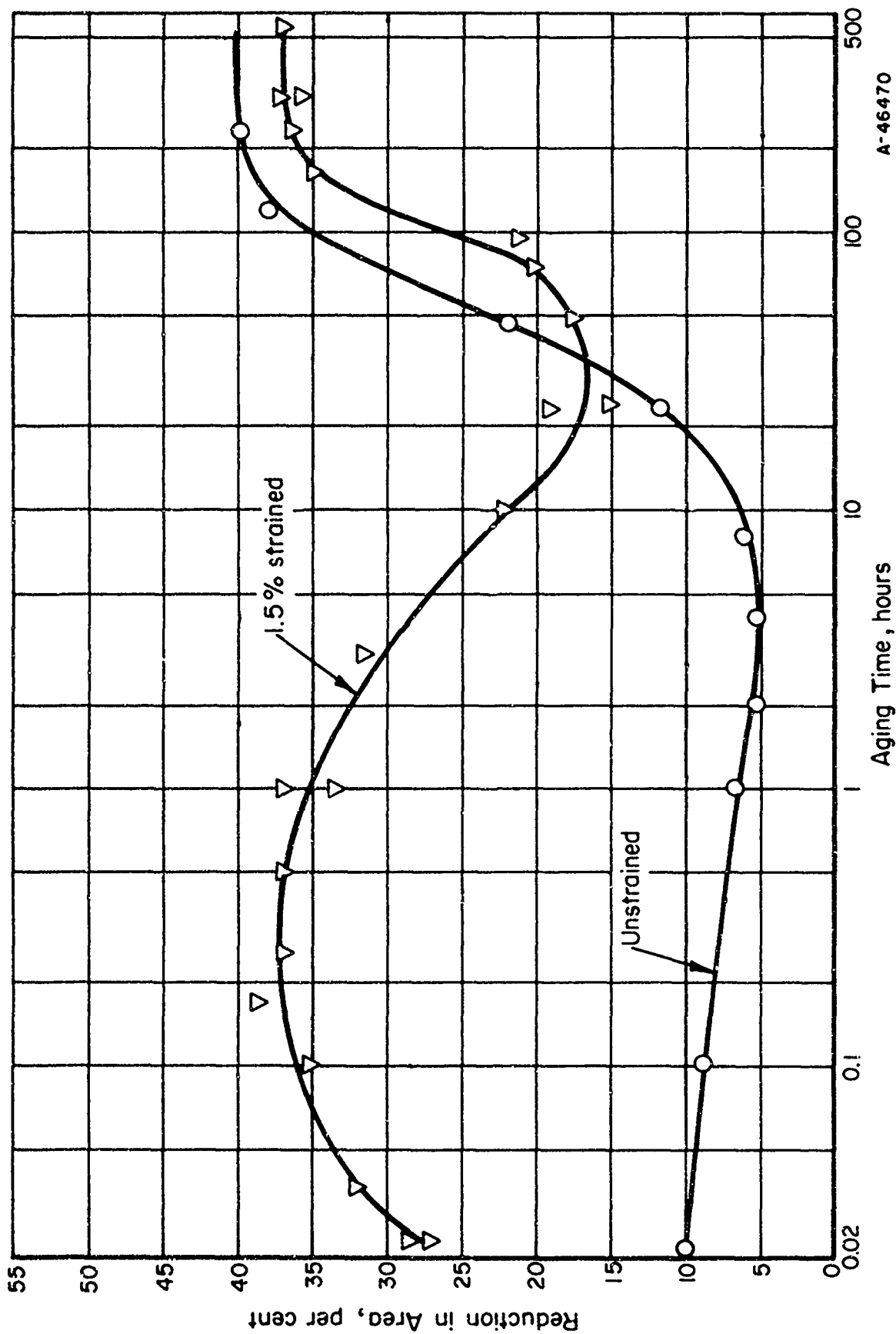


FIGURE 30. THE EFFECT OF AGING AT 150 F ON SPECIMENS UNSTRAINED AND STRAINED 1.5 PER CENT IN LIQUID NITROGEN(44)

A-46470



hydrogen outgassing. The difference in shape of the two aging curves resulted only from the strain and not from immersion in liquid nitrogen. This was shown by specimens that were treated identically except that, for the one group, no straining was done during the immersion in liquid nitrogen. Specimens of the latter group exhibited ductilities that fell on the aging curve for unstrained specimens.

These investigators used these data to evaluate proposed theories of hydrogen embrittlement. They considered that, prior to straining, a steady-state distribution exists between hydrogen in the lattice and hydrogen in the voids. Straining changes the steady-state distribution by increasing the occlusive capacity of the voids. Thus, establishment of a new steady-state distribution requires hydrogen to move from the lattice to the voids. During straining at  $-321$  F, hydrogen is immobile, however, at  $150$  F the hydrogen diffusion rate is vastly increased, and hydrogen will diffuse to the voids during the aging treatment. These workers discussed both the pressure theory and the classical adsorption theory and showed that both required increasing embrittlement during initial aging. Since this requirement was at variance with the experimental results shown in Figure 30, they concluded that neither mechanism was satisfactory. Therefore, they developed a new theory which is discussed later. However, according to their hypothesis, the strain magnitude influences the aging characteristics. As the strain is increased, the steady-state hydrogen content of the voids will increase, and the lattice hydrogen content must decrease.

Other experiments showed that the pseudorecovery observed in the first stage of aging is accelerated by increasing strain, which is in agreement with the postulated mechanism. This behavior is shown by the aging curves for hydrogenated specimens strained 3 per cent or 6 per cent at  $-321$  F and aged at  $150$  F (see Figure 31). The influence of strain on the aging characteristics is summarized in Figure 32. As the strain is increased, the driving force for hydrogen diffusion from the lattice to the voids is increased. Also, as the strain is increased, the level of ductility observed at the minimum at the end of the second stage of aging is increased and displaced to longer aging times. This observed behavior can be accounted for by two factors — the depletion of the lattice hydrogen content with increasing strain, and the increasing importance of outgassing at long aging times. Extrapolation of the shapes of the aging curves to larger strains suggested that the embrittlement will essentially disappear at a sufficiently large strain. This was found to be the case for specimens strained 12 per cent at  $-321$  F and aged at  $150$  F, as shown in Figure 33. The recovery curve is a horizontal line at a level of ductility equal to, or only slightly below, the ductility of uncharged specimens.

It was concluded that the strain-induced recovery is due entirely to the redistribution of hydrogen, the gross hydrogen content of the specimens remaining constant during the process. For the test conditions used for the above-described experiments, 12 per cent strain increased the occlusive capacity of the voids enough to completely drain the lattice of damaging hydrogen in establishing the new steady-state distribution. On the other hand, these investigators found that elastic straining did not affect the aging characteristics, for unstrained and elastically strained specimens exhibited identical aging curves. This is striking evidence of the localized redistribution of hydrogen resulting from plastic deformation.

The aging characteristics exhibited after room-temperature straining also were studied. Premature crack formation limited strain of the hydrogenated steel at room temperature to 0.2 per cent reduction in area. Qualitatively, room-temperature straining exerted the same effect as straining at  $-321$  F, but the magnitude of the effect was

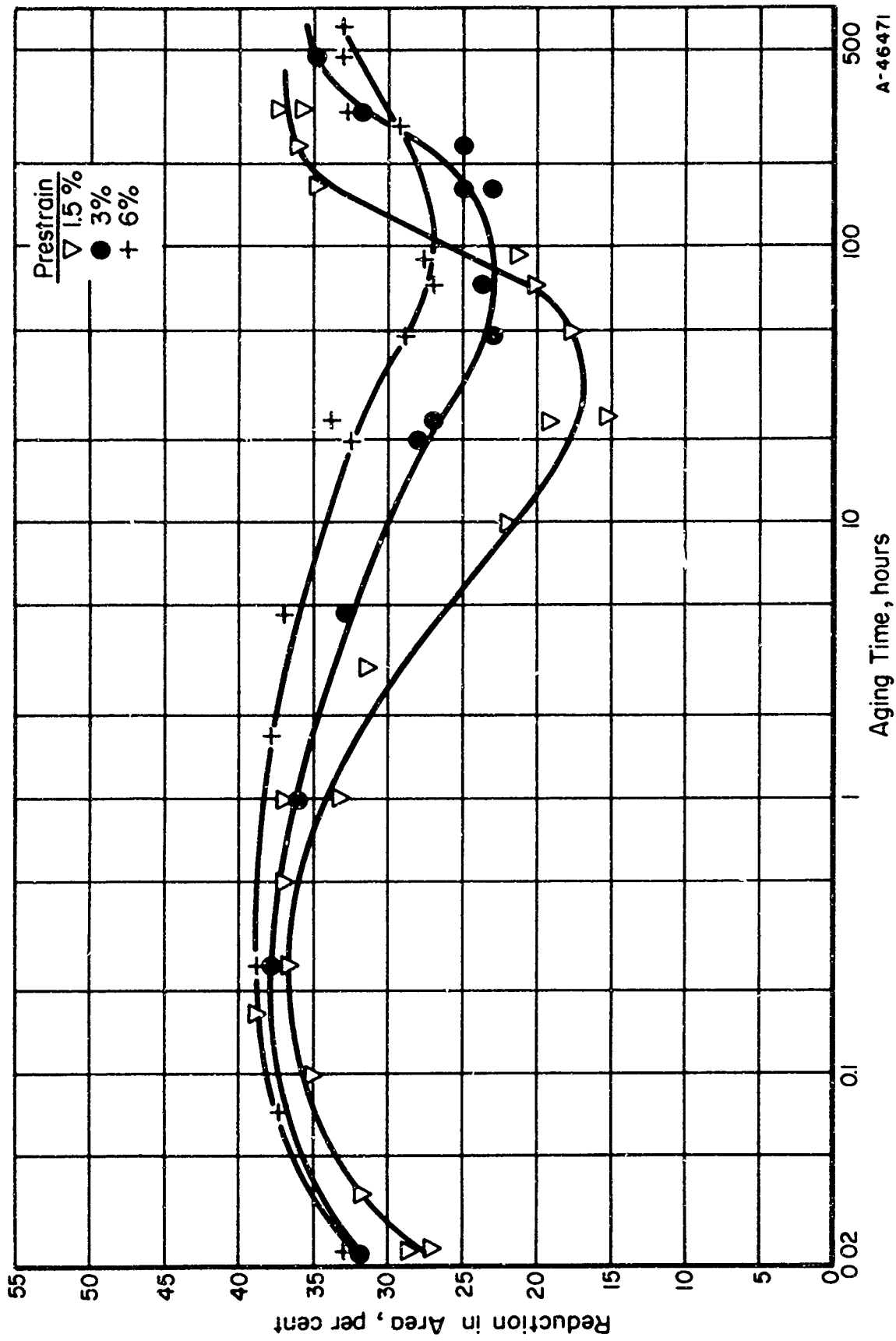


FIGURE 31. THE EFFECT OF AGING AT 150 F ON SPECIMENS STRAINED DIFFERENT AMOUNTS IN LIQUID NITROGEN<sup>(44)</sup>

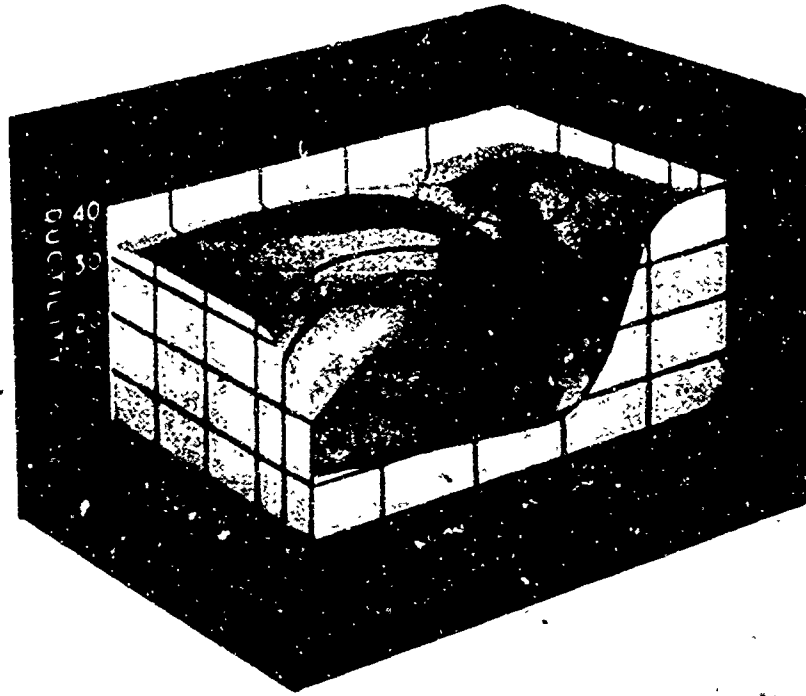


FIGURE 32. AGING CHARACTERISTICS OF SPECIMENS STRAINED DIFFERENT AMOUNTS IN LIQUID NITROGEN AFTER CHARGING<sup>(44)</sup>

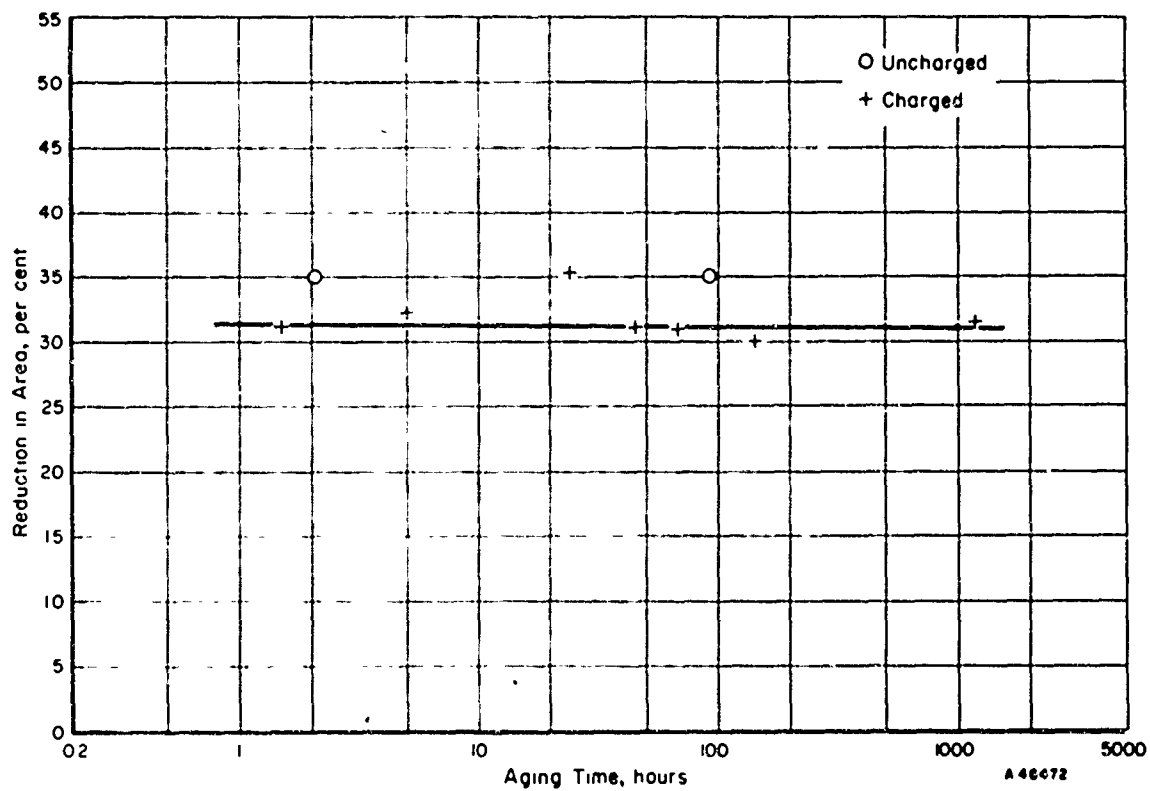


FIGURE 33. THE EFFECT OF AGING AT 150 F ON SPECIMENS STRAINED 12 PER CENT IN LIQUID NITROGEN<sup>(44)</sup>

much less. It was possible to introduce larger strains at room temperature by taking advantage of the ductility increase that occurs during the first stage of aging of strained hydrogenated steel. Specimens strained 1.5 per cent at -321 F and aged 30 minutes at 150 F had a reduction in area of about 37 per cent. Under these conditions a second strain of 1.5 per cent could be introduced at room temperature without crack formation. The results of aging such double-strained material showed that no essential difference was introduced by variation in straining temperature.

To complete the picture, Morlet et al.<sup>(44)</sup> investigated the effect of prior deformation on the aging characteristics after hydrogenation. Aging curves were determined for specimens of the same steel strained to 1.5 per cent or 6 per cent reduction in area and then subjected to the standard hydrogenation, cadmium plating, and baking. When aged at 150 F, prior strain raised the initial ductility, which, they concluded, resulted from the greater void capacity for hydrogen. However, some differences were found between straining before or after hydrogenation, particularly in the strain dependence of the ductility minima and in the recovery rates.

Johnson, Johnson, Morlet, and Troiano<sup>(45)</sup> investigated the effects of prestressing on the delayed-failure characteristics of SAE 4340 steel using sharp-notch specimens. The steel was heat treated to have an ultimate tensile strength of 240,000 psi. Prestressing prior to the introduction of hydrogen by cathodic charging (conditions which resulted in a surface concentration of hydrogen) exerted a strong influence on the parameters of delayed failure under static loading. The two levels of prestressing employed, 250,000 and 275,000 psi on the area under the notch, produced reductions in the area under the notch of approximately 0.5 and 0.8 per cent, respectively. In Figure 34, the delayed-failure behavior of these materials is compared with that obtained for specimens of the same strength level which had been charged in a similar manner but not prestressed. The charged notched tensile strength was increased by 35,000 psi as a result of the higher level of prestressing. Also, the lower critical stress was raised substantially - more than 50,000 psi - by the higher prestress. The failure time may have increased, but only slightly. To obtain more information on the effect of prestressing on rupture time, the crack-propagation characteristics were determined as a function of prestressing by the electrical resistivity method, for an applied stress of 125,000 psi. Figure 35, a plot of crack area versus static-loading time, shows that the initial crack area (the cracking occurring on loading) of 26 per cent was reduced to 13 per cent and to 2 per cent by prestresses of 250,000 psi and 275,000 psi, respectively. In addition, the initial crack-propagation rate was reduced by prestressing, but the rates in the later stages appeared to be comparable. The differences in crack-propagation characteristics as a result of prestressing were even more pronounced when the crack depth was plotted as a function of the square root of the static-loading time, as in Figure 36. The parabolic relationship between crack depth and time that was normally observed without prestressing (see the linear portion between the arrows on the curve representing no prestressing) was altered appreciably in the initial stages by prestressing prior to charging with hydrogen. A similar dependence of the crack-propagation characteristics upon prestressing also was obtained for applied stresses of 175,000 and 200,000 psi.

The investigators were not able to fully interpret the results of this experiment at the time the work was completed, because they could be rationalized on more than one basis. One viewpoint was that the plastic strain produced in prestressing inhibits crack initiation and propagation. A second approach was that the plastic strain affects the

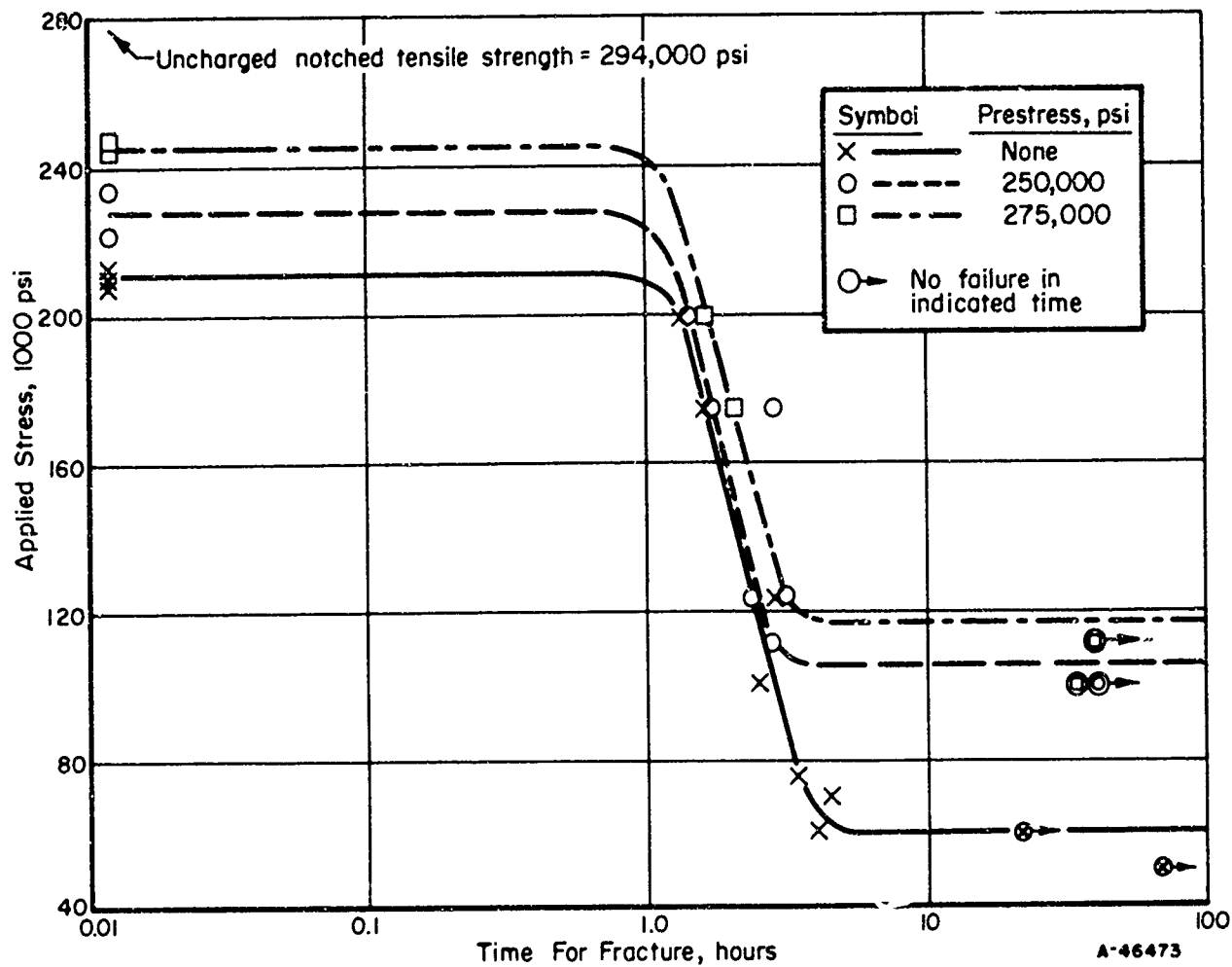


FIGURE 34. DELAYED-FAILURE BEHAVIOR FOR VARIOUS LEVELS OF PRESTRESSING FOR SHARP-NOTCH SPECIMENS AT THE 240,000-PSI STRENGTH LEVEL<sup>(45)</sup>

Charged after prestressing.

Aged 5 minutes at room temperature.

Case Institute of Technology Charging Condition A:

Electrolyte: 4 per cent  $H_2SO_4$  in water

Poison: None

Current density: 20 ma/in.<sup>2</sup>

Charging time: 5 minutes

Aging time: Measured from end of charging to start of test.

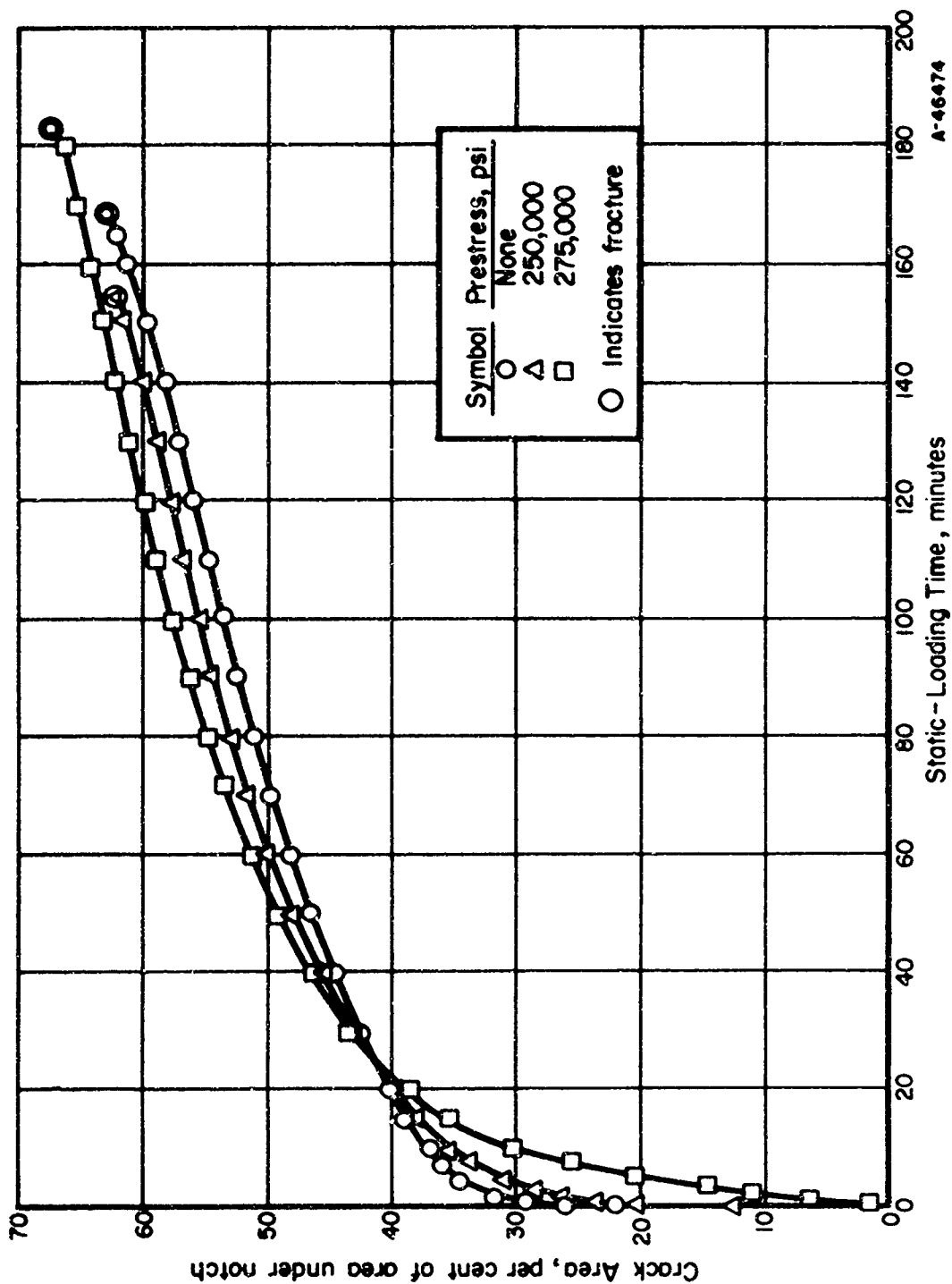


FIGURE 35. CRACK AREA VERSUS STATIC-LOADING TIME AT AN APPLIED STRESS OF 125,000 PSI FOR VARIOUS LEVELS OF PRESTRESSING OF SPECIMENS HEAT TREATED TO THE 240,000-PSI STRENGTH LEVEL(45)

Charged after prestressing.

Aged 5 minutes at room temperature.

Case Institute of Technology Charging Condition A, as given in Figure 34.

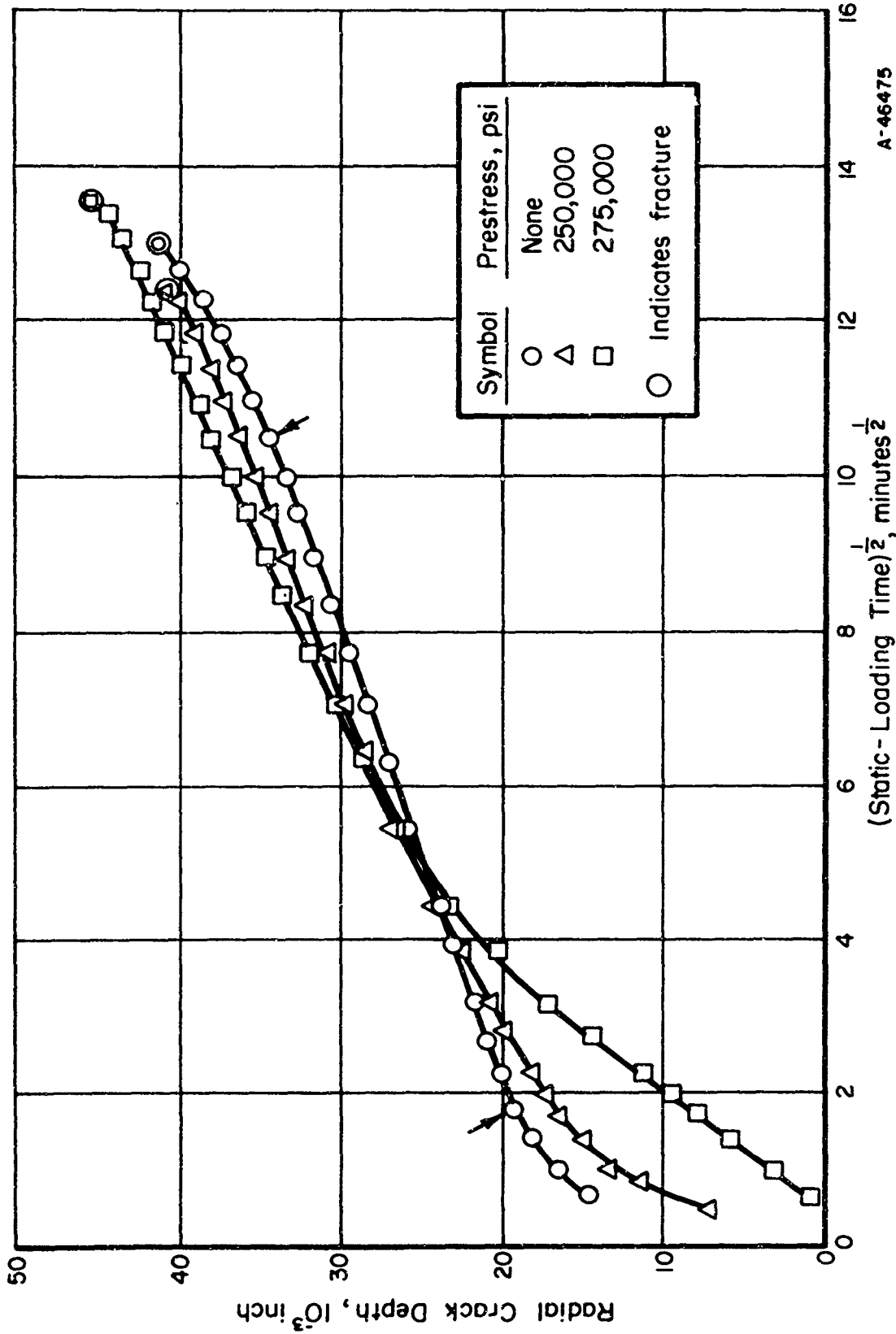


FIGURE 36. RADIAL CRACK DEPTH VERSUS THE SQUARE ROOT OF THE STATIC-LOADING TIME AT AN APPLIED STRESS OF 125,000 PSI FOR VARIOUS LEVELS OF PRESTRESSING OF SPECIMENS HEAT TREATED TO THE 240,000-PSI STRENGTH LEVEL(45)

Case Institute of Technology Charging Condition A, as given in Figure 34.

hydrogen distribution resulting from a given external charging condition. Both approaches were based on sound physical evidence found throughout the literature. On the other hand, the experiment did have some very important results. It had been suggested previously that plastic strain is necessary to initiate delayed failure (in a study of notched specimens)<sup>(5)</sup>. However, some of the specimens in the present experiment were prestressed at 275,000 psi before charging, so no additional plastic strain would be anticipated when stressed at 125,000 psi subsequent to charging. Even so, delayed failure occurred at the lower stress. If strain were necessary to initiate delayed failure, prestressing would be expected to enhance rather than retard the phenomenon.

The conclusion that plastic strain is not necessary to initiate delayed failure in notched specimens is in agreement with the finding of Elsea and co-workers, discussed earlier, that appreciable plastic strain is not required to initiate failure in unnotched specimens.

Bastien and Amiot<sup>(46)</sup>, in studying the delayed failure in a hydrogenated 0.08 per cent carbon steel with a pearlitic structure, found that different results could be obtained depending on the sequence of loading and charging with hydrogen. The tensile strength of the material was 37.5 kg/mm<sup>2</sup> (53,400 psi) and the upper yield strength was 24.0 kg/mm<sup>2</sup> (34,200 psi). When the specimens were charged electrolytically prior to being subjected to the static tensile stress, the maximum load which did not produce failure during 100 hours (the lower critical stress) was 21 kg/mm<sup>2</sup>, or 29,900 psi. However, when stressed for 24 hours before the beginning of hydrogenation, stresses of 28.5 kg/mm<sup>2</sup> (40,500 psi) did not induce failure even after 300 hours.

### THE EFFECT OF HYDROGEN CONTENT

From data presented in the preceding sections, it is apparent that there is a definite correlation between the presence of hydrogen and delayed, brittle failures of high-strength steel. This was clearly demonstrated by the early studies of these failures at Case Institute of Technology<sup>(4, 5)</sup>, Battelle Memorial Institute<sup>(7)</sup>, Syracuse University<sup>(10)</sup>, and the Naval Research Laboratory<sup>(12)</sup>. Therefore, this aspect of the effect of hydrogen will not be discussed further here, except to refer the reader to a comparison of charged and uncharged specimens under static loading in Figure 1 (page 5). Also, it has been shown earlier in this report that delayed, brittle failures occur when a critical combination of stress, hydrogen content, and time is exceeded, provided conditions permit the hydrogen in the steel to move freely, either under a hydrogen gradient or under a stress gradient.

Numerous investigators have studied the effects of variations in hydrogen content. Because the problems in hydrogen analysis are very great as a result of the small amount usually present and the great mobility of hydrogen even at room temperature, many of the investigations relied upon such criteria as variations in cathodic charging time, variations in current density, variations in aging time after charging, or variations in the concentration of, or time of exposure to, nonelectrolytic liquid environments (usually acids) as the basis for evaluating the effects of variations in hydrogen content. Although hydrogen has been introduced into steel under a multitude of conditions, the results of the various investigations nearly all concur in showing that the delayed



failures depend directly on the hydrogen content. If the hydrogen can be kept out or removed from the steel before the part is subjected to conditions which result in permanent damage, the problem is circumvented. However, this is not easy to do because of the numerous processing operations that are potential sources of hydrogen and because of the very small amount of hydrogen (as little as 1 ppm, or possibly less) that can induce failure. Another important point that has been demonstrated numerous times is that, although baking to "remove" hydrogen can result in full recovery of ductility as determined in a standard tensile test, frequently such a treatment is not sufficient to prevent delayed failure at a low stress under conditions of static loading.

Bucknall, Nicholls, and Toft<sup>(47)</sup> reported encountering delayed failures in several high-strength steels without the intentional introduction of hydrogen after heat treatment and with no obvious source of hydrogen, such as acid pickling or an electroplating operation, being used after heat treatment. They did not recognize that hydrogen was the culprit. Conical disk specimens similar to Bellville springs were compressed by tightening a bolt and then were observed periodically, usually for 100 days. The most important factor governing the tendency to crack after some time delay appeared to be the hardness of the plate. There was a hardness below which, under the conditions of stressing, no specimens cracked during the 100-day test period. For a given material, at some higher hardness all specimens cracked, and at some intermediate hardness, some specimens cracked and others did not, the proportion which cracked rising as the hardness increased. For all steels examined, the water-quenched condition was most susceptible to delayed cracking, the oil-quenched condition was less susceptible, and the tempered material was least susceptible. The following example shows the results for a Ni-Cr-Mo-V steel.

<u>Hardness, BHN</u>	<u>Number of Specimens Tested</u>	<u>Number Cracked Within 100 Days</u>	<u>Proportion Cracked Within 100 Days, per cent</u>
>521	1	1	100
491-520	5	4	80
461-490	13	8	60
431-460	11	0	0
401-430	2	0	0

The investigators concluded that every precaution should be taken to reduce internal stresses, and the plates should be used at the minimum hardness consistent with the required properties.

Barnett and Troiano<sup>(6)</sup> showed that the susceptibility to delayed failures which Bucknall et al. observed was most prevalent when the material in processing had been subjected to an environment conducive to the absorption of hydrogen.

Bell and Sully<sup>(48)</sup> also obtained delayed failures in a high-strength steel without intentionally charging it with hydrogen after heat treatment. However, these investigators also introduced hydrogen electrolytically in other specimens of the same steel and obtained delayed failures at far lower stresses. They studied a plain-carbon steel (0.8 to 0.9 per cent carbon) at hardness levels of approximately 560 DPN and approximately 500 DPN. Static stresses were obtained in bending by using a Seeger-circlip specimen, one end of which was held stationary and the other end moved away from the fixed end by a screw arrangement with a vernier scale attached. As stress relieved for 24 hours at 160 C (320 F), the average breaking deflection was 1.110 inch. When

electrolytically pickled and tested immediately, this value was reduced to 0.300 inch. However, storage at room temperature gave gradual recovery, and after 115 hours at room temperature 93 per cent of the breaking deflection of uncharged specimens was achieved. When unpickled clips of the 560-DPN material were set to a certain deflection less than that required to cause immediate fracture, 80 per cent broke within the duration of the test (250-350 hours). The average delay for all those that broke was 2580 minutes, but 7.7 per cent broke in less than 10 minutes. When electrolytically pickled 560-DPN clips were allowed to recover for 115 hours at room temperature prior to static testing, the proportion of clips that failed was about the same as for those that were not charged electrolytically. However, the proportion of the failed clips that broke in less than 10 minutes was much higher, being 71 per cent. Particularly significant was the finding that electrolytically charged clips which were aged 115 hours at room temperature and then were baked up to 16 hours at 200 C (392 F) still showed some effects of the electrolytic charging treatment, and this was without cadmium or other plating to retard hydrogen outgassing. These results demonstrated quite clearly that the introduction of hydrogen into steel of a high hardness level has a marked effect on the tendency of the steel to delayed failure at stresses below the ultimate tensile strength, even after the steel is stored or baked to remove absorbed hydrogen and after recovery of the short-time mechanical properties, as normally measured, is substantially complete.

In the work of Elsea and co-workers described in previous sections, continuous cathodic charging with 4 per cent sulfuric acid with the phosphorus poison at a current density of 8 ma/in.<sup>2</sup> (their Condition A) produced relatively high contents of hydrogen in the unnotched static-loading specimens. They recognized that service parts almost certainly have lower hydrogen contents than those produced in their statically loaded specimens. Therefore, both static-loading tests and experiments involving the permeability of hydrogen through steel were employed to find cathodic charging conditions which would result in low hydrogen contents<sup>(8)</sup>. In the static-loading tests, it was assumed that, other conditions being constant, an increase in the minimum stress for failure would be the result of a lower hydrogen content. The validity of this assumption was verified later by hydrogen analyses performed on specimens that were cathodically charged in a manner similar to that used in the static-loading tests.

The concentration of hydrogen cathodically charged into a steel, per unit of time, is observed to decrease as current density is decreased. However, in efforts to achieve low hydrogen contents, full advantage could not be taken of this current density-hydrogen content relationship when the sulfuric acid electrolyte was used. The current density could not be permitted to be less than about 8 ma/in.<sup>2</sup> because of the danger of losing the cathodic protection necessary to prevent attack by the electrolyte. If cathodic protection were lost, pitting-type corrosion would occur. This would reduce the cross-sectional area and introduce stress concentration. Also, the metal-acid reaction would result in varying and uncontrolled amounts of hydrogen being absorbed by the specimen.

One would expect that lower current densities would be required for cathodic protection against weak acids than against strong acids. To investigate this surmise, static-loading tests were conducted in which the electrolyte was composed of 10 per cent acetic acid, 45 per cent ethylene glycol, and 45 per cent water by volume and the current density was 1 ma/in.<sup>2</sup>. This was referred to as Charging Condition B. The results, shown in Figure 37, were similar to those obtained with the sulfuric acid electrolyte (Condition A), except that higher stresses and longer times were required to

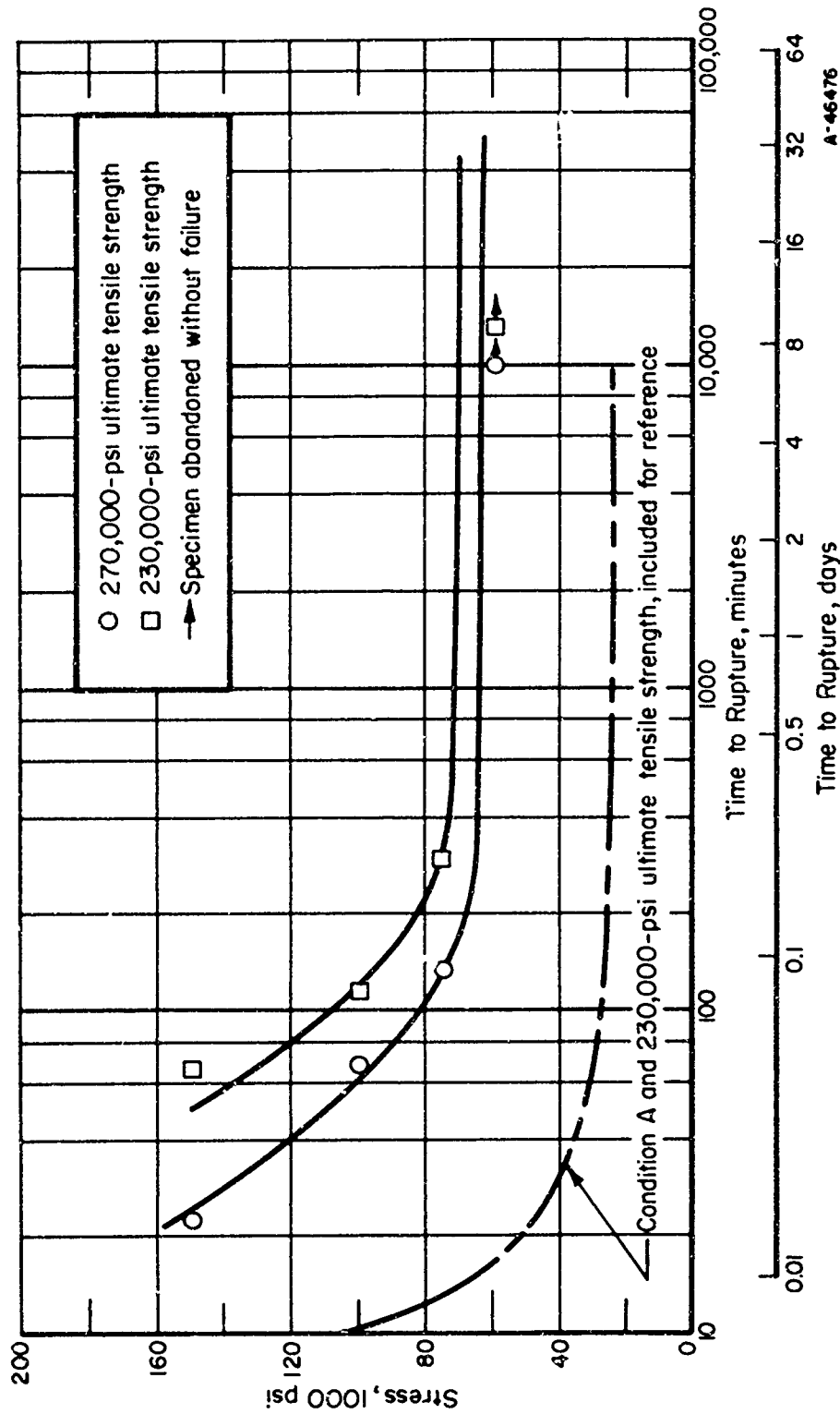


FIGURE 37. DELAYED-FAILURE BEHAVIOR OF AN SAE 4340 STEEL DURING CATHODIC CHARGING IN AN ACETIC ACID ELECTROLYTE AT 1 MA/IN.<sup>2</sup>(8)

Battelle Charging Condition B:

Electrolyte: 10 per cent acetic acid, 45 per cent ethylene glycol,  
and 45 per cent water by volume

Current density: 1 ma/in.<sup>2</sup>.

produce rupture. The minimum stress for failure was apparently between 60,000 and 75,000 psi for SAE 4340 steel at the 230,000-psi strength level, in contrast to the minimum stress for failure of about 25,000 psi with Condition A. However, cathodic protection of the specimen was lost when the current density was reduced below 1 ma/in.<sup>2</sup> for this electrolyte. Therefore, the series of experiments with this electrolyte was abandoned without hydrogen analyses to confirm the presumably lower hydrogen content. However, data from the permeability experiments indicated that Charging Condition B produced an equilibrium hydrogen content that was approximately 1/3 that produced by Charging Condition A.

No further effort was made to find an acid solution with which cathodic protection could be provided at much lower current densities. Instead, several other electrolytes were used in exploratory experiments. These consisted of either buffered solutions of weak acids or solutions of sodium hydroxide of various concentrations. The results of static-loading tests involving cathodic charging in 1/2 per cent sodium hydroxide solution at two current densities are shown in Figure 38. Cathodic charging in 1/2 per cent sodium hydroxide at 125 ma/in.<sup>2</sup> was Condition C, charging at 500 ma/in.<sup>2</sup> was Condition D. Compared with the time to rupture in the sulfuric acid electrolyte with phosphorus poison at 8 ma/in.<sup>2</sup> (Condition A), it was found that the time to rupture in the sodium hydroxide electrolyte was greater by one order of magnitude for the higher current density and by about two orders of magnitude for the lower current density. One specimen, cathodically charged continuously at 125 ma/in.<sup>2</sup> and stressed at 100,000 psi, failed after 11.4 days. The minimum stress for failure was not determined for these conditions.

Although the data contain some apparent contradictions, the results of hydrogen analyses made on specimens charged under Conditions A, C, and D (see Table 10) indicate that the minimum stress for failure was a function of the hydrogen content; the minimum stress for failure decreased with increasing hydrogen content. In the

TABLE 10. HYDROGEN CONTENT OF AN SAE 4340 STEEL (230,000-PSI ULTIMATE TENSILE STRENGTH) AFTER CATHODIC CHARGING UNDER VARIOUS CONDITIONS (8)

Condition	Cathodic Charging Conditions			Hydrogen Content <sup>(b)</sup> , ppm
	Electrolyte	Current Density, ma/in. <sup>2</sup>	Time, hours	
--	--	Uncharged <sup>(a)</sup>	--	0.4, 1.3
A	4% sulfuric acid and poison	8	24	6.7, 8.6
A	Ditto	8	48	1.8
D	1/2% sodium hydroxide	500	24	0.6
D	Ditto	500	336	2.9, 5.0
C	Ditto	125	336	0.8, 2.1

(a) The uncharged specimens were aged for 18 days at room temperature after final heat treatment and then were stored in liquid nitrogen prior to analysis.

(b) Two values indicate duplicate tests, cathodically charged and analyzed separately. All specimens were stored in liquid nitrogen within 3 minutes of completion of cathodic charging.

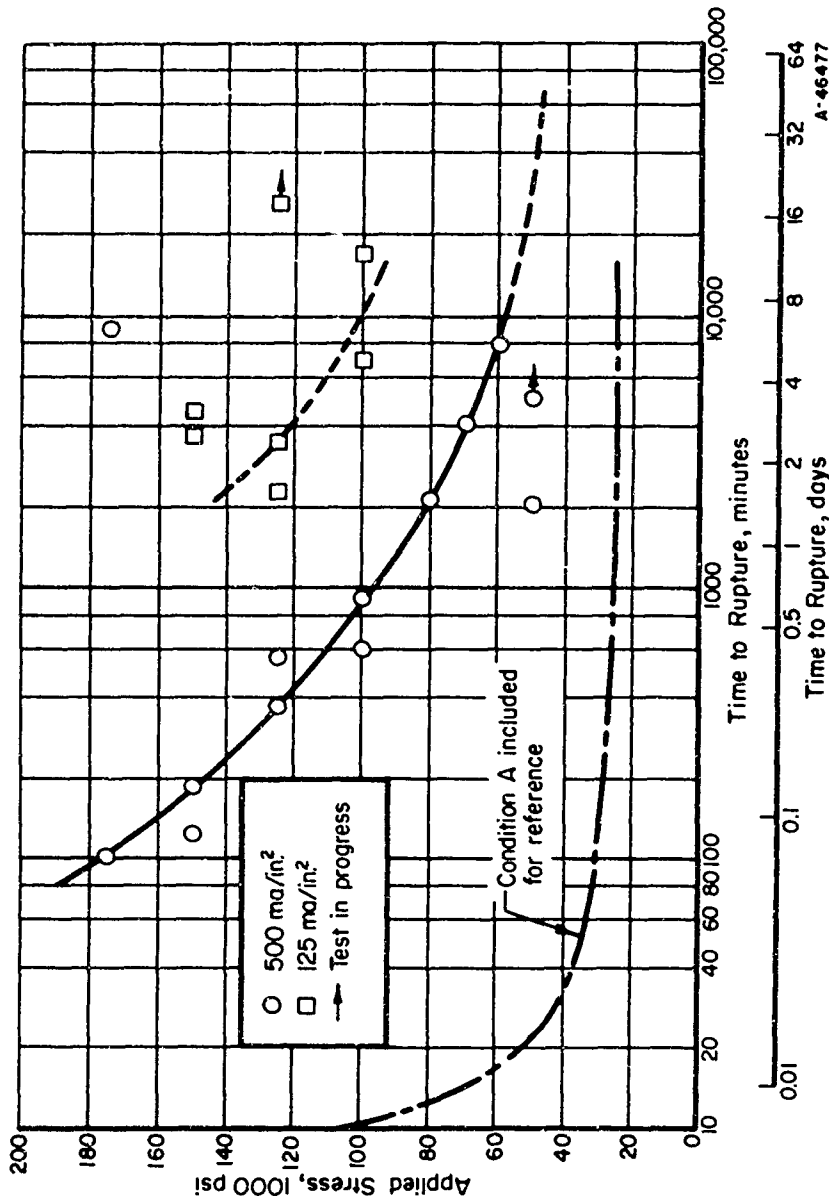


FIGURE 38. DELAYED-FAILURE BEHAVIOR OF AN SAE 4340 STEEL WITH AN ULTIMATE STRENGTH OF 230,000 PSI DURING CATHODIC CHARGING IN A 1/2 PER CENT SODIUM HYDROXIDE ELECTROLYTE(8)

Battelle Charging Condition C:

Electrolyte: 1/2 per cent sodium hydroxide in water  
 Current density: 125 ma/in. <sup>2</sup>.

Battelle Charging Condition D:

Electrolyte: 1/2 per cent sodium hydroxide in water  
 Current density: 500 ma/in. <sup>2</sup>.

permeability experiments, the flow of hydrogen through the specimen charged at 8 ma/in.<sup>2</sup> in the sulfuric acid electrolyte with phosphorus poison was approximately 6 times the flow through the specimen charged at 500 ma/in.<sup>2</sup> in the sodium hydroxide electrolyte. However, the hydrogen contents for those charging conditions of electrolyte and current density and for times of 24 and 336 hours, respectively, were in the ratio of roughly 2. The longer time, 336 hours, for the sodium hydroxide electrolyte was used as a basis for comparison, because the permeability experiments indicated that steady-state permeability was achieved with the alkaline electrolyte only after a much longer time than with the acid electrolyte.

In a continuation of this work<sup>(9)</sup>, a study was undertaken to determine the range in rupture times which could be obtained by varying the rate at which hydrogen entered an unnotched specimen being charged continuously while under a constant sustained load. The rate was varied by using different electrolytes and by varying the current density with a given electrolyte. The rupture times are shown as a function of the applied stress in Figure 39 for the 1/2 per cent sodium hydroxide electrolyte at 500 ma/in.<sup>2</sup> current density and for the 4 per cent sulfuric acid electrolyte at both 10 and 500 ma/in.<sup>2</sup>. The rupture time increased markedly with decreasing current density in the sulfuric acid electrolyte, and increased further by changing from the sulfuric acid to the sodium hydroxide electrolyte. There was little variation in the lower critical stress for failure with variations in charging conditions.

It was concluded that the observed variations in rupture time must reflect variations in the rate at which hydrogen was introduced into the steel. To verify this, a series of permeability experiments was performed in which the composition of the electrolyte, the current density, and the thickness of the permeation specimen were varied. The results of these experiments are shown in Figure 40, where the log of the steady-state permeation rate is plotted as a function of the log of the current density for two different electrolytes. In all cases, the data fit a straight line reasonably well. The hydrogen permeation rates obtained with the sulfuric acid electrolyte and a 0.010-inch-thick cathode specimen ranged from  $0.3 \times 10^{-3}$  to  $5.0 \times 10^{-3}$  in.<sup>3</sup>/in.<sup>2</sup>/min when the current density was increased from 10 to 300 ma/in.<sup>2</sup>. The permeation rates were considerably less for the sodium hydroxide electrolyte; they ranged from  $0.002 \times 10^{-3}$  to  $0.05 \times 10^{-3}$  in.<sup>3</sup>/in.<sup>2</sup>/min when the current density was increased from about 40 to 600 ma/in.<sup>2</sup> for a specimen of the same thickness. These data showed a considerable difference in the permeation rates between the sodium hydroxide and sulfuric acid electrolytes. It was concluded that these variations in permeation rates probably were responsible for the variation in rupture times shown in Figure 39.

The effect of variations in hydrogen-absorption rate on the rupture time was determined by subjecting unnotched tensile specimens to sustained static tensile loads while at the same time charging them cathodically at various current densities in both the 4 per cent sulfuric acid and the 1/2 per cent sodium hydroxide electrolytes. The data obtained at various applied stresses are shown in Figure 41 for the steel with 230,000-psi ultimate tensile strength, and in Figure 42 for the steel with 190,000-psi ultimate tensile strength. In these figures, the log of the rupture time was plotted as a function of the log of the permeation rate obtained through the 0.010-inch-thick steel for the particular charging conditions used in the rupture tests. The steady-state permeation rate through the 0.010-inch specimen was selected as a criterion of absorption rate because of the short time required to establish the steady-state condition. The data fit a straight line reasonably well, with a separate curve for each applied-stress level. These data indicate that the rupture time can be influenced considerably by the rate at

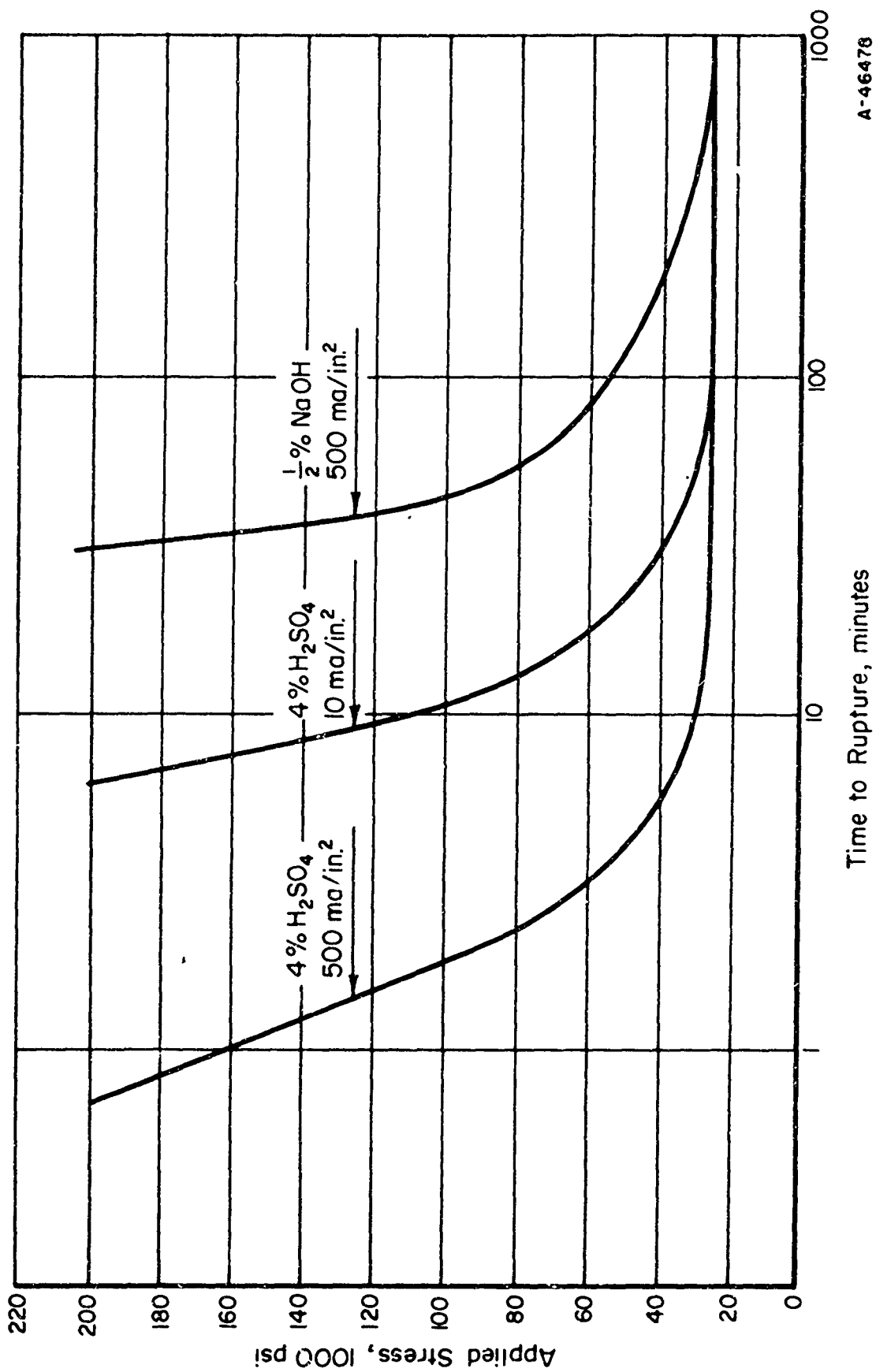


FIGURE 39. TIME FOR FAILURE AS A FUNCTION OF APPLIED STRESS FOR VARIOUS CHARGING CONDITIONS(9)

SAE 4340 steel, 230,000-psi ultimate tensile strength

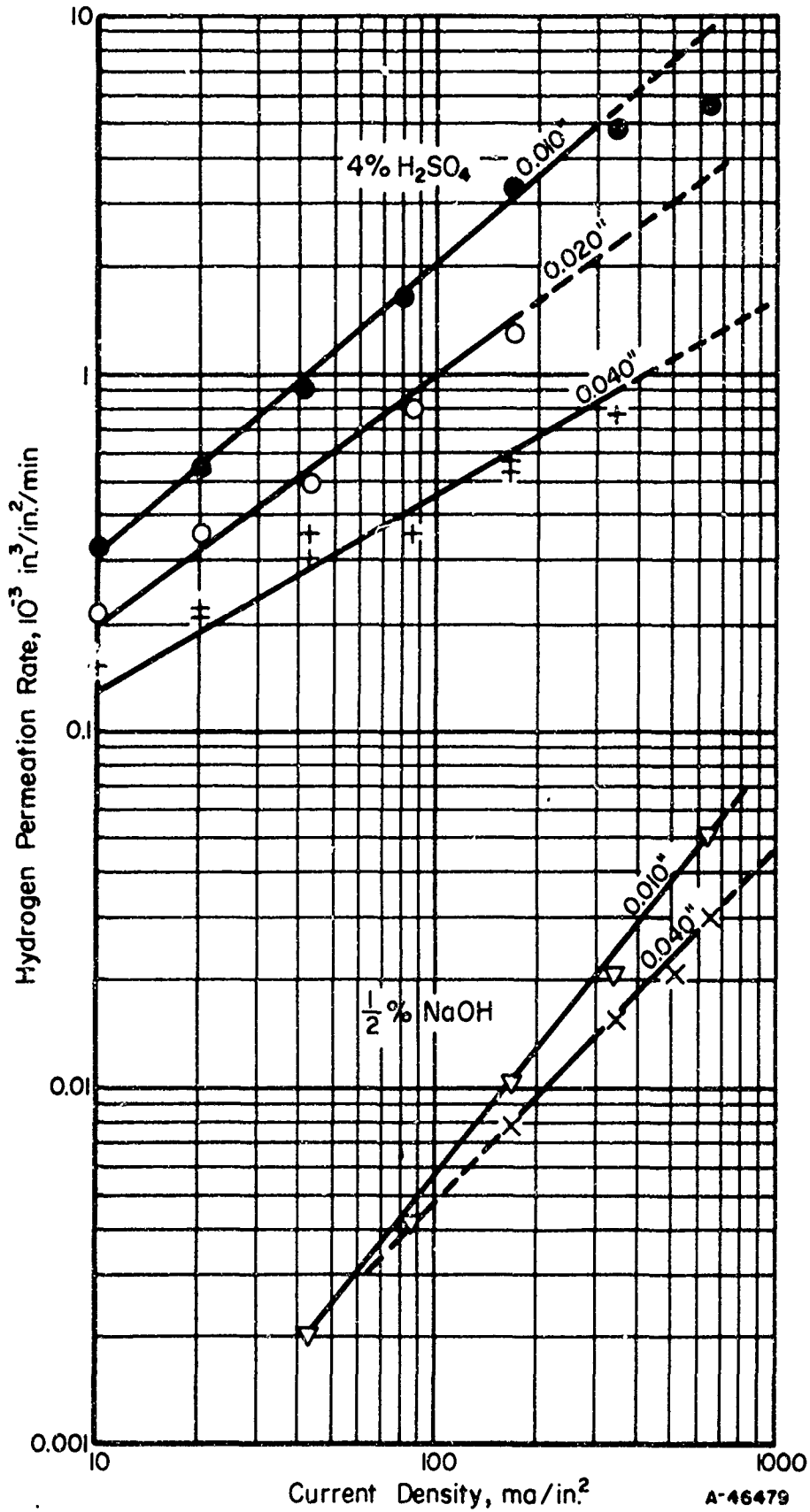
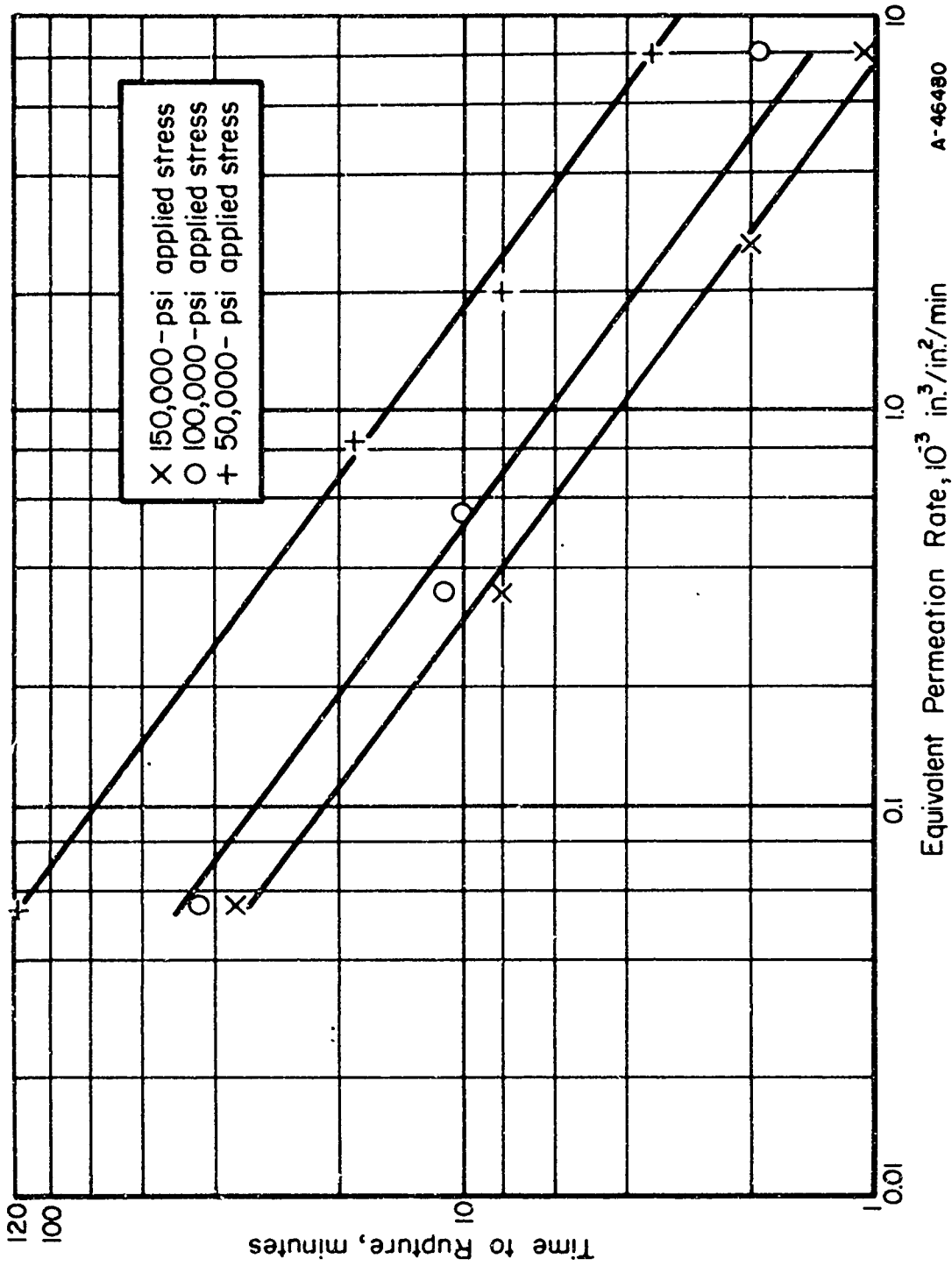


FIGURE 40. PERMEATION RATE OF HYDROGEN AS A FUNCTION OF CURRENT DENSITY FOR BOTH 4 PER CENT  $\text{H}_2\text{SO}_4$  AND 1/2 PER CENT  $\text{NaOH}$  ELECTROLYTES AND FOR VARIOUS THICKNESSES OF SPECIMENS(9)





A-46480

FIGURE 41. RUPTURE TIME FOR THE 230,000-PSI-STRENGTH STEEL AS A FUNCTION OF THE CATHODIC CHARGING CONDITION WHERE THE CHARGING CONDITION IS DEFINED AS THE EQUIVALENT PERMEATION RATE THROUGH A 0.010-INCH SPECIMEN(9)

SAE 4340 steel.

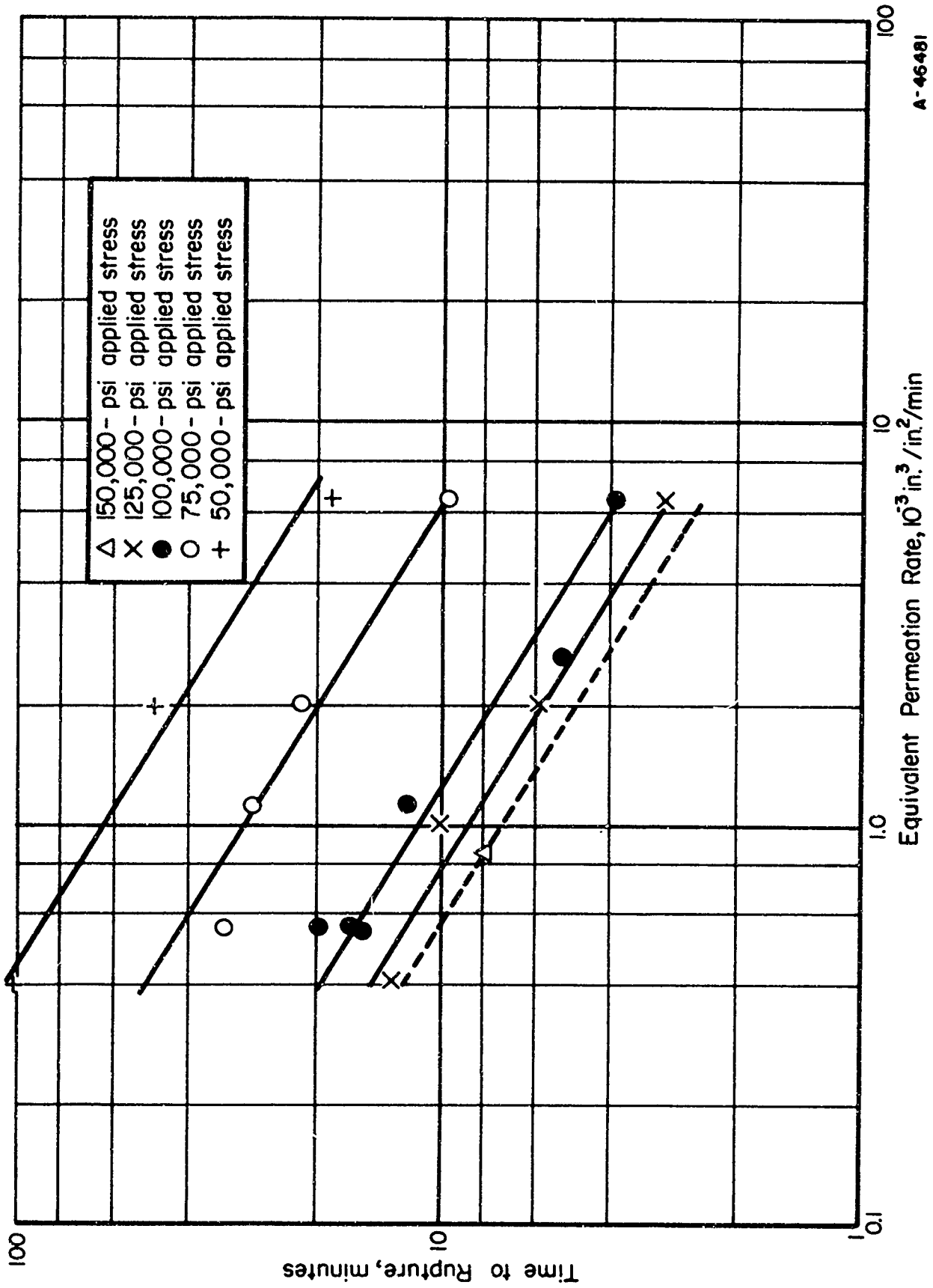


FIGURE 42. RUPTURE TIME FOR THE 190,000-PSI-STRENGTH STEEL AS A FUNCTION OF THE CATHODIC CHARGING CONDITION WHERE THE CHARGING CONDITION IS DEFINED AS THE EQUIVALENT PERMEATION RATE THROUGH A 0.010-INCH SPECIMEN(9)

SAE 4340 steel.

A-46481

which hydrogen is introduced into the steel. The curves shown in Figures 41 and 42 can be expressed by the equation

$$T_f = K \cdot P^n,$$

where

$T_f$  = time for failure to occur

$P$  = permeation rate

$K, n$  = constants.

The slopes (the constant  $n$ ) of the nearly parallel lines for the steel with 230,000-psi ultimate tensile strength were approximately  $-0.7$ , while those for the curves for the 190,000-psi strength level were approximately  $-0.6$ . Since  $n$  showed such little variation with changes in ultimate tensile strength, it was suggested that an average value of approximately  $-2/3$  might more adequately describe the reaction. No physical significance was attached to the values obtained for these slopes.

It is evident from Figures 41 and 42 that variations in the rate at which hydrogen was introduced into the steel had a greater effect on the rupture time than did variations in the applied stress, except when the applied stress was near the minimum critical stress for failure. Variations in the absorption rate had about as great an influence on the rupture time as did variations in the ultimate tensile strength of the steel. Since it is possible to obtain even wider ranges of hydrogen-charging conditions than those investigated, it appears that much greater variations in rupture time can be obtained by varying the rate at which hydrogen is introduced into the steel than can be obtained by altering the strength level of the steel. From this, one might conclude that the rate at which hydrogen is charged into a steel specimen is the most significant factor in producing delayed, brittle failures. However, in practice, much less hydrogen is introduced into a part during pickling and cleaning operations than was introduced into the tensile specimens of this investigation. Therefore, it was concluded that the strength level of the steel probably is the most important factor after all in practical considerations of delayed, brittle failure.

The bend tests performed by Slaughter et al. (8) which were described previously in discussing the effects of applied stress, also were useful in determining whether delayed failures are dependent on the hydrogen content or on the total quantity of hydrogen which traverses a given region by diffusion. Specimens stressed in bending were charged only on the compression side, and the tension side was notched so that the thickness of the specimens at the base of the notch varied from 0.075 inch to 0.250 inch. These specimens were cathodically charged in 4 per cent sulfuric acid electrolyte with added poison at a current density of approximately 33 ma/in.<sup>2</sup>. Under these conditions, a hydrogen gradient was established through the specimen, with the hydrogen content being highest at the cathodically charged compression surface and lowest at the tension surface where hydrogen was escaping to the atmosphere. As shown in Figure 26 (page 43), one specimen failed after a delay of 15 days. Since this specimen was only 0.075 inch thick at the minimum section, the steady-state concentration gradient of hydrogen should have been obtained in approximately 400 minutes as shown by permeability experiments for the conditions used. Therefore, the period for establishing the necessary hydrogen content within the specimen was a very small portion of the 15-day delay.

These data also indicated that an unlimited amount of hydrogen can traverse a region by diffusion without producing rupture, provided that a critical combination of hydrogen content and stress is not exceeded. For example, a bend specimen was charged cathodically for 43 days without rupture, while the surface from which the hydrogen was escaping was stressed to 80,000 psi. At this stress level, and under charging conditions to produce a high content of hydrogen, a tensile static-loading specimen failed in about 15 minutes. In the 43-day period, much more hydrogen diffused through the bend specimen than could have been absorbed by a tensile specimen in 15 minutes. Thus, it is a critical hydrogen content rather than the total amount of hydrogen passing a point that determines whether a delayed failure will occur.

Troiano and his co-workers<sup>(49)</sup> used a different approach to show that the delayed-failure behavior of high-strength steel is sensitive to hydrogen concentration. Sharp-notched specimens of SAE 4340 steel heat treated to the 230,000-psi strength level were precharged with hydrogen electrolytically, cadmium plated, and baked for various lengths of time at 300 F. The hydrogen concentration was varied by using different baking times. The results of static-loading tests, plotted in Figure 43, show that both the lower critical stress and the fracture times increased with decreasing hydrogen concentration (as indicated by baking time). These investigators concluded that, for a given notch sharpness, the lower critical stress is controlled by an interaction between hydrogen concentration and applied stress. These results of the Case studies are somewhat different from those of the Battelle studies. At Case, precharged notched specimens were aged at an elevated temperature to produce different hydrogen contents; under these conditions, the lower critical stress increased as the hydrogen content decreased (that is, as the baking time increased). In the Battelle studies, unnotched specimens were continuously charged while under static load, using different electrolytes and different current densities to produce different hydrogen contents; under these conditions, the lower critical stress remained about the same. Both approaches gave longer failure times with conditions that should result in lower hydrogen contents.

The recovery behavior of the material is shown by the increase of the lower critical stress from 75,000 psi to about 240,000 psi by baking for times up to 24 hours to remove hydrogen (Figure 43). A baking time of 20 hours was sufficient to restore full ductility to unnotched specimens, as determined in a standard tensile test. This attainment of full recovery indicated that the cadmium plate per se does not influence ductility. However, delayed, brittle failures still occurred and with appreciable loss in load-carrying ability in material baked 18 or 24 hours and then subjected to static loading. After baking for 7 hours, the notched tensile strength of charged and uncharged specimens was the same. However, the lower critical stress of 125,000 psi showed that delayed failure may still occur at very low applied stress after baking 7 hours.

The hydrogen content of the as-heat-treated specimens (1.5 cc/100 g) was essentially nonembrittling, because a significant loss of load-carrying ability under static loading was observed only after electrolytic introduction of hydrogen. This behavior was in accord with the suggestion by Darken and Smith<sup>(50)</sup> that hydrogen may exist in steel in two forms, since analysis for hydrogen showed that the amount introduced electrolytically was negligible compared with the as-heat-treated hydrogen content. In an exhaustive series of analyses, conventional vacuum-fusion techniques, with a precision of  $\pm 0.2$  cc hydrogen per 100 g, were unable to detect the presence of the electrolytically introduced hydrogen. Evidently, the as-received hydrogen is in an innocuous, probably

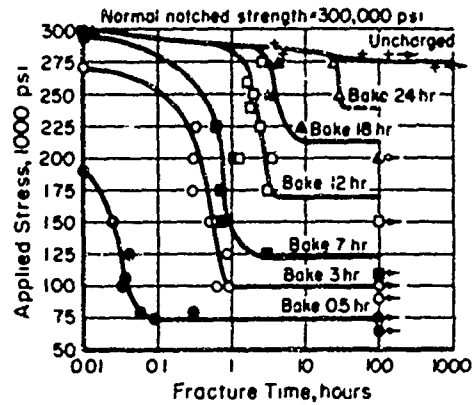


FIGURE 43. DELAYED-FAILURE BEHAVIOR FOR VARIOUS HYDROGEN CONCENTRATIONS CORRESPONDING TO DIFFERENT BAKING TIMES AT 300 F<sup>(49)</sup>

Sharp-notch specimens, SAE 4340 steel, 230,000-psi strength level

Case Institute of Technology Charging Condition A:

Electrolyte: 4 per cent H<sub>2</sub>SO<sub>4</sub> in water

Poison: None

Current density: 20 ma/in.<sup>2</sup>

Charging time: 5 minutes.

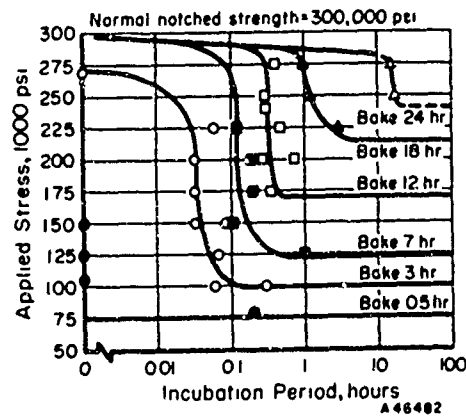


FIGURE 44. VARIATION OF INCUBATION PERIOD WITH APPLIED STRESS AND HYDROGEN CONCENTRATION CORRESPONDING TO DIFFERENT BAKING TIMES AT 300 F<sup>(49)</sup>

Sharp-notch specimens, SAE 4340 steel, 230,000-psi strength level.

Case Institute of Technology Charging Condition A, as in Figure 43.

molecular, state; severe embrittlement arises from a very small quantity of atomic hydrogen, which is presumably in solution.

H. H. Johnson et al. (49) also studied the effects of variations in hydrogen content on crack initiation and propagation by the electrical-resistance method. The results, contained in Figure 44, show that as the hydrogen content decreases (as indicated by increased baking time) the incubation period for crack initiation becomes longer. The incubation period was found to be relatively insensitive to the applied stress. Incubation periods ranging from a few seconds to 18 hours were observed, and longer ones undoubtedly could be produced.

Troiano and co-workers(5) also studied the effect of varying the room-temperature aging time before applying a static load. The procedure was to charge heat-treated SAE 4340 steel with hydrogen, age various times at room temperature, then apply a static load to failure. Again, sharp-notch specimens were used. At the 230,000-psi strength level, the time to fracture was plotted as a function of the aging time for several values of applied stress; see Figure 45. These curves were of the same form as curves showing the effect of room-temperature aging on notched tensile strength, which exhibited a marked minimum at approximately 2 hours while unnotched specimens showed a more or less continuous increase in ductility. At low values of applied stress, the sensitivity to delayed failure was lost in less than an hour, while for higher stresses, delayed failure occurred in specimens aged for a considerably longer time. Conventional delayed-failure curves for various aging times are shown for the 270,000-psi material in Figures 46 and 47. The results are summarized in Figure 48. Aging 100 hours at room temperature subsequent to charging did not eliminate the phenomenon of delayed failure. However, after the same aging time of 100 hours, the reduction in area of an unnotched specimen had recovered to the value associated with an uncharged specimen. This finding is typical of the findings of several investigators that delayed failure may occur in a high-strength steel which exhibits full ductility as determined by conventional tensile tests. This means that a normal value of reduction in area is no guarantee that delayed failure cannot occur. The lower critical stress, below which delayed failure did not occur, increased continuously with aging time.

In other work at Case(39), the effect of room-temperature aging on crack propagation was studied, with the results shown in Figure 49. For short times of static loading, variations in hydrogen content produced by aging had a large effect on the crack area.

Rinebolt(12) studied the effect of hydrogen charging for different times on the tensile properties of steels of three different strength levels. The comparisons shown in Figure 14 (page 29) are based on per cent of original tensile strength. After 4 hours of charging, about 60 per cent of the tensile strength was lost by a steel heat treated to a 209,000-psi strength level. The same percentage loss in tensile strength was obtained for the 287,000-psi strength level after about 1/2 hour of charging. However, the reduction in area and the elongation decreased to less than 1 per cent after charging for only 5 minutes for all three strength levels. Raring and Rinebolt(17) studied the effect of baking at 350 F for 1-1/2 hours on cadmium-plated, vacuum-melted SAE 4340 steel at the 230,000-psi strength level. Although the baking treatment restored the breaking strength of the plated specimens in the short-time test nearly to that of the unplated specimens, the susceptibility to delayed, brittle failure was not changed appreciably. After plating and baking, the lower critical stress was about 47 per cent of the notched

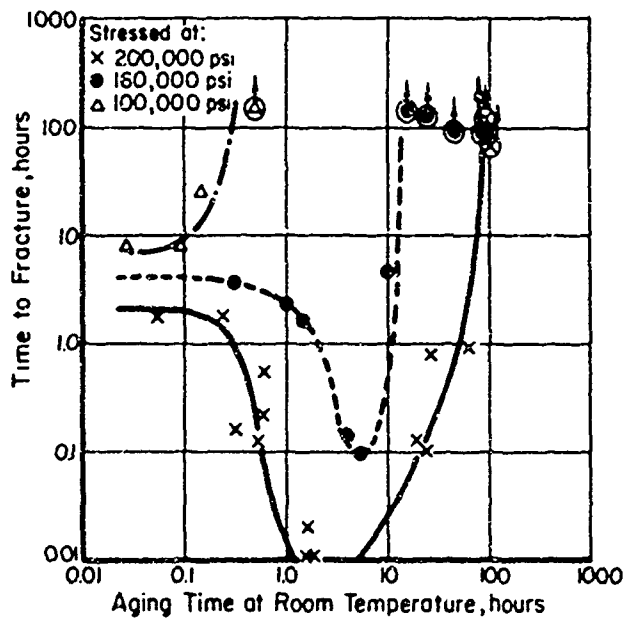


FIGURE 45. EFFECT OF AGING TIME AT ROOM TEMPERATURE ON TIME TO FRACTURE FOR SAE 4340 STEEL HEAT TREATED TO 230,000 PSI<sup>(5)</sup>

Sharp-notch specimens. Case Institute of Technology Charging Condition A, as in Figure 43.

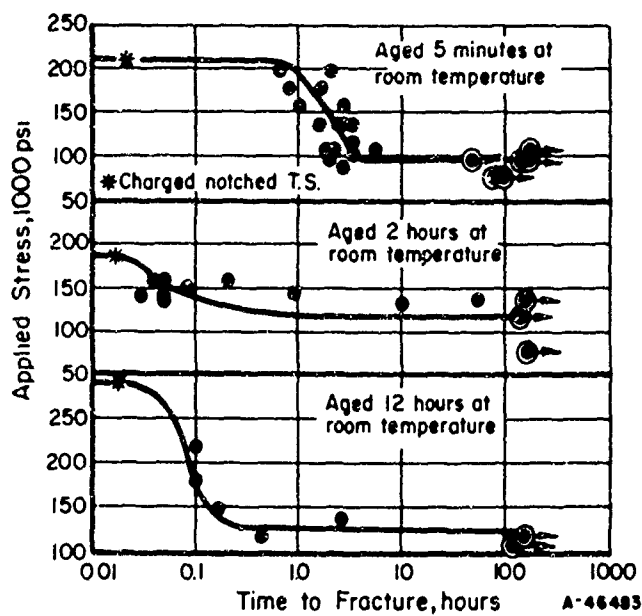


FIGURE 46. STATIC-LOADING TESTS ON SAE 4340 STEEL HEAT TREATED TO 270,000 PSI AND AGED AS INDICATED<sup>(5)</sup>

Sharp-notch specimens. Case Institute of Technology Charging Condition A, as in Figure 43.

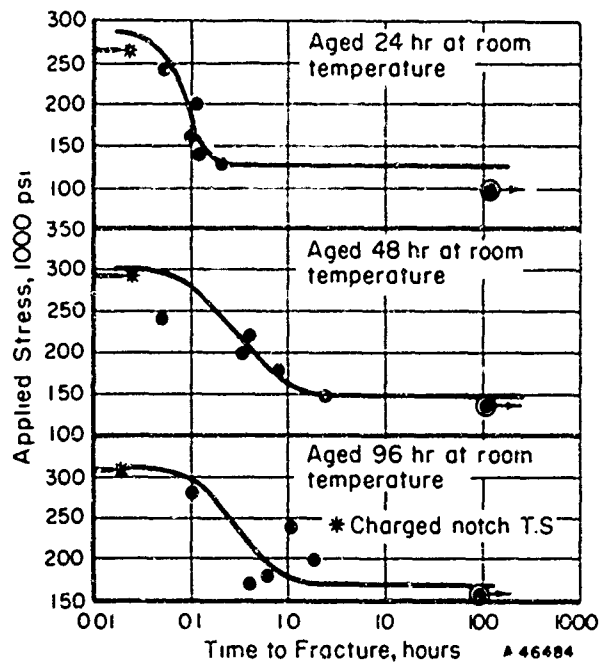


FIGURE 47. STATIC-LOADING TESTS ON SAE 4340 STEEL HEAT TREATED TO 270,000 PSI AND AGED AS INDICATED<sup>(5)</sup>

Sharp-notch specimens.

Case Institute of Technology Charging Condition A, as in Figure 43.

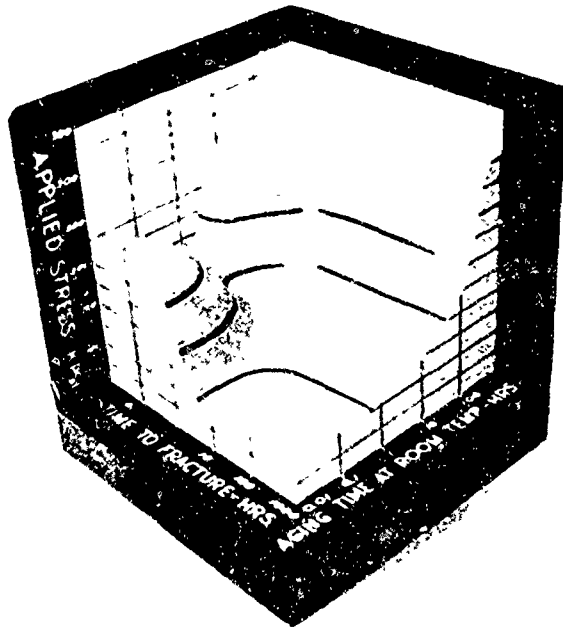


FIGURE 48. EFFECT OF AGING AT ROOM TEMPERATURE ON THE DELAYED-FAILURE CHARACTERISTICS OF A HIGH-STRENGTH STEEL<sup>(39)</sup>

Data obtained by Frohberg et al., Reference 5.



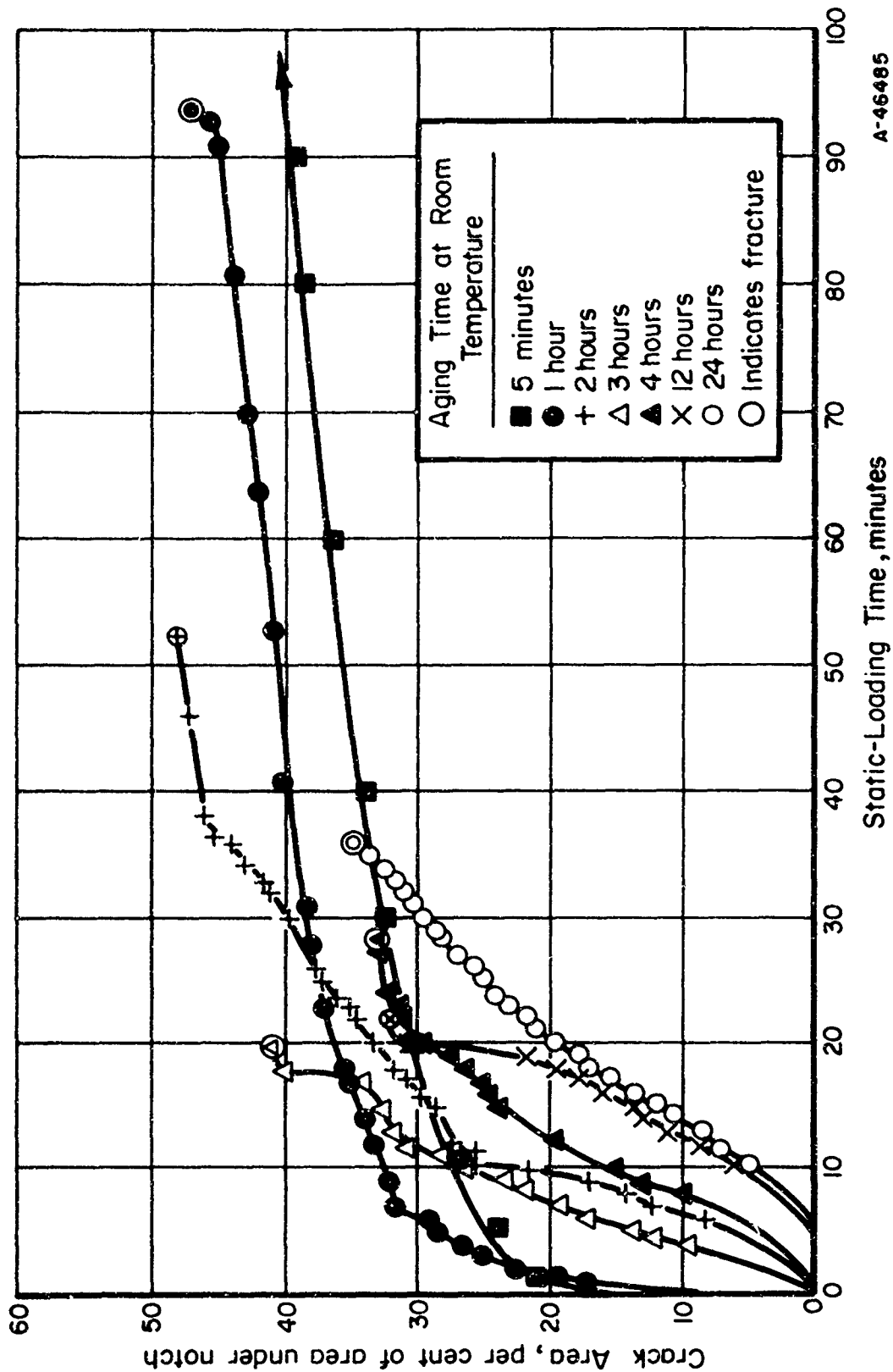


FIGURE 49. EFFECT OF PRIOR ROOM-TEMPERATURE AGING ON CRACK PROPAGATION IN SAE 4340 STEEL AT AN APPLIED STRESS OF 175,000 PSI(39)

Sharp-notch specimens. Case Institute of Technology Charging Condition A, as in Figure 43.

tensile strength of specimens that were not plated. The hydrogen content before baking was 0.7 to 1.1 ppm; after baking it was 0.6 to 0.7 ppm. The effect of the treatment on the short-time tensile properties of unnotched tensile specimens was as follows:

	<u>Before Plating</u>	<u>After Plating and Baking 1-1/2 Hours at 350 F</u>
Tensile Strength, psi	234,000	230,000
Yield Strength, psi	208,000	208,000
Elongation, per cent in 1 inch	15.0	15.0
Reduction in Area, per cent	57.0	52.5

Again, it is apparent that full recovery may be indicated by the conventional tensile tests, whereas the static-loading tests of notched specimens may indicate essentially no recovery.

The early investigations of hydrogen embrittlement induced by pickling in acid solutions or by electrolysis also showed that aging at room temperature or heating to moderately elevated temperatures (known as baking) causes a gradual recovery of the original ductility. Some investigators reported that complete recovery had been obtained, while others found that recovery was incomplete at either room temperature or at elevated temperatures. This early work was done largely with low-carbon steel.

Introducing hydrogen into the steel by different methods has been found to have little effect on the rate of recovery at room temperature. For example, it was found to be only slightly different for low-carbon steel wire embrittled by cathodic treatment from that for wire embrittled by heating in hydrogen<sup>(51)</sup>. However, variation in the cross-sectional area of the test piece has a large effect on the rate of recovery, at either room temperature or elevated temperature, because the recovery depends on the diffusion of hydrogen. For this reason, elevated temperatures are increasingly more effective. A severely embrittled low-carbon steel wire 0.040 inch in diameter was found to recover 50 per cent of the initial bending value at room temperature in about 1 week, while a wire of the same composition but 0.160 inch in diameter recovered to only 40 per cent of the original bend value in 3 months<sup>(51)</sup>. Figures 50 and 51 show the hydrogen content and ductility of embrittled 4-inch-square steel castings as a function of aging time at 400 F and room temperature, respectively. Whereas the ductility was substantially recovered in 125 hours at 400 F, extrapolation from the data points in Figure 51 indicated that it would require about 6 years to recover the original properties by aging at room temperature.

Apparently, low-alloy steels, heat treated to high strength levels, completely recover the ductility lost because of hydrogen introduced by acid pickling if they are stored for a long time before use or if they are baked at a sufficiently high temperature, provided that they are not electroplated after pickling. For example, tensile tests performed on SAE 4340 steel, heat treated to a hardness of Rockwell C 47, indicated that complete recovery from the effects of pickling in HCl for 1 hour was accomplished by aging at room temperature for 5 hours or more (see Figure 52, page 76).

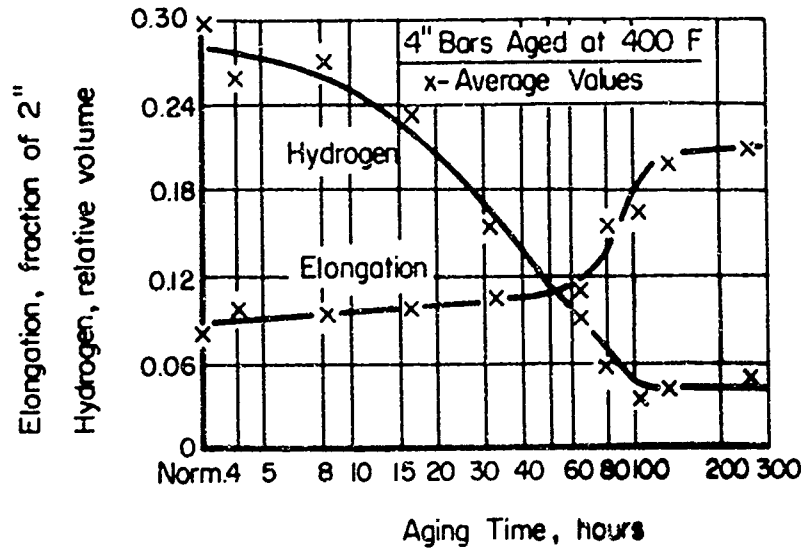


FIGURE 50. COMPARATIVE CHANGE OF HYDROGEN AND DUCTILITY DURING AGING<sup>(52)</sup>

Values for center of cast steel bars.

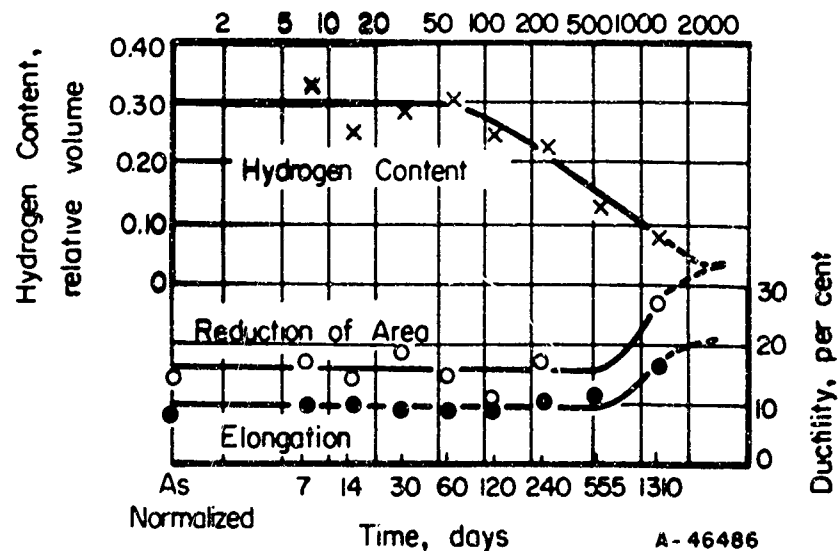


FIGURE 51. LOSS OF HYDROGEN FROM CENTER OF 4-INCH-SQUARE CAST-STEEL COUPONS AGED AT ROOM TEMPERATURE, AND EFFECT ON DUCTILITY<sup>(53)</sup>

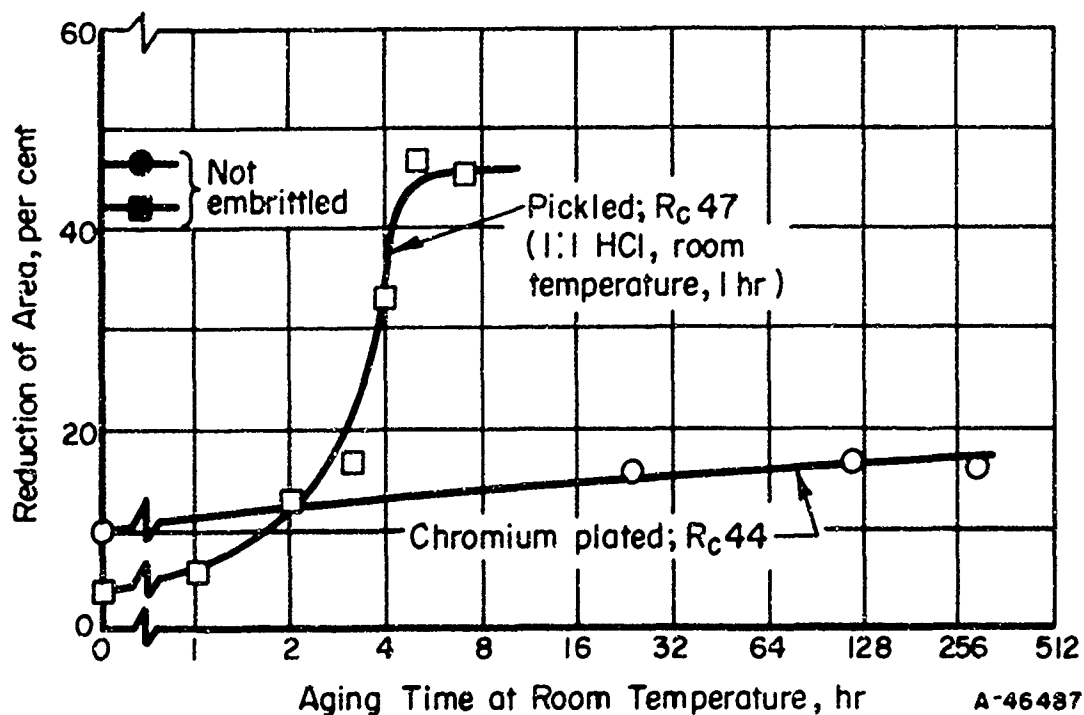


FIGURE 52. EFFECT OF AGING ON THE HYDROGEN EMBRITTLEMENT OF PICKLED AND CHROMIUM-PLATED 0.505-IN. -DIAMETER TENSILE SPECIMENS OF SAE 4340 STEEL<sup>(10)</sup>

Data by North American Aviation.

The ductility of steel may be markedly reduced as the result of an electroplating process. This results from hydrogen that is plated concurrently with the metal, part of the hydrogen being absorbed by the steel. Eakin and Lownie<sup>(31)</sup> reported substantial embrittlement of 1 per cent carbon-steel springs after cadmium plating. The embrittlement became more severe as the hardness level of the steel increased, and higher aging temperatures were required to produce complete recovery in a bend test. The strength-level dependence also was reported by Valentine<sup>(28)</sup>, who studied delayed failures of zinc-plated steel lockwashers. He found that the percentage of specimens failing a test, in which the lockwashers were loaded until they went flat, increased with hardness level. He reported that a subsequent aging treatment at 400 F eliminated or reduced the number of delayed failures. Stefanides<sup>(29)</sup> studied failures of acid-descaled and cadmium-plated steel dome lockwashers and also found that the percentage of failures increased as the hardness of the steel increased. However, in a study of many thousands of these dome lockwashers, he found no evidence that baking after plating was very helpful.

Zapffe and Haslem<sup>(54, 55, 56)</sup> conducted much research on the embrittlement of steel by electroplating. They studied mild steel and hardenable (17 per cent Cr, 1 per cent C) stainless steel wires electroplated with cadmium, chromium, zinc, tin, nickel, and lead. The hardenable stainless steel was embrittled by virtually all of the electroplating processes studied. Using their bend test for the stainless steel wires and fixed conditions of temperature and current density, they observed a much greater degree of embrittlement during chromium plating than during pure hydrogen plating (cathodic charging). They emphasized that a sufficiently heavy chromium plate can superimpose

its brittleness on that of the steel if the thickness of the base is not great enough compared with the thickness of the plate. Baking treatments were effective in recovering the original ductility.

Potak<sup>(57)</sup> presented experimental results concerning the embrittlement of a hardened high-carbon steel by a number of different electrolytic treatments. Figelman and Shreider<sup>(58)</sup> studied the effects of electroplating with chromium, copper, nickel, zinc, and cadmium on the ductility of heat-treated spring steel. The testing method consisted of measuring the bend angle necessary to produce failure of a flat specimen. They found that aging at 200 to 300 C (390 to 570 F) was almost always effective in recovery of ductility, but in the case of high stresses, a higher temperature was necessary for their removal.

From these few references and the results of some of the investigations described previously in this report, it is apparent that sufficient hydrogen is introduced into steel during a commercial-type electroplating process to cause substantial embrittlement and to cause delayed, brittle failure under many conditions.

Other work has shown that frequently more hydrogen is introduced in acid pickling to remove scale or in cathodic cleaning prior to electroplating than is introduced in electroplating itself<sup>(59)</sup>. These sources of hydrogen will be discussed more fully in a separate report.

Sachs and co-workers<sup>(19)</sup> performed hydrogen analyses on cadmium-plated sustained-load-type specimens of seven different high-strength steels. The analyses were obtained by cooling specimens in dry ice immediately after electroplating and keeping them at this reduced temperature until they were analyzed. The average hydrogen content for cylindrical stress-rupture specimens was approximately 2.5 ppm. Within the scatter of the data, steel composition had no effect on the amount of hydrogen contained in the specimen after cadmium electroplating. Comparison with earlier work where hydrogen was charged electrolytically without metal plating showed that hydrogen introduced into specimens during cadmium electroplating may be as high as that introduced through severe cathodic impregnation. The hydrogen content was shown to vary with section size, as would be expected.

Hobson and Sykes<sup>(42)</sup> showed that electrolytic charging and the introduction of hydrogen under pressure at 600 C (1112 F) gave the same embrittling effect, as measured by reduction in area.

R. D. Johnson et al.<sup>(60)</sup> showed that the delayed-failure behavior was almost identical for commercial cadmium-plated steel and the same steel cathodically charged with hydrogen under their Charging Condition A, for short-time aging (5 minutes) at room temperature. Figure 53 shows their results. At the 230,000-psi strength level, both methods of introducing hydrogen led to nearly identical delayed-failure curves (Figure 53b). The correlation at the 270,000-psi strength level is not as obvious, since sharp-notched specimens were used for cathodic charging, while specimens with a notch radius of only 0.010 inch were used for commercial cadmium plating. Allowing for the difference in notched tensile strength between the specimens with the two different notch radii, they concluded that the stress displacement of the delayed-failure curves in Figure 53a probably resulted from the difference in notch radii.

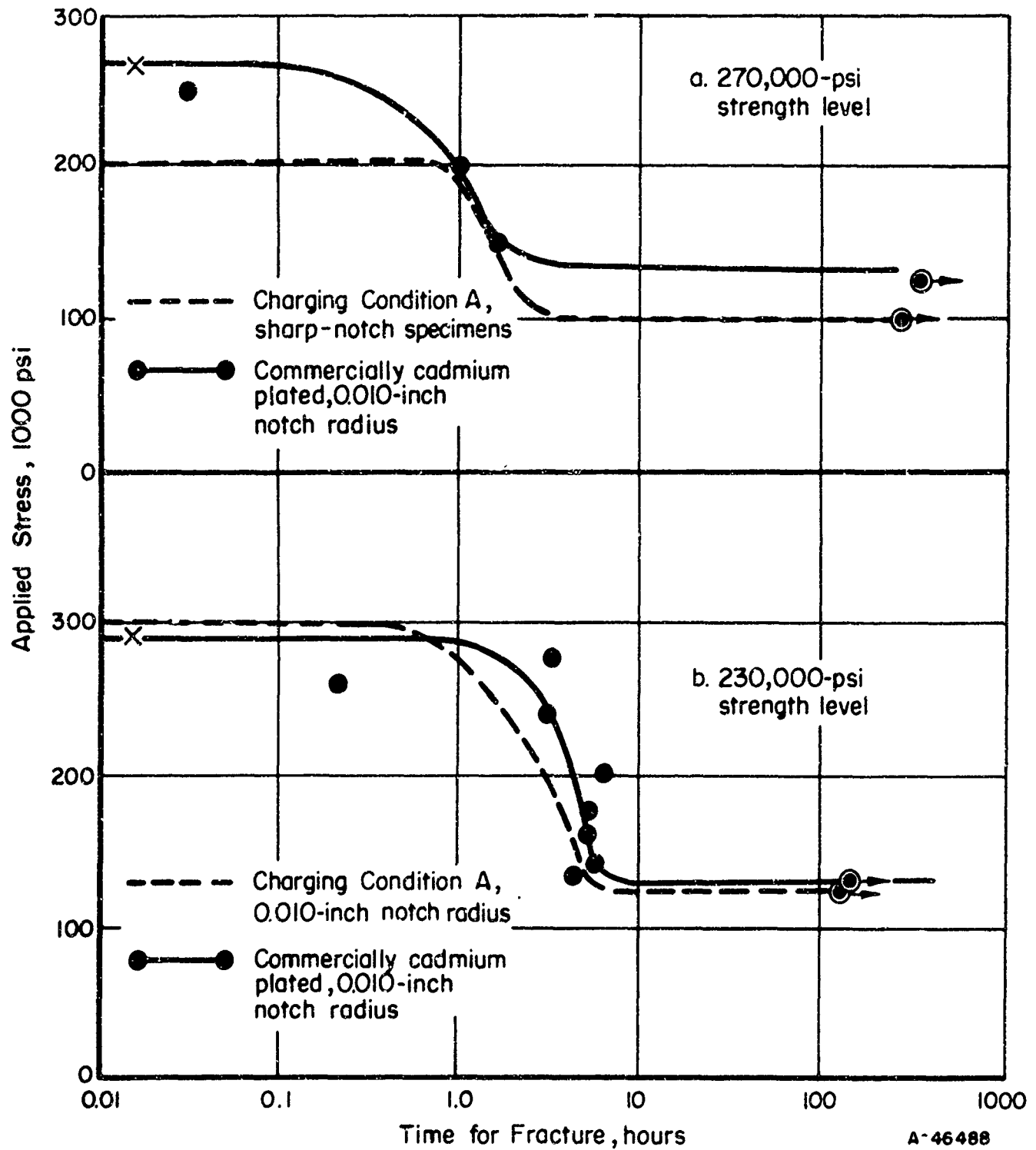


FIGURE 53. DELAYED-FAILURE BEHAVIOR OF SAE 4340 STEEL AT ROOM TEMPERATURE FOR SEVERAL CONDITIONS AS INDICATED<sup>(60)</sup>

Aged 5 minutes at room temperature.

Case Institute of Technology Charging Condition A:

Electrolyte: 4 per cent  $H_2SO_4$  in water

Poison: None

Current density: 20 ma/in.<sup>2</sup>

Charging time: 5 minutes

Aging time: Measured from end of charging to start of test.

Schuetz and Robertson<sup>(25)</sup> obtained a similar loss in ductility either from exposure to H<sub>2</sub>S solution or from cathodic charging. A number of other investigators have studied the hydrogen embrittlement and delayed, brittle fractures of steel resulting from exposure to H<sub>2</sub>S<sup>(61-67)</sup>.

Time-dependent delayed failures have been observed in rocket-motor cases when tested at constant pressure and exposed to aqueous environments<sup>(68, 69)</sup>. The first motor case failed unexpectedly on being pressure tested with water at intervals over a period of several months. In a series of experiments on small-size pressure vessels, both oil and water were used in pressure testing, and tests were performed under the following conditions:

- (1) No protection
- (2) Inside of vessel coated with primer, outside submerged in water bath
- (3) Inside and outside coated with primer.

When the metal was not allowed to come in contact with an electrolytic solution, failure occurred at high tangential stresses. Also, it was possible to transfer the origin of the fracture from the inside to the outside surface by protecting the inside and exposing the outside to the water. Thus, it was proved that the water used in hydrostatic testing was the cause of failure and that these failures were induced by hydrogen. Hydrogen embrittlement lowered the burst strength by 130,000 psi or more. These workers suggested that the role of water was twofold: (1) It provided the pit which, in turn, provided the essential triaxiality of stress, and (2) It was a medium for localized galvanic action which released the essential atomic hydrogen.

Spaeth concluded that hydrotesting with oil is an effective preventive measure against embrittlement, provided that the pressure-vessel steel is not loaded with hydrogen prior to hydrostatic testing.

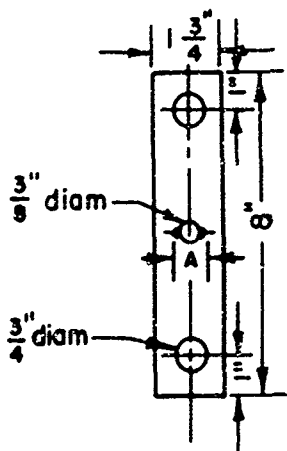
Norton<sup>(70)</sup>, using heavy water (D<sub>2</sub>O), showed that the hydrogen in water participates in the initial corrosion of steel, rather than the hydrogen present in the steel.

Steigerwald<sup>(71)</sup> carried out an investigation to systematically evaluate the influence of liquid environments (primarily aqueous) on the delayed-failure characteristics of high-strength steel in the presence of very sharp notches (fatigue cracks). This work was performed to help determine (1) whether or not slow crack growth was stimulated by the staining media sometimes used with precracked sheet tension tests for the measurement of the fracture-toughness parameter and the notched tensile strength of ultra-high-strength steels, and (2) whether any such stimulation affected the fracture toughness and strength values obtained.

A low-alloy martensitic steel (300M) and an H-11 type hot-work die steel were used in the investigation. The compositions, and the tensile properties for the various conditions of heat treatment used, are listed in Tables 11 and 12, respectively. Details of the precracked center-notch tensile specimen are given in Figure 54. The results of static-load tests on 300M steel with distilled water and recording ink as the environment are shown in Figures 55 and 56. Results for the H-11 steel in distilled water are shown in Figure 57. Both liquid media produced a considerable range of time for failure, depending on the level of applied stress. Failures occurred at a fraction of the notched

TABLE 11. COMPOSITION OF STEELS USED TO STUDY THE INFLUENCE OF LIQUID ENVIRONMENTS ON DELAYED-FAILURE BEHAVIOR<sup>(71)</sup>

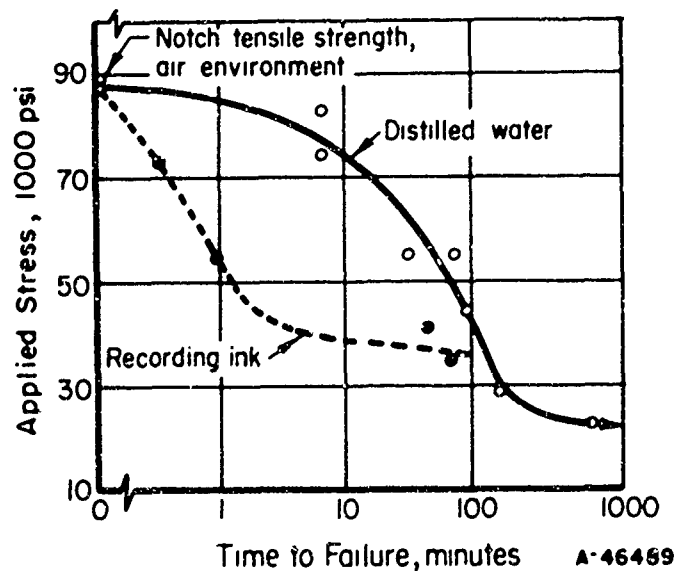
Material	Chemical Composition, per cent by weight							Sheet Thickness (As Received), in.
	Carbon	Manganese	Silicon	Chromium	Nickel	Vanadium	Molybdenum	
300M	0.43	0.89	1.78	0.90	1.92	0.13	0.43	0.080
H-11	0.39	0.30	1.00	5.14	--	0.49	1.30	0.097



Sawcut A approximately 0.600 in. extended by fatigue precracking to 0.750 in.

TABLE 12. TENSILE PROPERTIES OF 300M AND H-11 STEEL SPECIMENS USED IN THE STUDY OF THE EFFECT OF LIQUID ENVIRONMENTS ON DELAYED FAILURE<sup>(71)</sup>

Material	Tempering Temperature, F	0.2 Per Cent Offset Yield Strength, psi	Tensile Strength, psi	Elongation in 2 In., per cent
300M	600	245,000	295,000	6.0
300M	1025	200,000	226,000	8.5
300M	1150	160,000	187,000	11.0
H-11	1000	235,000	290,000	5.0

FIGURE 54. CENTER-PRECRACKED NOTCHED TENSILE SPECIMEN USED TO EVALUATE THE INFLUENCE OF LIQUID ENVIRONMENTS ON THE DELAYED-FAILURE CHARACTERISTICS OF HIGH-STRENGTH STEEL IN THE PRESENCE OF VERY SHARP NOTCHES (FATIGUE CRACKS)<sup>(71)</sup>FIGURE 55. DELAYED FAILURE OF 300M STEEL CENTER PRECRACKED SPECIMENS AT 295,000-PSI STRENGTH LEVEL WHEN SUBJECTED TO DISTILLED-WATER AND RECORDING-INK ENVIRONMENTS<sup>(71)</sup>



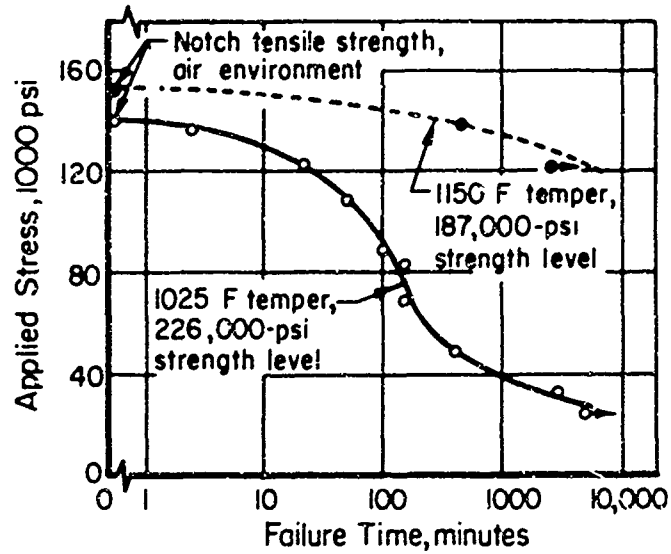


FIGURE 56. DELAYED FAILURE OF 300M STEEL CENTER-PRECRACKED SPECIMENS WHEN SUBJECTED TO A DISTILLED-WATER ENVIRONMENT<sup>(71)</sup>

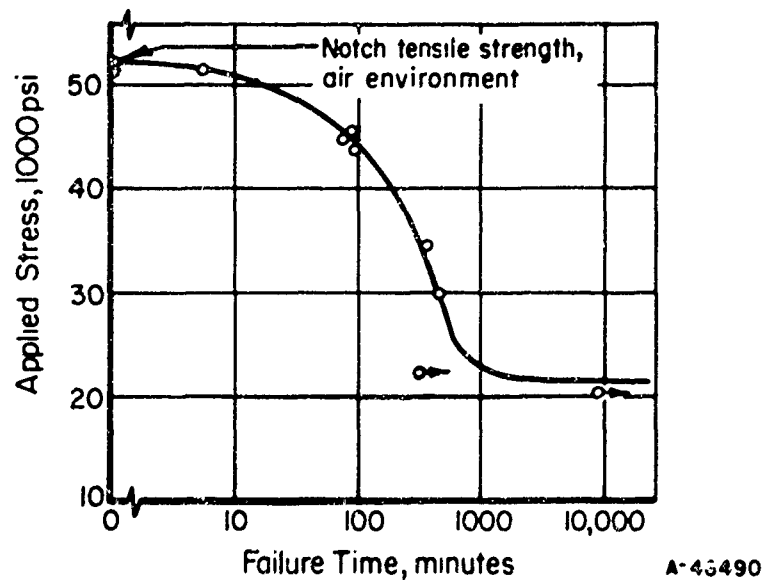


FIGURE 57. DELAYED FAILURE OF H-11 TOOL STEEL CENTER-PRECRACKED SPECIMENS AT THE 295,000-PSI-STRENGTH LEVEL WHEN SUBJECTED TO A DISTILLED-WATER ENVIRONMENT<sup>(71)</sup>

tensile strength determined in a standard tensile test performed in an air environment. As the strength level of the 300M steel was reduced, the material became more resistant to delayed, brittle failure. Also, as the material became more insensitive to notch effects, the tendency to delayed failure was reduced. Crack growth was followed by the electrical-resistance method, and all the curves exhibited discontinuities, as is typical of hydrogen embrittlement. The delayed failures described occurred by a process of slow crack growth until the crack reached a critical, unstable length, whereupon catastrophic failure occurred. Constant-load tests also were conducted on pre-cracked specimens to which no liquid was applied. In these cases, failure did not occur at stresses within 10,000 psi of the normal notched tensile strength after a 100-hour test time.

In an effort to obtain a medium which would not produce delayed failure and to gain some insight into the mechanism that was operative, the delayed-failure characteristics of fatigue-cracked 300M steel tempered at 600 F (295,000-psi ultimate tensile strength) were investigated for a number of liquid environments. In all cases, the specimens were loaded to a notched tensile stress of approximately 75,000 psi, which represented 83.5 per cent of the strength obtained in a conventional notched tensile test without a liquid in the crack. The results of the tests are shown in Table 13. The pH of aqueous solutions also was varied from 4.8 to 9.0 by the use of buffered solutions; this variation produced no significant difference in the failure time of 300M steel. Non-aqueous liquids consistently caused delayed failure, except for carbon tetrachloride, the only medium that contained no hydrogen. However, the failure times for the nonaqueous liquids were considerably longer than those produced by the aqueous environments. With those media having closed-ring structures and low dielectric constants (benzene and carbon tetrachloride), the steel was capable of sustaining the applied load for the greatest time periods.

TABLE 13. INFLUENCE OF VARIOUS CRACK ENVIRONMENTS ON FAILURE TIME OF 300M STEEL(71)

Environment	Failure Time, minutes
Recording ink	0.5
Distilled water	6.5
Amyl alcohol	35.8
Butyl alcohol	28.0
Butyl acetate	18.0
Acetone	120
Lubricating oil	150
Carbon tetrachloride	No failure in 1280
Benzene	2247
Air	No failure in 6000

Steigerwaid believed that the delayed failure induced by the liquid environments could be attributed to three possible factors: (1) lowering of the surface energy of the crack due to liquid adsorption, (2) hydrogen embrittlement, and (3) stress corrosion.

The data obtained were not sufficient to allow the particular mechanism or combination of factors to be defined conclusively. He considered that, in view of the fact that cracks were present and the organic environments caused delayed cracking, the mechanism involving a decrease in surface energy (Petch and Stables, 1952, Reference 72) was attractive. The apparent absence of an incubation time which he observed also is a necessary, but not sufficient, condition for a surface-adsorption mechanism. Therefore, a test was conducted on a 300M specimen that was not precracked but merely had a center jeweler's sawcut with a terminal radius of approximately 0.005 inch. The specimen was loaded to 90 per cent of the normal notched tensile strength and subjected to a distilled-water environment. Failure occurred in 15.2 hours. He found it difficult to visualize how surface adsorption on the face of the sawcut could lower the failure stress. Since the sawcut itself did not extend and a crack had to be initiated, most probably below the surface where the triaxiality favors fracture, another mechanism besides surface adsorption must be rate controlling. He concluded that, although hydrogen embrittlement and stress corrosion have both been observed in these high-strength steels, the manner in which sufficient hydrogen is produced or stress corrosion takes place in the various environments must be determined before these factors can be used to explain the observed delayed-failure process.

Davis<sup>(73)</sup> has studied stress corrosion and hydrogen embrittlement in two low-alloy high-strength steels, 4330M and SAE 4340. With electron-microscope fractography techniques, he claimed to be able to detect slight differences between hydrogen-embrittlement and stress-corrosion fractures; gross differences can be detected among ductile, fatigue, and intergranular brittle fractures. He reported that hydrogen-embrittlement and stress-corrosion fractures both appear to be intergranular with respect to the prior austenite grain boundaries. Metallographic microstructural differences between hydrogen-embrittlement and stress-corrosion cracking are not clearcut. However, fractographic studies with the electron microscope indicate that the two processes may be fundamentally related.

Swets and Frank<sup>(74)</sup> have reported on the pickup of hydrogen from a hydrocarbon lubricant by steel ball bearings. Swets, Frank, and Fry<sup>(75)</sup> found that grinding or abrading steel caused hydrogen pickup, apparently from water vapor in the air or from the cutting fluid when the latter was used.

In addition to the effect of concurrently plating hydrogen with the metal plate, the plate has another effect. The presence of a more-or-less impermeable metal coating, such as cadmium, makes the evolution of hydrogen from the interior of the base metal more difficult; this may serve to aggravate the effects of embrittlement and delayed failure of electroplated steel. Although appropriate baking treatments may restore most or all of the ductility to the plated steel, often such a treatment does not overcome the propensity toward delayed, brittle failure.

As was discussed previously, R. D. Johnson et al.<sup>(60)</sup> showed that the delayed-failure behavior was almost identical for commercial cadmium-plated steel and the same steel cathodically charged with hydrogen, for the conditions used. However, the room-temperature aging characteristics of cadmium-plated and hydrogen-charged specimens were markedly different, as is shown in Figure 58. Ductility was recovered more slowly in the case of the cadmium-plated specimens. Figure 52 (page 76) shows that chromium plate serves as a barrier to hinder evolution of hydrogen on aging, and, hence, to hinder recovery of ductility. Figure 59<sup>(10)</sup> for recovery by baking at 375 F shows

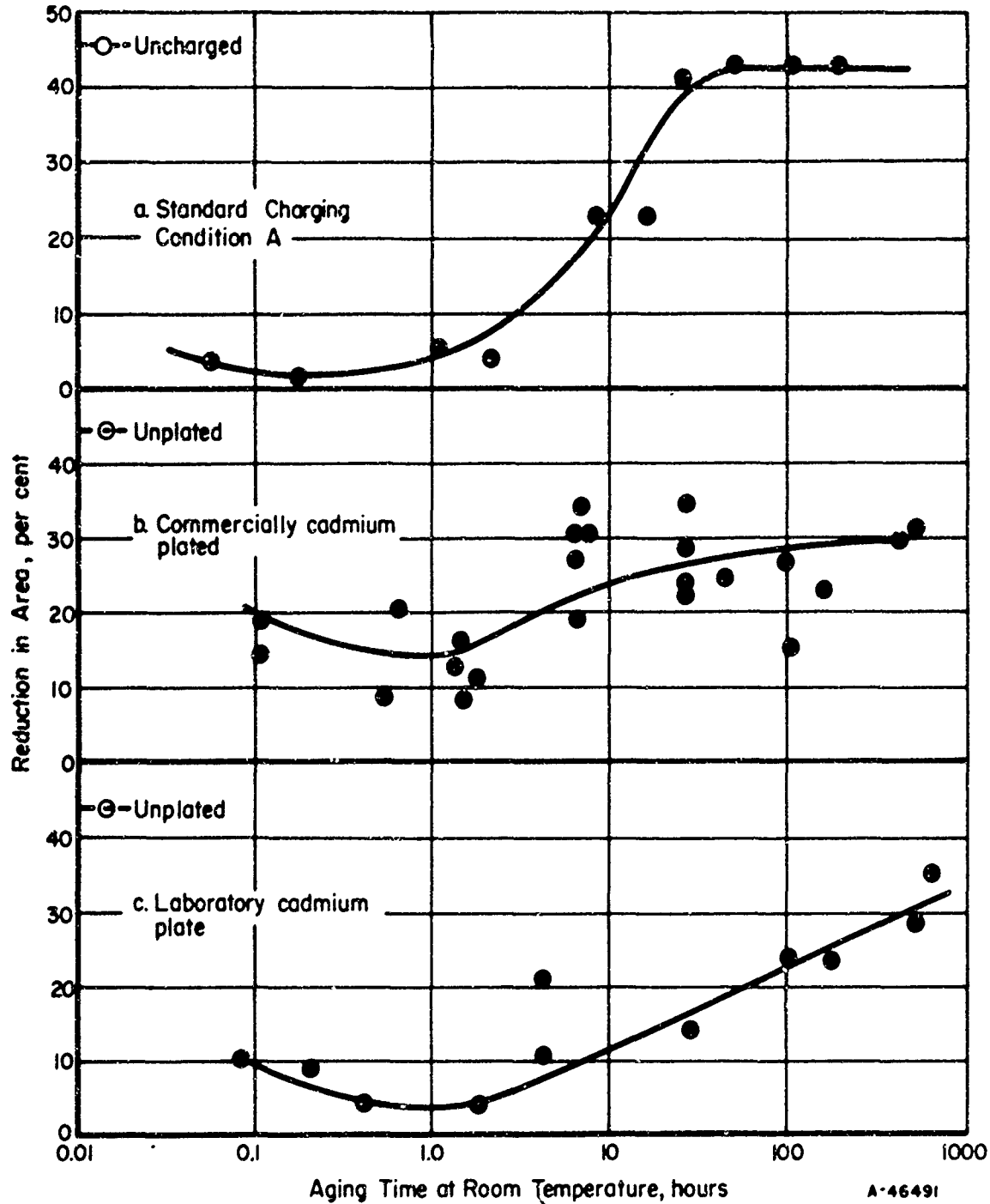


FIGURE 58. RECOVERY CURVES FOR AGING OF UNNOTCHED SPECIMENS AT THE 270,000-PSI STRENGTH LEVEL, PREVIOUSLY HYDROGEN EMBRITTLED AS INDICATED<sup>(60)</sup>

Case Institute of Technology Charging Condition A:

Electrolyte: 4 per cent  $H_2SO_4$  in water

Poison: None

Current density: 20 ma/in.<sup>2</sup>

Charging time: 5 minutes.

The laboratory cadmium plating was performed with the commercial cyanide bath containing the same brightening agent as was used for the commercial plating. A cadmium anode was used, the current density was 20 amp/ft<sup>2</sup>, and plating time was 10 minutes.

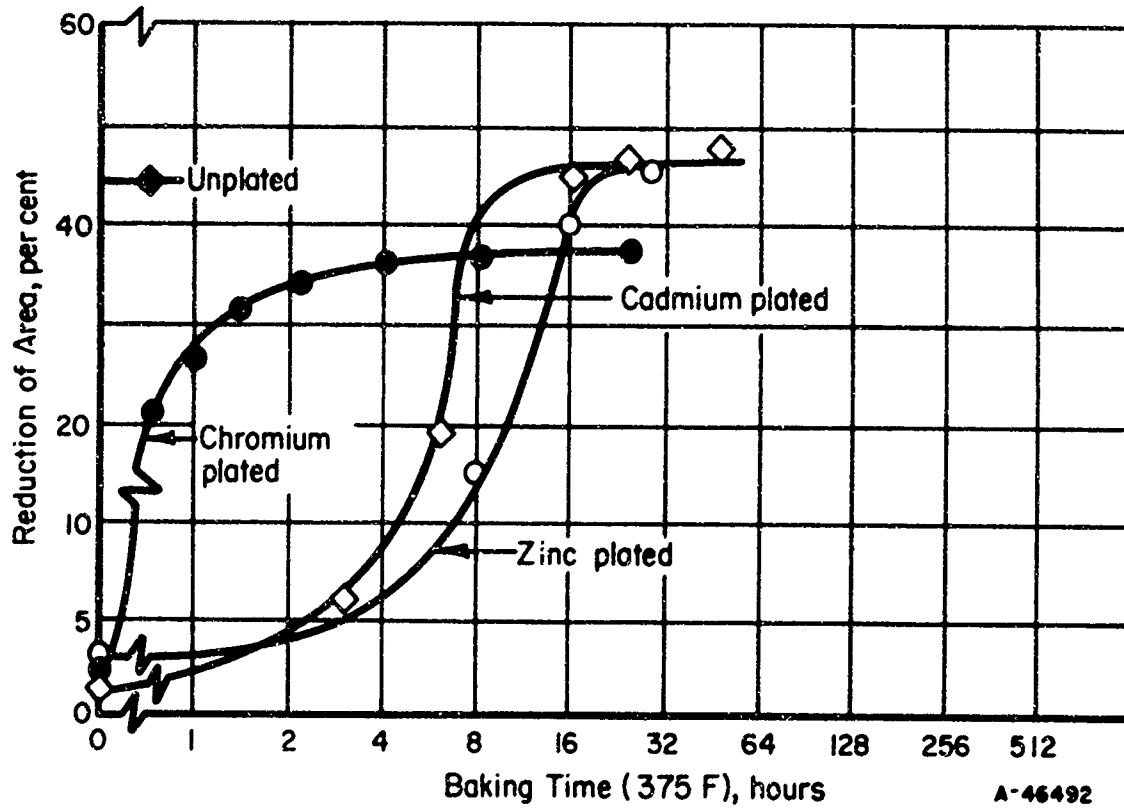


FIGURE 59. EFFECT OF BAKING TIME ON HYDROGEN EMBRITTLEMENT OF CHROMIUM-, CADMIUM-, AND ZINC-PLATED SPECIMENS(10)

Data by North American Aviation.

SAE 4340 steel, hardness = Rockwell C 45.

how the chromium plate also hinders recovery under these conditions and, further, that the cadmium plate commonly used for corrosion protection of high-strength steel parts acts as an even more effective barrier. The following data obtained by H. H. Johnson et al. (49) also show the barrier effect of cadmium plate on specimens with a reduction in area before plating of 40 to 42.5 per cent.

<u>Baking Treatment</u>	<u>Reduction in Area, per cent</u>	
	<u>Depleted Chemically</u>	<u>As Plated</u>
300 F, 0.5 hour	41.5	10.5
300 F, 2 hours	42.5	13.5

Geyer et al. (22) also performed an experiment to study cadmium as a barrier to hydrogen penetration. Four notched tensile specimens of SAE 4340 steel (290,000-psi ultimate tensile strength unnotched) were coated commercially with 0.0005 inch of cadmium by vacuum-metallizing techniques, rather than electroplating. The specimens sustained a load of 300,000 psi for 300 hours without failure. Three of the specimens then were exposed to 192 hours of salt fog, and light rusting occurred on the specimens. The specimens again sustained a load of 300,000 psi for 300 hours without failure. The sustained-load test after exposure to salt fog was performed to determine whether any detrimental hydrogen embrittlement resulted during the corrosion process, which is electrochemical in nature. Cadmium is anodic to steel; therefore, atomic hydrogen would be released at the steel (cathodic) areas during the corrosion process. The other vacuum-metallized specimen that withstood 300,000 psi for 300 hours without failure was subsequently electroplated with cadmium from a fluoborate bath containing peptone. The specimen was not baked after plating. It broke upon loading to 300,000 psi. Thus, the vacuum-metallizing cadmium-deposition process was nonembrittling, as would be expected. It was shown that, using this process, corrosion of the cadmium-coated steel in this instance did not cause hydrogen embrittlement. However, the vacuum-deposited cadmium did not prove to be a barrier to hydrogen penetration during subsequent cadmium electrodeposition.

The recovery of the original properties of cadmium-plated high-strength steel parts is an important problem in the aircraft industry. At room temperature, the recovery of ductility lost due to hydrogen embrittlement as the result of cadmium plating has been found to be extremely slow and often is incomplete after very long aging times. For example, cadmium-plated rings cut from a tubular part made of SAE 4340 steel with a hardness of Rockwell C 50 showed no recovery of ductility after aging for 2 weeks (Figure 60). However, the recovery of ductility increases rapidly with increasing temperature, as Eakin and Lownie(31) showed for thin, cadmium-plated clock-spring steel. This is illustrated in Figure 61. Although investigations such as this one on clock-spring steel indicate that temperatures up to at least 525 F greatly accelerate recovery of ductility lost as the result of hydrogen embrittlement, some tests conducted on SAE 4340 steel indicate that the higher temperatures may be detrimental to the ductility of high-strength cadmium-plated parts. In any event, temperatures over 610 F, the melting point of cadmium must be avoided, because liquid cadmium can cause cracking of low-hydrogen steel. Also, baking temperatures higher than 400 F produce discoloration of cadmium-plated parts and, thus, are undesirable. It has been suggested that the presence of such an oxide layer on the cadmium further interferes with the removal of hydrogen, and this may explain the adverse effect of baking at temperatures above 400 F that have been observed sometimes. Another possible explanation to account for such an effect is the formation of a brittle layer at the steel-cadmium interface as the result of diffusion of the cadmium into the steel.

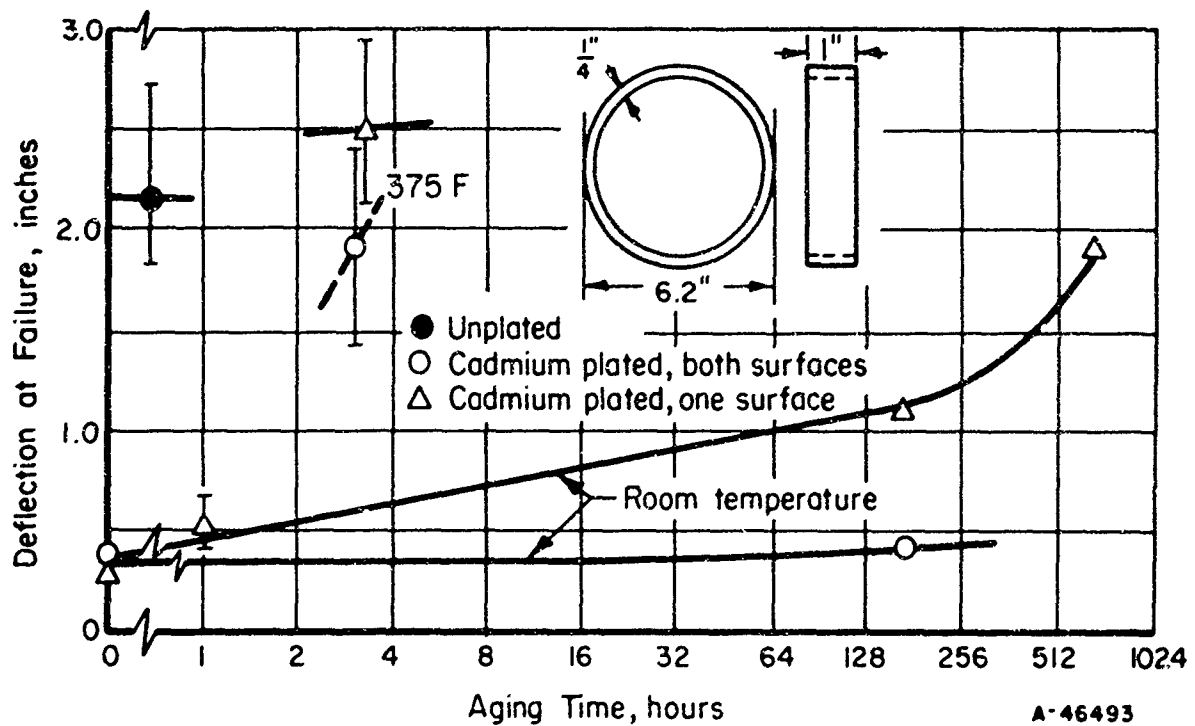


FIGURE 60. EFFECT OF ROOM-TEMPERATURE AGING AND BAKING AT 375 F ON HYDROGEN EMBRITTLEMENT OF CADMIUM-PLATED (0.001 INCH) STEEL TUBE(10)

Data by Menasco.

SAE 4340 steel; hardness = Rockwell C 50.

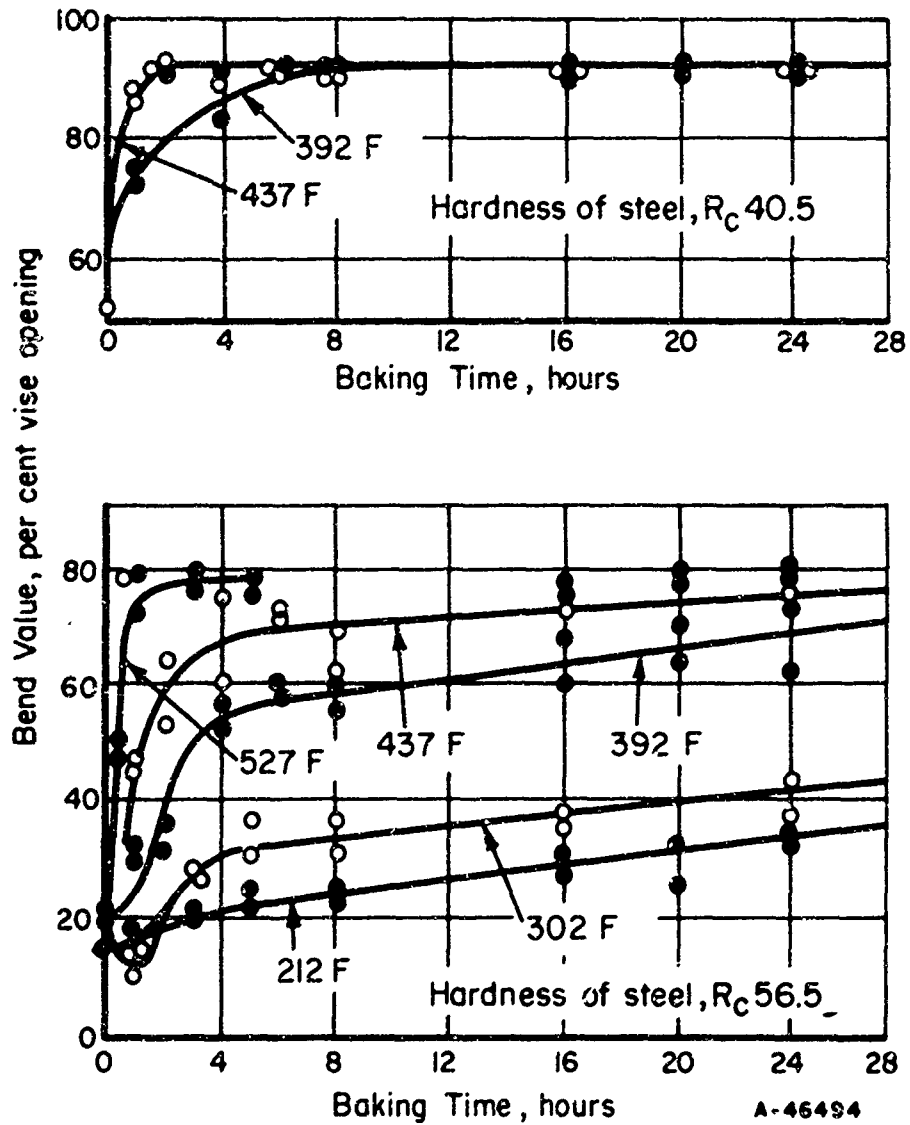


FIGURE 61. EFFECTS OF TEMPERATURE AND TIME ON RECOVERY FROM HYDROGEN EMBRITTLEMENT OF CADMIUM-PLATED CLOCK-SPRING-STEEL STRIP (0.008 IN.  $\times$  1/4 IN.)<sup>(10)</sup>

(After Eakin and Lownie, Reference 31).



Before strength levels were boosted to the point where delayed, brittle failures were encountered in service, the most common relief practice for hydrogen embrittlement resulting from cadmium plating consisted of baking at 375 to 400 F for 3 or 4 hours. When hydrogen-induced delayed, brittle failures were encountered, baking times often were increased to 23 hours, but this practice was only partially effective. The effects of room-temperature aging and of baking on the susceptibility to delayed, brittle failures have already been discussed because of their use to produce different hydrogen contents for laboratory investigations of the phenomenon. Various investigators showed that, although suitable baking treatments resulted in recovery of lost ductility, frequently such treatments do not eliminate susceptibility to delayed failures, especially for materials of the higher strength levels; for example, see Figure 43 (page 69). Delayed failures have occurred after baking for times at least as long as 100 hours. It was shown that data obtained in a short-time tensile test are not suitable criteria of the susceptibility to delayed, brittle failure.

The recovery of parts cadmium plated on only one surface is considerably faster than that of parts plated on both sides. Figure 60 illustrates the difference for hollow parts plated in the one case only on the outer surface and in the other case on both surfaces. Occasionally, a specific lot of material is found which is especially resistant to the relief of hydrogen embrittlement. Often this is due to variations in the cadmium plate. A dense plate offers more resistance to the effusion of hydrogen than does a more porous plate. One factor influencing the type of plate produced is the use of a brightener in a cadmium-plating solution. One investigation showed that very small amounts of such an additive greatly reduced the recovery from hydrogen embrittlement of SAE 4340 steel heat treated to a hardness of Rockwell C 48. Also, some plating baths are more efficient than others and plate out less hydrogen at the metal surface. Such factors will be discussed more fully in a separate report being prepared on the movement of hydrogen in steel.

### NEED FOR HYDROGEN MOVEMENT

A discussion of the chief requirements for delayed, brittle failures induced by hydrogen has been presented in preceding sections of this report. It has been shown that a critical combination of strength level, applied stress, and hydrogen content must be present in a region where failure can be initiated, usually in a region of triaxial stress state. Frequently, the necessary amount of hydrogen is not present at such a site, so movement of hydrogen must take place if failure is to be initiated. Also, as the failure propagates, the region of triaxial stress moves, so in most instances, hydrogen must move if propagation is to continue.

If hydrogen is to be free to move during the course of the failure, then conditions must be such as to favor diffusion of hydrogen. This, then, brings in considerations of temperature and time.

### Hydrogen Movement Demonstrated

In the work of Frohberg et al. (5), laboratory delayed failures were induced in sharp-notch specimens of high-strength SAE 4340 steel which had been electrolytically precharged with hydrogen and then subjected to a sustained load. Although the amount

of hydrogen introduced during the standard charging procedure was too small to be detected by analysis, specimens heat treated to the 270,000-psi strength level failed in a brittle manner after several hours' loading at stresses approaching 100,000 psi. One phase of this investigation concerned the hydrogen distribution within the specimen immediately after charging and the change in distribution upon aging. Unnotched tensile specimens were hydrogen charged and aged at room temperature. Surface layers of the specimens were removed by grinding under a flood of coolant, and the specimens were tested promptly. Five minutes after charging (the same interval used in sustained-loading tests of charged specimens), the hydrogen was highly concentrated in the surface layer of the specimen at the 270,000-psi strength level. Removal of an 0.020-inch-thick layer from the specimen surface increased the reduction in area from 3 per cent to a normal value of 43 per cent. After aging for 4 hours, the removal of 0.050 inch (2-1/2 times as much) from the surface increased the ductility to only 38 per cent reduction in area. These results indicate clearly that hydrogen diffuses into the specimen interior upon aging at a suitable temperature (in this case, room temperature).

Various investigators, including Troiano and co-workers<sup>(49)</sup>, Elsea and co-workers<sup>(7)</sup>, and Chilton<sup>(76)</sup> hypothesized that hydrogen in steel will migrate to areas of high stress. This could result in hydrogen concentration at the high-stress region and possibly result in brittle failure.

Geyer et al. <sup>(22)</sup> performed an experiment to ascertain if the residual hydrogen in steel migrates sufficiently to cause failure. The notched areas of four specimens of SAE 4340 steel heat treated to the 290,000-psi tensile-strength level were completely filled with wax, and then cadmium electroplated from the conventional cyanide bath. No baking treatment was used after plating so as to insure that residual hydrogen would be available for migration if it were to occur. Sustained-load tests gave the following results:

<u>Specimen</u>	<u>Load, psi</u>	<u>Time, hours</u>	<u>Results</u>
1	220,000	144	No failure
2	220,000	60	Failed
3	220,000	25	Failed
4	220,000	144	No failure

The load on the two specimens which had not failed in 144 hours was increased to 300,000 psi. One specimen failed in 55 hours and the other specimen failed after 73 hours at the new load. All unplated, notched specimens of the same steel at the same strength level sustained 220,000 psi for 400 hours and then 300,000 psi for 400 hours without failure. It can be deduced from this experiment that hydrogen in steel will migrate to points of high stress, with possible failure of the part.\*

\*The variation in the time to failure in this investigation points up some of the problems involved in studying the delayed-failure phenomenon experimentally. Because hydrogen diffuses in steel at an appreciable rate at room temperature and because one is dealing with at most only a few ppm of hydrogen, reliable analyses are difficult to obtain. Hence, many investigators rely upon electrolytic charging or electroplating under standardized conditions to introduce fairly reproducible amounts of hydrogen into the steel. However, recent work has shown that variations in preparation of the steel surface can have considerable effect on the rate at which the surface absorbs hydrogen.

Frohberg et al. (5) showed that the diffusion of hydrogen plays a very important role in the delayed-brittle-failure phenomenon. During room-temperature aging prior to loading, outgassing, which decreases the total amount of hydrogen present, competes with the inward diffusion of hydrogen to establish the hydrogen distribution at the time of loading. This is shown in Figure 62. The hydrogen distribution is a factor in determining the delayed-failure characteristics. In the case of precharged notched specimens, the lower critical stress increases continuously with prior aging, because the available hydrogen concentration at the base of the notch is decreasing continually(5). It was suggested that a critical combination of hydrogen and stress determines this limiting stress. However, as was shown previously, the notched tensile strength of charged specimens and the time to failure both pass through a minimum as a function of prior aging time after the same initial charging condition. Because of the relative insensitivity of the rupture time to strength level, it was suggested that the fracture time is related to the macroscopic diffusion of hydrogen inward from the initial surface concentration of electrolytically introduced hydrogen.

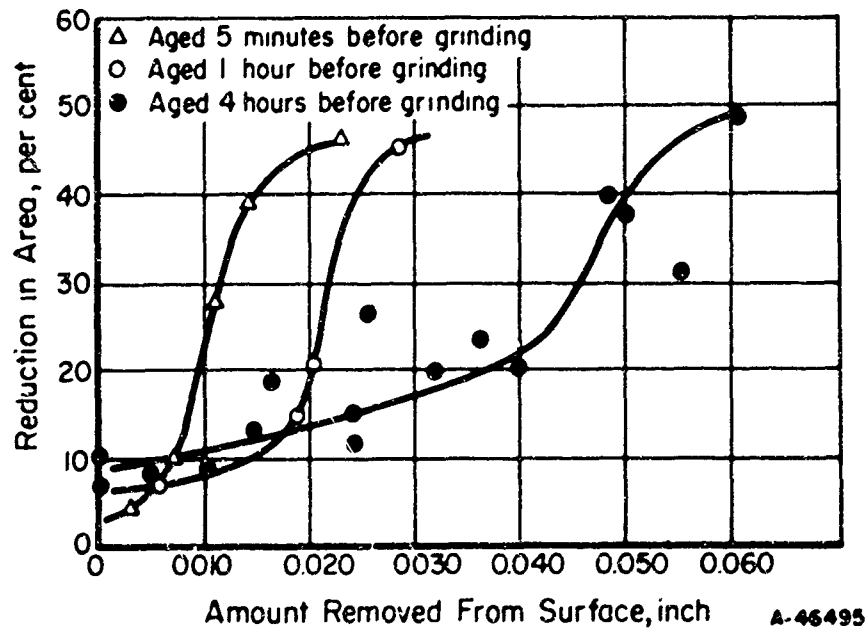


FIGURE 62. EFFECT OF REMOVING SURFACE LAYERS OF METAL FROM CHARGED UNNOTCHED TENSILE SPECIMENS AT THE 270,000-PSI STRENGTH LEVEL(5)

Case Institute of Technology Charging Condition A:

Electrolyte: 4 per cent  $H_2SO_4$  in water  
 Poison: None  
 Current density: 20 ma/in.<sup>2</sup>  
 Charging time: 5 minutes.

Barnett and Troiano(39) studied crack initiation and subsequent slow crack propagation of precharged notched specimens. For specimens aged 5 minutes at room temperature before loading, several important characteristics were observed that are related to the role of hydrogen in delayed failures. The specimens cracked (but did not

fracture) almost immediately upon application of a stress within the delayed-failure stress range. Below the lower critical stress, a crack did not form during an extended time interval in excess of 100 hours. Therefore, the lower critical stress represented the stress below which a crack was not initiated. After an initial crack formed, presumably to the depth of the existent hydrogen-rich zone, the crack depth increased in a manner proportional to the square root of the static-loading time. This relationship is analogous to the simplified diffusion equation,  $x^2 = Dt$ , where  $x$  is the penetration,  $t$  is the time at temperature, and  $D$  is the diffusion coefficient. This behavior suggested that crack propagation was controlled by macroscopic diffusion of the hydrogen front inward. In addition, the fracture strength determined from the uncracked area was approximately equal to the uncharged notched tensile strength, or slightly higher. Thus, it appeared that the crack front and the hydrogen front were moving inward simultaneously. At least the hydrogen front was not appreciably ahead of the crack front, or else some embrittlement would have been indicated in the measured fracture strength.

The importance of hydrogen diffusion in delayed, brittle failures is shown further by the results of the investigation of fracture stress performed by H. H. Johnson et al. (49). The crack formed under static-loading conditions grows slowly until the remaining nonhydrogenated core can no longer carry the applied load, at which time cataclysmic rupture occurs. The true stress at rupture is the fracture stress. In this study, SAE 4340 steel was heat treated to the 230,000-psi strength level, cathodically charged with hydrogen, immediately cadmium plated, and then baked to insure uniform hydrogen concentration throughout the section. Various baking times were used to provide a range of hydrogen concentrations. For various applied stresses and hydrogen concentrations, the fracture stress was found to be constant at approximately 330,000 psi, as is shown in Table 14. This value was obtained in two different ways, with excellent agreement between the two methods. In both methods, the applied load was divided by the uncracked area when sudden rupture occurred. The two methods differed in the way in which the uncracked area was determined. For the values of fracture stress shown in the table, the area at rupture was obtained from a calibration plot (determined by the heat-tinting technique) for converting resistance measurements into crack areas. Virtually the same results were obtained when the uncracked area was determined from visual examination of the fracture surface, which revealed two distinct modes of crack propagation. The rim, formed by slow, hydrogen-induced crack propagation, exhibited a fine texture that indicated brittle fracture. The inner fracture surface, formed by sudden rupture, was rougher and indicated a more ductile fracture.

Because a constant fracture stress was obtained, it appears that the average hydrogen concentration resulting from baking is not sufficient to propagate a crack. That is, crack propagation has to wait for a localized build-up of hydrogen concentration in front of the crack. Therefore, the rate of crack propagation cannot be greater than the rate at which the critical hydrogen concentration is attained by diffusion to the crack tip. Cataclysmic rupture, being characterized by a very high crack velocity, will occur only when the fracture strength of the nonhydrogenated core material is exceeded.

These concepts imply that crack propagation is a discontinuous process and actually consists of a series of separate crack initiations. The most severe triaxial stress state is to be found just in advance of the crack. When the critical hydrogen concentration is attained in that location, a small crack forms and then grows through the

hydrogen-enriched region until it joins the previous crack. Further crack growth must wait for diffusion of hydrogen, induced by the stress gradient, to the new region of maximum triaxial stress.

Other work performed at Case Institute verified the concept that crack growth in hydrogenated steel is discontinuous in fashion. This has been discussed in the section dealing with the effects of applied stress and plastic strain.

These various results have served to show that the degree of embrittlement encountered and the rate of crack propagation attained in delayed, brittle failure are controlled by the diffusion of hydrogen.

The localized redistribution of hydrogen resulting from plastic deformation has been discussed previously in the consideration of the effects of applied stress and plastic strain. Also, the stress-induced diffusion of hydrogen has been discussed. Interpretation of the data obtained from studies of these two aspects of the movement of hydrogen is consistent with the hypothesis that hydrogen exerts a maximum embrittling effect in the region of most severe stress state. Hydrogen occluded in internal voids is purported to be nondamaging, and embrittlement apparently results from hydrogen in solution.

TABLE 14. FRACTURE STRESS AT VARIOUS APPLIED STRESSES AND HYDROGEN CONCENTRATIONS OBTAINED IN A STUDY OF THE IMPORTANCE OF HYDROGEN DIFFUSION IN DELAYED FAILURE(a)(49)

Baking Time(b), hours	Applied Stress, psi	Fracture Stress, psi
3	200,000	308,000
3	225,000	319,000
7	200,000	334,000
7	225,000	327,000
12	200,000	335,000
12	200,000	342,000
12	225,000	346,000
18	225,000	329,000

(a) Ultimate tensile strength, uncharged specimen = 230,000 psi.

(b) The baking time was varied so as to provide different hydrogen concentrations.

#### Temperature Dependence

One of the unusual characteristics of hydrogen embrittlement is that the embrittlement disappears at low and high test temperatures and is, accordingly, most severe in an intermediate temperature range in the general vicinity of room temperature<sup>(77,78)</sup>.

This was discussed more fully in DMIC Memorandum 180 and is summarized in Figure 63 for SAE 1020 steel. The disappearance of hydrogen embrittlement at -321 F (liquid-nitrogen temperature) in SAE 4340 steel heat treated so as to have an ultimate tensile strength of 230,000 psi is evident from the data in Table 15<sup>(14)</sup>.

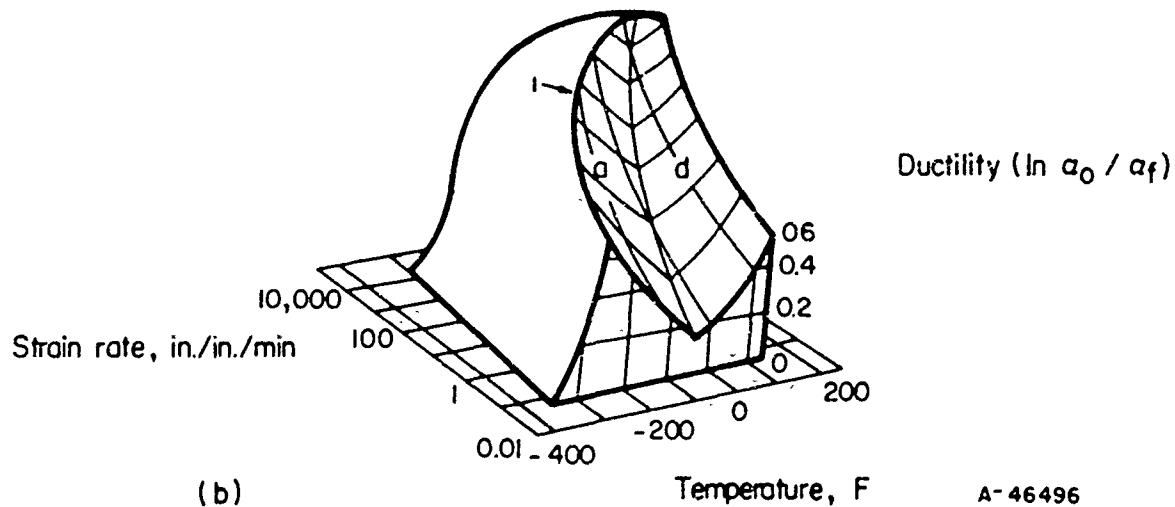
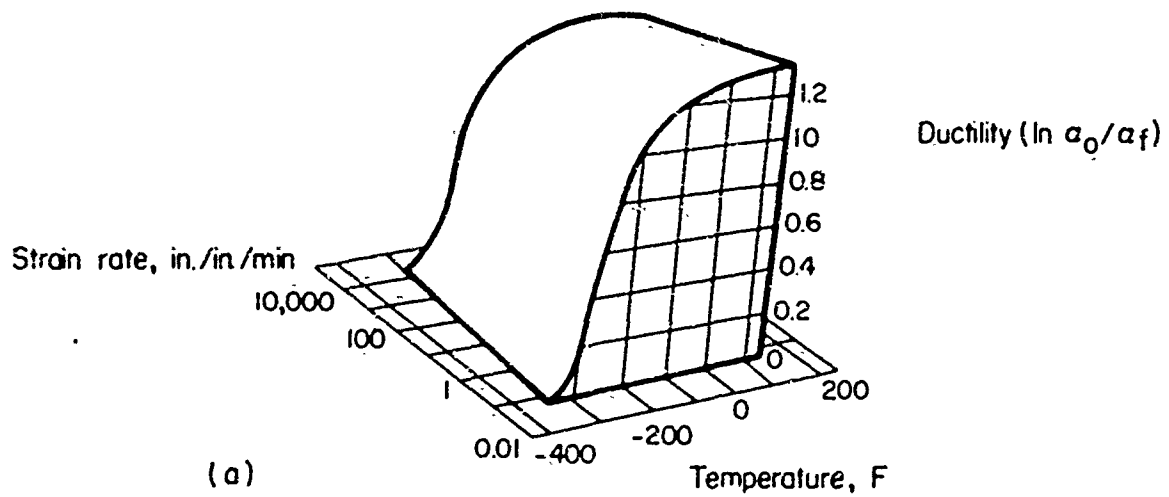
TABLE 15. EFFECT OF CHARGING CONDITIONS AND TEST TEMPERATURE ON THE DUCTILITY OF UNNOTCHED SAE 4340 SPECIMENS(a)(44)

Condition	Test Temperature, F	Reduction in Area, per cent
Uncharged specimen	Room	40
Specimen charged and cadmium plated	Room	5
Specimen charged and cadmium plated, baked 1 hour at 300 F	Room	10
Uncharged specimen	-321	22
Specimen charged and cadmium plated, baked 1 hour at 300 F	-321	22

(a) Heat treated to 230,000-psi tensile strength.

In this investigation by Morlet et al., an unnotched, hydrogenated specimen that was cadmium plated and then baked 1 hour at 300 F to provide a uniform hydrogen content was strained to 1.5 per cent reduction in area. This resulted in a multitude of tiny cracks, even though the specimen fractured with a ductility of 10 per cent reduction in area. However, at -321 F, it was possible to strain the hydrogenated specimens to more than 12 per cent reduction in area without forming any cracks. In studying the effect of plastic strain on hydrogen embrittlement, these investigators demonstrated the diffusion-controlled nature of the mechanism by aging at different temperatures. After straining 1.5 per cent at -321 F, specimens were aged at temperatures of 150 F, 80 F, 32 F, and -15 F. The results are summarized in Figure 64. The displacement of the aging curve to longer times at low aging temperatures is evidence that the behavior is diffusion controlled. The phenomenon is further indicated by an Arrhenius plot of the data, shown in Figure 65. As was discussed in a previous section\*, three separate stages were observed in the aging process for specimens that were strained after being charged with hydrogen. During the first stage, the reduction in area increased, then it decreased to a minimum value in the second stage, and finally in the third stage the ductility increased again and did so in a manner similar to that of the unstrained specimens. The variation in ductility during the first two stages of aging was particularly striking when compared with the aging behavior for the unstrained specimens. In Figure 65, the aging time at the midpoint of Stage One (corresponding to a reduction in area of 30 per cent) has been plotted against the reciprocal of the absolute aging temperature. The activation energy obtained from this plot was 8500 cal/g, which agreed well with the activation energy for diffusion of hydrogen through iron determined by Chang and Bennett<sup>(79)</sup>. Similar data for Stage Two of the aging curves are shown in Figures 66

\*The section "Effects of Applied Stress and Plastic Strain". See page 46.



A-46496

FIGURE 63. THE DUCTILITY OF AN SAE 1020 STEEL AS A FUNCTION OF STRAIN RATE AND TEMPERATURE<sup>(78)</sup>

(a) As annealed.

(b) As charged cathodically for 1 hr in 4 per cent sulfuric acid.

Curve i, in Figure 63b, bounds the range of strain rates and temperatures where embrittlement is found.

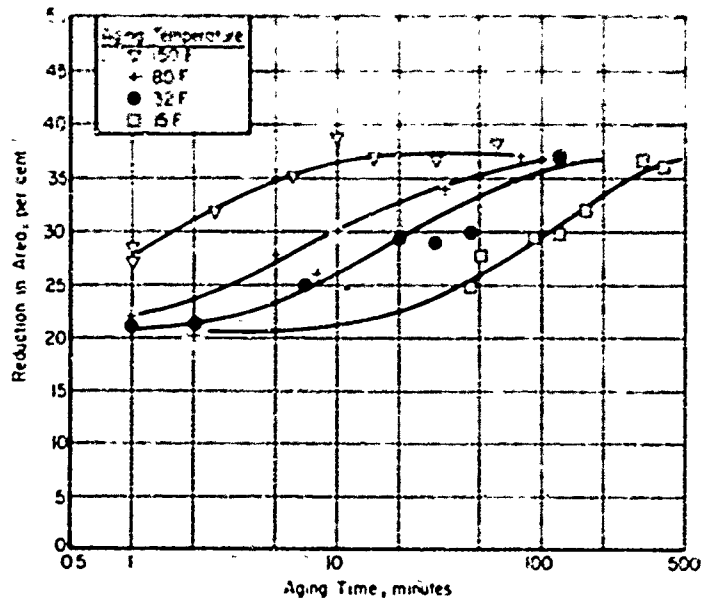


FIGURE 64. THE EFFECT OF AGING TIME AND TEMPERATURE ON THE RESULTING DUCTILITY IN THE FIRST STAGE OF AGING OF UNNOTCHED SPECIMENS PREVIOUSLY CHARGED WITH HYDROGEN AND STRAINED 1.5 PER CENT IN LIQUID NITROGEN(44)

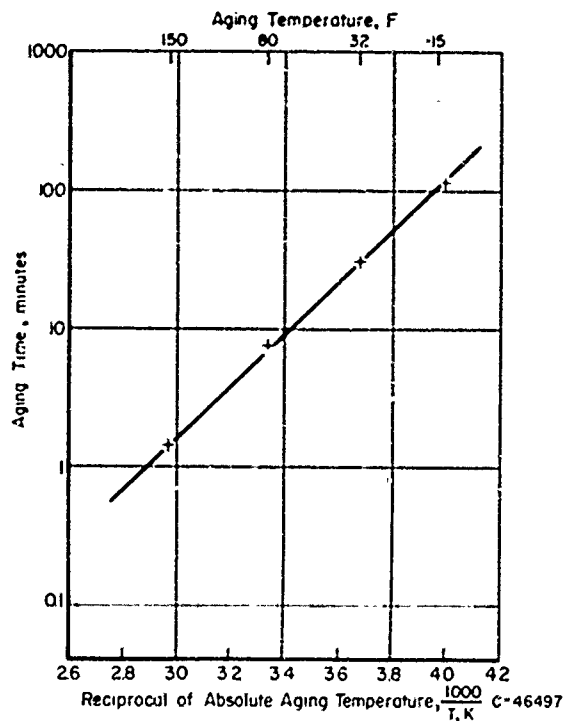


FIGURE 65. ARRHENIUS PLOT IN WHICH THE AGING TIME TO ACHIEVE HALF THE INCREASE IN DUCTILITY ASSOCIATED WITH THE FIRST STAGE OF AGING IS PLOTTED AGAINST THE RECIPROCAL OF THE ABSOLUTE AGING TEMPERATURE(44)

Activation energy 8500 cal/g.



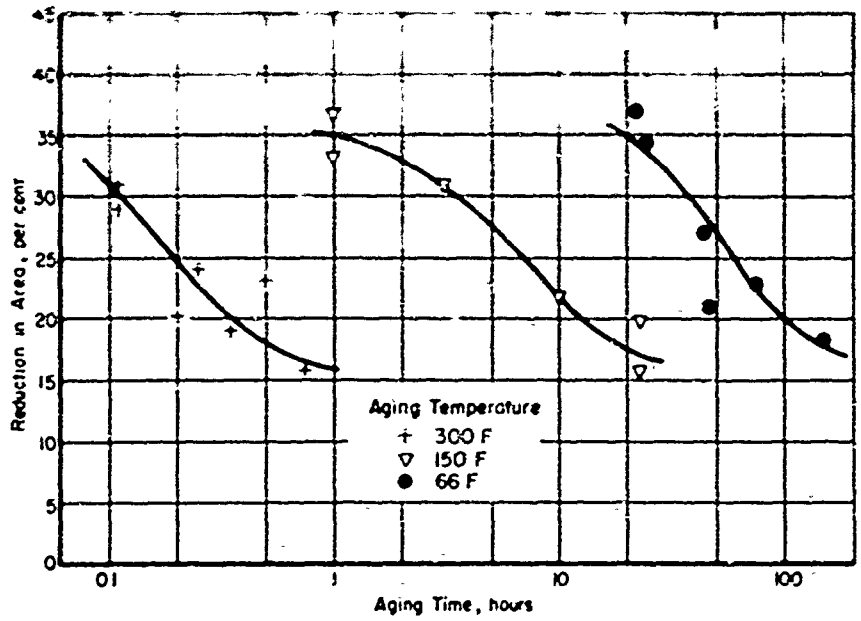


FIGURE 66. THE EFFECT OF AGING TIME AND TEMPERATURE ON THE RESULTING DUCTILITY IN THE SECOND STAGE OF AGING OF UNNOTCHED TENSILE SPECIMENS PREVIOUSLY CHARGED WITH HYDROGEN AND STRAINED 1.5 PER CENT IN LIQUID NITROGEN(44)

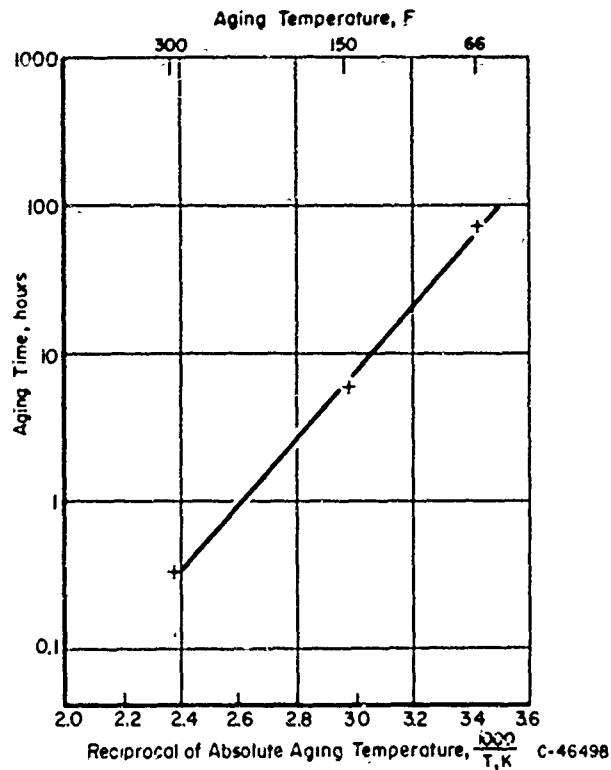


FIGURE 67. ARRHENIUS PLOT IN WHICH THE AGING TIME REQUIRED TO ACHIEVE HALF THE REDUCTION IN DUCTILITY ASSOCIATED WITH STAGE TWO OF AGING IS PLOTTED AGAINST THE RECIPROCAL OF THE ABSOLUTE AGING TEMPERATURE(44)  
Activation energy 9600 cal/g.

and 67. An activation energy of 9600 cal/g was obtained for Stage Two, a value well within the expected experimental error. These results confirm the diffusion-controlled nature of the hypothesis of hydrogen embrittlement.

Slaughter et al. (8) observed a potent effect of testing temperature on delayed failures. In these experiments, high-strength steel bolts were loaded statically by applying a measured torque. For the 230,000-psi strength level, bolts pickled 12 minutes in 10 per cent HCl failed in from 11 to 118 minutes after stressing at room temperature. One bolt, charged cathodically at 218 F after stressing, failed within 45 seconds after the beginning of electrolysis. Another bolt, pickled 12 minutes in 10 per cent HCl and cooled to -112 F before loading, was held in the stressed condition for 235 hours at -112 F without failure. This bolt (still under stress) failed within an hour after being warmed to room temperature.

Experimental work performed at Case Institute of Technology showed that test temperature strongly affects the parameters which describe the hydrogen-induced delayed-failure phenomenon. R. D. Johnson et al. (60) showed that the notched tensile strength of charged specimens aged 5 minutes at the test temperature prior to testing was reduced from the normal value of the notched tensile strength over the temperature range from -230 F to +190 F. At the extreme temperatures of -320 F and +250 F, there was little difference between the notched tensile strengths in the charged and the uncharged conditions. These results are shown in Figure 68. The rupture time was found to decrease and the lower critical stress continually increased as the test temperature of statically loaded, charged, notched specimens was raised from room temperature to 250 F, as is shown in Figures 69 and 70. A linear Arrhenius plot (log of the rupture time plotted versus the reciprocal of the absolute temperature) was not obtained over this temperature range (see Figure 71). Because crack propagation at room temperature appears to be controlled by diffusion, the nonlinearity of the Arrhenius plot was attributed primarily to the different initial hydrogen distributions existing at the time of loading, since different amounts of outgassing and redistribution of hydrogen presumably took place during the fixed 5-minute aging time at the various test temperatures.

In a continuation of this work (45), the temperature dependence of the failure time was measured from room temperature to about -50 F at two applied stresses for each of two initial hydrogen distributions. One distribution was essentially a highly concentrated surface layer of hydrogen obtained by aging 5 minutes at room temperature after charging. For this hydrogen distribution, previous work had shown that a static stress caused an initial crack to form to a given depth in a notched specimen immediately upon loading, from which point the increase in crack depth was proportional to the square root of the static-loading time. Figure 72 shows that reasonably linear Arrhenius plots were obtained for applied stresses of 125,000 and 200,000 psi, which supports the suggestion that the crack propagation is controlled by the macroscopic diffusion of hydrogen inward for this initially nonuniform hydrogen distribution in which the hydrogen was concentrated in the surface layers.

The other hydrogen distribution investigated was obtained by a 3-hour aging treatment at room temperature. This aging time was chosen after the rupture time and the crack-propagation characteristics had been determined as a function of aging time. It represented the deepest penetration of hydrogen that could be obtained by aging while still maintaining the hydrogen concentration at a level high enough that there would be essentially no incubation period before crack initiation in the sharp-notched specimens

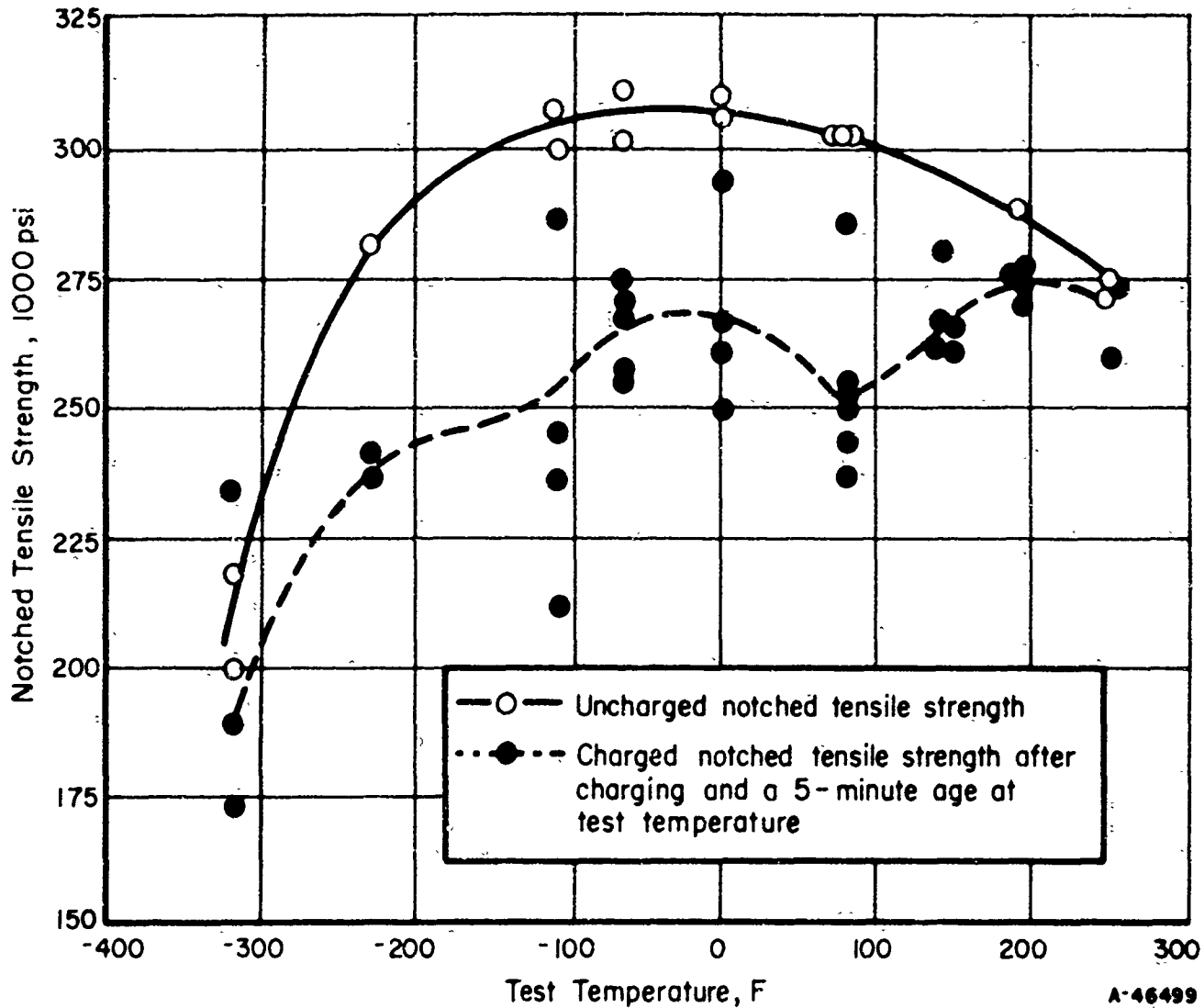


FIGURE 68. EFFECT OF TESTING TEMPERATURE ON THE NOTCHED TENSILE STRENGTH OF SAE 4340 STEEL IN THE CHARGED AND UNCHARGED CONDITIONS<sup>(60)</sup>

230,000-psi strength level, sharp-notch specimens

Case Institute of Technology Charging Condition A:

Electrolyte: 4 per cent  $H_2SO_4$  in water

Poison: None

Current density: 20 ma/in.<sup>2</sup>

Charging time: 5 minutes.

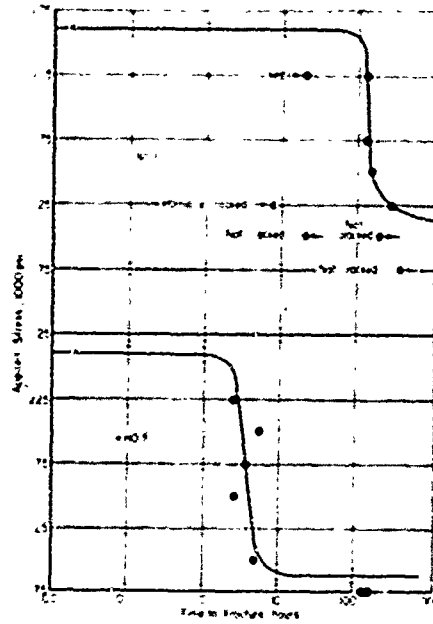


FIGURE 69. DELAYED-FAILURE BEHAVIOR AT -30 F AND 80 F FOR SAE 4340 STEEL SPECIMENS AT 230,000-PSI STRENGTH LEVEL<sup>(60)</sup>

Sharp-notch specimens, 5-minute age at test temperature

Case Institute of Technology Charging Condition A, as in Figure 68.

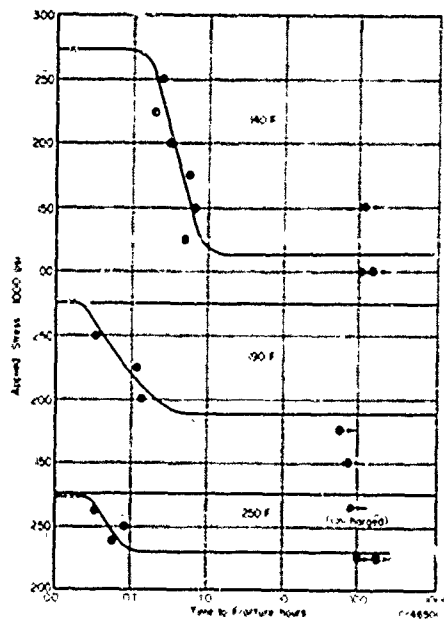


FIGURE 70. DELAYED-FAILURE BEHAVIOR AT 140 F, 190 F, AND 250 F FOR SAE 4340 STEEL SPECIMENS AT 230,000-PSI STRENGTH LEVEL<sup>(60)</sup>

Sharp-notch specimens, 5-minute age at test temperature.

Case Institute of Technology Charging Condition A, as in Figure 68.

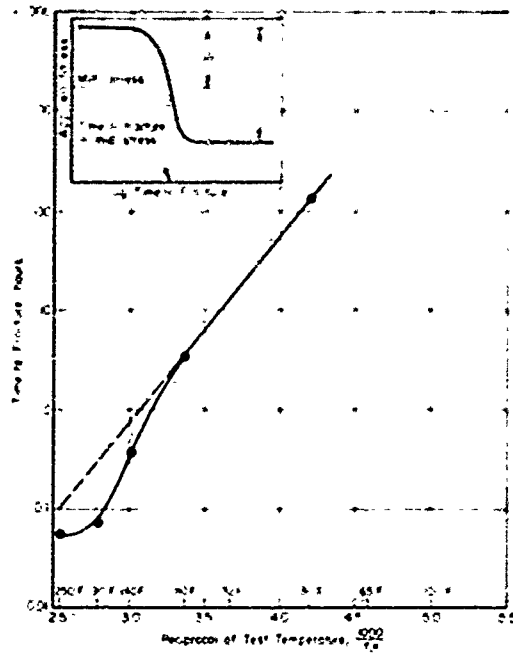


FIGURE 71. TIME FOR FRACTURE AS A FUNCTION OF RECIPROCAL OF ABSOLUTE TEST TEMPERATURE FOR SAE 4340 STEEL SPECIMENS AT 230,000-PSI STRENGTH LEVEL<sup>(60)</sup>

Sharp-notch specimens aged 5 minutes at test temperature. Fracture time taken midway between upper and lower critical stresses as indicated.

Case Institute of Technology Charging Condition A, as in Figure 68.

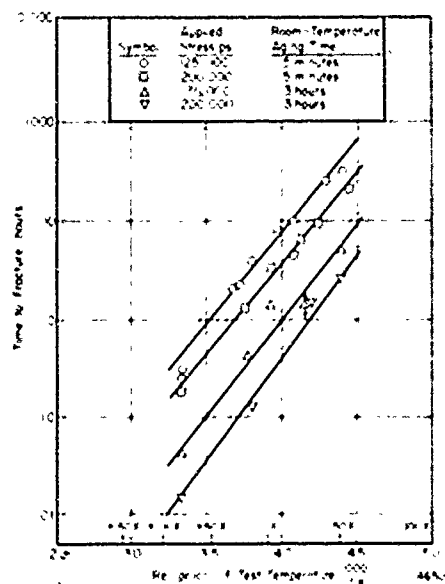


FIGURE 72. FRACTURE TIME VERSUS RECIPROCAL OF ABSOLUTE TEMPERATURE FOR CHARGED, SHARP-NOTCH SPECIMENS AT THE 230,000-PSI STRENGTH LEVEL, AGED AND STRESSED AS INDICATED<sup>(45)</sup>

used. The hydrogen penetration was deep enough that the propagating crack did not reach the hydrogen front prior to fracture for applied stresses of 175,000 and 200,000 psi. The temperature dependence of the rupture time for these conditions also is shown in Figure 72. Again, the Arrhenius plots were reasonably linear. The slopes of all four plots could be described by an activation energy of  $9,000 \pm 600$  cal/g-atom. This indicated that the crack-propagation rate was controlled by diffusion of hydrogen, even in the specimens aged for 3 hours in which the hydrogen had penetrated throughout the region through which the crack had to propagate to cause failure. These results also supported the hypothesis that the mechanism of crack propagation is diffusion-controlled on a microscopic scale at the tip of the crack.

Steigerwald, Schaller, and Troiano<sup>(80)</sup> studied the effect of testing at temperatures below room temperature on the delayed-failure behavior of SAE 4340 steel at the 230,000-psi strength level, using sharp-notch specimens precharged with hydrogen. The results are shown in Figures 73, 74, and 75. Incubation times were determined by the electrical-resistance method. Lowering the temperature prolonged both the incubation time and the fracture time. At -50 F and -95 F, the incubation time coincided with the fracture time, that is, once a crack was initiated, it immediately propagated through the specimen. In their analysis of the incubation period, these investigators showed that, if the local initiation of a crack at a given applied stress is dependent only on the diffusion of hydrogen, the log of the ratio of incubation time to the absolute temperature should vary linearly with the reciprocal of the absolute temperature. The results in Figure 76 show that such a relationship existed. This behavior indicates that the incubation time required for the formation of the first crack in a hydrogenated specimen tested under static loading is controlled principally by the diffusion of hydrogen. The activation energy of 9120 cal/g-atom is in excellent agreement with values for hydrogen embrittlement reported by Morlet and co-workers<sup>(44)</sup> and with reported values for the diffusion of hydrogen in iron for the temperature range employed.\*

The disappearance of hydrogen embrittlement and delayed, brittle failures at low temperatures results from the decrease in hydrogen-diffusion rate with decreasing temperature. For a test at a fixed strain rate, the stress-induced gradient diminishes with decreasing temperature, so the embrittlement decreases also. Troiano and his co-workers have suggested that the disappearance of hydrogen embrittlement at high temperatures also may be related to stress-induced hydrogen diffusion<sup>(44)</sup>. Because the driving force tending to concentrate hydrogen in the region of maximum triaxiality is stress induced, the driving force presumably is independent of the temperature. However, the force tending to homogenize the solution presumably increases with temperature. Thus, at high temperatures, the gradient cannot be created, and embrittlement should decrease. It should also be noted that the notch sensitivity of the steel decreases with increasing temperature; thus, the voids should be less effective in creating a region of severe stress state.

### Strain-Rate Dependence

It is a general rule that the severity of embrittlement increases with increasing strain rate. However, for hydrogen embrittlement, the reverse is true for all

\*The activation energy for hydrogen diffusion in iron exhibits two values which have been attributed to variations in the diffusion mechanism. At high temperatures, the activation energy is approximately 3000 cal/g-atom, while in the room-temperature range values from 6000 to 9200 cal/g-atom have been reported.

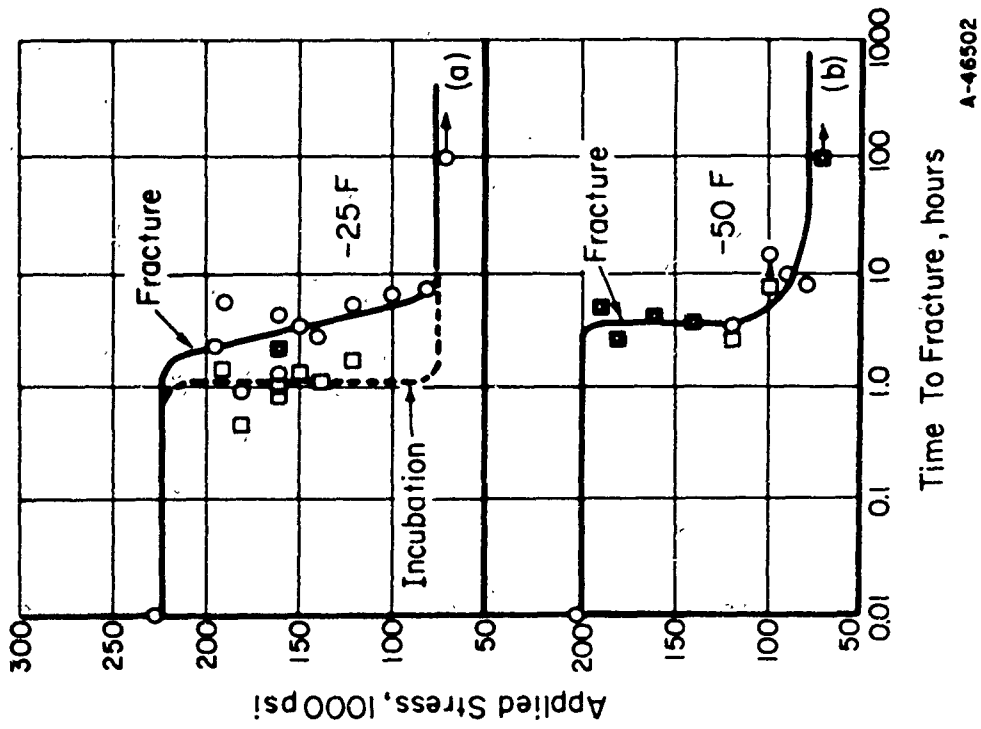


FIGURE 74. DELAYED-FAILURE BEHAVIOR OF HYDROGENATED HIGH-STRENGTH STEEL SPECIMENS TESTED AT -25 AND -50 F(80)

SAE 4340 steel heat treated to a tensile strength of 230,000 psi.

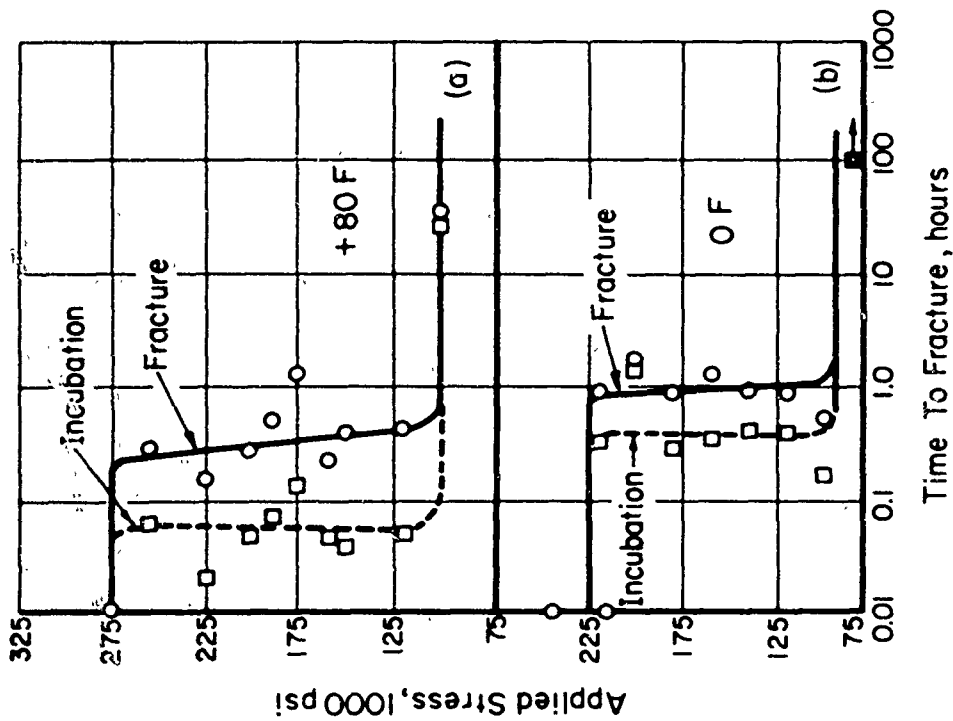


FIGURE 73. DELAYED-FAILURE BEHAVIOR OF HYDROGENATED HIGH-STRENGTH STEEL SPECIMENS TESTED AT 80 AND 0 F(80)

SAE 4340 steel heat treated to a tensile strength of 230,000 psi.

A-46502

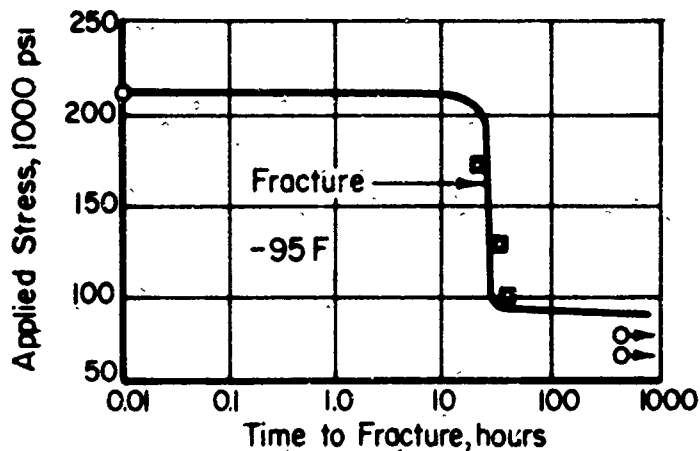
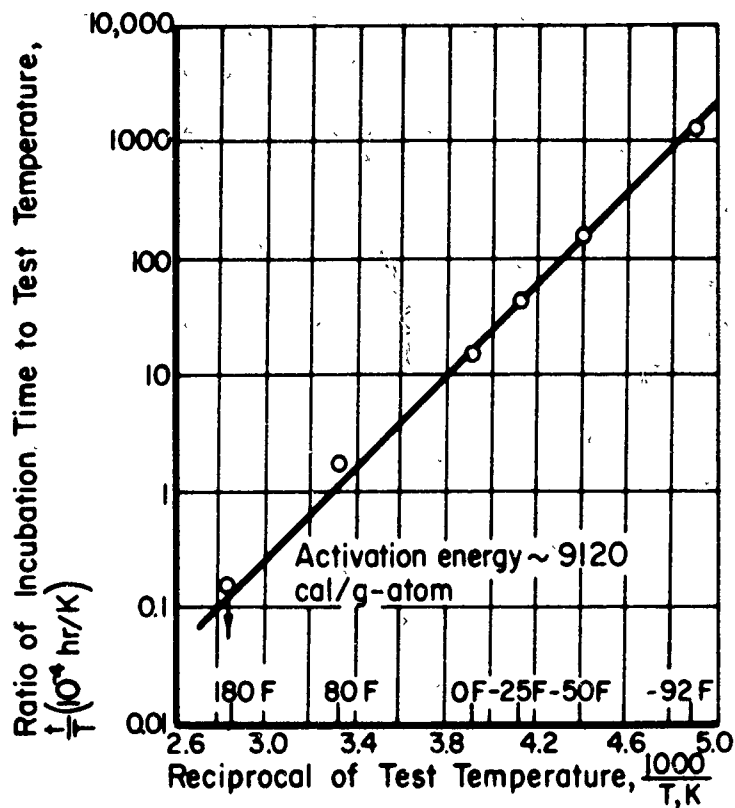


FIGURE 75. DELAYED-FAILURE BEHAVIOR OF HYDROGENATED HIGH-STRENGTH STEEL SPECIMENS TESTED AT -95 F<sup>(80)</sup>

SAE 4340 steel heat treated to a tensile strength of 230,000 psi.



A-46503

FIGURE 76. RATIO OF INCUBATION TIME TO ABSOLUTE TEMPERATURE AS A FUNCTION OF RECIPROCAL OF ABSOLUTE TEMPERATURE FOR AN APPLIED STRESS OF 150,000 PSI<sup>(80)</sup>



temperatures at which hydrogen embrittlement is observed. For this reason, hydrogen embrittlement sometimes is referred to as low-strain-rate embrittlement. This has been discussed in a previous report (DMIC Memorandum 180), is shown in Figure 77, and has been summarized for SAE 1020 steel in Figure 63 (page 95). Hydrogen

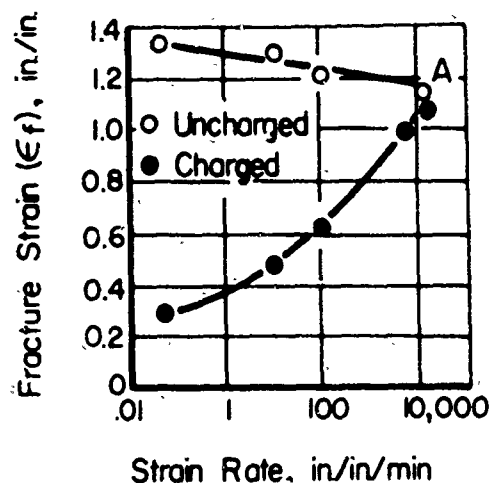


FIGURE 77. FRACTURE STRAIN AS A FUNCTION OF STRAIN RATE IN A CHARGED AND UNCHARGED, SPHEROIDIZED SAE 1020 STEEL AT ROOM TEMPERATURE<sup>(77)</sup>

embrittlement of high-strength steel is nil in an impact test. It may or may not be detected in a standard tensile test of unnotched specimens, depending on the hydrogen content and distribution; however, it is more apparent in a notched tensile specimen with the triaxial stress state introduced by the notch. The most sensitive test for hydrogen embrittlement is the static-loading test of a notched specimen. According to the generally accepted mechanisms for hydrogen embrittlement and delayed, brittle fracture, the strain-rate dependence of hydrogen embrittlement reflects differences in the time available for hydrogen to diffuse into the highly stressed regions. In a test at high strain rates, such as an impact test, the time is not sufficient to permit a damaging amount of hydrogen to diffuse into the region of maximum triaxiality, and embrittlement does not develop. However, as the strain rate is decreased, more hydrogen can diffuse into the highly stressed region, and embrittlement tends to occur. The ultimate in this direction is achieved in the static-loading test where the strain rate is zero. Hydrogen diffuses very rapidly in ferritic or martensitic steels at room temperature, in fact, faster than most intermetallic diffusion at temperatures approaching the melting point of the solvent metal. Therefore, although the phenomenon is diffusion controlled, under many conditions severe embrittlement can be detected in an ordinary tensile test where the crosshead speed may be about 0.05 inch per minute and the test time may be in the neighborhood of 2 minutes. Thus, the accepted mechanism for hydrogen embrittlement is in agreement with the observed effects of temperature and strain rate.

The most sensitive test for revealing hydrogen embrittlement and the only satisfactory way to study delayed, brittle fracture is the static-loading test. Use of this test, of course, precludes a study of variations in strain rate. However, a few examples of the results of variations in strain rate on embrittled high-strength steels will be

included to complete the picture. Using notched tensile strength as a measure of embrittlement, Barnett and Troiano<sup>(6)</sup> showed that the embrittlement was quite sensitive to small variations in strain rate (see Table 16).

TABLE 16. EFFECT OF STRAIN RATE ON NOTCHED TENSILE STRENGTH OF SAE 4340 STEEL AT THE 230,000-PSI STRENGTH LEVEL, CATHODICALLY CHARGED<sup>(a)</sup> AND AGED 24 HOURS AT ROOM TEMPERATURE<sup>(6)</sup>

Nominal Strain Rate (Crosshead Speed), in. /min	Total Time of Test, min	Time From 80,000 Psi to Maximum Load, min.	Notched Tensile Strength, psi
0.07	1.75	0.75	301,000
0.05	2.5	1.75	262,000
0.002	47.0	20.0	200,000

(a) Case Institute of Technology Charging Condition A:

Electrolyte : 4 per cent H<sub>2</sub>SO<sub>4</sub> in water

Poison : None

Current density: 20 ma/in.<sup>2</sup>

Charging time : 5 minutes

However, the results of different investigations (for example, Reference 5) have shown that delayed failures can be encountered under conditions for which full recovery was indicated by the conventional notch tensile test. Klier, Muvdi, and Sachs<sup>(81)</sup> studied the effects of strain rate on the deflection at fracture of an unnotched bend specimen for different charging times and current densities. Their results, given in Figure 78, showed severe embrittlement when the strain rate was 2 inches per minute or less, whereas none was detected in the impact test. They also studied the effect of strain rate on the notched tensile strength of embrittled specimens of different strength levels. In the results shown in Figure 79, note how much lower the notched tensile strength was as determined by the delayed-failure test (static loading) than as determined in even the slowest of the tensile tests.

### EFFECT OF MICROSTRUCTURE

Since the usual way to achieve high strength levels in structural components made of steel is to develop a tempered martensitic structure, most of the investigations of hydrogen-induced, delayed, brittle failures of high-strength steels have been performed with tempered-martensite structures. In the section on the effect of strength level, it was shown that, the higher the strength level of tempered martensite of a given composition, the more susceptible is the material to delayed, brittle failures and the lower is the lower critical stress. The loss in load-carrying ability incurred is the reason users of high-strength steels are concerned about this type of failure.

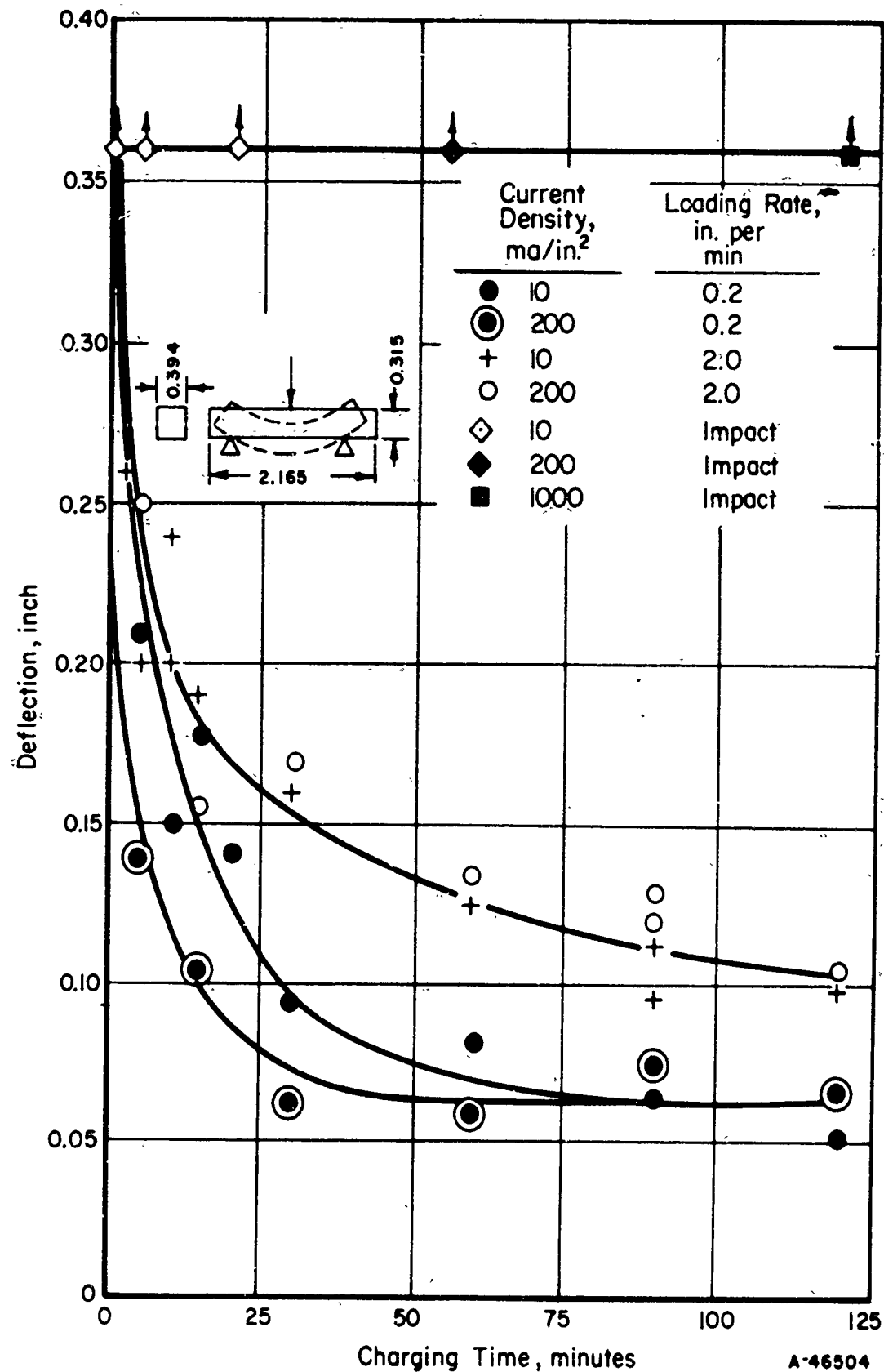


FIGURE 78. ROOM-TEMPERATURE DEFLECTION AT FRACTURE AS A FUNCTION OF ELECTROLYTIC CHARGING TIME FOR SMOOTH BEND SPECIMENS OF SAE 4340 STEEL WITH STRAIN RATE AND HYDROGEN CONTENT AS PARAMETERS<sup>(81)</sup>

Heat Treatment: Austenitized at 1600 F, oil quenched, tempered at 400 F.  
Bath: 10 per cent NaOH at 30 C.

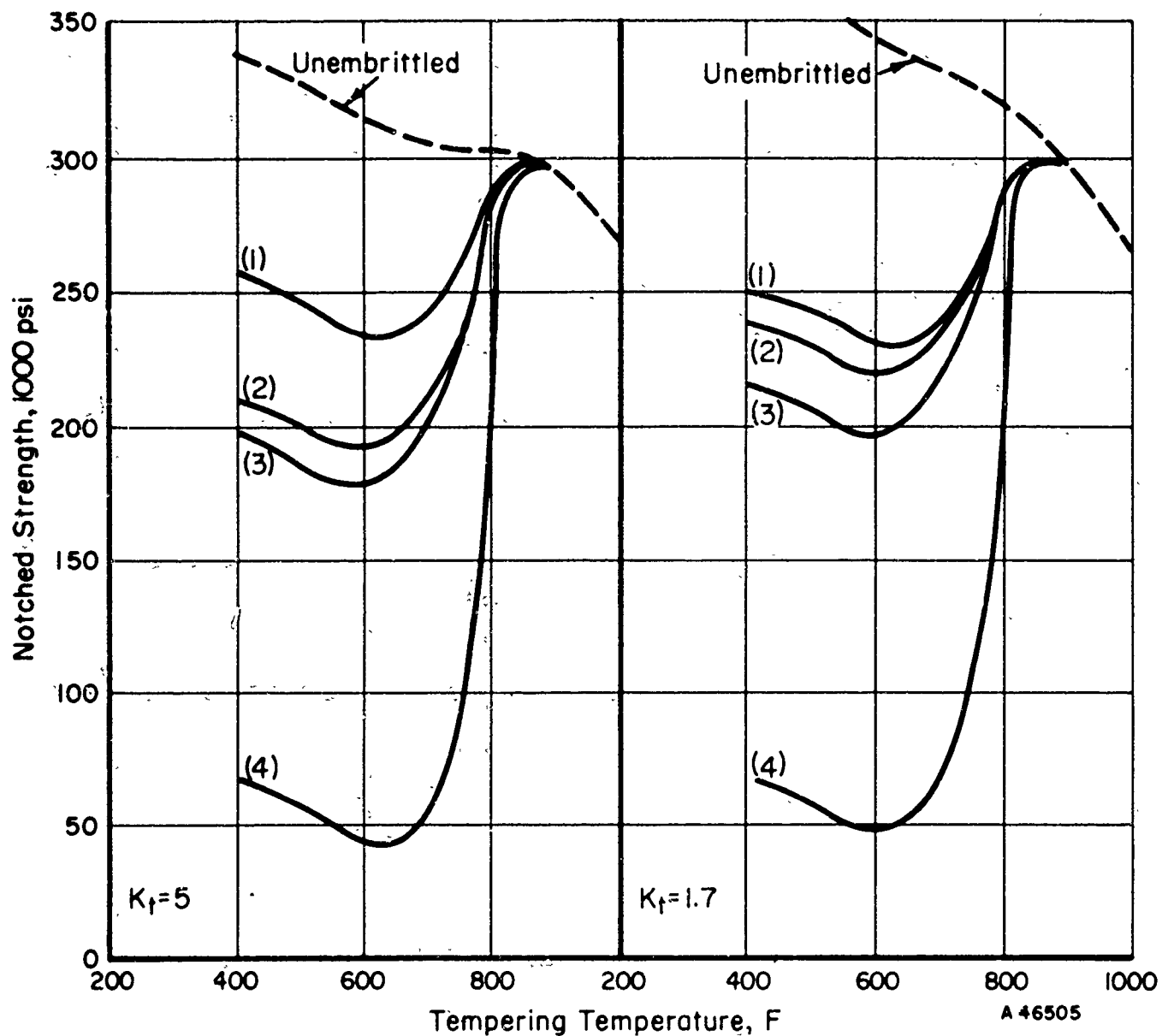


FIGURE 79. EFFECT OF LOADING RATE ON THE NOTCHED STRENGTH OF CATHODICALLY EMBRITTLED ( $C_1$ ) SAE 4340 STEEL<sup>(81)</sup>

(1) 2.00 in./min  
(2) 0.20 in./min

(3) 0.02 in./min  
(4) Static loading

Oil quenched from 1600 F.

Cathodically charged at 447 ma/in.<sup>2</sup> for 1/2 hr( $C_1$ ).

In the section of this report that describes the effect of composition, it was shown that hydrogen-induced, delayed failures are found only in body-centered-cubic steel structures, fully austenitic steels being highly resistant to embrittlement by hydrogen and apparently immune to delayed, brittle failure. A few investigations have been concerned with structures other than tempered martensite or austenite, and some of these will be reviewed here.

Various investigators showed that tensile strength is a major factor in the loss of ductility by hydrogen embrittlement. It was recognized that differences in microstructure were the underlying cause, but the relationship between the two was not understood. Hobson and Hewitt<sup>(1)</sup> investigated differences in microstructure in a 3 Cr-Mo steel at various levels of tensile strength, each reached by alternative heat treatments which, of course, resulted in different microstructures. They found that, with the amounts of hydrogen normally found in finished steel (about 1 to 4 cc/100 g), the effect of hydrogen on ductility at room temperature was severe only when the steel was in one of two extreme conditions of heat treatment - either hardened (martensite or bainite) and very lightly tempered or very highly spheroidized.

Bastien and Amiot<sup>(46)</sup> studied the delayed failure of hydrogenated plain-carbon steels that had different carbon contents and had been heat treated differently so that they differed in structure. Their results are shown in Table 17. They found that the sorbitic structure had the greatest susceptibility to hydrogen-induced, delayed, brittle failure, and globular pearlite exhibited the least susceptibility. Lamellar pearlite gave intermediate results. Sorbite, a term that is obsolete in the United States, refers to a fine mixture of ferrite and cementite, either fine pearlite or tempered martensite. Considering the strength level, their sorbite must have been tempered martensite. Their results for globular pearlite (spheroidite) appear to be inconsistent with the results of Hobson and Hewitt.

TABLE 17. INFLUENCE OF COMPOSITION AND STRUCTURE ON THE DELAYED FAILURE<sup>(a)</sup> IN HYDROGENIZED CARBON STEELS (AFTER BASTIEN AND AMIOT)<sup>(1,4)</sup>

Steel Designation	Carbon Content, per cent	Microstructure	Mechanical Properties, kg/mm <sup>2</sup> <sup>(b)</sup>				
			Proportional Limit	Upper Yield Point	Tensile Strength	Lower Critical Stress	Ratio, L.C.S./T.S.
E	0.08	Lamellar pearlite	22	24.0	37.5	21	0.56
F	0.1	Lamellar pearlite	31	35.3	44.3	30	0.68
G	0.42	Lamellar pearlite	39	41.6	60.0	39	0.65
G	0.42	Lamellar Pearlite	37	40.0	77.5	35	0.45
H	0.96	Sorbite	160	--	177.8	65	0.37
H	0.96	Globular pearlite	--	51.0	61.0	55.5	0.90

(a) Electrolytic charging began 15 hours before application of the load. L.C.S. = maximum stress which did not induce fracture of charged specimens (lower critical stress) and T.S. = tensile strength.

(b) 1 kg/mm<sup>2</sup> = 1422 psi.

It was suggested early in the studies of hydrogen embrittlement and delayed, brittle failure of high-strength steel that the decomposition of retained austenite under an applied stress in the presence of hydrogen may play a significant role. Austenite has

a considerably greater solubility for hydrogen than does alpha iron. This suggests that, as the austenite transforms to martensite during the hardening operation, the hydrogen in the steel will tend to be rejected from the transformed material and be concentrated more and more in the remaining austenite. If retained austenite with a high hydrogen content were to transform under an applied stress, the resulting martensite would be supersaturated with respect to hydrogen. At least two investigations considered this possibility. In each one, a high strength level was achieved by producing a fully bainitic structure in SAE 4340 steel and comparing the susceptibility to delayed failure of this material with that of the quenched-and-tempered martensitic structure that would contain retained austenite. In one investigation, Slaughter et al. (8) prepared specimens with bainitic structures by austenitizing in a dry argon atmosphere, quenching into a salt bath at 650 F, and then transferring the specimens to an air furnace at 650 F. The specimens were held at 650 F for 18 hours to insure completion of the transformation, giving a fully bainitic structure. The nominal tensile strength of this material was 190,000 psi. Other specimens, quenched to martensite (plus retained austenite), were tempered to give the same strength level. The results of static-loading tests of smooth specimens cathodically charged continuously while under load are shown in Figures 2 and 13 (pages 6 and 26) and in Table 18. As shown in the figures, specimens with a bainitic structure behaved much like the specimens with a martensitic structure of the same strength. In the higher stress range, specimens with bainitic and martensitic structures showed almost identical behavior; in the lower stress range, the bainitic structure appeared to be affected more adversely by the cathodic charging.

In the investigation conducted by Frohberg et al. (5), a fully bainitic structure tempered to a tensile strength of 230,000 psi was produced for comparison with tempered martensite heat treated to the same strength level. Examination of the bainitic material by X-ray diffraction gave no indication of retained austenite. Figure 80 shows that the precharged, sharp-notched specimens with a bainitic structure behaved basically the same as did those with a martensitic structure. The delayed-failure curve for the bainitic specimens was displaced slightly upward compared with that of the tempered-martensite specimens. It was suggested that this displacement could be attributed to the fact that the residual stress state in an austempered structure is inherently less severe than that of a quenched-and-tempered structure. In other words, the martensite with its higher residual stress state required a smaller externally applied stress to cause delayed failure. The room-temperature aging characteristics of charged specimens with a bainitic structure are shown in Figure 81, along with the curve for tempered martensite. The initial embrittlement was less severe for the bainite than for the martensite. However, the recovery of ductility with aging time appeared to be markedly slower for the specimens with a bainitic structure than for those with a tempered-martensite structure.

The results of these two investigations showed that retained austenite does not play a primary role in hydrogen embrittlement and delayed failure. Since, in both investigations, the two structures behaved similarly at a given strength level, it would appear that strength level and not microstructure was the important factor operating (along with applied stress and hydrogen content) in the delayed failures.

Slaughter et al. (8) also studied the effect of structure on the loss of strength in the static-loading test for annealed specimens of SAE 4340 steel. However, it was not possible to obtain equal strengths with a tempered-martensite structure and an annealed structure. The annealed structure was obtained by isothermally transforming austenitized specimens at 1200 F for 24 hours. The results of these tests also are included in

TABLE 18. RESULTS OF ROOM-TEMPERATURE DELAYED-FAILURE TESTS OF UNNOTCHED SPECIMENS OF SAE 4340 STEEL CATHODICALLY CHARGED WITH HYDROGEN<sup>(a)</sup> WHILE SUBJECTED TO STATIC TENSILE STRESS<sup>(8)</sup>

Specimen	Applied Stress, psi	Time to Rupture, minutes
<u>Tempered Martensite, 190,000-psi UTS</u>		
A97	168,000	19.3
A94	150,000	33.3
A90	100,000	41
A95	43,000	67
A91	35,000	98
A96	35,000	113
<u>Bainite, 190,000-psi UTS</u>		
A115	>189,000 <sup>(b)</sup>	23.1
A111	150,000	51.5
A112	100,000	46
A113	30,000	114
A114	25,000	192
A116	20,000	312

(a) 4 per cent H<sub>2</sub>SO<sub>4</sub> electrolyte with phosphorus poison; current density 8 ma/in.<sup>2</sup>.

(b) Specimens A115 necked down visibly, so that the true stress at the minimum section exceeded the value of 189,000 psi based on original cross-sectional area.

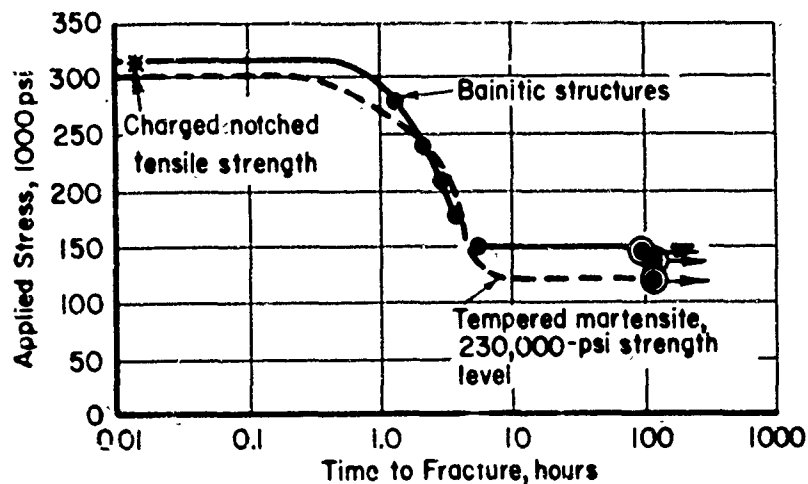


FIGURE 80. STATIC-LOADING TESTS ON SAE 4340 STEEL OF TEMPERED BAINITIC STRUCTURE AT 230,000-PSI STRENGTH LEVEL<sup>(5)</sup>

Sharp-notch specimens aged 5 minutes at room temperature before testing.

Case Institute of Technology Charging Condition A:

Electrolyte: 4 per cent  $H_2SO_4$  in water

Poison: None

Current density: 20 ma/in.<sup>2</sup>

Charging time: 5 minutes.

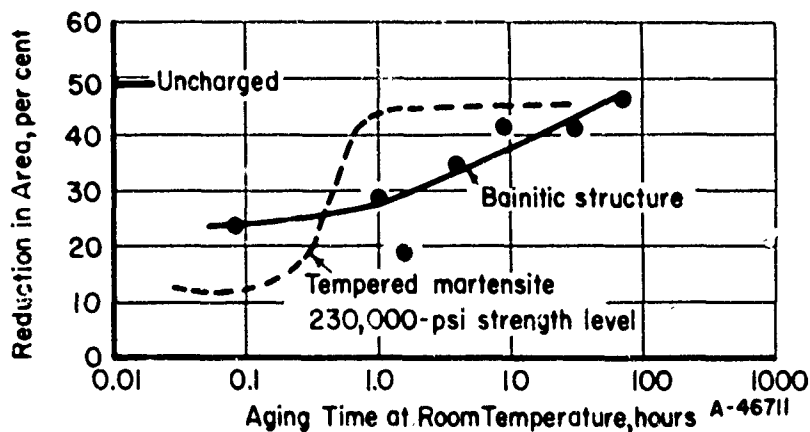


FIGURE 81. EFFECT OF AGING TIME ON DUCTILITY OF SAE 4340 STEEL OF TEMPERED BAINITIC STRUCTURE AT THE 230,000-PSI STRENGTH LEVEL<sup>(5)</sup>

Unnotched specimens.

Case Institute of Technology Charging Condition A, as in Figure 80.



Figures 2 and 13 (pages 6 and 26). As shown in Figure 13, extrapolation of the curve for the martensitic structure is consistent with the properties of the annealed, pearlitic structure which had a nominal tensile strength of 75,000 psi. These results, along with the other results for tempered martensite at several strength levels and for bainite that are included in the figures, show that structure, per se, did not have a large effect on the stress-rupture behavior of unnotched specimens during cathodic charging.

Hydrogen-induced cracks nucleate and grow much more readily in the lightly tempered martensite of a high-strength steel than in the softer pearlitic and ferritic structures. This suggested that a duplex structure consisting of a fine dispersion of a soft phase, such as ferrite, within a martensite matrix might retard the initiation and/or growth of these cracks. To produce such a dispersion, Elsea and co-workers<sup>(9)</sup> austenitized several specimens in the usual manner, but isothermally transformed them at 1200 F for times varying from 5 to 30 minutes before oil quenching. These specimens were tempered to obtain an ultimate tensile strength of approximately 230,000 psi. In Table 19, the results of delayed-failure tests on these specimens are compared with the results for a completely martensitic structure tempered to the same strength level. The finely dispersed particles of ferrite had no noticeable effect on the total time delay to failure.

TABLE 19. EFFECT OF FERRITE DISPERSED IN MARTENSITE ON RUPTURE TIME AT AN APPLIED STRESS OF 100,000 PSI<sup>(a)</sup>(9)

Isothermal Transformation Time at 1200 F, minutes	Approximate Amount of Ferrite, per cent	Rupture Time, minutes
0	0	10.0
5	5	5.5
15	15	6.3
30	25	10.0

(a) SAE 4340 steel heat treated to the 230,000-psi strength level. Unnotched specimens cathodically charged in  $H_2SO_4$  under standard conditions while under the static load.

Because segregations of nonmetallic inclusions have a considerable influence on the formation of cracks and hydrogen blowholes, Foryst<sup>(82)</sup> conducted an investigation to determine their effect on the sensitivity of mild steel to the action of hydrogen. Ingots were produced with various amounts of oxide inclusions, and they were processed into wire. The various materials were studied in three conditions, as follows:

- (1) Initial state (wire as produced with oxide inclusions)
- (2) Heated for 24 hours in moist hydrogen
- (3) Vacuum degassed at 800 C (1470 F).

Specimens representing the various materials and conditions were cathodically charged with hydrogen in a sulfuric acid electrolyte that contained arsenic as a cathodic poison.

Then the charged specimens were bent repeatedly through 180 degrees to failure. It was found that there was no connection between the brittleness of the steel resulting from charging with hydrogen and the content of oxide inclusions.

Schuetz and Robertson<sup>(25)</sup> studied the delayed fracture of ferrite and martensite in a 10 per cent nickel steel charged cathodically. The results, shown in Figure 27 (page 45) indicate that the time dependence of fracture was similar for both structures, but the failures occurred at much lower applied stresses for the martensite than for the ferrite. They suggested that this was due to the combination of the internal stresses existing in martensite and the external applied load.

### EFFECT OF SECTION SIZE

Elsa and co-workers<sup>(8)</sup> conducted a series of experiments with small specimens in order to study the incubation period for hydrogen cracking. The results are shown in Figure 82. At the higher range of applied stress, rupture occurred more rapidly as the section size decreased. Thus, the predominant part of the delay in this stress range was the time required for the absorption of hydrogen, since these tests were conducted during cathodic charging. However, in the lower range of stress, the time to rupture became almost independent of specimen size as the applied stress approached the minimum stress for failure. The fact that the delay was independent of section size indicated that the incubation period became the predominant part of the delay in this lower stress range. Bars of various thickness stressed in bending also showed that the time for failure increased with increasing specimen size.

Sachs and co-workers<sup>(19)</sup> performed a limited study of the effect of section size by using notched, electroplated specimens. In previous work, they showed that, after tempering in the range to produce high strength, the notched strength of uncharged specimens is dependent on the specimen size. With increase in specimen size, the notched strength is lowered. However, the notched strength still was much higher than that measured under sustained loads for hydrogen-embrittled steel. In the sustained-load tests, the effect of hydrogen is effectively to reduce the section and, in this way, to promote failure. They reasoned that, if a larger specimen is employed so that the surface to volume ratio is reduced, the average hydrogen content of the specimen will be reduced and the crack will penetrate a relatively shorter distance through the specimen. They suggested that, as a consequence, the notched strength of larger electroplated (and hence hydrogen embrittled) specimens should be relatively raised, that is, the susceptibility to sustained-load failures should decrease. A limited number of tests supported this prediction, as shown in Figure 83. In other experiments, they showed that the hydrogen content of these cadmium-plated specimens varied with section size in the manner they had predicted.

Of course, section size is a big factor in the recovery of properties by aging, where the mechanism is the diffusion of hydrogen out of the part. Since the aging time increases as the square of the diameter or thickness, hydrogen removal from large masses is very slow. This is shown by the work of Sims and co-workers<sup>(52, 83)</sup> and by Hobson<sup>(84)</sup>. Based on an extrapolation of data obtained on the loss of hydrogen from the center of 4-inch-square cast-steel bars aged up to 3-1/2 years at room temperature, Sims<sup>(53)</sup> estimated that 6 years would be required to reduce the hydrogen to the

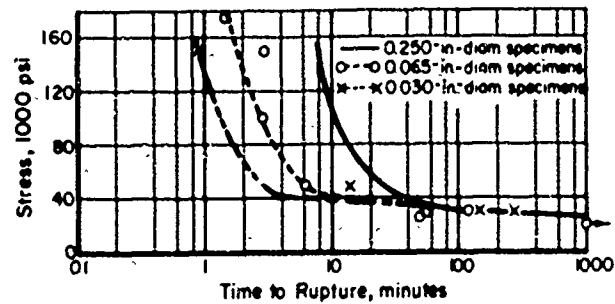


FIGURE 82. EFFECT OF SPECIMEN SIZE ON DELAYED-FAILURE CHARACTERISTICS OF AN SAE 4340 STEEL DURING CATHODIC CHARGING WITH HYDROGEN UNDER BATTELLE CONDITION A<sup>(8)</sup>

230,000-psi strength level.

Battelle Charging Condition A:

Electrolyte: 4 per cent by weight of  $H_2SO_4$  in water

Poison: 5 drops per liter of cathodic poison composed of 2 g phosphorus dissolved in 40 ml  $CS_2$

Current density: 8 ma/in.<sup>2</sup>.

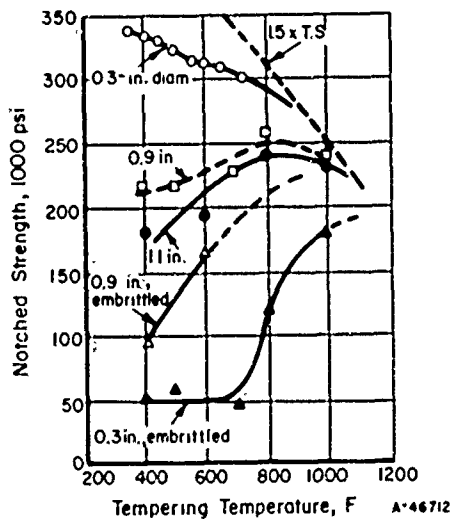


FIGURE 83. THE NOTCHED STRENGTH MEASURED FOR EMBRITTLLED AND UNEMBRITTLLED SPECIMENS OF THE INDICATED SIZES VERSUS TEMPERING TEMPERATURE<sup>(19)</sup>

The notch strength for the embrittled specimens was measured under sustained loading.

"equilibrium" level. Even though aging to remove hydrogen is vastly accelerated at a suitable elevated temperature, such as 400 F, hydrogen removal is still a big problem in the hydrogen embrittlement of large forgings. Here the solution seems to lie in vacuum processing so that hydrogen is removed before the steel solidifies.

### EFFECT OF NOTCH ACUITY

A number of the investigators that have used notched specimens to study hydrogen-induced, delayed, brittle failures have studied the effect of notch acuity. Most of these investigations have been performed with precharged specimens, and each showed that increasing the notch severity drastically lowered the applied load necessary to produce delayed, brittle failures. With notch-root radii of <0.001, 1/32, and 2 inches, and with the area under the notch and the notch depth (50 per cent) held constant, the delayed-failure curves shown in Figure 20 (page 36) were obtained for SAE 4340 steel heat treated to the 230,000-psi strength level<sup>(5)</sup>. It is readily apparent that the lower critical stress was raised as the notch sharpness was decreased. Also, as the notch acuity was increased, the spread between the upper and lower critical-stress values increased; the ratio between the two is shown in Table 20. The smallest notch radius,

TABLE 20. EFFECT OF NOTCH ACUITY ON THE CRITICAL STRESS FOR DELAYED, BRITTLE FAILURE<sup>(5)</sup>

Notch Radius, inch	Notched Tensile Strength, psi (A)	Minimum Critical Stress for Delayed Failure, psi (B)	Ratio A/B
<0.001	300,000	120,000	2.5
1/32	270,000	165,000	1.6
2	220,000	215,000	1.0

with the highest degree of stress concentration, produced failure with the smallest load. These results were produced with a highly heterogeneous hydrogen concentration in which the hydrogen was concentrated in the surface layers, because the charged specimens were aged only 5 minutes at room temperature before testing. With a similar material and similar specimens, but with a uniform hydrogen distribution produced by cadmium plating immediately after charging and then baking 0.5 hour at 300 F, the results shown in Figure 84 were obtained.<sup>(85)</sup> In this investigation, the notch sharpness was defined as one-half the diameter of the cross section at the notch divided by the notch radius. The lower critical stress increased markedly as the notch sharpness decreased from 100 to 0.4. With sharp notches, delayed failure was observed over a wide range of applied stresses, whereas the stress range was negligible for unnotched specimens, just as for the heterogeneous distribution. Since the charged and uncharged notched tensile strengths were found to vary with notch acuity in roughly the same manner (see Figure 85), this suggests that hydrogen embrittlement and notch embrittlement are additive. These are part of the data which show that a critical combination of stress state and hydrogen concentration must be attained to initiate a crack.

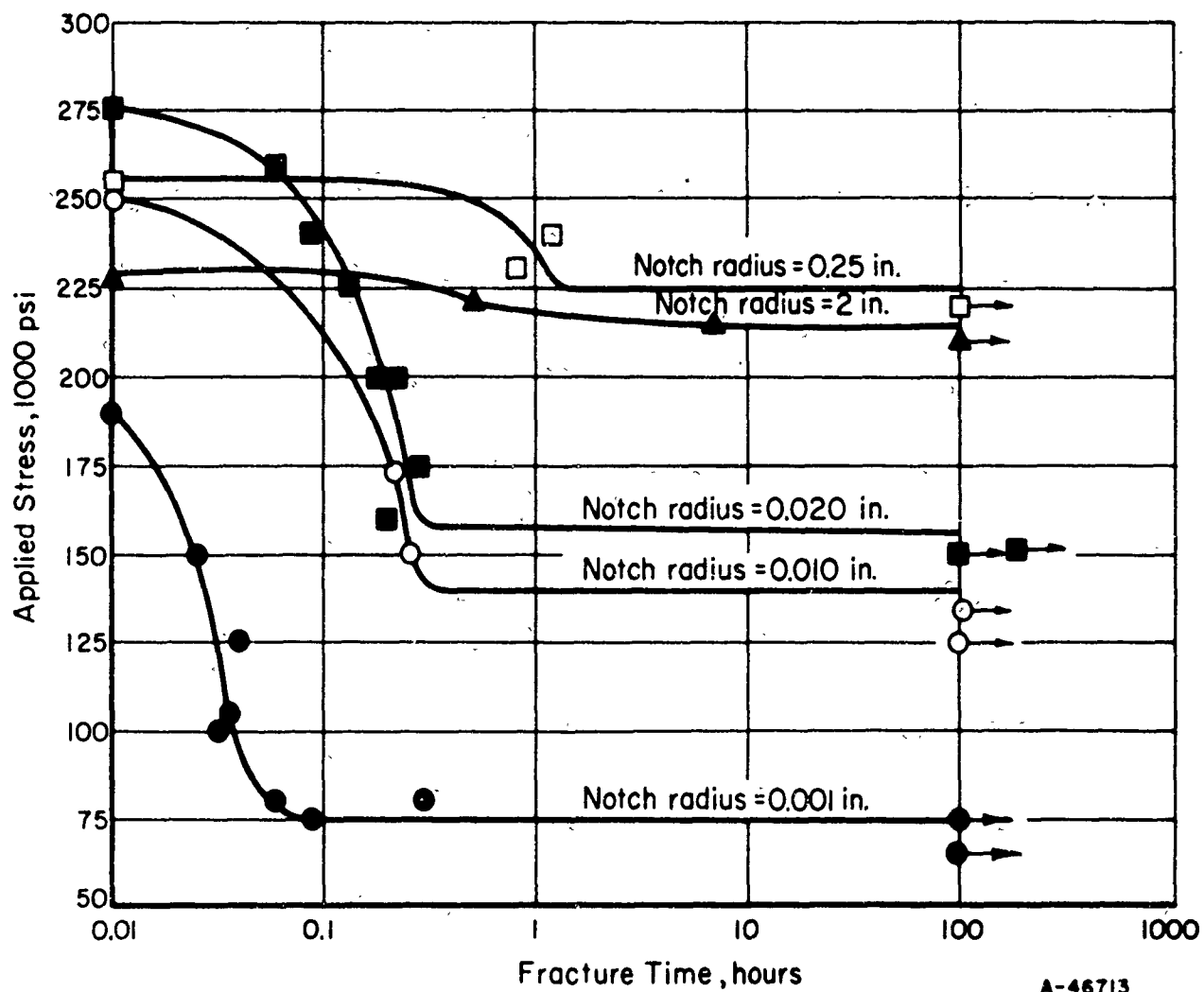


FIGURE 84. DELAYED-FAILURE CURVES FOR SPECIMENS OF DIFFERENT NOTCH SHARPNESSES<sup>(85)</sup>

Specimens baked 0.5 hour at 300 F; 50 per cent notch; 230,000-psi strength level.

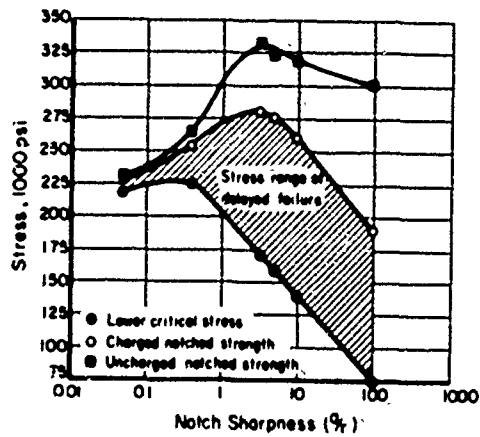
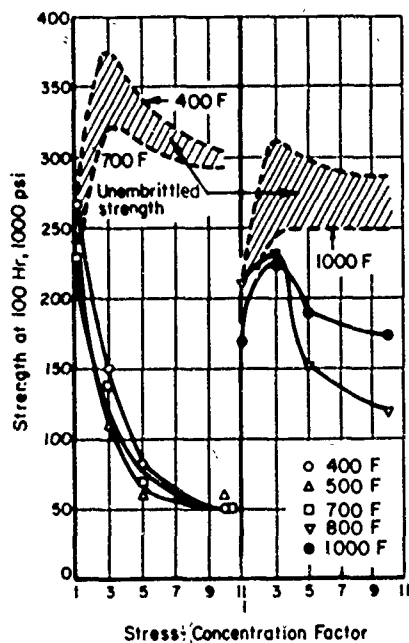


FIGURE 85. LOWER CRITICAL STRESS AND CHARGED AND UNCHARGED NOTCHED STRENGTH FOR DIFFERENT NOTCH SHARPNESSES, DERIVED FROM FIGURE 84<sup>(85)</sup>

$a$  is half diameter of the cross section at the notch,  $r$  is notch radius.



A-46714

FIGURE 86. THE RUPTURE STRENGTH AT 100 HOURS VERSUS STRESS CONCENTRATION WITH TEMPERING TEMPERATURE AS PARAMETER FOR CADMIUM-PLATED SAE 4340 STEEL<sup>(19)</sup>

Oil quenched from 1525 F.

Figures 15, 16, 17 and 18 (pages 32, 118, and 33) illustrate the effect of notch acuity on the level of applied stress and time delay to failure for two steels at various strength levels<sup>(19)</sup>. The plots are based on  $K_t$  values for theoretical stress concentration. Figures 16 and 18 clearly illustrate the drastic lowering of the lower critical stress as notch sharpness was increased. Other work by these investigators<sup>(11)</sup> showed the effect of notch acuity, as well as strain rate, on the notched strength of SAE 4340 steel at various strength levels, as precharged with hydrogen under two different conditions. The results are shown in Figures 87 and 88.

### EFFECT OF STRESS STATE

It has been shown in previous sections that delayed, brittle failures can be produced at low stresses in unnotched specimens subjected to uniaxial tensile loading, provided that the hydrogen content is high enough. This can be accomplished by continuous cathodic charging with hydrogen under suitable conditions. With precharged specimens, the lower critical stress usually is just a little below the short-time tensile strength of the material under this type of loading, as is shown in Figures 16 and 20 (pages 32 and 36). Numerous investigations have shown that a triaxial stress state, which is achieved by use of a notched tensile specimen, is much more conducive to the development of delayed, brittle failures in hydrogenated specimens than is uniaxial tension. This also is illustrated in the two figures just cited.

The authors are aware of no work in which the specimens were stressed in uniaxial compression. However, in some investigations, the differences between the compression and the tension surfaces of a bend specimen have been investigated. In one investigation<sup>(12)</sup>, the ends and three sides of smooth (unnotched) high-strength SAE 4340 specimens with a cross section 0.394 inch square were coated with Glyptal so that the hydrogen would enter only on the uncoated side during cathodic charging. After charging, the specimens were tested in a slow-bend jig with the side charged with hydrogen either in tension or compression. Figure 89a shows the effects of charging time on maximum load for specimens tested in the two orientations. The maximum load withstood by specimens with the charged side in tension decreased rapidly as the charging time was increased, whereas only a small drop in maximum load was observed when the uncharged side was tested in tension. It was noted that when the charged side was tested in tension, the depth of cleavage fracture increased with increased charging time (see Figure 89b), illustrating progressive embrittlement to deeper positions. This is added evidence that, on charging, a high concentration of hydrogen is developed initially at the surface and that a gradual penetration occurs with time.

At Battelle<sup>(8)</sup>, a study was made of the delayed failure of specimens statically loaded in bending and charged cathodically on the compression side while under stress. The tension side, which was exposed to the atmosphere, was notched to various depths. During cathodic charging, a hydrogen gradient was established through the specimen, with the hydrogen content being highest at the cathodically charged compression surface and lowest at the tension surface where hydrogen was escaping to the atmosphere.

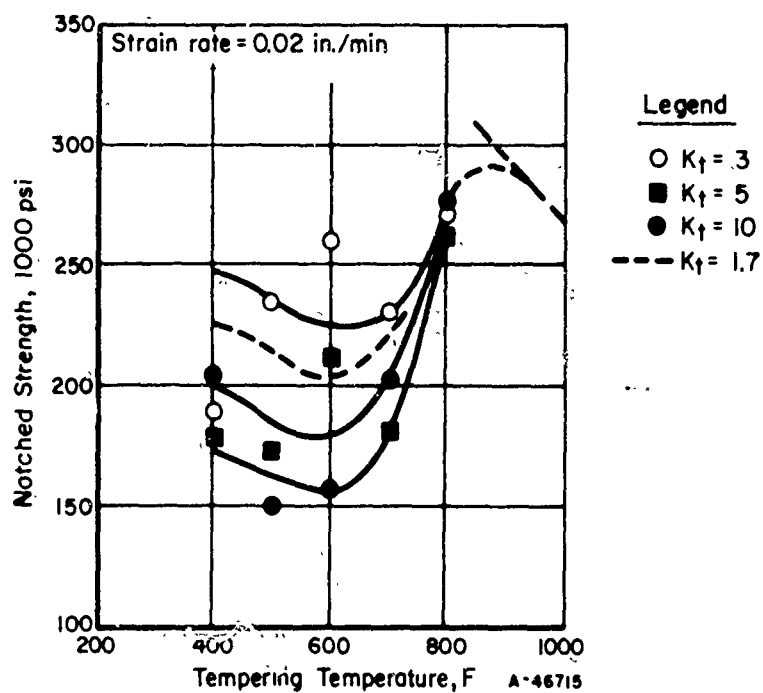
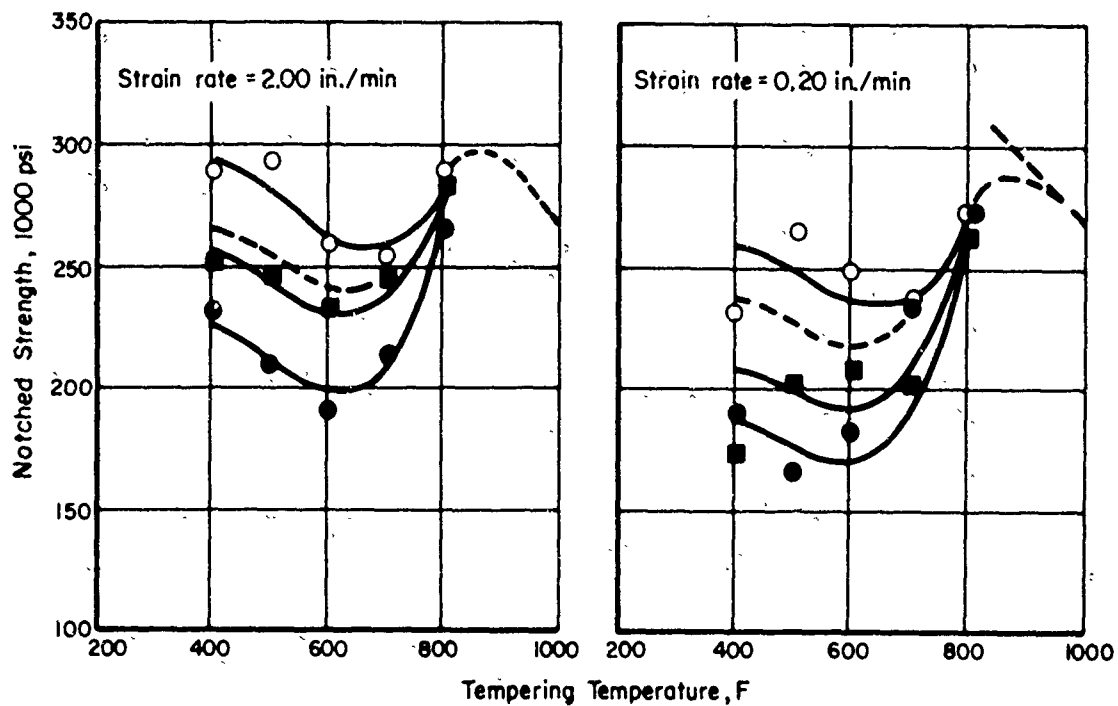


FIGURE 87. ROOM-TEMPERATURE NOTCHED STRENGTH OF 0.3-IN.-DIAM NOTCHED TENSILE SPECIMENS OF SAE 4340 STEEL HYDROGEN EMBRITTLED BY CHARGING CONDITION  $C_1$  <sup>(11)</sup>

Charging Condition  $C_1$ :

447 ma/in.<sup>2</sup> for 1/2 hr;

Bath; 10% NaOH at 30 C.



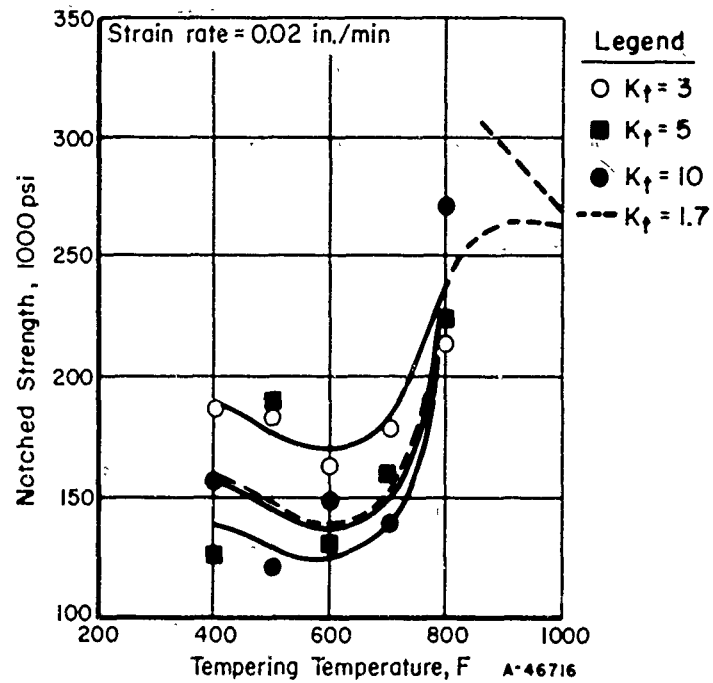
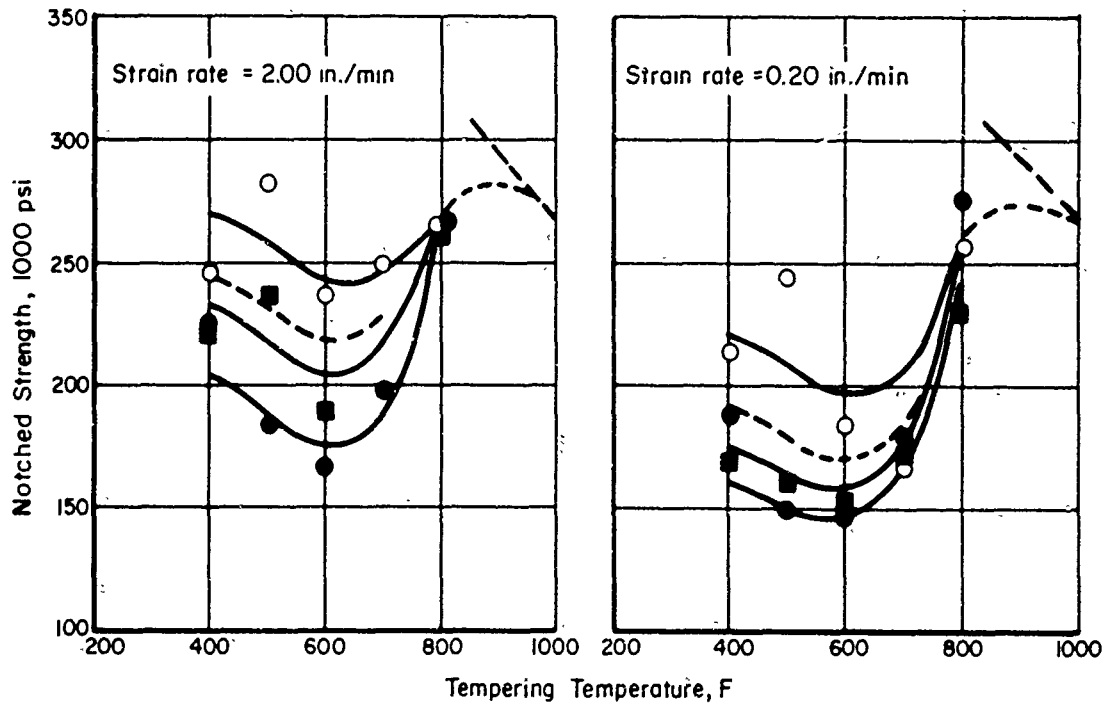
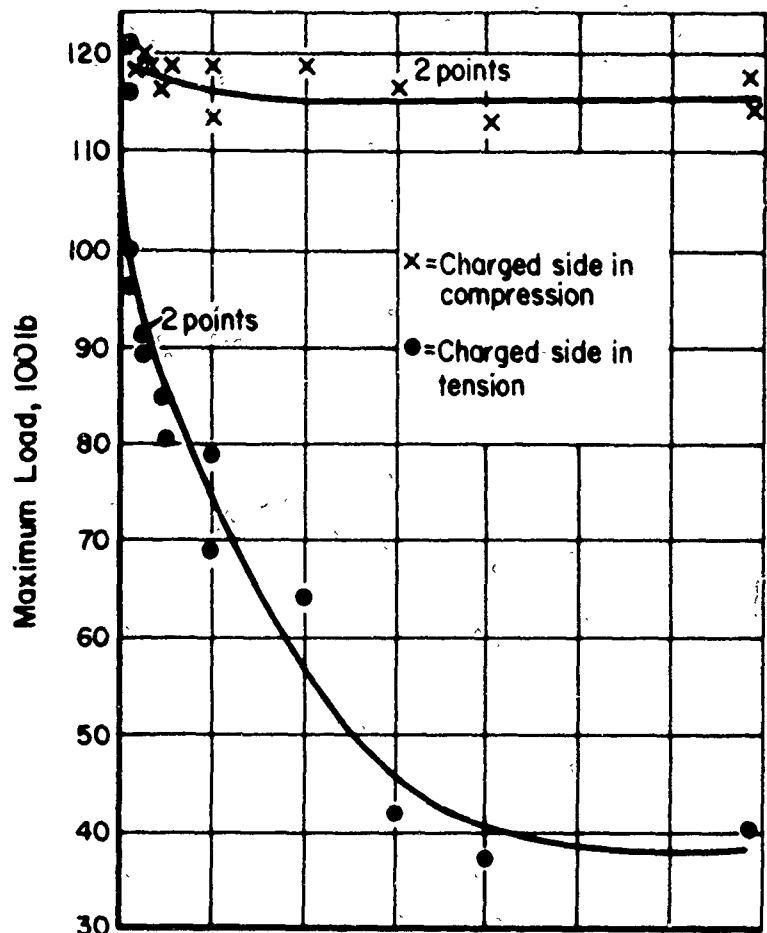


FIGURE 88. ROOM-TEMPERATURE NOTCHED STRENGTH OF 0.3-IN.-DIAM. NOTCHED TENSILE SPECIMENS OF SAE 4340 STEEL HYDROGEN EMBRITTLED BY CHARGING CONDITION  $C_2$ <sup>(11)</sup>

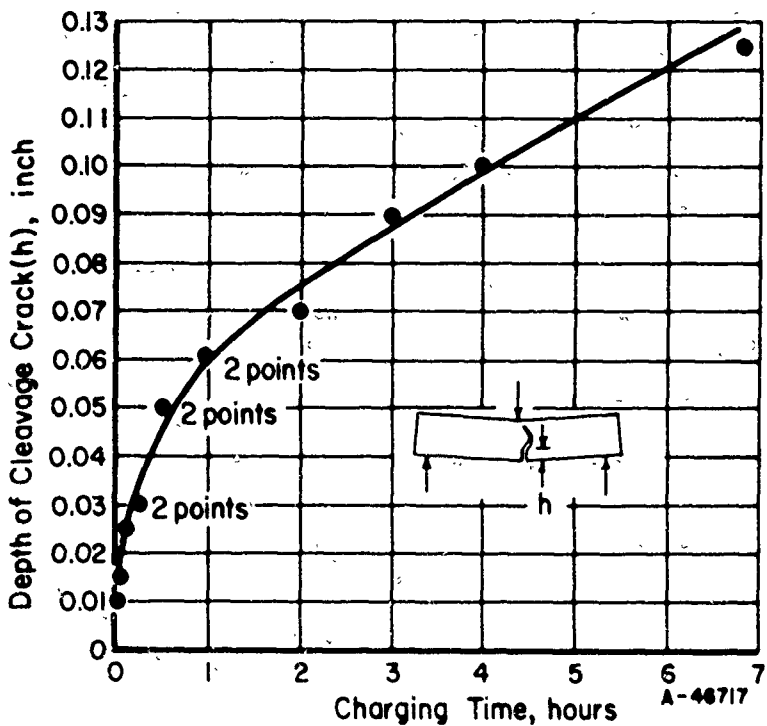
Charging Condition  $C_2$ :

447 ma/in.<sup>2</sup> for 2-1/2 hr;

Bath: 10% NaOH at 30 C.



a. Differences in load to failure when hydrogen is charged in the compression or the tension surfaces of bend specimens, with maximum load for each orientation plotted as a function of charging time.



b. When the charged side was tested in tension, the depth of cleavage fracture showed the extent of hydrogen penetration for various charging times.

FIGURE 89. RESULTS OBTAINED FROM SLOW-BEND TESTS OF UNNOTCHED SPECIMENS CHARGED WITH HYDROGEN<sup>(12)</sup>

Air-melted AISI 4340 steel charged at 0.59 amp/in.<sup>2</sup>.

Delayed failures were obtained, but none of them originated at the cathodically charged surface. The region near the cathodically charged surface behaved in a ductile manner. The results obtained are shown in Figure 26 (page 43).

Probert and Rollinson<sup>(23)</sup> also studied specimens that were stressed by bending and which were completely protected on all surfaces except the compressively stressed side. These specimens were found to be cracked on the tension side after cathodic treatment. Some of the results were as follows:

<u>Treatment</u>	<u>Bend Angle at Fracture, degrees</u>
Without charging	120
Charged from all sides	45
Hydrogen on tension side only	45
Hydrogen on compression side only	55

Sustained-load bend tests also were performed with hydrogen introduced on the compression side only. The following results were obtained:

<u>Sustained-Load Angle, degrees</u>	<u>Time to Failure, hours</u>
52	1
50	8
45-50	No failure

This is added evidence that the existence of compressive stress (induced by bending) in the surface being charged will not prevent hydrogen embrittlement. These investigators also showed that a compressive stress induced by shot peening will not prevent hydrogen pickup nor the embrittlement of the areas stressed in tension.

The workers at Battelle Memorial Institute<sup>(9)</sup> also studied the effect of torsion loading on rupture time under sustained load. With the unnotched specimens loaded in torsion and with standard charging conditions, delayed failures were obtained as shown in Figure 90. The time for failure is plotted as a function of the principal tensile stress. The curve for the results of the standard uniaxial tension test under the same charging conditions is shown for comparison. The time for failure to occur was about the same for both the torsion test and the uniaxial tension test. The slight difference between the two curves was attributed to the error involved in loading the torsion specimens. The load, which was transmitted to the specimen by a system of pulleys, probably resulted in the actual load being slightly less than the calculated load. These data suggest that for all practical purposes the only stress that influences the delay time for failure is the maximum tensile stress.

A number of investigations have been performed in which precharged specimens have been subjected to bending stresses. Some of these have been short-time tests in which the deflection at fracture was measured. An example of the results of this type of test was given in Figure 78 (page 107). Also, delayed failures have been obtained in bend tests of precharged notched specimens and of unnotched specimens under continuous charging. However, the sustained-load tensile test of notched specimens is generally accepted as being a more sensitive and more reproducible measure of the susceptibility of hydrogenated steel to delayed, brittle failure.

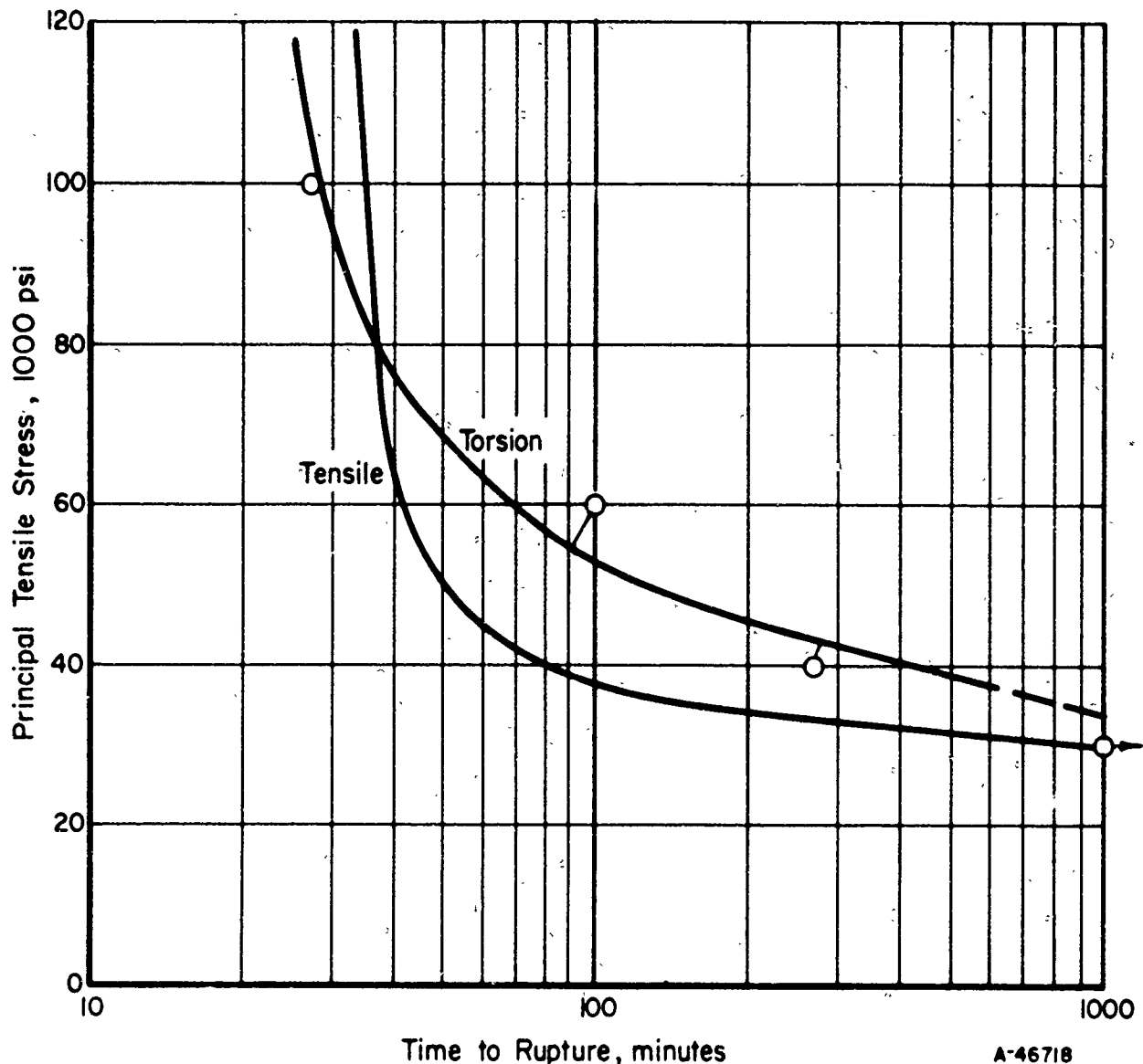


FIGURE 90. TIME FOR FAILURE AS A FUNCTION OF APPLIED STRESS FOR TENSILE AND TORSION LOADS<sup>(9)</sup>

SAE 4340 steel.

Ultimate tensile strength, 190,000 psi.

Charging conditions, 4% H<sub>2</sub>SO<sub>4</sub>, 10 ma/in.<sup>2</sup>.

Most of the delayed, brittle failures encountered have been sustained-load failures observed after a part was under an applied load for a certain length of time. Also, most of the laboratory investigations of delayed failures have used sustained loading. However, such failures can also occur under repeated loading. Muvdi, Sachs, and Klier<sup>(86)</sup>, with certain aircraft applications in mind, studied the fatigue properties of embrittled steel in an exploratory way and compared the results with those obtained with unembrittled material. Their tests were limited to a low number of cycles, ranging between about 10 and 10,000, because, in general, aircraft parts such as landing gears are subjected only to a rather limited number of repeated load cycles. SAE 4340 steel was studied at several strength levels between 290,000 and 210,000-psi ultimate tensile strength. Rotating-beam fatigue tests were performed on both notched ( $K_t = 2.5$  and 8) and smooth ( $K_t = 1$ ) specimens at a speed of 250 rpm. For the specimens to be studied

in the hydrogenated condition, hydrogen was introduced into the specimens cathodically just prior to testing. The charging conditions selected were intended to be rather mild. Analyses for hydrogen content of both smooth and notched ( $K_t = 8$ ) specimens at two different strength levels ranged between 0.4 and 0.8 ppm. Some of the results for the highest and lowest strength levels are shown in Figures 91 and 92. The S-N curves for hydrogen-embrittled material had the general appearance expected for low-cycle fatigue curves of steels heat treated to high strength levels. For the higher strength levels, the curves for smooth specimens were located entirely above those for notched specimens, while for the 210,000-psi strength level the notch-fatigue curve intersected the curve for smooth specimens at approximately 200 cycles. Between 1,000 and 10,000 cycles, the notch-fatigue strength generally was roughly one-half the smooth-fatigue strength, which was in agreement with the results of unembrittled specimens. Compared to the results for unembrittled specimens, an adverse effect of hydrogen was usually observed in the range of lowest cycles. The lone exception to this was for the smooth specimens of the 210,000-psi material, for which the fatigue strengths of embrittled and unembrittled specimens were found to be identical. In all instances, the effect of hydrogen appeared to vanish at between 1,000 and 10,000 cycles, for both smooth and notched specimens. Although the speed of these tests (250 rpm) is rather low for rotating-beam fatigue tests, it still represented a high rate of loading, namely, less than about 0.06 second from zero to maximum tension in each cycle. Thus, the loading rate for these tests was intermediate between impact and the rate used in tensile tests. The authors explained the quite small effects observed on the basis of the high rate of loading. They concluded that the normal, high-speed fatigue test is of little value as a tool for the evaluation of hydrogen embrittlement.

### THEORIES OF HYDROGEN EMBRITTLEMENT

In spite of the many investigations of hydrogen embrittlement and delayed, brittle fracture reported in the technical literature, there still is no general agreement regarding the mechanism by which hydrogen reduces the ductility of steel.

A suitable theory must explain the characteristics of hydrogen embrittlement, which are quite different from those of the more conventional forms of embrittlement. Hydrogen embrittlement disappears at low and high test temperatures and, therefore, is most severe in an intermediate temperature range, usually in the vicinity of room temperature. Also, hydrogen embrittlement is inversely related to the strain rate, which is just the reverse of most other forms of embrittlement.

One of the unique characteristics of delayed, brittle failure induced by hydrogen is that there is a lower critical stress below which failure will not occur. Different investigations showed quite early that the hydrogen-induced, delayed, brittle failure process occurs in three distinct stages:

- (1) The incubation period
- (2) A period of relatively slow crack growth, or crack propagation
- (3) Sudden rupture with extremely rapid crack growth through the central core essentially free of hydrogen.

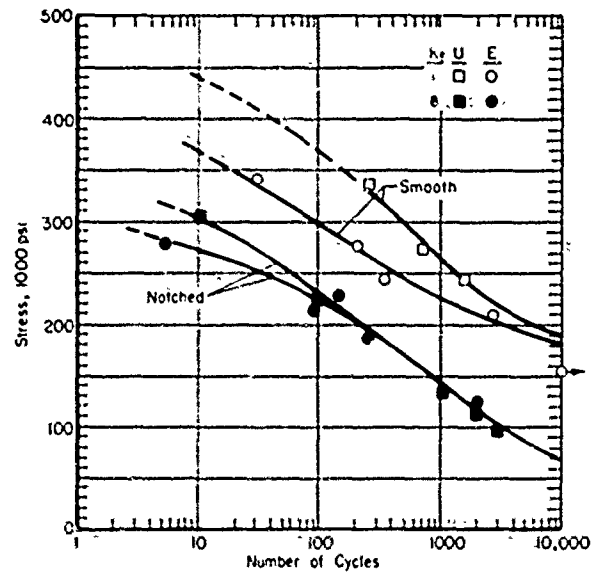


FIGURE 91. S-N CURVES FOR UNEMBRITLED AND EMBRITLED, SMOOTH AND NOTCHED, ROTATING-BEAM FATIGUE SPECIMENS FROM 9/16-INCH-DIAMETER SAE 4340 STEEL AT THE 290,000-PSI STRENGTH LEVEL<sup>(86)</sup>

U = unembrittled

E = embrittled

$K_t$  = stress-concentration factor

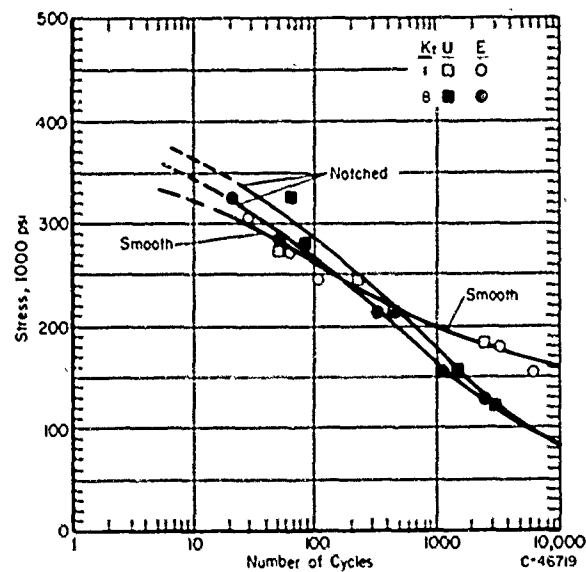


FIGURE 92. S-N CURVES FOR UNEMBRITLED AND EMBRITLED, SMOOTH AND NOTCHED, ROTATING-BEAM FATIGUE SPECIMENS FROM 9/16-INCH-DIAMETER SAE 4340 STEEL AT THE 210,000-PSI STRENGTH LEVEL<sup>(86)</sup>

U = unembrittled

E = embrittled

$K_t$  = stress-concentration factor.

In subsequent work, crack initiation and propagation were studied in detail, and it was found that crack propagation is a discontinuous process which consists of a series of separate crack initiations and propagations. The average hydrogen concentration is not sufficient to propagate a crack. Thus, crack propagation cannot occur until the hydrogen concentration increases in a localized region in front of the crack. This increase occurs through hydrogen diffusion, which is induced either by a stress gradient or a hydrogen gradient. Both the incubation period and crack-propagation phase are controlled and paced by the diffusion of hydrogen. Thus, above a particular threshold stress, the conditions necessary for localized cracking are dependent essentially only on the development of a critical hydrogen content. Crack initiation and crack growth have been discussed previously in other sections of this report, particularly in the sections dealing with the effects of various hydrogen concentrations and the movement of hydrogen. For further information, the reader is referred to some of the more recent papers discussing these aspects of the hydrogen problem; these include References 49, 80, and 87.

Because delayed failure consists of a series of many individual crack initiations, the factors that determine the incubation time are particularly important in explaining the delayed-failure mechanism. In Reference 87, it is suggested that the initiation of a hydrogen-induced crack is dependent on two factors, as follows:

- (1) The stress-induced diffusion of hydrogen that produces an appreciable build up of hydrogen in a localized region
- (2) The basic effect of hydrogen on the material that causes localized failure, that is, a crack.

The first factor has been dealt with at some length in preceding sections. The second factor, the ability of hydrogen to lower the fracture stress, has been the main part of several of the more recent theories proposed to explain hydrogen embrittlement. Most investigators have concluded that the hydrogen pressure in certain voids or imperfections which act as the fracture embryos tends to lower the applied stress at which these embryo fractures become active. Each of the theories advanced to explain hydrogen embrittlement depends on a critical combination of hydrogen and stress. Therefore, they can be applied to a certain extent to the delayed-failure process also. However, most of them do not explain the observed insensitivity of the incubation time to variations in applied stress.

Except for Troiano's theory<sup>(88)</sup>, most of the newer theories involve the surface adsorption of hydrogen through the precipitation of hydrogen gas on the surface of a crack or lattice imperfection, and this adsorption is seen as lowering the surface energy necessary for the extension of the crack.

Troiano, who has studied the delayed-failure process at great length, believes the implication is strong that delayed failure is the result of a lowering of the true fracture strength of the iron lattice which results from the segregation of interstitial hydrogen atoms in the lattice at the region of maximum triaxiality near the tip of the crack.

The theories advanced to explain the phenomena of hydrogen embrittlement and delayed, brittle failure of high-strength may be arranged in four groups.

The first theory was the planar-pressure theory of Zapffe and co-workers. They assumed that molecular hydrogen precipitates in internal voids of the crystal structure

and builds up a pressure great enough to result in a triaxial stress state sufficient to cause premature failure. This theory was advanced before delayed, brittle failures were known. Refinements of this theory have been proposed by Bastien and Azou, and by De Kazinczy. These differ mainly in the way hydrogen is delivered to the voids and in the way pressure extends the internal crack. Strain rate, degree of strain, and temperature are believed to regulate the size of the void or triaxial region and also the rate at which hydrogen is delivered to this region.

Petch and Stables in 1952 apparently were the first to propose a mechanism to explain the effect of hydrogen on the delayed, brittle fracture of steel under static load. They assumed that hydrogen is adsorbed on the surface of microcracks, thereby lowering the surface energy and allowing the cracks to be extended by reduced stresses.

These two types of theories explain most of the experimental results obtained from studies of hydrogen embrittlement, but they do not explain the effect of plastic deformation, performed subsequent to hydrogenation, on the recovery curves obtained upon aging. This shortcoming led Troiano and co-workers to propose a theory in which embrittlement results from hydrogen in solution and which considers that the hydrogen contained in voids is not damaging.

Subsequently, Bastien and co-workers revised their theory. They assumed that hydrogen is grouped in microcracks by plastic deformation; this gives a possible explanation of the experimental results of Morlet, Johnson, and Troiano<sup>(88)</sup>.

These theories will now be discussed in somewhat more detail. However, the reader is referred to the original papers should he desire a full discussion.

Zapffe and Sims in 1940<sup>(89)</sup> and 1941<sup>(90)</sup> proposed that hydrogen embrittlement is the phenomenon of occlusion of molecular hydrogen under high pressure in voids which appear to be a fundamental part of the crystal structure of steel and which are related to slip and cleavage phenomena. When the occlusion pressure exceeds the elastic strength of the steel, the lattice disjunctions are sprung, and slip and cleavage planes operate much as during cold deformation. The bright fracture that always characterizes the transcrystalline type of hydrogen embrittlement was explained as being the reflection from flat cleavage facets that separated along planes favorably oriented with the imposed stress. Opening of this ultramicroscopic structure of steel by hydrogen is illustrated experimentally by the ready penetration of hydrogen-embrittled steel by liquids. They reasoned that hydrogen embrittlement, if caused by aerostatic pressure within the substructure or the cleavage structure, must have the nature of triaxial stress and will, therefore, inhibit flow, so that an imposed stress may lead to rupture. This was extended by Zapffe and Haslem<sup>(33)</sup> and Zapffe<sup>(91, 92)</sup>, resulting in the planar-pressure theory.

Briefly, the planar-pressure theory follows from two simple, demonstrated facts: (a) hydrogen atoms dissolved in the iron lattice evaporate at all lattice openings until an opposing equilibrium pressure of molecular hydrogen is attained and (b) metal crystals in general, here specifically steel, inherently contain a systematic lattice and crystallographic looseness (commonly referred to as imperfection, or mosaic, structure), in whose voids molecular hydrogen must collect and compress according to Fact (a).



Thus, hydrogen embrittlement becomes nothing other than a phenomenon of internal precipitation along imperfectly disposed crystallographic planes much as in "age hardening", except that here the precipitate is a gas and, therefore, causes no hardening. Even in an unstrained crystal, molecular hydrogen collects in the planar separations which already exist as an inherent feature. The metal becomes embrittled when the gas pressure exceeds some critical value approximating the elastic strength of the crystal. On testing, however, the plastic movement opens the imperfections further, which logically reduces the pressure of molecular hydrogen within the voids to values which may be less than the critical. At the high pressures associated with embrittlement, an appreciable reserve of hydrogen atoms must lie within the adjoining lattice under conditions of quasi-equilibrium, as expressed by  $[H] = K \cdot (P_{H_2})^{1/2}$ . Reduction of  $P_{H_2}$  in the lattice void then causes further precipitation of those hydrogen atoms. If the rate of strain is not too rapid, precipitation will replenish  $P_{H_2}$  sufficiently rapidly to maintain the embrittled condition. If the rate of strain is increased, however, until the rate of decrease in  $P_{H_2}$  exceeds the rate of restoration through further precipitation of hydrogen, the apparent embrittlement should decrease, as is observed. The effect of temperature has an obviously similar relationship, since the pressure of a gas phase likewise decreases with decreasing temperature. Thus, there will be a critical temperature, also a critical rate of cooling, for any given set of conditions, such that the critical embrittlement pressure  $P_{H_2}$  is decreased more rapidly than it is replenished by precipitating hydrogen, and embrittlement will decrease, as is observed experimentally.

Bastien and Azou<sup>(93)</sup> proposed that hydrogen is concentrated around dislocations which discharge it into the voids during plastic straining. With this build up of molecular hydrogen in the voids, an increase of pressure occurs which causes embrittlement by raising triaxial stresses around the voids.

According to De Kazinczy<sup>(94,43)</sup>, hydrogen embrittlement is caused by a lowering of the shear strength and the cleavage strength. He explains this by assuming that molecular hydrogen of high pressure is included in a Griffith crack or some other crack which initiates fracturing. The energy necessary to open a crack and cause it to grow is assumed to arise from the expansion of the hydrogen gas and release of energy during crack growth, which results in a lowering of the fracture stress. It is shown that hydrogen diffusion into the crack is needed during crack spreading, and this diffusion explains the time and temperature effects of hydrogen embrittlement.

These results have been correlated with the diffusion of hydrogen by Toh and Baldwin<sup>(78)</sup> (see Figure 63, page 95).

One of the most characteristic features of hydrogen-induced failure in high-strength steels is the delay-time effect for failure to occur under the action of static loads. In 1952, Petch and Stables<sup>(72)</sup> published the first plausible explanation of this time-delay behavior which they predicted and which was soon observed experimentally by a number of investigators. Their proposed mechanism for delayed fracture was based on the Griffith mechanism for the fracture of completely brittle materials. They proposed a suitable modified form of the Griffith-Orowan<sup>(95)</sup> theory of static fatigue in glass. This theory requires the development of a suitable crack which, through reduction in the cross section, leads to eventual overloading of the remaining uncracked cross section and, thus, failure. Petch and Stables explain the delay feature of the fracture

of steels that contain hydrogen by assuming that at stresses above a certain minimum, the growth of a Griffith microcrack is arrested as soon as it begins to grow, because the newly developed crack surface is clean and, thus, possesses high surface energy. Hydrogen dissolved in the steel is assumed to migrate to the surface of the new crack where it lowers the surface energy. Because the surface energy has been lowered, the crack is enabled to grow slightly again. This sequence of intermittent crack growth is repeated until the crack becomes large enough that the remaining section cannot carry the load, thus resulting in sudden fracture. Petch<sup>(96)</sup> has demonstrated that the reduction in surface energy by hydrogen adsorption is sufficient to account for a significantly reduced stress for crack propagation. The calculated lowering of fracture stress as the result of surface adsorption was in good agreement with measured fracture stresses of hydrogen-embrittled material. As with the De Kazinczy model, the time-dependent growth of these cracks is governed by the diffusivity of hydrogen.

The crack formation proposed by Petch and Stables has been verified experimentally by numerous investigations, as References 17, 8, 6, and 81 will attest. Also, the discontinuous nature of crack growth in hydrogen-induced, delayed, brittle failures was well demonstrated, first by the acoustical method used by Elsea and co-workers and, subsequently, by the electrical-resistance method of studying crack initiation and propagation used by Troiano and his co-workers<sup>(6, 80)</sup>. Petch and Stables in 1952 had predicted that their proposed hydrogen-induced failures would propagate by intermittent crack growth in stepwise fashion.

Brown and Baldwin pictured hydrogen embrittlement as being the contribution of two separate domains that yielded a C-curve<sup>(77)</sup>. One domain is at low temperatures and the other at high temperatures. They believed that the first domain explains the results obtained by Zapffe and Sims, and by Petch and Stables. The second is purported to explain why the rate of embrittlement decreases with increasing temperature at higher temperatures. They determined the effect of hydrogen on the ductility,  $\epsilon$ , of SAE 1020 steel at strain rates,  $\dot{\epsilon}$ , from 0.05 in./in./min to 19,000 in./in./min and at temperatures,  $T$ , from +150 to -320 F. The ductility surface of the embrittled steel revealed two domains: one in which  $(\partial \epsilon / \partial \dot{\epsilon})_T > 0$  and  $(\partial \epsilon / \partial T)_{\dot{\epsilon}} < 0$ , and the other in which  $(\partial \epsilon / \partial \dot{\epsilon})_T > 0$  and  $(\partial \epsilon / \partial T)_{\dot{\epsilon}} > 0$ . Apparently, the explanations of hydrogen embrittlement of Zapffe and Sims, and of Petch and Stables are in accord with the first of these domains only. The C-type plot Brown and Baldwin obtained is shown in Figure 93.

Elsea and co-workers<sup>(7)</sup> early suggested a mechanism to explain the delayed-type brittle failure of high-strength steels. Their hypothesis was based on the diffusion of hydrogen in steel from regions of low stress to regions of high stress, that is, stress-induced diffusion of hydrogen.

The theory to explain hydrogen embrittlement and delayed failure evolved by Troiano and co-workers in a series of reports and papers over the period 1954 through 1962 is the only theory that relies upon the ability of hydrogen, the smallest interstitial solute element, to initiate cracks. According to their model, hydrogen migrates under the driving force of a stress gradient to the triaxial region of a crack nucleus and thus reduces the "true cohesive strength" of the material. Their theory leads to the conclusion that the requirements which must be fulfilled in order to observe hydrogen-induced, delayed, brittle failure are as follows:

- (1) The ability of the hydrogen to interact with the appropriate stress field

- (2) Sufficient mobility of the hydrogen to allow the phenomenon to be observed in a reasonable period of time under the chosen test conditions
- (3) A material with a sufficiently high yield strength, in order that a critical interaction energy between local stress fields and the hydrogen may be attained.

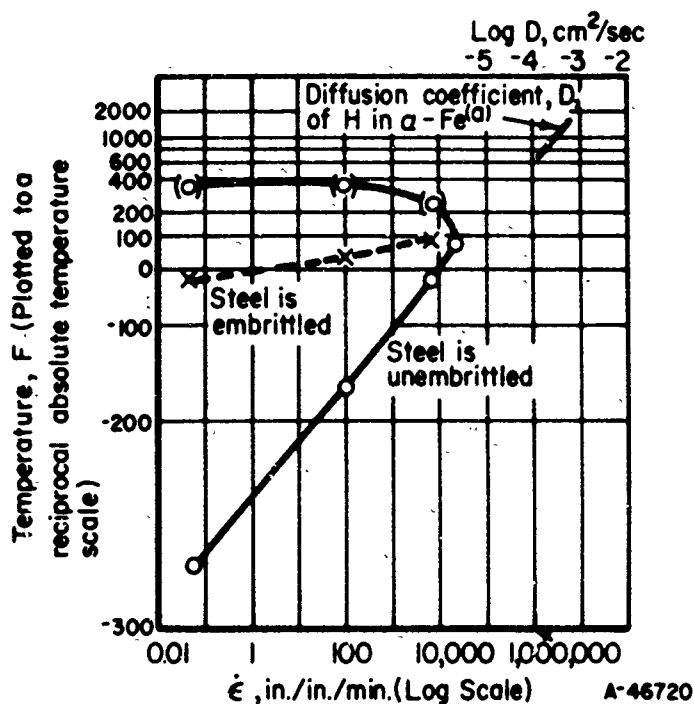


FIGURE 93. A PLOT OF TEMPERATURES AT WHICH DUCTILITY OF CHARGED STEELS RETURNS TO THE DUCTILITY CURVE OF UNCHARGED STEELS AS A FUNCTION OF STRAIN RATE (CIRCLES)<sup>(77)</sup>.

The crosses indicate the combinations of temperature and strain rate at which a minimum in the ductility curves occurred. The diffusion coefficient of hydrogen in  $\alpha$  iron is plotted to the upper scale.

Note that the reciprocal absolute temperature scale is inverted.

(a) Geller, W., and Sun, Tak-Ho, *Archiv. Eisenhüttenwesen*, 21, 423-430 (1950).

Based on the results they obtained by prestraining-and-aging experiments on hydrogenated high-strength steel, Morlet, Johnson, and Troiano<sup>(44, 97)</sup> concluded that the hydrogen concentration in the triaxial region in front of a void or large imperfection, rather than the pressure within the void, is the determining factor for embrittlement. This mechanism to explain the nature of crack kinetics of the delayed failure is based on the stress-induced diffusion of hydrogen to the area of maximum triaxiality. When the hydrogen concentration in this region reaches a critical value, a crack is nucleated. This initial crack propagates instantaneously until it is stopped, presumably by some degree of plastic flow or by the higher fracture stress of the adjacent material outside the region of maximum triaxiality. For cracking to resume, hydrogen must diffuse to

the new region of triaxiality near the base of the newly extended portion of the crack, whereupon another cycle of crack initiation and propagation will occur. Crack propagation then is a series of incubations, as has been observed experimentally, rather than a process of continuous, uninterrupted growth. The specimen eventually fails when the stress becomes greater than the fracture stress of the uncracked material that remains. This explanation of delayed failure implies two conditions: (a) the incubation period is controlled by the rate of stress-induced diffusion of hydrogen and (b) the crack grows in a discontinuous manner.

Some of the experimental work supporting this concept will be referred to briefly.

Immediately after a short-time cathodic charging operation, such as is used in most studies of delayed failure of notched specimens, the hydrogen concentration is extremely heterogeneous, the hydrogen being localized at the surface of the specimen. From experiments using an electrical-resistance method to measure the kinetics of crack growth in such specimens, Barnett and Troiano<sup>(6)</sup> concluded that the delayed failure was dependent on the growth of the crack which accompanies the macroscopic diffusion of hydrogen into the specimen. Under these conditions, however, a quantitative study of the delayed-failure mechanism was difficult to carry out because, with the heterogeneous hydrogen distribution, the hydrogen content was continually changing by redistribution and outgassing.

A more refined approach to the delayed-failure problem was that used by Johnson, Morlet, and Troiano<sup>(85,49)</sup>. They used a procedure that produced specimens with a relatively low, but apparently uniform, hydrogen concentration. Through a series of experiments involving static loading of such specimens, they were able to show that the general nature of the delayed-failure phenomenon of uniformly hydrogenated material was similar to that obtained for specimens with a heterogeneous hydrogen distribution. However, the kinetics of cracking was different. With a uniform hydrogen content, a definite incubation period preceded the initiation of a crack which ultimately led to failure of the specimen. They suggested that the incubation period was the time required for sufficient hydrogen to concentrate in a localized triaxial region and initiate a crack. Elsea and co-workers at Battelle also had made this suggestion as a result of their studies of unnotched specimens continuously charged with hydrogen while under a static load<sup>(8,9)</sup>.

The results of tests performed at low temperatures (0 F and -25 F) showed that the hydrogen-induced slow crack growth occurred discontinuously and that the delayed-failure process involved a series of crack initiations with instantaneous, but limited, propagation, rather than the continuous growth of a single crack<sup>(98)</sup>. The results obtained at low temperatures also showed that the activation energy for the incubation time agreed with that for the diffusion of hydrogen in alpha iron and that the relationship between stress and hydrogen required for crack initiation was not significantly affected by temperature variation over the range investigated.

Troiano and co-workers<sup>(49)</sup> demonstrated that cracks initiate below the surface of a notch, approximately in the region of highest triaxiality of stress, rather than at the root of the notch. Also, the location of the initial crack varies with notch acuity, just as does the location of maximum triaxiality. These findings are illustrated in Figure 94. Sharply notched specimens cracked just below the notch surface; the crack then propagated inward and outward. Cracks initiated well below the surface of mild

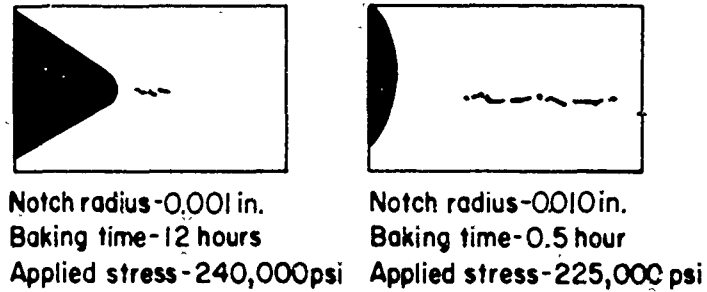


FIGURE 94. CRACKS OBSERVED IN NOTCHED SPECIMENS SECTIONED AFTER STATIC LOADING<sup>(49)</sup>

Specimens were hydrogenated, cadmium-plated, and baked at 300 F. Longitudinal sections at 100X; reduced approximately 50 per cent for reproduction.

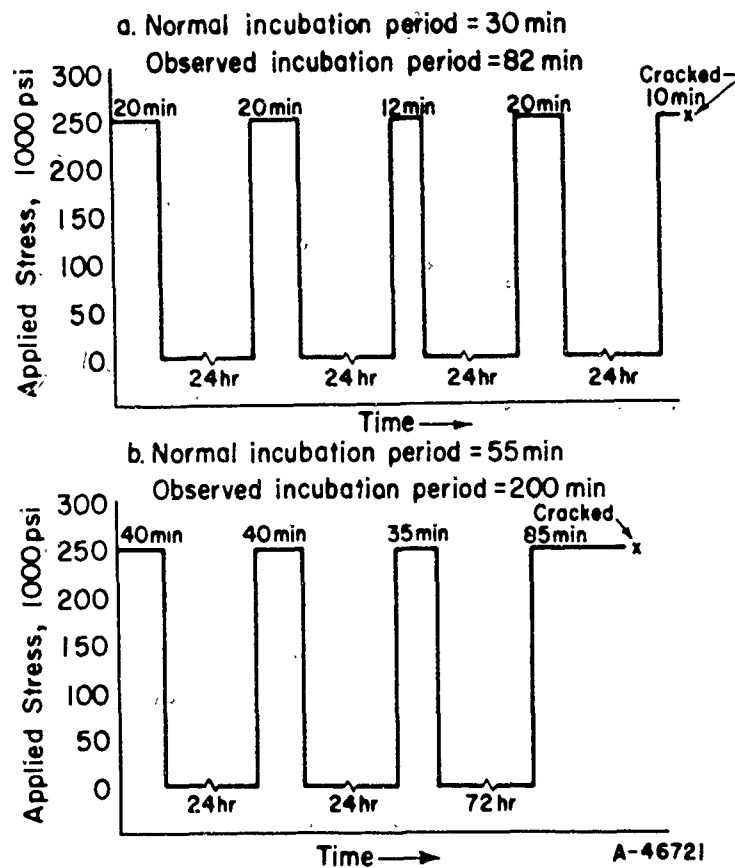


FIGURE 95. SCHEMATIC REPRESENTATION OF LOADING AND AGING TREATMENTS WHICH PRODUCE INCUBATION PERIODS MUCH LONGER THAN NORMAL INCUBATION PERIODS FOR THESE HYDROGEN CONCENTRATIONS<sup>(49)</sup>

Sharp-notch specimens, 230,000-psi strength level.

notches; the presence of a shear lip at the root of the mild notch (showing that the fracture was ductile in that area) demonstrated that the crack did not propagate to the surface until final rupture.

These investigators reasoned that, if the diffusion process is stress-induced, the incubation period should be reversible, in the sense that the direction of hydrogen diffusion should reverse upon removal of the stress. They demonstrated that this was indeed the case in experiments that are summarized in Table 21. Sharp-notch specimens were treated to give a hydrogen concentration corresponding to an incubation period of

TABLE 21. REVERSIBILITY OF THE INCUBATION PERIOD<sup>(49)</sup>

Normal incubation period = 25, 30, and 30 minutes  
for triplicate specimens.

Loading Time at 250,000 Psi, minutes	Aging Time	Incubation Period on Reloading at 250,000 Psi, minutes
17	1 min	8
20	24 hr	18
20	24 hr	30
20	24 hr	30

about 30 minutes. (Tests on three specimens gave incubation times of 30, 30, and 25 minutes, respectively.) The specimens were then stressed at 250,000 psi for the indicated times (which were shorter than the incubation period), unloaded, and aged at room temperature. The specimens that were aged for 24 hours exhibited normal incubation periods upon reloading, but the one that was aged for only 1 minute displayed a much shorter incubation period, since the aging time was too short to allow hydrogen diffusion. Since the incubation period is reversible, total incubation periods much longer than the normal periods may be produced by alternate loading and aging treatments, as shown in Figure 95. A total incubation period of 82 minutes was produced by this procedure for conditions that normally would give an incubation period of 30 minutes. In the other example, the special treatments extended the incubation period from 55 minutes to 200 minutes.

Thus, it has been shown that delayed failure is merely a series of crack initiations.

Certain combinations of hydrogen content and stress are required to cause crack initiation, and the relationship between these two factors is a fundamental part of the incubation time. It had been shown that the incubation time for delayed failure is relatively insensitive to the applied stress above a certain threshold stress. Investigators at Case Institute of Technology and Battelle Memorial Institute had postulated that, above some threshold stress, the initiation of a hydrogen-induced crack is dependent upon the development of a critical hydrogen content in the region where fracture starts. Steigerwald, Schaller, and Troiano<sup>(87)</sup> performed an experiment which demonstrated the validity of this concept. This relationship cannot be obtained from an ordinary

tensile test conducted at room temperature, because it is necessary to measure the hydrogen content. Hence, the tests were conducted in liquid nitrogen (-321 F), at which temperature diffusion during the test that might alter the local hydrogen content would be nil. A series of unnotched SAE 4340 tensile specimens heat treated to the 230,000-psi strength level were electrolytically precharged with hydrogen for 24 hours in a poisoned 4 per cent sulfuric acid solution. The hydrogen content was varied over a considerable range by adjusting the charging current. A linear relation was obtained between the hydrogen content and the log of the current density over a range of current densities, just as had been reported by other investigators. The point where the hydrogen content as a function of charging current deviated from linearity for a fixed charging time (8 ppm in this experiment) corresponded to local failure by cracking or blistering and the start of irreversible embrittlement.

Tensile tests were conducted at -321 F, and reduction in area was used to indicate the degree of embrittlement. Figure 96 shows the effect of hydrogen content (indicated by the current density) on the ductility of the high-strength steel at -321 F. The results show that the relationship between hydrogen and stress necessary to initiate a crack depends primarily on the hydrogen content. At these low temperatures, where diffusion of hydrogen was nil, no embrittlement occurred for hydrogen contents below about 5 ppm. However, when this critical hydrogen content was reached, catastrophic embrittlement took place. Inasmuch as the basic nature of delayed failure is not markedly affected by temperature, it was concluded that the initiation of a crack at room temperature also would be dependent on the development of a critical hydrogen content. It therefore was concluded that once above some threshold value, the stress in the delayed-failure process merely serves to produce sufficient hydrogen grouping (called stress-induced diffusion) to initiate a crack in the region where a fracture embryo exists.

Troiano and co-workers went through a theoretical treatment of the role of stress-induced diffusion, considering such factors as the number of hydrogen atoms arriving at the point of maximum binding energy in a given time, the distortion of the lattice due to hydrogen, the elastic constants, test temperature, the particular notch geometry, and the applied stress. They concluded that, in order for embrittlement (that is, local crack initiation) to occur, the number of hydrogen atoms arriving at the point of maximum binding energy in a given time (which would now correspond to the incubation time) must equal the critical hydrogen content. Therefore, for a given temperature and notch geometry, the following simplified relationship applies:

$$p_i \cdot t_i = \text{constant},$$

where  $t_i$  is the incubation time corresponding to an applied stress of  $p_i$ . On this basis, the incubation time as a function of applied stress can be calculated using only one experimental point to evaluate the constant for a given temperature and notch geometry. Figure 97 presents a comparison of the relationship between stress and time as determined by the above equation and by experiment. The slopes of the predicted curves agree reasonably well with the results obtained experimentally.

Each of the various theories of hydrogen embrittlement depends on a critical combination of hydrogen and stress, and each also depends in some way on the calculated pressure developed by the hydrogen in a certain type of void or imperfection. As was seen above, the mechanisms proposed by Zapffe, De Kazinczy, Bastien and Azou, and Petch and Stables depend directly on the pressure in an imperfection. In the concept of

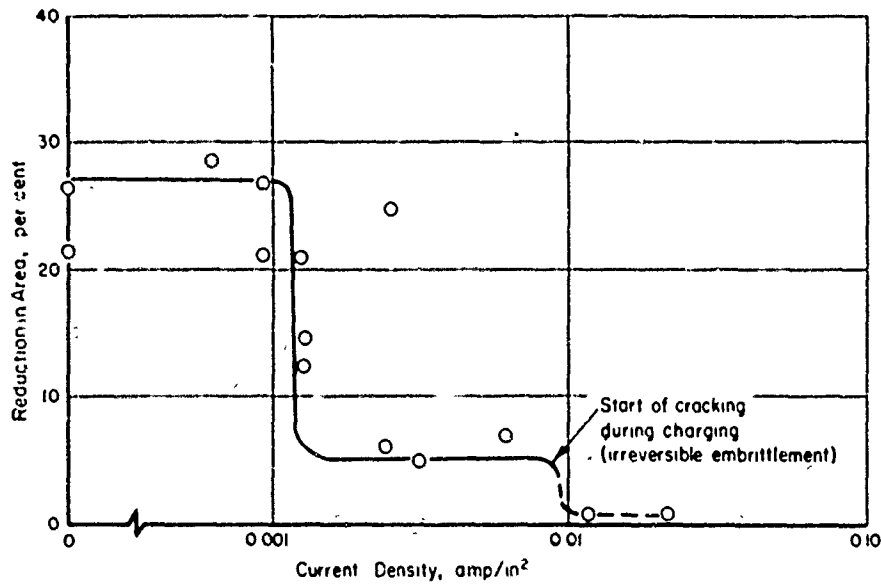


FIGURE 96. EFFECT OF HYDROGEN CONTENT (CURRENT DENSITY) ON THE DUCTILITY OF AISI 4340 STEEL TESTED AT  $-321\text{ F}^{(87)}$

Specimens precharged 24 hours in 4%  $\text{H}_2\text{SO}_4$  + poison.

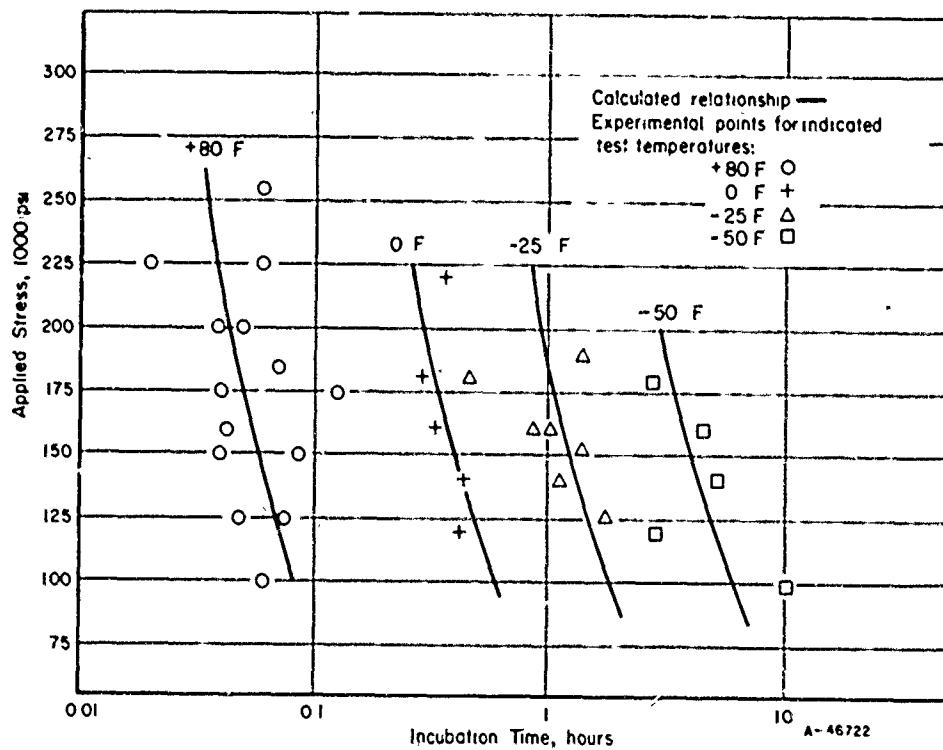


FIGURE 97. COMPARISON OF CALCULATED RELATIONSHIP BETWEEN APPLIED STRESS AND INCUBATION TIME AND EXPERIMENTAL DATA FOR HYDROGENATED AISI 4340 STEEL AT 230,000-PSI STRENGTH LEVEL<sup>(87)</sup>

Specimen Type B, 0.001-inch notch radius.



embrittlement presented by Troiano and his co-workers, the hydrogen pressure in the void influences the embrittlement by regulating the hydrogen content in the lattice in the triaxial region adjacent to the void. Recently Bilby and Hewitt<sup>(99)</sup> published the first results of an incomplete study of the stability of a wedge-shaped microcrack under constant external stress and internal pressure. Their results suggested that only a very small quantity of lattice-dissolved hydrogen is required to exert an embrittling effect directly through pressure in wedge cracks. A number of methods have been used to calculate the relationship between hydrogen content and pressure in a void, and several give essentially the same results — for example, the methods in References 43 and 32. Using the method of De Kazinczy<sup>(43)</sup>, Steigerwald et al.<sup>(87)</sup> calculated the pressure for a steel with 0.008 per cent voids; the results they obtained are plotted in Figure 98. These results indicate that the calculated pressure rises extremely rapidly over a very narrow range of hydrogen contents. The calculated relationship between pressure and hydrogen content (Figure 98) is similar to that obtained experimentally between stress and hydrogen content (based on the results in Figure 96). In agreement with the postulated mechanisms, these results indicate qualitatively that the hydrogen pressure in a void is the critical parameter influencing embrittlement. However, the exact mechanism by which hydrogen lowers the fracture stress, thus causing embrittlement, still is not understood.

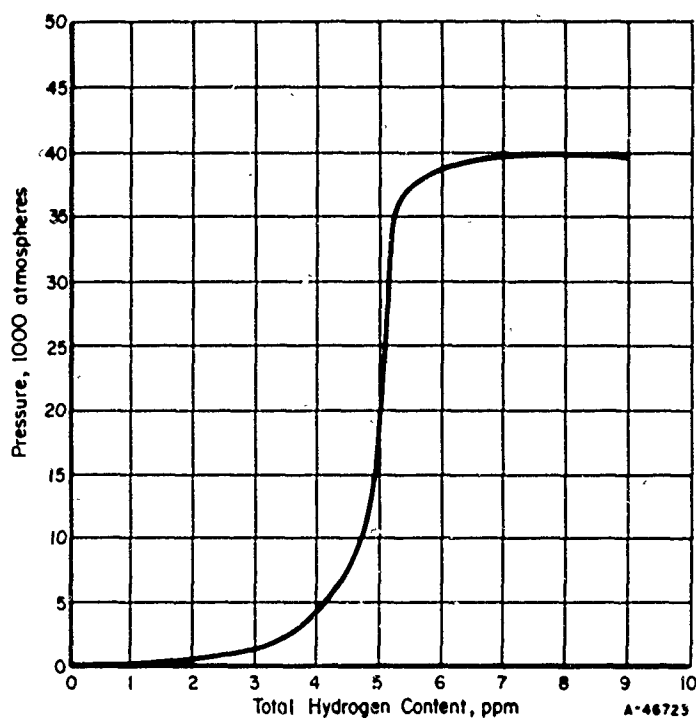


FIGURE 98. RELATIONSHIP BETWEEN PRESSURE AND HYDROGEN CONTENT CALCULATED BY METHOD OF DE KAZINCZY (REFERENCE 43) FOR STEEL WITH 0.008 PER CENT VOIDS<sup>(87)</sup>

Temperature = -321 F

Garofalo, Chou, and Ambegaokar<sup>(100)</sup> recently considered the combined effects of pressure and adsorption, using current ideas on the dislocation theory of fracture. This work is rather similar to that of Bilby and Hewitt<sup>(99)</sup>, but the two analyses appear to differ in certain important respects and suggest rather different conclusions.

De Kazinczy recently published a paper on crack formation in steel during electrolytic hydrogen absorption<sup>(101)</sup>. He considers that hydrogen dissolved in steel can cause cracking by two separate mechanisms. Blister-type cracks (observed by a number of investigators) are caused by deposition of molecular hydrogen gas within the metal, due to a high activity of molecular hydrogen. Cracks also occur at much lower hydrogen activities and at stresses below the yield stress. Here he considers that hydrogen causes creep by unpinning dislocations, and brittle fracture occurs by the Stroh or Cottrell mechanisms. This type of mechanism is similar to the cracking which occurs at high temperatures in the absence of hydrogen, where thermal energy causes the unpinning of dislocations.

Tetelman and Robertson employed the technique of decorating dislocations to investigate deformation and fracture resulting from precipitation of hydrogen in Fe-3Si single crystals<sup>(102)</sup>. They showed that cracks are produced on {100} planes inside crystals, as a consequence of the precipitation of hydrogen gas, either when crystals are quenched from a hydrogen atmosphere at elevated temperatures or when they are cathodically charged with hydrogen at room temperature. Plastic deformation in the vicinity of cracks was observed as arrays of decorated dislocations, which conformed with the calculated stress distribution about a crack containing an internal pressure. Also, the observations provided information permitting a detailed analysis of the mechanics of crack growth. The fracture characteristics of crystals containing internal cracks were evaluated at 25 and -196 C (room temperature and the temperature of liquid nitrogen), and the results are related to the mechanism of hydrogen embrittlement in terms of the growth of pre-existing cracks.

Siede and Rostaker<sup>(103)</sup> found that hydrogen-charged iron has strain-aging characteristics that are indistinguishable from those of uncharged iron. Based on these results they presented the case that hydrogen displaces carbon and nitrogen from dislocation centers, and the hydrogen embrittlement derives from the stabilization of transient and thermally generated crack nuclei formed at lower stress levels.

Blanchard and Troiano<sup>(104)</sup> attempted to apply a fracture mechanism proposed by Cottrell to the case of hydrogenated steel and other metals susceptible to hydrogen embrittlement. Hydrogen was assumed to enhance the growth of cracked arrays of dislocations by increasing their energy. An interpretation of the increase of energy of the cracks due to hydrogen was proposed. This interpretation, based on the consideration of the electronic structure of hydrogenated metals, accounts for two aspects of hydrogen embrittlement:

- (1) Only transition metals have been embrittled by hydrogen thus far.
- (2) The susceptibility of Ni-base Ni-Cr-Fe alloys decreases with increasing (Cr + Fe) content.

The theory is said to explain part of the experimental results obtained on the variation of the ductility of steel with its hydrogen content at low temperature.

Most recently, Scott and Troiano<sup>(105)</sup> carried out an investigation with the purpose of evaluating the possibility of extending the concept of hydrogen-induced, delayed, brittle failure, developed previously by Troiano and co-workers, to other interstitial alloy systems, specifically carbon in steel. Delayed, brittle failures were obtained in a nonhydrogenated high-temperature die steel tested at elevated temperatures

(850-950 F). The characteristics of the failures were similar to those obtained with hydrogenated high-strength steel at ambient temperatures. The almost perfect correspondence of the behavior of the two systems led to the conclusion that the same mechanism was operative in both cases. This mechanism is based on the idea of a local lowering of the cohesive strength of the lattice due to an accumulation of interstitial solute atoms in regions of high elastic strains. Thus, these appear to have been carbon-induced, delayed, brittle failures. The elevated temperature was required so that carbon would have sufficient mobility to move in response to the stress gradient. This paper restates their proposed mechanism for hydrogen-induced, delayed, brittle failure.

### TESTS FOR HYDROGEN EMBRITTLEMENT

The purpose of this section is to discuss tests that can be used to determine if a hydrogen-embrittlement problem, and specifically a delayed-brittle-failure problem, exists. Most of these tests depend on a comparison of the properties of a material carefully processed so as to have a minimum hydrogen content with those of a material processed under suspect conditions.

For careful processing, the heat-treating atmosphere should not be conducive to hydrogen pickup from the steam reaction, so the water vapor content should be relatively low. Also, the partial pressure of hydrogen should be low. (Treatment at elevated temperatures in a wet hydrogen atmosphere is one method that is used to intentionally introduce hydrogen into steel.) A dry argon atmosphere is ideal for use in laboratory investigations, but often this is not practicable in the plant. No acid pickling, cathodic cleaning, nor electroplating operations are permissible, as these operations usually introduce hydrogen into the steel.

In some laboratory investigations, in order to obtain a uniform base material and minimize variations in hydrogen content resulting from steelmaking operations, a procedure has been adopted to reduce the hydrogen content of the steel as much as possible. To accomplish this, the steel is austenitized at a suitable temperature and furnace cooled to a temperature in the pearlite-formation range where complete isothermal transformation can be achieved on holding for a reasonable time (a few hours), allowing ample margin for heat-to-heat variations in transformation time. Then the temperature is lowered to approximately 500 F, and the material is held for an additional time of perhaps 24 hours to achieve the lower equilibrium solubility associated with the lower temperature. After rough machining of test specimens, the specimens are heated for hardening by austenitizing in a dry argon atmosphere. They are quenched and tempered in the usual fashion.

Suspect treatments include acid pickling, cathodic cleaning, electroplating, electrochemical machining, heating in moist atmospheres or hydrogen-bearing atmospheres, exposure of steel to moisture sufficient to cause corrosion (including the use of water for pressure testing of pressure vessels), and exposure to hydrogen at elevated temperatures and pressures. Also, especially for heavy sections, hydrogen introduced in the steelmaking operations may be a factor unless suitable vacuum processing has been used to minimize hydrogen pickup from these sources. However, in the aircraft and

missile industries where lighter sections prevail, the bulk of the hydrogen problems are related to cleaning and electroplating operations.

Throughout this report, in discussing the effects of different variables on delayed, brittle failure, various tests have been encountered. Some of these include the conventional tensile test, the tensile test of notched specimens, the sustained-load test of smooth specimens with continuous cathodic charging, the sustained-load test of pre-charged notched specimens, various bend tests of notched or smooth specimens, the torsion test, fatigue tests, and impact tests.

For some time, it has been recognized generally that hydrogen embrittlement is minimized as the strain rate is increased, while it is enhanced as the strain rate is decreased. For this reason, notched impact tests, such as Charpy V-notch tests, are of no value in detecting the presence of the hydrogen-embrittlement condition or the susceptibility of a material to delayed, brittle fracture. The reader is referred to the section that treats the effect of strain rate for a fuller discussion of this aspect of the problem. Also, the test should be performed in the vicinity of room temperature, as the hydrogen embrittlement is a maximum at temperatures in this general vicinity. See Figure 63 (page 95) for a summary of the effects of strain rate and test temperature.

The various test methods differ in their capability to detect the susceptibility of a material to delayed, brittle failure. If a tensile test of an unnotched specimen shows an appreciable loss in reduction in area, the condition is severe. However, a normal value of reduction in area is no guarantee that delayed failure cannot occur at low applied stresses. The results of a number of investigations have shown that delayed failure frequently may occur in a high-strength steel which exhibits full ductility as determined by the reduction in area obtained from a conventional tensile test. The notched tensile strength is a somewhat more sensitive measure of susceptibility to delayed, brittle failure, at least under some conditions. However, instances have been cited earlier in this report where a recovery treatment resulted in full recovery of notched tensile strength, and still delayed failures occurred under static-loading conditions. For example, see References 85 and 5. Also, Frohberg, Barnett, and Troiano<sup>(5)</sup> showed that the time for complete recovery by aging is greater in the static-loading test than in the notched tensile test for identically charged specimens.

It is difficult to determine the susceptibility to delayed, brittle failure using pre-charged unnotched tensile specimens and static loading if the specimens are truly straight and true axial loading is achieved. Elsea and co-workers<sup>(8)</sup> obtained delayed, brittle failures after several hours in small-diameter wire specimens in which uniaxial stresses would have been approached very closely. These were unnotched specimens, but it was necessary to charge them cathodically during the sustained-load period. These same investigators observed that delayed failure in a few preliminary tests of precharged unnotched specimens of larger diameter was associated with slight bending that occurred inadvertently during heat treatment of the premachined specimens so that the stresses were not uniaxial. They regularly obtained delayed failures with straight, unnotched tensile specimens when they were cathodically charged continuously while under sustained load. Frohberg, Barnett, and Troiano<sup>(5)</sup> obtained delayed, brittle failures at lower stresses with notched specimens than with smooth specimens. The results obtained in both these early investigations indicated that triaxial stresses are more likely to lead to delayed, brittle failure than are uniaxial stresses. This behavior

was clearly demonstrated in work of Frohmberg et al.<sup>(5)</sup> and Klier, Muvdi, and Sachs<sup>(19)</sup> in which variations in notch acuity were studied. This work has been described in the section dealing with the effect of notch acuity. Figures 20, 86, and 18 (pages 36, 118, and 33, respectively) clearly show the effect.

The sustained-load test of cadmium-plated notched specimens has seen wide use as an indicator of hydrogen embrittlement that occurs as the result of hydrogen introduced into high-strength steel by cleaning and electroplating operations. The reason for this is that the plots of applied stress versus failure time in the sustained-load test are strongly influenced by the quantity of hydrogen present. If all other variables are held constant, the lower critical stress (the stress level below which failure is not obtained) has been shown to increase with decreasing levels of hydrogen. Some of the other variables that affect the lower critical stress at room temperature are the strength level of the material, notch acuity or stress-concentration factor, and eccentricity of loading during testing.

No reports are known of failures in compression, and failures have not initiated in the compression side of bend specimens, as was discussed in the section that deals with the effects of different stress states. The rotating-beam fatigue test was studied by Sachs' group<sup>(86)</sup>. They concluded that, as a tool for the evaluation of hydrogen embrittlement, the normal high-speed fatigue test is of little value. Also, the high cost of specimen preparation makes the test uneconomical. However, in a study of inhibitors for hydrogen pickup during acid pickling at Aberdeen Proving Ground, as discussed by Dauerman<sup>(106)</sup>, embrittlement was measured with the Moore fatigue test. Other experimental work on specimens loaded in torsion showed that the failure times were not influenced by the state of the stress and, for all practical purposes, the only stress that influenced the delay time for failure was the maximum tensile stress<sup>(9)</sup>. The plane of the cracks in torsion specimens was normal to the maximum tensile stress.

As a result of these various tests, it is apparent that the most sensitive test for revealing hydrogen embrittlement and the most satisfactory way to study delayed, brittle failures is the static-loading test. Under carefully controlled conditions, this sustained-load test of notched tensile specimens is a satisfactory indicator of susceptibility to delayed, brittle failure. However, this test involves a stress-rupture machine of some sort, and care must be taken to secure good alignment of specimen axis and grips so as to attain virtually uniaxial tensile loading, with bending stresses at a minimum. Therefore, there has been considerable effort to develop other tests.

Figure 99 shows a static-loading device that can be used in place of more expensive stress-rupture machines. The load is measured by means of strain gages attached to a reduced section of the loading screw. Belleville springs are provided to reduce the effect of any relaxation of the specimen or apparatus. This device has been used with precharged specimens, and, with the electrolytic cell in place as shown in the figure, it is suitable for continuous charging while under load. The slight decrease in the indicated stress during the test is considerably less than the probable error in loading. The Gregg tension ring is a small and simple device for applying and maintaining a tensile load on a notched stress-rupture specimen. The load is applied to the test specimen through an elastic ring and is measured by the change in diameter of the ring. The static bend test is favored by some investigators, and others use a constant-rate bend test to detect embrittlement but not susceptibility to delayed failures. References 81 and 107 describe a constant-rate bend test, and results obtained with it are compared with those from other tests. For sustained loading, a notched C-ring (the specimen) stressed by a hollow bolt, the load upon which is detected by a strain gage, has

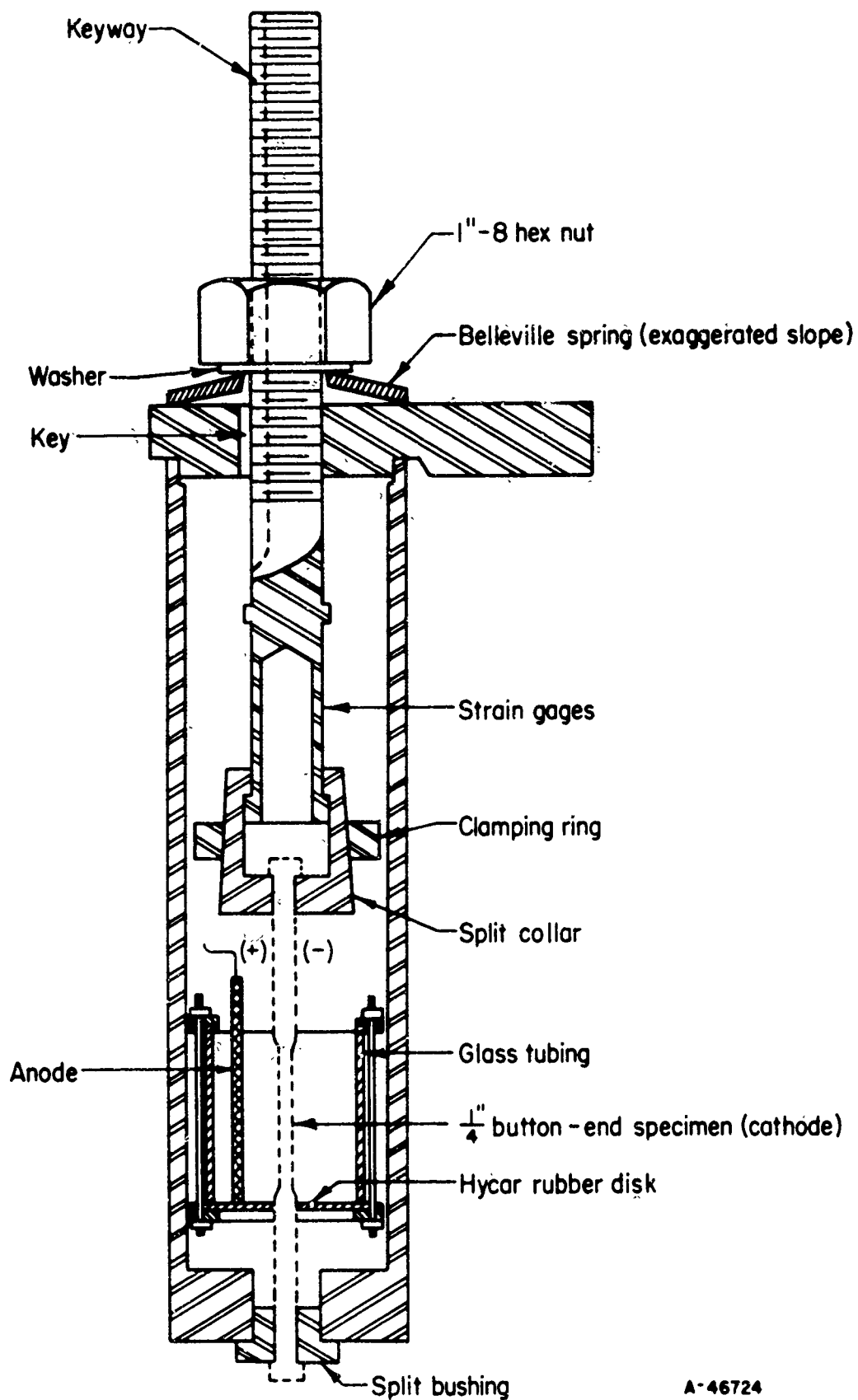


FIGURE 99. STATIC-LOADING DEVICE FOR 1/4-INCH BUTTON-END SPECIMENS<sup>(8)</sup>

Electrolytic cell, for charging specimens with hydrogen while under stress, is shown in place.

been devised(108, 109, 110). Jones(111) has described a test in which a long slender column is bent by loading in compression. Other devices and test methods are described in References 112, 113, and 114. A recent article has suggested that neutrons may soon be used as a nondestructive test to locate hydrogen in metals(115).

A survey in 1957 of 25 companies concerned with hydrogen embrittlement of ferrous metals used in aircraft and missiles showed the need for standardizing the engineering test methods for detecting hydrogen embrittlement. Methods then in use included the standard tensile test, the notched tensile test, either of these two types of tensile test in conjunction with a sustained load test, seven types of bend tests, and sustained-load tests of notched or smooth tensile bars, torqued bolts, flat bars, round rings, and C-rings. The Aerospace Research and Testing Committee set up Project W-95 to select or develop a standard test, preferably a short-term test, that would give an accurate indication of the degree of hydrogen embrittlement in ferrous materials. In this project, six basic methods of testing for hydrogen embrittlement were investigated. They were the tensile test, stressed-ring test, sustained-load notched tensile test, constant-rate bend test, torqued-bolt test, and static-bend test. Modifications of the test specimen and procedures brought the total number of methods investigated to 12. Of all the methods investigated, the sustained-load notched tensile test was found to be the most sensitive and reproducible. However, two versions of this test were used (the chief difference being in the root radius of the notch), and they showed considerable difference in time to failure for specimens embrittled under identical conditions by the same laboratory. Therefore, further work was recommended to arrive at a standard sustained-load notched tensile test. This work is described in detail in Reference 116.

In a recent paper, Johnson(117) has discussed a method for detecting hydrogen embrittlement resulting from electrolytic cadmium plating. Sustained-load tests were performed with specimens having notch root radii of 0.001, 0.003, 0.005, and 0.025 inch. The three sharper notches all indicated good sensitivity to high degrees of embrittlement. For low degrees of embrittlement, it was concluded that the notch root radius should be 0.003 inch or smaller for maximum sensitivity.

### CONCLUSIONS:

- (1) Composition is not an important factor in the hydrogen-induced, delayed, brittle failure of steels. No alloying element, either substitutional or interstitial, has eliminated the tendency for hydrogen-induced, delayed, brittle failure, and none has been truly effective in retarding failures of this type. All ferritic and martensitic steels studied have been susceptible to this type of failure when tested under appropriate conditions. No instance of hydrogen-induced failure of a completely austenitic steel is known. However, with very severe charging conditions, austenitic steels can suffer some loss in ductility. The resistance of austenitic steels to this type of failure appears to be related to the face-centered-cubic structure.
- (2) Under practicable conditions of processing steel, the strength level appears to be the most important factor governing the occurrence of delayed, brittle failure. As the nominal tensile strength of the steel is increased, both the minimum applied stress for failure and the time required to produce failure decrease. Thus, high-strength steel

parts are especially susceptible. However, in the presence of sufficient hydrogen, delayed, brittle failures have been obtained in steels with tensile strengths as low as 53,400 psi.

(3) Delayed, brittle failures may occur in steel over a wide range of applied tensile stress. For given specimens, hydrogen-charging conditions, and test procedures, there is a critical value of applied stress below which these failures do not occur, and the material is able to support the stress indefinitely. For a given strength level, the time to failure depends only slightly on applied stress, so long as it is well above the critical level. Experimental data indicate that failure does not occur until a certain combination of applied stress, hydrogen content, and time is exceeded. The critical stress for failure and also the time required to produce failure decrease as the strength level of the steel is increased. It has been shown that measurable plastic flow is not required for hydrogen to initiate brittle failure. Also, straining the material a few per cent prior to the introduction of hydrogen has no appreciable effect on the time for failure. With continuous cathodic charging, there was no effect of a few per cent plastic strain on the lower critical stress, but with specimens precharged before being loaded statically, prior plastic strain raised the lower critical stress. Failure is initiated most readily in regions of triaxial stress state. No failures have been reported for uniaxial compression.

(4) Because of the small amounts of hydrogen involved and the ease and speed with which hydrogen moves through steel and leaves the steel surface at ordinary temperatures, reliable hydrogen analyses are virtually impossible to obtain. Even so, the results of many investigations concur in showing that delayed, brittle failures depend directly on the hydrogen content. Such failures are not a problem if the hydrogen can be kept out of the steel or if it can be removed from the steel before permanent damage occurs. However, this is not easy to do, considering the many sources of hydrogen and the fact that as little as 1 ppm of hydrogen or even less can lead to failure.

(5) Normally, the critical amount of hydrogen to induce failure is not present at the stress sites which favor delayed failure. Therefore, hydrogen diffusing to these sites is an important part of the failure mechanism. Since the site of maximum triaxial stress moves as failure progresses, hydrogen must continue to move if crack propagation is to continue. The necessity for hydrogen to move explains why this type of failure occurs only under low strain rates. The diffusion of hydrogen is, of course, temperature and time dependent, and numerous experiments have shown that the degree of embrittlement encountered and the rate of crack propagation are controlled by the diffusion of hydrogen. However, the movement of hydrogen is quite rapid at temperatures in the vicinity of room temperature, and failures occur readily at ordinary temperatures. Lowering the temperature prolongs both the incubation time and the fracture time. This movement of hydrogen can occur in response to a hydrogen composition gradient, and it is generally accepted that it also can occur in response to a stress gradient. It is hypothesized that hydrogen exerts a maximum embrittling effect in the region of most severe tensile stress.

(6) As a rule, the severity of most types of embrittlement increases with increasing strain rate. However, hydrogen embrittlement shows just the opposite behavior. For this reason, it is often called low-strain-rate embrittlement. Even for high-strength steel, hydrogen embrittlement is nil in an impact test. It may or may not be detected in an ordinary tensile test, depending upon the hydrogen content and distribution, but it



is more severe in a notched tensile specimen with the triaxial stresses introduced by the notch. The most sensitive test for hydrogen embrittlement and delayed, brittle failure is the static-loading test of a notched specimen.

(7) In steels, hydrogen-induced, delayed, brittle failures are found only in body-centered cubic microstructures; fully austenitic steels are quite resistant to hydrogen embrittlement. Tempered martensite, bainite, lamellar pearlite, and spheroidized structures all are susceptible to hydrogen embrittlement, and delayed failures occur in all four. It has been established that the transformation of retained austenite is not a primary cause of these failures. Structure per se appears to be relatively unimportant so long as it is body-centered cubic. Rather, the ultimate tensile strength of the material, regardless of structure, is the chief factor influencing delayed, brittle failures.

(8) The section size also is a factor, at least in instances where the hydrogen is initially concentrated at the surface, as it is shortly after electroplating, pickling, or electrolytic charging, or when hydrogen is introduced electrolytically or by corrosive attack while the part is under sustained load. Increased section size results in longer delays before brittle failure. In addition, section size has a marked influence on the recovery of properties by aging to remove hydrogen from the steel; hydrogen removal from large masses is very slow.

(9) Because the delayed, brittle failure induced in steel by hydrogen is a low-strain-rate phenomenon, it is relatively easy to study crack initiation and propagation. Acoustical, electrical resistance, and metallographic methods have been used in these studies; they have shown that the delayed-brittle-failure process consists of the following three stages:

- (1) Incubation
- (2) A period of slow crack growth (propagation)
- (3) Sudden rupture through the central core that frequently is essentially free of hydrogen.

Crack propagation has been shown to be a discontinuous process that consists of a series of separate crack initiations and propagations. Both the incubation period and crack propagation are controlled by the diffusion of hydrogen. Above a certain threshold stress, the conditions necessary for localized cracking depend almost entirely on the development of a critical hydrogen content. This level of hydrogen is built up by diffusion, induced either by a hydrogen gradient or by a stress gradient. However, there still is no general agreement regarding the mechanism by which hydrogen reduces the ductility of steel and lowers its load-carrying ability. Several theories of hydrogen embrittlement have been proposed. Each of them depends on a critical combination of stress and hydrogen, and each depends in some way on the development of a hydrogen pressure in a certain type of void or imperfection.

REFERENCES

- (1) Hobson, J. D., and Hewitt, J., "The Effect of Hydrogen on the Tensile Properties of Steel", *J. Iron and Steel Inst.*, 173, 131-140 (1953).
- (2) Eisenkolb, F., and Ehrlich, G., "Absorption of Hydrogen by Austenitic Steels Under Cathodic Loading", *Arch. Eisenhüttenwesen*, 25 (3,4), 167-194 (1954). Brucher Translation No. 3412.
- (3) Blanchard, P. A., and Troiano, A. R., "Hydrogen Embrittlement in Steels, Titanium Alloys, and Several Face-Centered Cubic Alloys. Section III. Hydrogen Embrittlement of Several Face-Centered Cubic Alloys", WADC TR 59-172 (April, 1959).
- (4) Frohmberg, R. P., Barnett, W. J., and Troiano, A. R., "Delayed Failure and Hydrogen Embrittlement in Steel", WADC TR 54-320 (1954).
- (5) Frohmberg, R. P., Barnett, W. J., and Troiano, A. R., "Delayed Failure and Hydrogen Embrittlement in Steel", *Trans. Am. Soc. Metals*, 47, 892-923 (1955).
- (6) Barnett, W. J., and Troiano, A. R., "Crack Propagation in the Hydrogen-Induced Brittle Fracture of Steel", *Trans. Am. Inst. Mining, Met., and Petroleum Engrs.*, 209, 486-494 (1957); *J. Metals*, 9 (4), 486-494 (April, 1957).
- (7) Slaughter, E. R., Fletcher, E. E., Elsea, A. R., and Manning, G. K., "An Investigation of the Effects of Hydrogen on the Brittle Failure of High-Strength Steels", Third Quarterly Progress Report to WADC, Contract AF 33(616)-2103 (March 31, 1954).
- (8) Slaughter, Edward R., Fletcher, E. Ellis, Elsea, Arthur R., and Manning, George K., "An Investigation of the Effects of Hydrogen on the Brittle Failure of High-Strength Steels", WADC TR 56-83 (June, 1955).
- (9) Simcoe, Charles R., Elsea, Arthur R., and Manning, George K., "An Investigation of Absorbed Hydrogen in Ultra-High-Strength Steel", WADC TR 56-598 (November 15, 1956).
- (10) Sachs, George, and Beck, Walter, "Survey of Low-Alloy Aircraft Steels Heat-Treated to High Strength Levels: Part 1. Hydrogen Embrittlement", WADC TR 53-254, Part 1 (June, 1954).
- (11) Klier, E. P., Muvdi, B. B., and Sachs, George, "Design Properties of High-Strength Steels in the Presence of Stress-Concentrations and Hydrogen Embrittlement: Part 1. Effects of Hydrogen Embrittlement on High-Strength Steels - Static Properties", WADC TR 55-18, Part 1 (November, 1954).
- (12) Rinebolt, J. A., "Progress Report on the Effect of Gases in Steel", Naval Research Laboratory Memorandum Report 345 (March, 1953, to July, 1954).

- (13) Gasior, E., and Prajsnar, T., Private communication to M. Smialowski in 1959 and described by him on page 241 in his book Hydrogen in Steel, Pergamon Press (1962).
- (14) Smialowski, Michael, Hydrogen in Steel, Pergamon Press, New York (1962), pp 239, 241.
- (15) Johnson, H. H., Johnson, R. D., Frohberg, R. P., and Troiano, A. R., "Static Fatigue in Twelve Heats of 4340 Steel Embrittled with Hydrogen", WADC TN 55-306 (August, 1955).
- (16) Blanchard, P., and Troiano, A. R., "Delayed Failure and Notch Tensile Properties of a Vacuum Melted 4340 Steel", WADC TN 58-176 (September, 1958).
- (17) Raring, R. H., and Rinebolt, J. A., "Static Fatigue of High-Strength Steel", NRL Memorandum Report 452 (April, 1955).
- (18) Raring, R. H., and Rinebolt, J. A., "Static Fatigue of High Strength Steel", Trans. Am. Soc. for Metals, 48, 198-212 (1956).
- (19) Klier, E. P., Muvdi, B. B., and Sachs, G., "The Response of High-Strength Steels in the Range of 180,000 to 300,000 psi to Hydrogen Embrittlement From Cadmium-Electroplating", Am. Soc. Testing Materials, Proceedings, 58, 597-619 (1958).
- (20) Klier, E. P., Muvdi, B. B., and Sachs, G., "Design Properties of High-Strength Steels in the Presence of Stress Concentrations and Hydrogen Embrittlement. Part 3. The Response of High-Strength Steels in the Range of 180,000-300,000 psi to Hydrogen Embrittlement From Cadmium Electroplating", WADC TR 56-395, Part 3 (March, 1957).
- (21) Srawley, J. E., "Hydrogen-Embrittlement Susceptibility of Some Steels and Nonferrous Alloys", NRL Report No. 5392 (October 19, 1959).
- (22) Ceyer, N. M., Lawless, G. W., and Cohen, B., "A New Look at the Hydrogen Embrittlement of Cadmium Coated High Strength Steels", WADC TR 58-481 (December, 1958).
- (23) Probert, L. E., and Rollinson, J. J., "Hydrogen Embrittlement of High Tensile Steels During Chemical and Electrochemical Processing", Electroplating and Metal Finishing, 14, 323-326, 342 (September, 1961); 356-360, 382 (October, 1961); 396-401, 406 (November, 1961); 15, 6-9 (January, 1962).
- (24) Beachum, E. R., Johnson, H. H., and Stout, R. D., "Hydrogen and Delayed Cracking in Steel Weldments", Welding J., 40 (4), 155-s - 159-s (April, 1961).
- (25) Schuetz, A., and Robertson, W., "Hydrogen Absorption, Embrittlement and Fracture of Steel", Corrosion, 13, 437t-458t (1957).

- (26) Uhlig, H. H., "Action of Corrosion and Stress on 13% Cr Stainless Steels", *Metal Progress*, 57 (4), 486 (1950).
- (27) Lillys, P., and Nehrenberg, A. E., "Effect of Tempering Temperature on Stress-Corrosion Cracking and Hydrogen Embrittlement of Martensitic Stainless Steels", *Trans. Am. Soc. Metals*, 48, 327-346 (1955).
- (28) Valentine, K. B., "Stress Cracking of Electroplated Lockwashers", *Trans. Am. Soc. Metals*, 38, 488-494 (1947).
- (29) Stefanides, Victor, Discussion of Reference 28, *Trans. Am. Soc. Metals*, 38, 495-502 (1947).
- (30) Noble, H. J., "Hydrogen Embrittlement", *The Iron Age*, 148, 45-52 (November 27, 1941).
- (31) Eakin, C. T., and Lownie, H. W., Jr., "Reducing Embrittlement in Electroplating", *The Iron Age*, 158, 69-72 (November 21, 1946).
- (32) Sykes, C., Burton, H. H., and Gegg, C. C., "Hydrogen in Steel Manufacture", *J. Iron and Steel Inst.*, 156, 155-180 (1947).
- (33) Zapffe, C. A., and Haslem, M. E., "A Test for Hydrogen Embrittlement and Its Application to 17% Chromium 1% Carbon Stainless Steel Wire", *Metals Technology*, 13 (1), Tech. Paper 1954 (January, 1946); *Trans. Am. Inst. Mining and Met. Engrs.*, Iron and Steel Div., 167, 281 (1946).
- (34) Houdremont, E., and Schrader, H., "Effect of Hydrogen on Plasticity of Steels", *Arch. Eisenhüttenwesen*, 15, 87 (1941/2), In German.
- (35) Mills, Robert L., and Edeskuty, Frederick, "Hydrogen Embrittlement of Cold-Worked Metals", *Chem. Engr. Prog.*, 25, 477-480 (1956).
- (36) Uhlig, Herbert H., "Influence of Hydrogen on Mechanical Properties of Some Low-Carbon Manganese-Iron Alloys and on Hadfield Manganese Steel", *Metals Technology*, Tech. Paper 1701 (June, 1944).
- (37) Blanchard, P., and Troiano, A. R., "La Fragilisation des Métaux par L'hydrogène. Influence de la Structure Cristallographique et Electronique", *Memoires Scientifiques Revue de Metallurgie*, 57 (6), 409-422 (1960).
- (38) Jones, R. L., "The Susceptibility of Materials to Hydrogen Embrittlement From Chemical Milling Operations", Convair (Astronautics), Div. of General Dynamics Corp., San Diego, California, MRG-219 (March 16, 1961).
- (39) Barnett, W. J., and Troiano, A. R., "Crack Propagation in the Hydrogen-Induced Brittle Fracture of Steel", WADC TN 55-405 (August, 1955).
- (40) Steigerwald, E. A., Schaller, F. W., and Troiano, A. R., "The Lower Critical Stress for Delayed Failure", WADC TR 59-445 (August, 1959).

- (41) Steigerwald, E. A., Schaller, F. W., and Troiano, A. R., "The Role of Stress in Hydrogen Induced Delayed Failure", *Trans. Met. Soc. AIME*, 218, 832-841 (October, 1960).
- (42) Hobson, J. D., and Sykes, C., "Effect of Hydrogen on the Properties of Low Alloy Steels", *J. Iron and Steel Inst.*, 169, 209-220 (1951).
- (43) De Kazinczy, F., "A Theory of Hydrogen Embrittlement", *J. Iron and Steel Inst.*, 177, 85-92 (1954).
- (44) Morlet, J. G., Johnson, H. H., and Troiano, A. R., "A New Concept of Hydrogen Embrittlement in Steel", WADC TR 57-190 (March, 1957).
- (45) Johnson, R. D., Johnson, H. H., Morlet, J. G., and Troiano, A. R., "Effects of Physical Variables on Delayed Failure in Steel", WADC TR 56-220 (June, 1956).
- (46) Bastien, Paul, and Amiot, Pierre, "The Influence of Hydrogen in Steel on the Phenomenon of Delayed Fracture", *Compt. Rend.*, 241, 1760-1762 (1955), In French.
- (47) Bucknall, E. H., Nicholls, W., and Toft, L. H., "Delayed Cracking in Hardened Alloy Steel Plates", *Symposium on Internal Stresses in Metals and Alloys*, Monograph and Report Series No. 5, Institute of Metals, 351-365 (1948).
- (48) Bell, W. A., and Sully, A. H., "Some Effects of Hydrogen on the Delayed Fracture of High-Tensile Steel", *J. Iron and Steel Inst.*, 178, 15-18 (1954).
- (49) Johnson, H. H., Morlet, J. G., and Troiano, A. R., "Hydrogen, Crack Initiation, and Delayed Failure in Steel", *Trans. Met. Soc. AIME*, 212 (4), 528-536 (August, 1958).
- (50) Darken, L. S., and Smith, R. F., "Behavior of Steel During and After Immersion in Acid", *Corrosion*, 5, 1-16 (1949).
- (51) Bardenheuer, P., and Ploum, H., "The Hydrogen Embrittlement of Steel in Dependence on the Amount of Absorbed Hydrogen", *Mitt. Kaiser-Wilhelm Inst. Eisenforschung*, 16, 137-140 (1934), In German.
- (52) Sims, C. E., Moore, G. A., and Williams, D. W., "The Effect of Hydrogen on the Ductility of Cast Steels", *Trans. Am. Inst. Mining Met. Engrs.*, 176, 283 (1948).
- (53) Sims, C. E., "Hydrogen Elimination by Aging", *Trans. Am. Inst. Mining Met. Engrs.*, 188, 1321 (1950); *J. Metals*, 188 (11), 1321 (November, 1950).
- (54) Zapffe, C. A., and Haslem, M. E., "Measurement of Embrittlement During Chromium and Cadmium Electroplating and the Nature of Recovery of Plated Articles", *Trans. Am. Soc. Metals*, 39, 241-258 (1947).
- (55) Zapffe, C. A., and Haslem, M. E., "Hydrogen Embrittlement in Cadmium and Zinc Electroplating", *Plating*, 37, 366-371 (April, 1950).

- (56) Zapffe, C. A., and Haslem, M. E., "Hydrogen Embrittlement in Nickel, Tin and Lead Electroplating", *Plating*, 37, 610-613 (June, 1950).
- (57) Potak, Ya. M., "Brittle Fracture of Steel and Steel Elements", *Khrupkoe Razrushenie Stali i Stalnykh Detalei*, Moscow (1955), In Russian. Data taken from Smialowski, M., Hydrogen in Steel, Pergamon Press, New York (1962), pp 384-385.
- (58) Figelman, M. A., and Shreider, A. V., "Hydrogen Embrittlement of Steel by Electroplating with Cu, Ni, Zn, Cd, Cr", *Zh. Prikladnoi Khim*, 31, 1184 (1958). This work is summarized in Smialowski, M., Hydrogen in Steel, Pergamon Press, New York (1962), p 385.
- (59) Gurklis, J. A., McGraw, L. D., and Faust, C. L., "Hydrogen Embrittlement of Cadmium Plated Spring Steel", *Plating*, 47 (10), 1146-1154 (October, 1960).
- (60) Johnson, R. D., Johnson, H. H., Barnett, W. J., and Troiano, A. R., "Hydrogen Embrittlement and Static Fatigue in High Strength Steel", WADC TN 55-404 (August, 1955).
- (61) Greco, Edward C., and Wright, William B., "Corrosion of Iron in an H<sub>2</sub>S-CO<sub>2</sub>-H<sub>2</sub>O System", *Corrosion*, 18, 119t-124t (March, 1962).
- (62) Skei, T., Wachter, A., Bonner, W. A., and Burnham, H. D., "Hydrogen Blistering of Steel in Hydrogen Sulfide Solutions", *Corrosion*, 9, 163-172 (1953).
- (63) Fraser, J. P., and Treseder, R. S., "Cracking of High Strength Steels in Hydrogen Sulfide Solutions", *Corrosion*, 8, 342-360 (1952).
- (64) Karpenko, G. V., and Stepurenko, V. T., "The Effect of Hydrogen Sulfide Solution Upon the Mechanical Properties of Steel", *Akademiya Nauk Ukrainskoy SSR. Institut Mashinovedeniya i Avtomatiki. The Effect of Working Media Upon the Properties of Steel. No. 1. Media Which Cause Hydrogen Absorption of Steel*, Kiev, Izd-vo AN UkSSR (1961), In Russian.
- (65) Herzog, E., and Malinowsky, E., "Embrittlement and Fractures of Steels Subjected to Stress in Saturated Solutions of H<sub>2</sub>S", *Memoires Scientifiques de la Revue de Metallurgie*, 57, 535-549 (July, 1960), In French.
- (66) Grundig, W., "Hydrogen Embrittlement as a Cause of Fracture of Steel Wires for Concrete Reinforcement", *Bol. ABM*, 14, 473-515 (October, 1958), In Portuguese; Abstract in *J. Iron and Steel Inst.*, 194, 274 (1960).
- (67) Bastien, Paul, and Amiot, Pierre, "Mechanism of the Effect of Ionized Solutions of Hydrogen Sulfide on Iron and Steel", *Comp. Rend.*, 235, 1031-1033 (1952), In French.
- (68) Shank, M. E., Spaeth, C. E., Cooke, V. W., and Coyne, J. E., "Solid-Fuel Rocket Chambers for Operation at 240,000 Psi and Above", *Parts I and II, Metal Progress*, 76, 74-82 (November, 1959); 84-92 (December, 1959).

- (69) Spaeth, C. E., "Defects, Surface Finishes, and Hydrogen Embrittlement", Mechanical and Metallurgical Behavior of Sheet Materials, Proc. 7th Sagamore Ordnance Materials Research Conf., Racquette Lake, N. Y., pp III-11 to III-37, August 16-19, 1960.
- (70) Norton, Francis J., "Diffusion of D<sub>2</sub> from D<sub>2</sub>O Through Steel", J. Appl. Phys., 24, 499 (1953).
- (71) Steigerwald, E. A., "Delayed Failure of High-Strength Steel in Liquid Environments", Proc. Am. Soc. Testing Materials, 60, 750-760 (1960).
- (72) Petch, N. J., and Stables, P., "Delayed Fracture of Metals Under Static Load", Nature, 169, 842-843 (May 17, 1952).
- (73) Davis, Robert A., "Stress Corrosion Investigation of Two Low Alloy High Strength Steels", paper presented at the 18th Conference and Corrosion Show of the National Assoc. of Corrosion Engrs., Kansas City, Missouri, March 19-23, 1962.
- (74) Swets, D. E., and Frank, R. C., "Hydrogen from a Hydrocarbon Lubricant Absorbed by Ball Bearings", Trans. Met. Soc. AIME, 221, 1082-1083 (October, 1961).
- (75) Swets, D. E., Frank, R. C., and Fry, D. L., "Environmental Effects on Hydrogen Permeation Through Steel During Abrasion", Trans. Met. Soc. AIME, 212 (2), 219-220 (April, 1958).
- (76) Chilton, J. E., "Development of Electroplating Processes to Eliminate Hydrogen Embrittlement in High-Strength Steel", WADC TR 57-514 (November 4, 1957).
- (77) Brown, Jack T., and Baldwin, William M., Jr., "Hydrogen Embrittlement of Steels", Trans. Am. Inst. Mining and Met. Engrs., 200, 298-303 (1954); J. Metals, 6 (2), 298-303 (February, 1954).
- (78) Toh, Taiji, and Baldwin, William M., Jr., "Ductility of Steel with Varying Concentrations of Hydrogen", Stress Corrosion Cracking and Embrittlement, W. D. Robertson, editor, John Wiley and Sons, Inc., New York (1956), pp 176-186.
- (79) Chang, P. L., and Bennett, W. D. G., "Diffusion of Hydrogen in Iron and Iron Alloys at Elevated Temperatures", J. Iron and Steel Inst., 170, 205-213 (1952).
- (80) Steigerwald, E. A., Schaller, F. W., and Troiano, A. R., "Discontinuous Crack Growth in Hydrogenated Steel", Trans. Met. Soc. AIME, 215, 1048-1052 (December, 1959).
- (81) Klier, E. P., Muvdi, B. B., and Sachs, G., "Hydrogen Embrittlement in an Ultra-High-Strength 4340 Steel", J. Metals, 9 (1), 106-112 (January, 1957); Trans. Am. Inst. Mining, Met., and Petroleum Engrs., 209, 106-112 (1957).

- (82) Foryst, J., "The Dependence of the Hydrogen Brittleness of Steel on the Content of Oxide Inclusions", *Hutnicke Aktuality*, 14, 47-59 (1958); Abstract in *J. Iron and Steel Inst.*, 194, 523-524 (1960).
- (83) Sims, C. E., "The Behavior of Gases in Solid Iron and Steel", *Gases in Metals*, Am. Soc. Metals, Cleveland (1953), pp 157-161.
- (84) Hobson, J. D., "The Removal of Hydrogen by Diffusion from Large Masses of Steel", *J. Iron and Steel Inst.*, 191, 342-352 (April, 1959).
- (85) Johnson, H. H., Morlet, J. G., and Troiano, A. R., "Hydrogen, Crack Initiation, and Delayed Failure in Steel", WADC TR 57-262 (May, 1957).
- (86) Muvdi, B. B., Sachs, G., and Klier, E. P., "Design Properties of High-Strength Steels in the Presence of Stress Concentrations and Hydrogen Embrittlement. Suppl. 1. Effects of Hydrogen Embrittlement on High-Strength Steels (Fatigue Properties)", WADC TR 55-18, Supplement 1 (February, 1956).
- (87) Steigerwald, E. A., Schaller, F. W., and Troiano, A. R., "Hydrogen Embrittlement in Steels, Titanium Alloys, and Several Face-Centered Cubic Alloys. Section 1. Delayed Failure in High Strength Steel", WADC TR 59-172, Section 1 (April, 1959).
- (88) Morlet, J. G., Johnson, H. H., and Troiano, A. R., "A New Concept of Hydrogen Embrittlement in Steel", *J. Iron and Steel Inst.*, 189, 37-44 (1958).
- (89) Zapffe, C. A., and Sims, C. E., "Defects in Weld Metal and Hydrogen in Steel", *Welding J.*, 19 (10), 377s-395s (1940).
- (90) Zapffe, C. A., and Sims, C. E., "Hydrogen Embrittlement, Internal Stress and Defects in Steel", *Trans. Am. Inst. Mining and Met. Engrs.*, 145, 225-259 (1941).
- (91) Zapffe, C. A., "Neumann Bands and the Planar-Pressure Theory of Hydrogen Embrittlement", *J. Iron and Steel Inst.*, 154, 123P-130P (1946).
- (92) Zapffe, C. A., Discussion of "Metal Arc Welding of Steel" by S. A. Herres in *Trans. Am. Soc. Metals*, 39, 162-189 (1947), *Trans. Am. Soc. Metals*, 39, 190-191 (1947).
- (93) Bastien, P., and Azou, P., "Effect of Hydrogen on the Deformation and Fracture of Iron and Steel in Simple Tension", *Proc. of the First World Met. Cong.*, Am. Soc. Metals, 535-552 (1951).
- (94) De Kazinczy, F., "Synpunkter På Väteförsprödnings Natur", *Jernkontorets Annaler*, 138, 271-287 (1954), An English summary is given.
- (95) Orowan, E., "Fundamentals of Brittle Behavior in Metals", *Fatigue and Fracture of Metals*, Technology Press, Mass. Inst. Technol. and John Wiley and Sons, New York (1952), p 139.



- (96) Petch, N. J., "The Lowering of Fracture Stress Due to Surface Adsorption", *Phil. Mag.*, Series 8, 1, 331-337 (1956).
- (97) Morlet, J. G., Johnson, H. H., and Troiano, A. R., "A New Concept of Hydrogen Embrittlement in Steel", *J. Iron and Steel Inst.*, 189, 37-44 (May, 1958).
- (98) Steigerwald, E. A., Schaller, F. W., and Troiano, A. R., "Effect of Temperature on the Static Fatigue Characteristics of Hydrogen Embrittled 4340 Steel", WADC TR 58-178 (April, 1958).
- (99) Bilby, B. A., and Hewitt, J., "Hydrogen in Steel - The Stability of Micro-Cracks", *Acta Met.*, 10, 587-600 (June, 1962).
- (100) Garofalo, F., Chou, Y. T., and Ambegaokar, V., "Effect of Hydrogen on Stability of Microcracks in Iron and Steel", *Acta Met.*, 8, 504-512 (August, 1960).
- (101) De Kazinczy, F., "Crack Formation in Steel During Electrolytic Hydrogen Absorption", *TVF*, 32 (3), 159-165 (1961), In English.
- (102) Tetelman, A. S., and Robertson, W. D., "The Mechanism of Hydrogen Embrittlement Observed in Iron-Silicon Single Crystals", *Trans. Met. Soc. AIME*, 224 (4), 775-783 (August, 1962).
- (103) Siede, A., and Rostaker, W., "On the Problem of Hydrogen Embrittlement of Iron", *Trans. Met. Soc. AIME*, 212 (6), 852-855 (December, 1958).
- (104) Blanchard, P. A., and Troiano, A. R., "Hydrogen Embrittlement In Terms of Modern Theory of Fracture", WADC TR 59-444 (August, 1959).
- (105) Scott, T. E., and Troiano, A. R., "Interstitial Induced Delayed Failure of Steel", U. S. Air Force, Aeronautical Research Laboratories, ARL 62-425 (September, 1962).
- (106) Dauerman, L., "A Study of the Mechanism of the Action of Inhibitors Which Prevent Hydrogen Embrittlement of Carbon Steels Resulting from Acid Pickling", Rutgers University, Final Report for Paint and Chemical Research Laboratory, Aberdeen Proving Ground, on Contract No. DA-30-069-ORD-1680 (January 1, 1956, to November 30, 1960).
- (107) Beck, W., Klier, E. P., and Sachs, G., "Constant Strain Rate Bend Tests on Hydrogen-Embrittled High Strength Steels", *Trans. Am. Inst. Mining and Met. Engrs.*, 206, 1263-1268 (October, 1956).
- (108) Morgan, William A., "New Test for Hydrogen Embrittlement", *Digest of Reference 109, Metal Prog.*, 82 (1), 154, 156 (July, 1962).
- (109) Williams, F. S., Beck, W., and Jankowsky, E. J., "A Notched Ring Specimen for Hydrogen Embrittlement Studies", paper presented at 63rd Annual Meeting of the ASTM, Atlantic City, N. J. (June, 1960).

- (110) Jar'owsky, E. J., and Beck, W., "Investigation of Crack Propagation in Hydrogen Embrittled Steel", Naval Air Material Center, Rept. No. NAMC-AML-AE-1102 (August 28, 1959). PB 150780, AD-227511.
- (111) Jones, R. L., "A New Approach to Bend Testing for the Determination of Hydrogen Embrittlement Susceptibility of Sheet Materials", Convair (Astronautics), Div. of General Dynamics Corp., San Diego, Calif., Report No. 235 (June 15, 1961).
- (112) Raring, R. H., and Rinebolt, J. A., "A Small and Inexpensive Device for Sustained Loading Testing", Am. Soc. Testing Materials, Bulletin No. 213, 74-76 (April, 1956).
- (113) Klingler, R. F., "A Mechanical Test for Indicating Hydrogen Embrittlement in Alpha-Beta Titanium Alloys", WADC TN 55-774 (December, 1955).
- (114) Sachs, G., "Test Methods for Evaluating Hydrogen Embrittlement", Proc. of the Third Sagamore Ordnance Materials Research Conf., pp 496-516, December 5-7, 1956, OTS PB 131783.
- (115) Anon., "Watch for These New Nondestructive Testing Tools", Steel, 150, 62-66 (January 22, 1962).
- (116) Carlisle, M. E., "Methods of Testing for Hydrogen Embrittlement", Northrop Report No. NOR-59-472, Aerospace Research and Testing Committee, Proj. W-95, Final Report (October 21, 1959).
- (117) Johnson, B. G., "Method of Test for Hydrogen Embrittlement Due to Electrolytic Cadmium Plating", Paper No. 61, Presented at ASTM meeting, Los Angeles, California, October 1-5, 1962.

ARE:EEF/js

LIST OF DMIC TECHNICAL REPORTS ISSUED  
DEFENSE METALS INFORMATION CENTER

Battelle Memorial Institute

Columbus 1, Ohio

Copies of the technical reports listed below may be obtained from DMIC at no cost by Government agencies, and by Government contractors, subcontractors, and their suppliers. Others may obtain copies from the Office of Technical Services, Department of Commerce, Washington 25, D. C. See PF numbers and prices in parentheses.

DMIC Report Number	Title
46D	Department of Defense Titanium Sheet-Rolling Program - Uniform Testing Procedure for Sheet Materials, September 12, 1958 (PB 121649 \$1.25)
46E	Department of Defense Titanium Sheet-Rolling Program - Thermal Stability of the Titanium Sheet-Rolling-Program Alloys, November 25, 1958 (PB 151061 \$1.25)
46F	Department of Defense Titanium Sheet-Rolling Program Status Report No. 4, March 20, 1959 (PB 151065 \$2.25)
46G	Department of Defense Titanium Sheet-Rolling Program - Time-Temperature-Transformation Diagrams of the Titanium Sheet-Rolling Program Alloys, October 19, 1959 (PB 151075 \$2.25)
46H	Department of Defense Titanium Sheet-Rolling Program, Status Report No. 5, June 1, 1960 (PB 151087 \$2.00)
46I	Statistical Analysis of Tensile Properties of Heat-Treated Ti-4A1-3Mo-1V Sheet, September 16, 1960 (PB 151095 \$1.25)
46J	Statistical Analysis of Tensile Properties of Heat-Treated Ti-4A1-3Mo-1V and Ti-2.5A1-16V Sheet, June 6, 1961 (AD 259284 \$1.25)
106	Beryllium for Structural Applications, August 15, 1958 (PB 121648 \$3.00)
107	Tensile Properties of Titanium Alloys at Low Temperature, January 15, 1959 (PB 151062 \$1.25)
108	Welding and Brazing of Molybdenum, March 1, 1959 (PB 151063 \$1.25)
109	Coatings for Protecting Molybdenum From Oxidation at Elevated Temperature, March 6, 1959 (PB 151064 \$1.25)
110	The All-Beta Titanium Alloy (Ti-13V-11Cr-3Al), April 17, 1959 (PB 151066 \$3.00)
111	The Physical Metallurgy of Precipitation-Hardenable Stainless Steels, April 20, 1959 (PB 151067 \$2.00)
112	Physical and Mechanical Properties of Nine Commercial Precipitation-Hardenable Stainless Steels, May 1, 1959 (PB 151068 \$3.25)
113	Properties of Certain Cold-Rolled Austenitic Stainless Sheet Steels, May 15, 1959 (PB 151069 \$1.75)
114	Ductile-Brittle Transition in the Refractory Metals, June 25, 1959 (PB 151070 \$2.00)
115	The Fabrication of Tungsten, August 14, 1959 (PB 151071 \$1.75)
116R	Design Information on 5Cr-Mo-V Alloy Steels (H-11 and 5Cr-Mo-V Aircraft Steel) for Aircraft and Missiles (Revised), September 30, 1960 (PB 151072-R \$1.50)
117	Titanium Alloys for High-Temperature Use Strengthened by Fibers or Dispersed Particles, August 31, 1959 (PB 151073 \$2.00)
118	Welding of High-Strength Steels for Aircraft and Missile Applications, October 12, 1959 (PB 151074 \$2.25)
119	Heat Treatment of High-Strength Steels for Aircraft Applications, November 27, 1959 (PB 151076 \$2.50)
120	A Review of Certain Ferrous Castings Applications in Aircraft and Missiles, December 18, 1959 (PB 151077 \$1.50)
121	Methods for Conducting Short-Time Tensile, Creep, and Creep-Rupture Tests Under Conditions of Rapid Heating, December 20, 1959 (PB 151078 \$1.25)
122	The Welding of Titanium and Titanium Alloys, December 31, 1959 (PB 151079 \$1.75)
123	Oxidation Behavior and Protective Coatings for Columbium and Columbium-Base Alloys, January 15, 1960 (PB 151080 \$2.25)
124	Current Tests for Evaluating Fracture Toughness of Sheet Metals at High Strength Levels, January 28, 1960 (PB 151081 \$2.00)
125	Physical and Mechanical Properties of Columbium and Columbium-Base Alloys, February 22, 1960 (PB 151082 \$1.75)
126	Structural Damage in Thermally Cycled René 41 and Astroloy Sheet Materials, February 29, 1960 (PB 151083 \$0.75)
127	Physical and Mechanical Properties of Tungsten and Tungsten-Base Alloys, March 15, 1960 (PB 151084 \$1.75)
128	A Summary of Comparative Properties of Air-Melted and Vacuum-Melted Steels and Superalloys, March 28, 1960 (PB 151085 \$2.75)
129	Physical Properties of Some Nickel-Base Alloys, May 20, 1960 (PB 151086 \$2.75)
130	Selected Short-Time Tensile and Creep Data Obtained Under Conditions of Rapid Heating, June 17, 1960 (PB 151088 \$2.25)
131	New Developments of the Welding of Metals, June 24, 1960 (PB 151089 \$1.25)
132	Design Information on Nickel-Base Alloys for Aircraft and Missiles, July 20, 1960 (PB 151090 \$3.00)
133	Tantalum and Tantalum Alloys, July 25, 1960 (PB 151091 \$5.00)
134	Strain Aging of Refractory Metals, August 12, 1960 (PB 151092 \$1.75)
135	Design Information on PH 15-7 Mo Stainless Steel for Aircraft and Missiles, August 22, 1960 (PB 151093 \$1.25)

## DMIC REPORTS

DMIC Report Number	Title
136A	The Effects of Alloying Elements in Titanium, Volume A. Constitution, September 15, 1960 (PB 151094 \$3.50)
136B	The Effects of Alloying Elements in Titanium, Volume B. Physical and Chemical Properties, Deformation and Transformation Characteristics, May 29, 1961 (AD 260226 \$3.00)
137	Design Information on 17-7 PH Stainless Steels for Aircraft and Missiles, September 23, 1960 (PB 151096 \$1.00)
138	Availability and Mechanical Properties of High-Strength Steel Extrusions, October 26, 1960 (PB 151097 \$1.75)
139	Melting and Casting of the Refractory Metals Molybdenum, Columbium, Tantalum, and Tungsten, November 18, 1960 (PB 151098 \$1.00)
140	Physical and Mechanical Properties of Commercial Molybdenum-Base Alloys, November 30, 1960 (PB 151099 \$3.00)
141	Titanium-Alloy Forgings, December 19, 1960 (PB 151100 \$2.25)
142	Environmental Factors Influencing Metals Applications in Space Vehicles, December 27, 1960 (PB 151101 \$1.25)
143	High-Strength-Steel Forgings, January 5, 1961 (PB 151102 \$1.75)
144	Stress-Corrosion Cracking - A Nontechnical Introduction to the Problem, January 6, 1961 (PB 151103 \$0.75)
145	Design Information on Titanium Alloys for Aircraft and Missiles, January 10, 1961 (PB 151104 \$2.25)
146	Manual for Beryllium Prospectors, January 18, 1961 (PB 151105 \$1.00)
147	The Factors Influencing the Fracture Characteristics of High-Strength Steel, February 6, 1961 (PB 151106 \$1.25)
148	Review of Current Data on the Tensile Properties of Metals at Very Low Temperatures, February 14, 1961 (PB 151107 \$2.00)
149	Brazing for High Temperature Service, February 21, 1961 (PB 151108 \$1.00)
150	A Review of Bending Methods for Stainless Steel Tubing, March 2, 1961 (PB 151109 \$1.50)
151	Environmental and Metallurgical Factors of Stress-Corrosion Cracking in High-Strength Steels, April 14, 1961 (PB 151110 \$0.75)
152	Binary and Ternary Phase Diagrams of Columbium, Molybdenum, Tantalum, and Tungsten, April 28, 1961 (AD 257739 \$3.50)
153	Physical Metallurgy of Nickel-Base Superalloys, May 5, 1961 (AD 258041 \$1.25)
154	Evolution of Ultrahigh-Strength, Hardenable Steels for Solid-Propellant Rocket-Motor Cases, May 25, 1961 (AD 257976 \$1.25)
155	Oxidation of Tungsten, July 17, 1961 (AD 263598 \$3.00)
156	Design Information on AM-350 Stainless Steel for Aircraft and Missiles, July 28, 1961 (AD 262407 \$1.50)
157	A Summary of the Theory of Fracture in Metals, August 7, 1961 (PB 181081 \$1.75)
158	Stress-Corrosion Cracking of High-Strength Stainless Steels in Atmospheric Environments, September 15, 1961 (AD 266005 \$1.25)
159	Gas-Pressure Bonding, September 25, 1961 (AD 265133 \$1.25)
160	Introduction to Metals for Elevated-Temperature Use, October 27, 1961 (AD 268647 \$2.50)
161	Status Report No. 1 on Department of Defense Refractory Metals Sheet-Rolling Program, November 2, 1961 (AD 267077 \$1.00)
162	Coatings for the Protection of Refractory Metals from Oxidation, November 24, 1961 (AD 271384 \$3.50)
163	Control of Dimensions in High-Strength Heat-Treated Steel Parts, November 29, 1961 (AD 270045 \$1.00)
164	Semiaustenitic Precipitation-Hardenable Stainless Steels, December 6, 1961 (AD 274805 \$2.75)
165	Methods of Evaluating Welded Joints, December 28, 1961 (AD 272088 \$2.25)
166	The Effect of Nuclear Radiation on Structural Metals, September 15, 1961 (AD 265839 \$2.50)
167	Summary of the Fifth Meeting of the Refractory Composites Working Group, March 12, 1962 (AD 274804 \$2.00)
168	Beryllium for Structural Applications, 1958-1960, May 18, 1962 (AD 278723 \$3.50)
169	The Effect of Molten Alkali Metals on Containment Metals and Alloys at High Temperatures, May 18, 1962 (AD 282932 \$1.50)
170	Chemical Vapor Deposition, June 4, 1962 (AD 281887 \$2.25)
171	The Physical Metallurgy of Cobalt-Base Superalloys, July 6, 1962 (AD 283356 \$2.25)
172	Background for the Development of Materials To Be Used in High-Strength-Steel Structural Weldments, July 31, 1962 (AD 284265 \$3.00)
173	New Developments in Welded Fabrication of Large Solid-Fuel Rocket-Motor Cases, August 6, 1962 (AD 284829 \$1.00)
174	Electron-Beam Processes, September 15, 1962 (AD 287433 \$1.75)
175	Summary of the Sixth Meeting of the Refractory Composites Working Group, September 24, 1962 (AD 287029 \$1.75)
176	Status Report No. 2 on Department of Defense Refractory Metals Sheet-Rolling Program, October 1, 1962 (AD 288127 \$1.25)
177	Thermal Radiative Properties of Selected Materials, November 15, 1962, Vol. I (AD 294348 \$3.00)
177	Thermal Radiative Properties of Selected Materials, November 15, 1962, Vol. II (AD 294349 \$4.00)
178	Steels for Large Solid-Propellant Rocket-Motor Cases, November 20, 1962
179	A Guide to the Literature on High-Velocity Metalworking, December 3, 1962
180	Design Considerations in Selecting Materials for Large Solid-Propellant Rocket-Motor Cases, December 10, 1962
181	Joining of Nickel Base Alloys, December 20, 1962
182	Structural Considerations in Developing Refractory Metal Alloys, January 31, 1963
183	Binary and Ternary Phase Diagrams of Columbium, Molybdenum, Tantalum, and Tungsten (Supplement to DMIC Report 152), February 7, 1963
184	Summary of the Seventh Meeting of the Refractory Composites Working Group, May 31, 1963
185	The Status and Properties of Titanium Alloys for Thick Plate, June 14, 1963
186	The Effect of Fabrication History and Microstructure on the Mechanical Properties of Refractory Metals and Alloys, July 1, 1963

DMIC REPORTS  
(Continued)

DMIC  
Report Number

Title

---

188	The Engineering Properties of Columbium and Columbium Alloys, September 6, 1963
189	The Engineering Properties of Tantalum and Tantalum Alloys, September 13, 1963
190	The Engineering Properties of Molybdenum and Molybdenum Alloys, September 20, 1963
191	The Engineering Properties of Tungsten and Tungsten Alloys, September 27, 1963
192	Hot-Cold Working of Steel to Improve Strength, October 11, 1963
193	Tungsten Research and Development Review, October 23, 1963
194	A Discussion of the Physical Metallurgy of the 18 Per Cent Nickel Maraging Steels, November 15, 1963
195	Properties of Coated Refractory Metals, January 10, 1964